53239

ACTA CLIMATOLOGICA
ET CHOROLOGICA

TOMUS XL-XLI.

ACTA UNIVERSITATIS SZEGEDIENSIS

ACTA CLIMATOLOGICA ET CHOROLOGICA

TOMUS XL-XLI.

CONTENTS

ANNUAL MEAN URBAN HEAT ISLAND VERSUS 2D SURFACE PARAMETERS: MODELLING, VALIDATION AND EXTENSION

B. BALÁZS[1], J. GEIGER[2] and Z. SÜMEGHY[1]

[1]Department of Climatology and Landscape Ecology, University of Szeged, P.O.Box 653, 6701 Szeged, Hungary
E-mail: balazsb@geo.u-szeged.hu
[2]Department of Geology and Paleontology, University of Szeged, P.O.Box 653, 6701 Szeged, Hungary

Összefoglalás – Feltételezésünk az, hogy az alföldi városok átlagos évi hősziget intenzitása megközelíthető a felszíni jellemzőik alapján. Tanulmányunk célja – szegedi és debreceni hőmérsékleti és felszínborítottsági adatok alapján – egy többváltozós modell készítése az átlagos hősziget területi eloszlásának megbecslésére, e modell validálása, majd kiterjesztése más olyan, hasonló földrajzi adottságú városokra, ahol nem áll rendelkezésre hőmérsékleti mérés.

Summary – Our assumption is that the mean daily maximum heat island of towns situated on a plain can be assessed on the basis of their surface features. Based on temperature and surface cover data from Szeged and Debrecen, the aim of our research is to construct a multiple variable model for estimating the spatial distribution of the mean heat island, the validation of this model and then to extend our results to other towns situated in a similar environment with no temperature measurements available.

Key words: urban heat island, urban surface parameters, geoinformatic methods, Szeged, Hungary

1. INTRODUCTION

Urban environments differ significantly from the surrounding natural lands, because they have different surface geometry, material- and air composition, and the anthropogenic heat emission also affects them. This leads to a local-scale alteration of climate: e.g. the formation of the urban heat island (UHI). This is a positive thermal alteration, namely that the town is usually warmer than its surroundings. The effect has dual characteristics: in summer it means a problem because of the slowly cooling air at night, but in winter this same influence is advantageous, since the heating demand of buildings and the length of heating period decreases in the urban areas (*Unger*, 1997). Furthermore, the composition of urban vegetation is changed and a postponement of phenological phases is observable (*Lakatos and Gulyás*, 2003). Its investigation is important because of the large number of inhabitants.

The aim of our research is to calculate a statistical estimation for the intensity of the annual mean maximal heat island. Its research can provide important information for example for urban planning (*Kuttler*, 1998).

The quantitative determination of the role of factors affecting the development and intensity of UHI is difficult because of the complex vertical and horizontal structure of the town and because of the artificial emission of heat and pollutants. Detailed data collection

is also complicated and it demands significant technical investments. Our assumption is that satellite images of the settlements situated on plain (simple morphology, no orographical influence) can serve as a tool to estimate the annual mean UHI, because some parameters (e.g. the built-up ratio) of the modified urban surface can be calculated with the help of these images.

According to the aim of this research we construct a multiple variable model for the estimation of the spatial distribution of the mean heat island using the surface cover data of Szeged and Debrecen. Then we extend our results to other towns situated in a similar environment with no temperature measurements available.

2. STUDY AREAS

Szeged and Debrecen are situated on the Great Hungarian Plain, on Holocene sediments with a gentle relief. According to Trewartha's classification Szeged and Debrecen belong to the climatic type D.1 (continental climate with longer warm season), similarly to the predominant part of the country.

According to the geographical position it is possible to divide the Hungarian towns into three categories: located in a valley, at the meeting point of mountainous area and plain, and on the plain. From the point of view of urban climate development, in the case of the first two categories it is very difficult to separate the effects of topography and human impact. Szeged and Debrecen belong to the third category, so they have favourable conditions for urban climate research. For this reason the results of systematic measurements and analysis in these towns can be a basis of general conclusions (*Unger*, 1997).

The investigations are focused on the built-up areas of the towns, which mean about 30 km² areas in case of both towns. The towns have different structures: Szeged has one centre and an avenue-boulevard system, and the river Tisza flows across it. Debrecen is less structured and has more centres.

3. TEMPERATURE MEASUREMENTS

For the information on the UHI structure and intensity temperature data were collected by mobile measurements in Szeged and Debrecen (*Fig. 1a-b*). In order to systematise the collected datasets the study areas were divided into 500 m x 500 m grid-cells. The same grid size of 0.25 km² was applied in some other urban climate projects (e.g. *Park*, 1986; *Long et al.*, 2003; *Lindberg et al.*, 2003). The study areas consist of 107 (25.75 km²) and 105 cells (26 km²) in Szeged and in Debrecen, respectively. They cover the inner and suburban parts of the towns. In both towns one rural cell was used as a reference area for the comparison of temperature data.

The required data were collected with measurement cars on assigned routes, in a one-year-long period between April 2002 and March 2003). Such mobile measurements are wide-spread in studying urban climate parameters (e.g. *Oke and Fuggle*, 1972; *Moreno-Garcia*, 1994; *Santos et al.*, 2003).

In the study areas the representative temperature pattern derives from the measurements, which took place every 10th days. This means the measurements were taken

35 times in Szeged and Debrecen at the same time. The three-hour measurements were carried out under all weather conditions except rain. Based on experiences from previous studies the data collection took place at the expected time of the daily maximum development of the UHI, at 4 hours after sunset (*Oke*, 1981; *Boruzs and Nagy*, 1999).
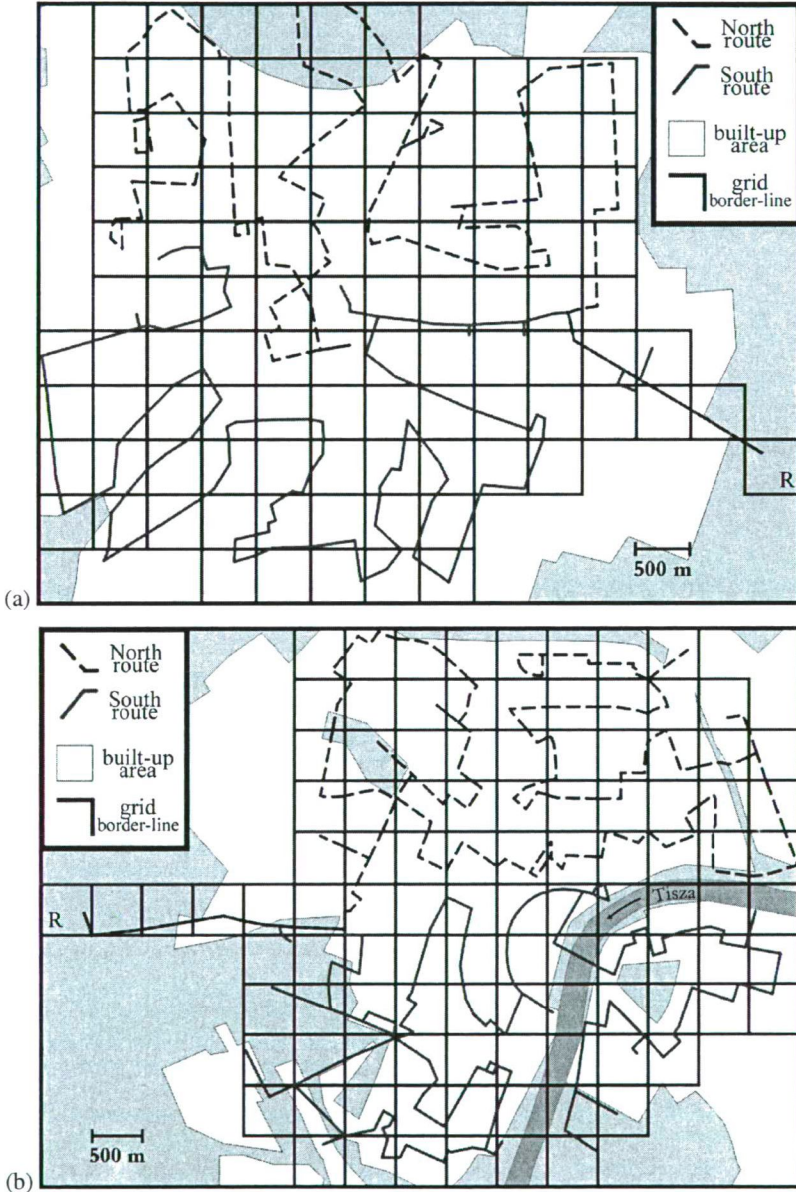

Fig. 1 Routes of the mobile UHI measurements (*a*) in Debrecen and (*b*) in Szeged (R = rural cell)

The areas were divided into two sectors because of the size of the study areas and the length of the measurement routes. The routes were planned to touch all the cells at least

once both ways (*Fig. 1a-b*). The temperature was measured by an automatic sensor connected to a digital data logger. The sensor measured the values every 10 seconds. It was placed on a bar, 0.6 m in front of the car and 1.45 m above the ground because of the thermic disturbing effect of the car. The car's speed was 20-30 kmh[-1] in order to provide the necessary ventilation to the sensor and a proper density of data. Accordingly there are data from every 55-83 m along the measurement routes. The values logged at the rare stops (e.g. red light, barrier) were later deleted from the database. The measured temperature data were averaged in each cell. In the hours after sunset the linear change of temperature was applied to the calculation of the measured data, with the assumption that it is only approximately valid in the suburban areas because of the different cooling gradients (*Oke and Maxwell, 1975*).

In our case the UHI intensity (ΔT) is defined as follows (*Unger et al., 2004*):

$$\Delta T = T_{cell} - T_{cell\,(R)}$$

where T_{cell} = temperature of the given urban cell; $T_{cell(R)}$ = temperature of the rural cell.

4. BUILT-UP RATIO AND FURTHER SURFACE PARAMETERS

The built-up ratio (B) characterizes the town horizontally. This parameter of land-use (streets, pavements, parking lots, building roofs, etc.) was determined for each grid cell using GIS (Geographical Information System) methods combined with remote sensing analysis of Landsat satellite images (*Unger et al., 2001*) not only for the study areas used for the temperature measurements but also for their extensions of 1.5 km in every direction. The nearest-neighbour method of resampling was employed, resulting in a root mean square value of less than 1 pixel. Because the geometric resolution of the image was 30 m x 30 m, small urban units could be assessed independently of their official (larger scale) land-use classification. The satellite images were taken in 2003, so they provide accurate data for the actual built-up conditions. Normalised Vegetation Index (*NDVI*) was calculated from the pixel values, according to the following equation (*Gallo and Owen, 1999*):

$$NDVI = (IR - R) / (IR + R)$$

where IR is the pixel value of the near-infrared band (0.72-1.1 μm) and R is the pixel value of the visible red band (0.58-0.68 μm). The value of *NDVI* is between -1 and +1. It depends on the quantity of biomass. If there is rich vegetation in the area, the $NDVI \approx 0.5\text{-}1$ (this means a full vegetation cover, e.g. forest). If there is grass vegetation in the area, the value of the $NDVI \approx 0.2\text{-}0.5$. If there is water surface, then the value approaches -1. With this index it is possible to determine the proportions of water, built-up and vegetated surfaces in percent by cells.

Fig. 2 shows the relation between the mean heat island intensity and the built-up ratio in Szeged and Debrecen together, so 212 element pairs were used. A strong positive relationship can be seen between the two parameters, namely the temperature difference increases as the built-up ratio increases. The strength of the linear relationship is supported by the value of the deterministic coefficient at the used element number ($R^2 = 0.2855$, n = 212).
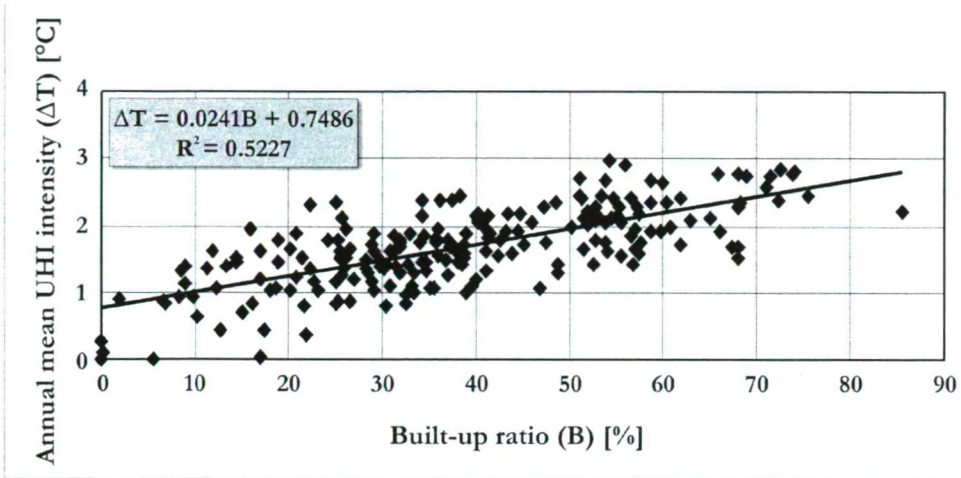
Fig. 2 Relationship between heat island intensity and built-up ratio in Szeged and Debrecen together
(n = 212)

The values of the built-up ratio can vary between 0% and 100%. In our case, in the study towns a built-up ratio of 2-84% was found. For example, in the case of Szeged *Fig. 3* shows the relation between the spatial distribution of the heat island and the built-up ratio, as the heat island intensity follows the change of built-up values. The distribution of the UHI intensity is roughly concentric, which is the consequence of the structure of the town.

It is important to consider the surroundings of the cells, because the temperature of the surroundings influences the temperature of a given cell, and *B* changes rapidly from the city centre. A set of predictors can be determined from the surface built-up ratio and its areal extensions in the following way, similar to *Bottyán and Unger* (2003):

- parameter value in the grid cell B with $\Delta i^2 + \Delta j^2 = 0$
- mean parameter value of all grid cells B_1 with $1 \leq \Delta i^2 + \Delta j^2 < 2^2$
- mean parameter value of all grid cells B_2 with $2^2 \leq \Delta i^2 + \Delta j^2 < 4^2$

Here, i and j are cell indices in the two dimensions, and Δi and Δj are the differences of grid cell indices with respect to a given cell. The obtained zones of predictors cover the entire investigated area and their extensions in Debrecen and Szeged. Now we have three predictors to build a linear statistical model. This procedure creates the right conditions for applying our model to predict the UHI intensity in other cities with different size. *Fig. 4* shows the structure of the constructed B, B_1, B_2 parameters.
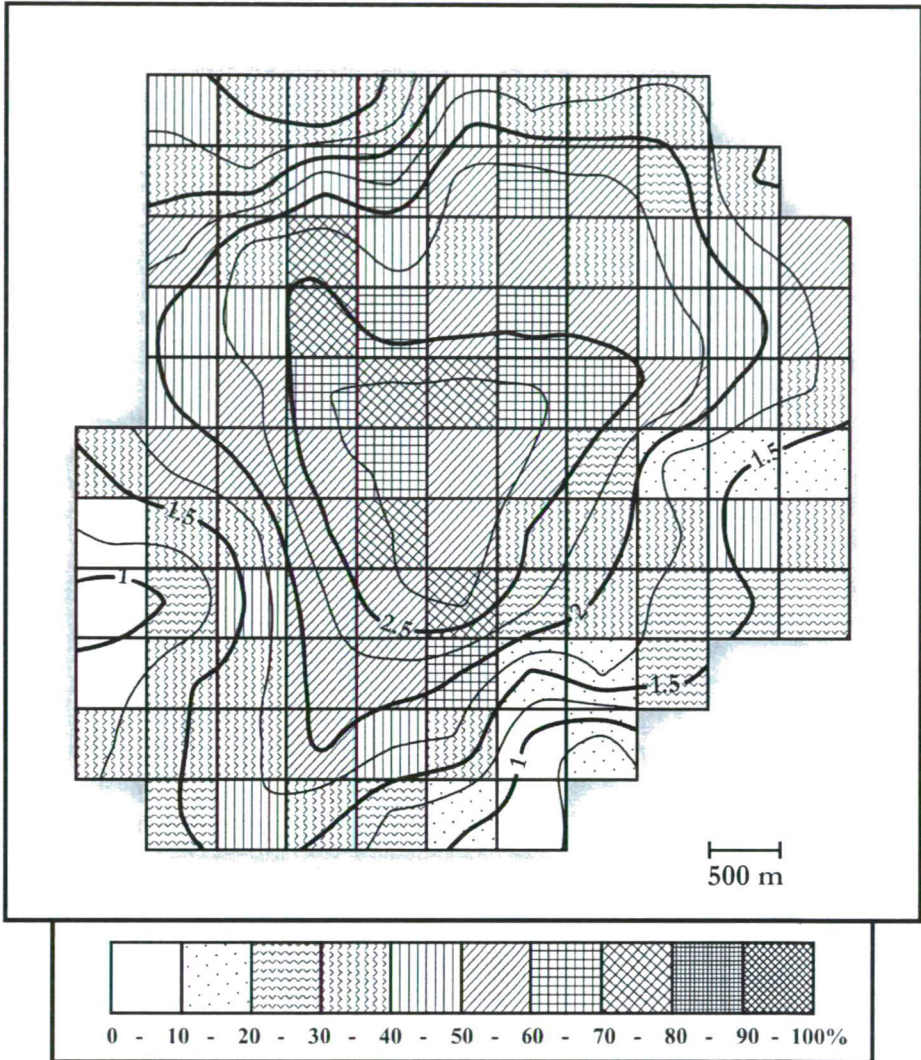
Fig. 3 Spatial distribution of the built-up ratio and the UHI intensity (in °C) in Szeged
(the 4 cells in the westernmost part of the study area are not shown)
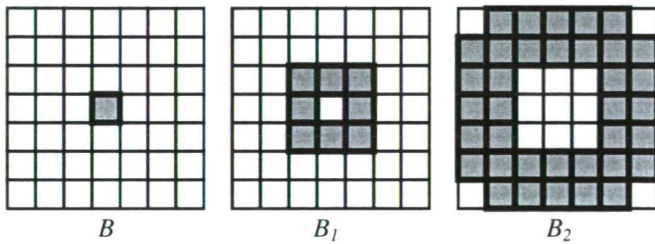
Fig. 4 The cells which take part in the calculation of B, B_1, B_2 parameters

5. CONSTRUCTION OF THE MULTIPLE-PARAMETER MODEL

The task is to quantitatively define the relationship between the above-mentioned urban surface parameters and the annual mean UHI intensity. As mentioned earlier our aim is to create a general multiple-parameter model on the basis of data from Szeged and Debrecen, which can be used for the estimation of heat island structure in other towns situated on a plain.

The elements of our multiple-parameter model:
- ΔT, as variable parameter (°C),
- B, B_1, B_2, as invariable parameters (%).

The multiple regression analysis of the Statgraphics Plus software was used to compute a model equation for the spatial distribution of the intensity of the annual mean heat island:

$$\Delta T = 0.0040*B + 0.0167*B_1 + 0.0267*B_2$$

The three parameters are responsible for the development of the temperature excess in more than 90% ($r^2 = 0.94$). In the data of Szeged and Debrecen, used together (212 element pairs) in creating the model, the value of B is between 0% and 84%, the value of B_1 is between 3% and 63%, the value of B_2 is between 12% and 49%, and the value of ΔT is between 0°C and 2.96°C.

Our model results can be considered appropriate, if the values of the study area are in the same interval. Henceforth this general model can be extended to other, different-sized towns, where the environmental situation, like topography and climate, is similar to that of Szeged and Debrecen. As mentioned earlier only the satellite images of the settlements are necessary for this, from which the built-up ratio and its areal extensions can be determined as predictors.

6. VALIDATION

Between September 2002 and January 2005 temperature measurements were taken in some towns situated on plain (Hajdúböszörmény, Hajdúdorog) by *Szegedi* (2005). These towns are situated near Debrecen, so they have similar topography and climate, but they are smaller than Debrecen. These towns both have avenue-boulevard systems, which is favourable for the development of the regular heat island structure type.

Hajdúböszörmény has 29,000 inhabitants and its (mostly urban) study area consists of 56 cells (14 km^2). Here the annual mean UHI intensity is 0.9°C in the centre according to the temperature measurement. The estimated annual ΔT is also 0.9°C (*Fig. 5*). 10,000 people live in Hajdúdorog and it has a study area of 35 cells (8.75 km^2). The annual mean UHI intensity is 0.3°C in the centre according to the temperature measurements. The estimated annual ΔT is also 0.3°C (*Fig. 5*).

So there is a good correspondence between the measured and estimated intensity values.
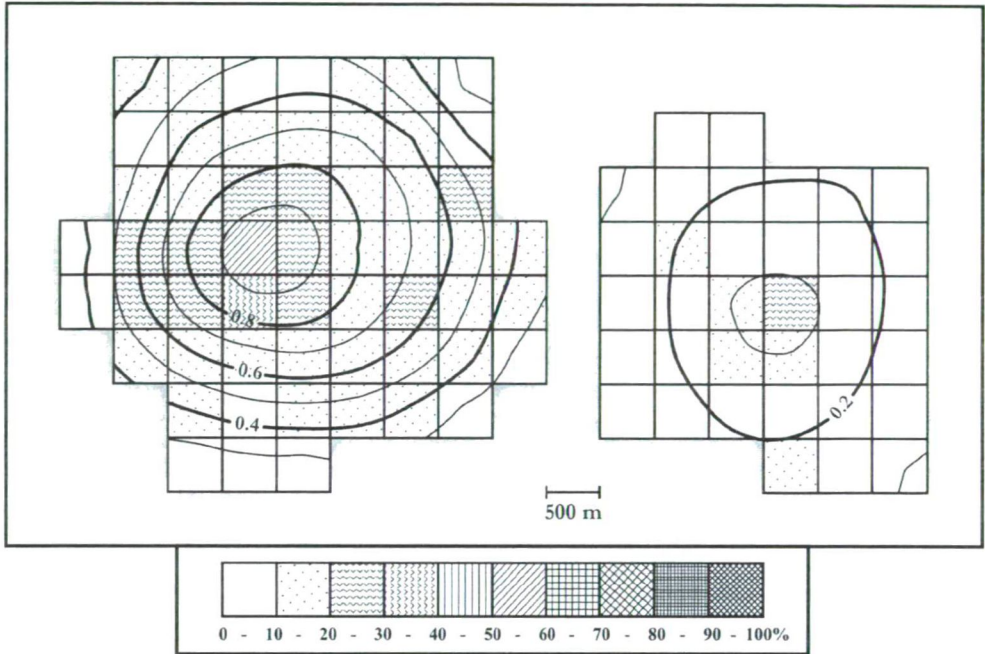
Fig. 5 Spatial distribution of the predicted mean UHI intensity (in °C)
for Hajdúböszörmény and Hajdúdorog

7. APPLICATION – EXTENSION

Presently sixteen towns with different size and population situated on a plain (Great Hungarian Plain) are examined in order to extend our model results. Three towns are not situated in Hungary: one is in Serbia and two in Romania. The towns studied are as follows: Arad, Baja, Békéscsaba, Cegléd, Hódmezővásárhely, Karcag, Kecskemét, Kiskunfélegyháza, Makó, Nagykőrős, Nyíregyháza, Orosháza, Szabadka (Subotica), Szolnok, Temesvár (Timisoara) and Pest (east side of Budapest, which is an almost plain area).

In this section, as examples, we show some of our results on the modelling of the spatial distribution of the annual mean UHI intensity in the case of Kecskemét and Békéscsaba.

Kecskemét has 109,000 inhabitants with a (mostly urban) study area of 61 cells (15.25 km^2). According to our model equation it has a rather regular heat island development with a center in the historical city centre and with a largest value of about 2.9°C (*Fig. 6*).
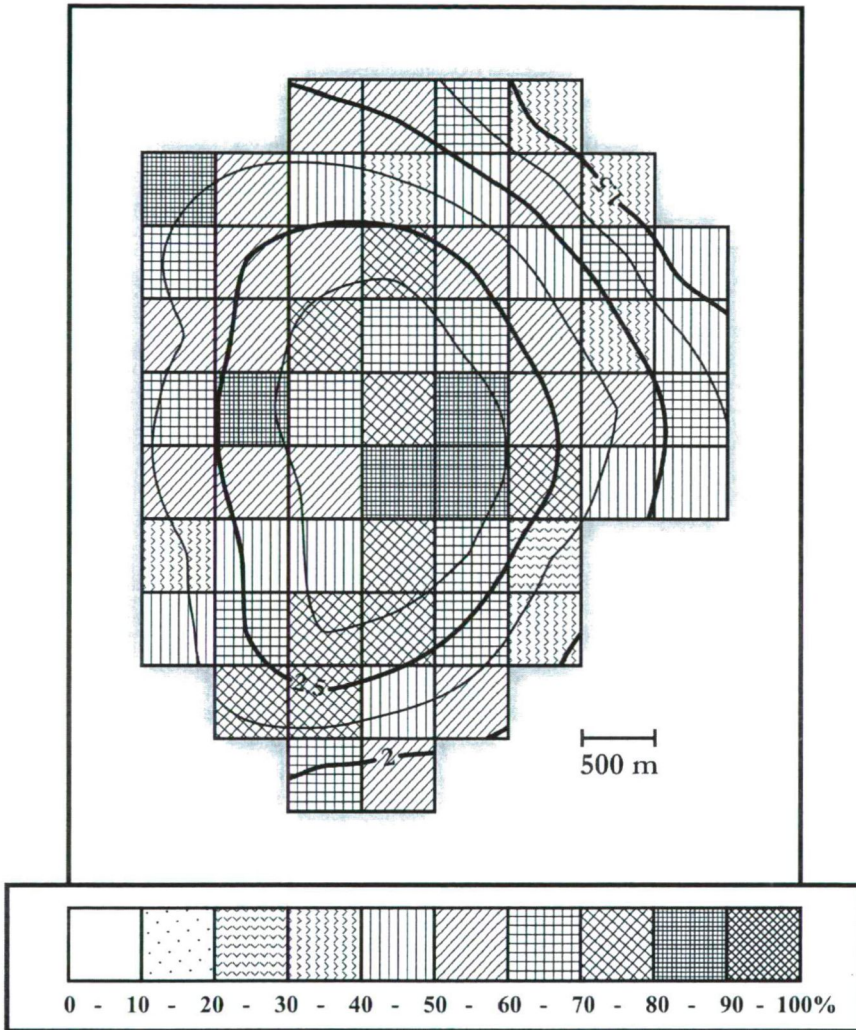
Fig. 6 Spatial distribution of the predicted mean UHI (in °C) intensity in Kecskemét

64,000 people live in Békéscsaba and its study area consists of 73 cells (18.25 km^2). As *Fig. 7* shows, it also has a regular heat island structure type with a largest value of about 1.8°C.
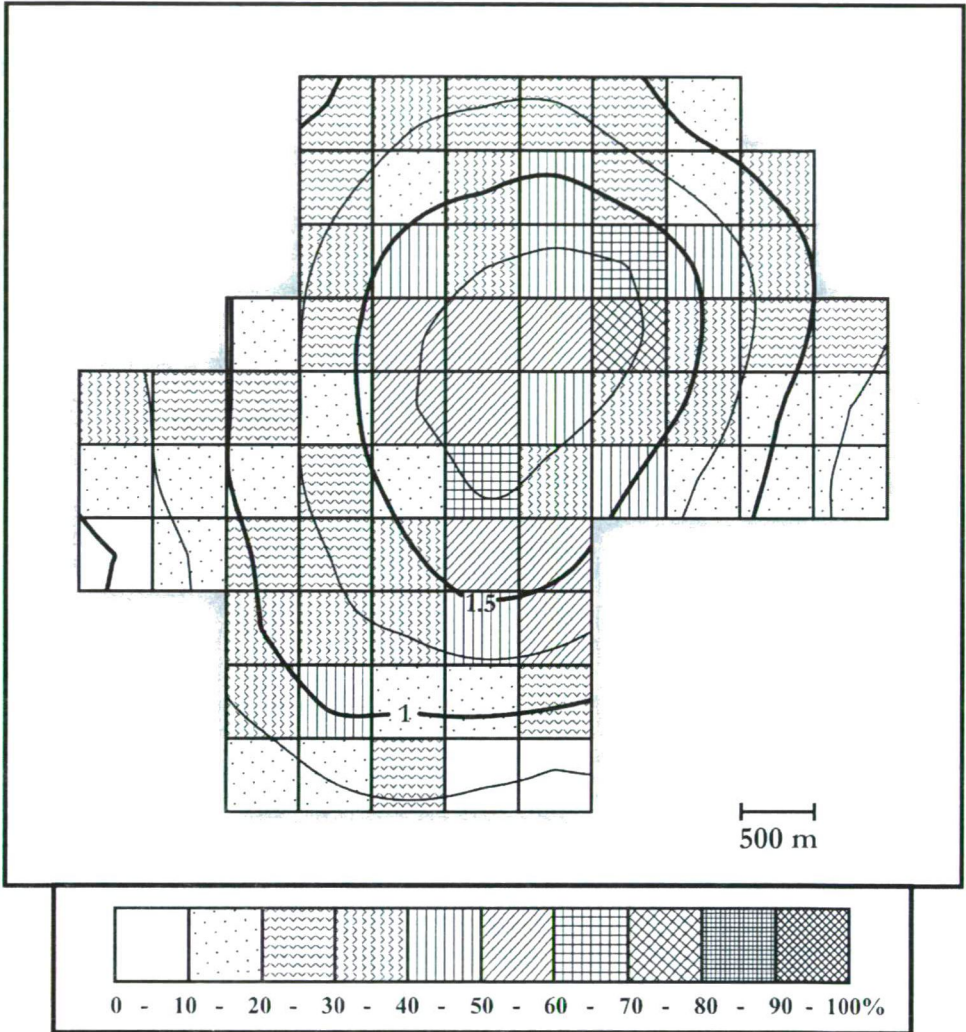
Fig. 7 Spatial distribution of the predicted mean UHI intensity (in °C) in Békéscsaba

8. CONCLUSIONS

This study presents a general multiple-parameter model based on surface cover parameters. There is a good correspondence between the measured and estimated intensity values. It can be used for the estimation of heat island structure in the case of towns situated on a plain. The knowledge of the estimated structure of mean UHI may provide useful basic information for the development projects of towns.

14

Our further aims are the verification of the model with temperature measurements, the extension of the model for other towns and to follow up the changes in the built-up ratio.

REFERENCES

Boruzs, T. and Nagy, T., 1999: A város hatása a klímaelemekre. [The influence of city on the climate elements (in Hungarian)]. MSc Thesis (manuscript). József Attila Tudományegyetem, Szeged.

Bottyán, Z. and Unger, J., 2003: A multiple linear statistical model for estimating the mean maximum urban heat island. *Theor. Appl. Climatol. 75*, 233-243.

Gallo, K.P. and Owen, T.W., 1999: Satellite-based adjustments for the urban heat island temperature bias. *J. Appl. Meteorol. 38*, 806-813.

Kuttler, W., 1998: Stadtklima. In *Heyer, E.* (ed): *Witterung und Klima*. Teubner, Stuttgart-Leipzig, 328-364.

Lakatos, L. and Gulyás, Á., 2003: Connection between phenological phases and urban heat island in Debrecen and Szeged, Hungary. *Acta Climatologica Univ. Szegediensis 36-37*, 79-83.

Lindberg, F., Eliasson, I. and Holmer, B., 2003: Urban geometry and temperature variations. In *Klysik, K., Oke, T.R., Fortuniak, K., Grimmond, C.S.B. and Wibig, J.* (eds.): *Proceed. Fifth Int. Conf. on Urban Climate Vol. 1*, University of Lodz, Lodz, Poland. 205-208.

Long, N., Mestayer, P.G. and Kergomard, C., 2003: Urban database analysis for mapping morphology and aerodynamic parameters: The case of St Jerome sub-urban area, in Marseille during ESCOMTE. In *Klysik, K., Oke, T.R., Fortuniak, K., Grimmond, C.S.B. and Wibig, J.* (eds.): *Proceed. Fifth Int. Conf. on Urban Climate Vol. 2*, University of Lodz, Lodz, Poland. 389-392.

Moreno-Garcia, M.C., 1994: Intensity and form of the urban heat island in Barcelona. *Int. J. Climatol. 14*, 705-710.

Oke, T.R., 1981: Canyon geometry and the nocturnal urban heat island: comparison of scale model and field observations. *J. Climatol. 1*, 237-254.

Oke, T.R. and Fuggle, R.F., 1972: Comparison of urban/rural counter and net radiation at night. *Bound.-Lay. Meteorol. 2*, 290-308.

Oke, T.R. and Maxwell, G.B., 1975: Urban heat island dynamics in Montreal and Vancouver. *Atmos. Environ. 9*, 191-200.

Park, H-S., 1986: Features of the heat island in Seoul and its surrounding cities. *Atmos. Environ. 20*, 1859-1866.

Santos, L.G., Lima, H.G. and Assis, E.S., 2003: A comprehensive approach of the sky view factor and building mass in an urban area of city of Belo Horizonte, Brazil. In *Klysik, K., Oke, T.R., Fortuniak, K., Grimmond, C.S.B. and Wibig, J.* (eds.): *Proceed. Fifth Int. Conf. on Urban Climate Vol. 2*, University of Lodz, Lodz, Poland. 367-370.

Szegedi, S., 2005: Települési hősziget-mérések jellegzetes méretű alföldi településeken. [Urban heat island measurements on different sized settlements with situated on a plain. (in Hungarian)] *Debreceni Földrajzi Disputa – Desputatio Geographica Debrecina 2003-2005*, 157-180.

Unger, J., 1997: Városklimatológia – Szeged városklímája. [*Urban climatology – Urban climate of Szeged*. (in Hungarian)] *Acta Climatologica Univ. Szegediensis 31/B (Urban Climate Special Issue)*, 69 p.

Unger, J., Sümeghy, Z., Gulyás, Á., Bottyán, Z. and Mucsi, L., 2001: Land-use and meteorological aspects of the urban heat island. *Meteorol. Applications 8*, 189-194.

Unger, J., Bottyán, Z., Sümeghy, Z. and Gulyás, Á., 2004: Connection between urban heat island and surface parameters: measurements and modeling. *Időjárás 108*, 173-194.

COMPARISON BETWEEN SKY VIEW FACTOR VALUES COMPUTED BY TWO DIFFERENT METHODS IN AN URBAN ENVIRONMENT

T. GÁL[1], M. RZEPA[2], B. GROMEK[3] and J. UNGER[1]

*[1]Department of Climatology and Landscape Ecology, University of Szeged, P.O. Box 653, 6701 Szeged, Hungary
E-mail: tgal@geo.u-szeged.hu
[2]Department of Meteorology and Climatology, University of Lodz, Poland
[3]Department of Theoretical Physics, University of Lodz, Poland*

Összefoglalás – Munkánkban bemutatásra kerül az égboltláthatóság (SVF) egy GIS alapú kiszámítási módja, ami egy városi 3D adatbázist alkalmaz. Ez a módszer lehetővé teszi egy város terület egészére kiterjedő folytonos SVF mező kiszámítását. Az chhcz hasonló városgeometriai adatbázisok elengedhetetlen kellékei a városi hőszigettel foglalkozó kutatásoknak. Munkánkban továbbá bemutatásra kerül egy terepi mérés is, ami az SVF halszem objektívvel készített fotókon alapuló kiértékeléséhez szükséges. Ez a fotografikus eljárás különösen alkalmas a városi környezethez és emellett elterjedt módja is az SVF meghatározásnak. A két módszer összevetése rámutat a kapott értékek eltérésére, amit többnyire a mérési pont körüli növényzettel magyarázhatunk. A növényzet hatásától eltekintve szignifikáns kapcsolat mutatható ki a két módszerrel számolt értékek között, ami alátámasztja a vektoros SVF számítási eljárás alkalmazásának lehetőségét városi környezetben. Ezzel a vektoros módszerrel (terepi mérések nélkül) egy folytonos SVF mező meghatározása egy teljes város területére csupán néhány napot vesz igénybe (aminek nagy része számítási idő), ha az épület adatbázis rendelkezésre áll. A vektoros számítási eljárás hibáját csökkenthetjük, ha felhasználunk a számításhoz városi növényzet adatbázisokat is.

Summary – In our study we present a GIS method for SVF calculation, which uses an urban 3D building database. This method provides opportunity to evaluate the continuous SVF field in an entire urbanized area. This kind of urban surface geometric database is essential for the researches on urban heat island. In this study we also present field measurements for the fish-eye photo based SVF calculation. This photographic technique is particularly well suited for urban environments and it is also a prevalent way of SVF determination. The comparison of the two methods shows that there are some differences – mostly caused by the presence of the vegetation around the measurement site – in the computed values. Apart from the vegetation there is significant correlation between the two values therefore the vector-based method can be considered capable of SVF calculation in an urban environment. With the vector-based method the calculation (without field measurements) of the continuous SVF field for an entire urban environment takes a few days (principally the computing time) if the building database is available. The error of the vector-based calculation can be decreased if a database of the intra-urban vegetation is applied.

Key words: urban environment, SVF calculations, 3D building database, fish-eye photographs, comparison

1. INTRODUCTION

Urban areas are an example of the most dramatic anthropogenic land use changes where primarily the geometry and surface characteristics have been, and are constantly being, altered. As a consequence, urban environments modify the energy and water balance which often results in higher urban temperature compared to the relatively natural surroundings (urban heat island – UHI). Different kinds of heat islands can be

distinguished: UHI under surface, on the surface, in the urban canopy layer (UCL) and in the urban boundary layer. The UHI is typically presented as a temperature difference between the air within the UCL (below the rooftops in the spaces between buildings) and that measured in a rural area outside the settlement (*Oke*, 1982). Generally, its strongest development occurs at night when the heat, stored in the daytime, is released (*Landsberg*, 1981; *Oke*, 1987).

Nocturnal cooling processes are primarily regulated by outgoing long wave radiation. In cities, narrow streets and high buildings create deep canyons. This 3D geometrical configuration plays an important role in regulating long-wave radiative heat loss, since due to the horizontal and vertical unevenness of the surface elements the outgoing long-wave radiation loss is more restricted here than in rural areas. Therefore, urban geometry is an important factor contributing to intra-urban temperature variations below roof level (e.g. *Oke*, 1981; *Eliasson*, 1996).

The sky view factor (SVF) is often used to describe urban geometry (e.g. *Upmanis*, 1999; *Svensson*, 2004). By definition, SVF is the ratio of the radiation received (or emitted) by a planar surface to the radiation emitted (or received) by the entire hemispheric environment (*Watson and Johnson*, 1987). It is a dimensionless measure between zero and one, representing totally obstructed and free spaces, respectively (*Oke*, 1988).

There are several techniques for the calculation of the SVF: using surveying techniques (e.g. *Bottyán and Unger*, 2003), digital camera with fish-eye lens (e.g. *Grimmond et al.*, 2001; *Chapman and Thornes*, 2004; *Rzepa and Gromek*, 2006), signals from GPS receivers (*Chapman et al.*, 2002; *Chapman and Thornes*, 2004) or more recently thermal fish-eye imagery (*Chapman et al.*, 2007). The photographic technique is particularly well suited for urban environments, where buildings are variable in size and shape, and vegetation is present.

Modern 3D models describing the complex urban surface provide the opportunity of the GIS-based SVF evaluation. Among these software methods both raster- (e.g., *Brown et al.*, 2001; *Ratti et al.*, 2003; *Lindberg*, 2005) and vector-based approaches (e.g., *Souza et al.*, 2003; *Gulyás et al.*, 2006; *Gál et al.*, 2007) are known.

The overall purpose of this study is to analyze the differences between SVF values computed with a vector-based algorithm (*Gál et al.*, 2007) and with a photographic method, the so called BMSky-view (*Rzepa and Gromek*, 2006). The specific objectives are (i) to present and apply two different methods for SVF calculation in the same study area, (ii) to compare the two methods and analyze the difference between the values.

2. THE STUDY AREA AND THE 3D BUILDING DATABASE

Szeged (46°N, 20°E) is located in southeast Hungary, in the southern part of the Great Hungarian Plain at 79 m above sea level on a flat plain (*Fig. 1*). The region of Szeged belongs to the climatic type D.1 by Trewartha's classification which means continental climate with longer warm season (*Unger*, 1996). The urbanized area is around 30 km^2 within a larger administrative area (281 km^2). Szeged is a medium-sized city among the Hungarian settlements with a population of about 160,000.

The creation of the applied 3D building database for Szeged was based on local municipality data of building footprints and aerial photos for the determination of individual building heights. The creation of the database is described in detail in *Unger*

(2006, 2007). For cross-checking, theodolite measurements were carried out and as a result, the mean ratio of the differences in the heights of the buildings was around 5%. The database covers the whole study area (27 km^2) and consists of more than 22,000 buildings. Smaller, room-sized buildings are difficult to determine from the aerial photos, moreover their heat absorption and emission are negligible. Thus, buildings smaller than 15 m^2 were excluded from the database.

The measurement campaign for SVF determination in urban environment was carried out in a sample area of 0,41 km^2 in Szeged. There are various building types (with different footprint area and height) and density in this area thus it is suitable for the comparison of the values computed by the two different methods (*Fig. 1*).

To determine the elevation of the measurement points a Digital Elevation Model (DEM) is needed. This DEM for Szeged represents a bare surface with a small vertical variation of the surface (75.5–83 m a.s.l.). Both applied databases (elevation and building) use the Unified National Projection (EOV in Hungarian).
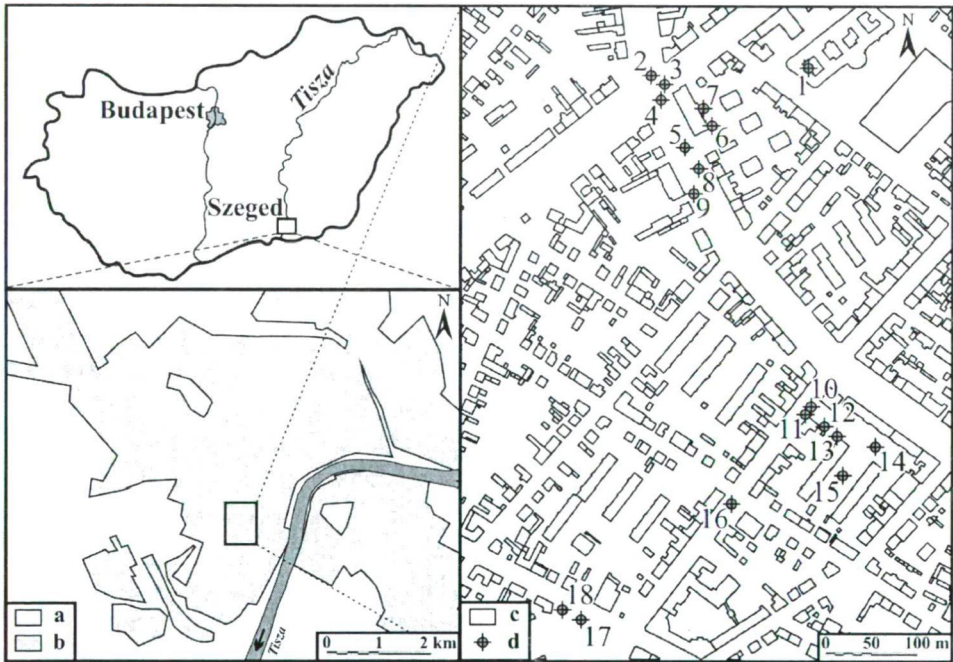
Fig. 1 The location of Szeged in Hungary and the location of the sample area in Szeged: (a) open area, (b) built-up area, (c) buildings (from the 3D building database) and (d) SVF measurement points

3. METHODS FOR THE SVF CALCULATIONS

As the main objective of our study is the comparison of the SVF values calculated from the 3D building database and from the fish-eye photographs, we selected 18 points in the sample area (*Fig. 1*). For these points SVF values were calculated with both methods resulting in two SVF values for each point:

    – SVF$_{vector}$ (computed by vector-based method from the 3D building database),

– SVF$_{\text{BMSky-View}}$ (computed by the BMSky-View algorithm from fish-eye photo-graphs).

Before examining the differences it is necessary to present the fundamental characteristics of the two methods.

3.1. Algorithm for SVF$_{vector}$ calculation using an urban vector database

The 3D building database of Szeged is a model of the real situation, which represents a simplified urban surface (containing buildings only). In this model all buildings have flat roof, and all walls of a building are of the same height.

The projection of every building on the sky is managed as the projection of their walls visible from a given surface point and polygon g(x) is the border of the visible sky (*Fig. 2a*). After dividing the hemisphere equally into slices by rotation angle α, 'rectangles' are drawn whose heights are equal to the g(x) values in the middle points of the intervals.
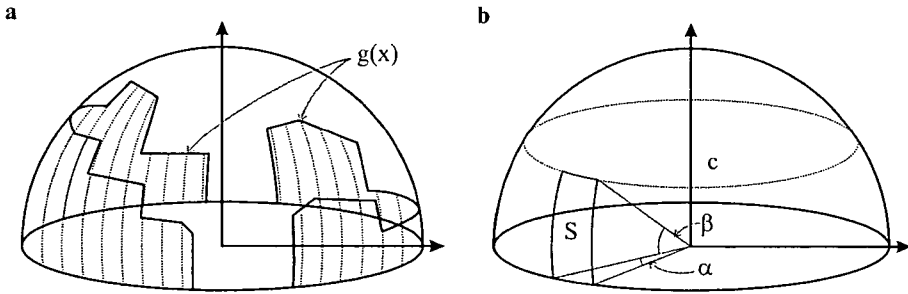
Fig. 2 (*a*) Polygon g(x) as a border of the visible sky and dividing the hemisphere under g(x) equally into slices by angle α (heights are equal to the g(x) values in the middle points of the intervals), (*b*) a slice of a 'width' of α (S) of a basin with an elevation angle β

SVF values for a couple of common geometric arrangements are given by *Oke* (1987). In the case of the regular basin, where β is the elevation angle from the centre to the wall, the SVF value (referring to the centre) is: SVF$_{\text{basin}} = \cos^2\beta$. So the view factor (VF) of a basin with an elevation angle β is VF$_{\text{basin}} = 1-\cos^2\beta = \sin^2\beta$, therefore the view factor for a slice (S) with a width of α (*Fig. 2b*) can be calculated as:

$$\text{VF}_S = \sin^2\beta \cdot (\alpha/360)$$

The algorithm draws a target line by the angle α from the selected point and along this line it searches the building which obstructs the largest part of the sky in that direction. The accuracy of the algorithm depends on the magnitude of the rotation angle (α). Smaller α angles result in a more accurate estimation of the SVF$_{\text{vector}}$ but also mean longer computation time. After calculating the VF values by slices their sum is subtracted from 1 to get the SVF$_{\text{vector}}$.

For the automation of the process described above the ESRI ArcView 3.2 software (*www.esri.com*, 2006) is appropriate. It has a built-in object-oriented program language (Avenue). With the help of this language the software is programmable so that every element of the software is accessible (see also *Souza et al.*, 2003). Our application is compiled from 9 scripts (graphical surface, control of the parameters, calculation of SVF$_{\text{vector}}$, etc.). *Fig. 3* illustrates the schematic description of the developed algorithm.
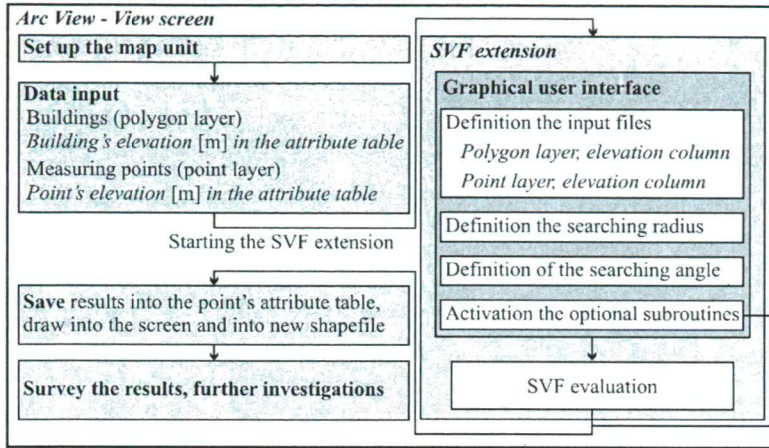
Fig. 3 Schematic description of the algorithm for the SVF_{vector} calculation using vector database

According to *Fig. 3* values for two parameters have to be selected. These are (i) the radius of the area around the site where the algorithm takes the heights and positions of the buildings into consideration and (ii) the interval of the rotation angle (α) which determines the density of the target lines starting from the site. In our case a radius of 200 m and a rotation angle of 1° seemed to be appropriate (see more details in *Unger, 2007*).

3.2. Determining sky view factor using fish-eye photographs

BMSky-view is a user friendly application enabling to compute the SVF values directly from photos taken by digital camera with fish-eye lens.

This application works under Windows (*Fig. 4*). The algorithm of computing SVF was implemented using C++ programming language and based on a slight modification of the Steyn-method (*Steyn, 1980*). Steyn describes a method for determining the sky view factor from fish-eye lens photographs, which are divided into a number of concentric annuli of equal width, each representing an interval of zenith angles. Within each annulus he manually estimated the fraction of sky and derived the following formula:

$$SVF = \frac{1}{2 \cdot n} \sum_{i=1}^{n} \sin\left(\frac{\pi\left(i - \frac{1}{2}\right)}{2 \cdot n}\right) \cos\left(\frac{\pi\left(i - \frac{1}{2}\right)}{2 \cdot n}\right) \alpha_i$$

where α_i is the angular width of sky in the i-th annulus and n is the number of annuli (*Bärring et al., 1985*).

3.3. Details of the field measurement and the application of the vector-based algorithm

For the determination of the $SVF_{BMSky-View}$ values photographs were taken with a camera equipped with fish-eye lens. We used a Nikon Coolpix 4300 camera with Nikon FC-E8 lens which is a prevalent tool for this application (e.g., *Grimmond et al., 2001; Chapman and Thornes, 2004; Rzepa and Gromek, 2006*). The fish-eye photographs were taken on 4 January 2006 therefore tree foliage was minimal. The camera was mounted to a

folding tripod and we recorded its height above the surface at each of the 18 selected points. At the same time we have located the points in a large-scale ortophoto-map (with a pixel resolution of 0.2 m). The $SVF_{BMSky-View}$ values were evaluated with the BMSky-view software from these fish-eye photographs.
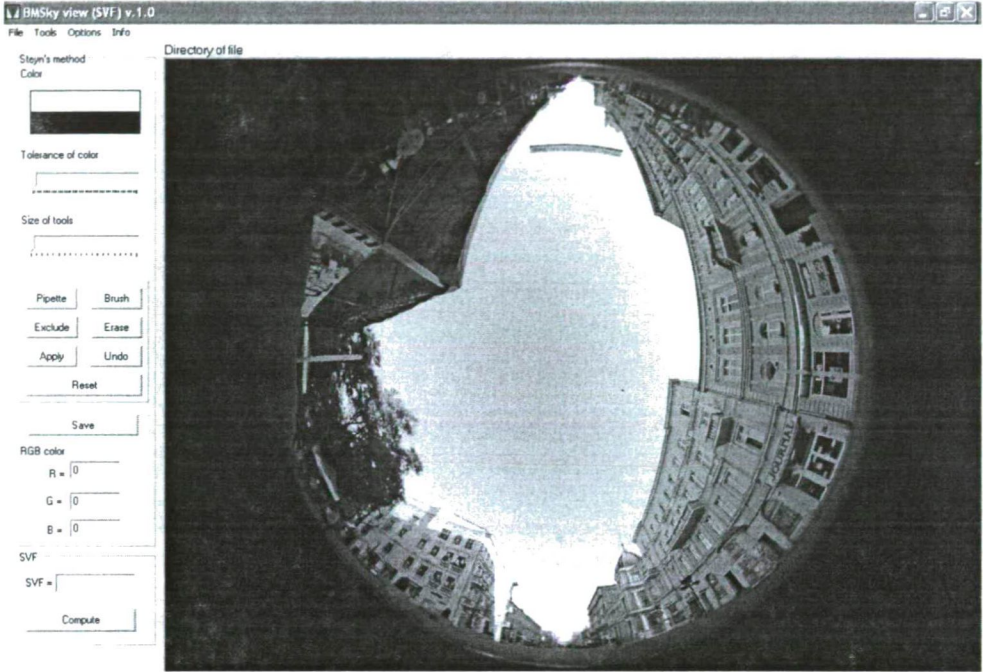
Fig. 4 Menu to recognize the sky area

The SVF_{vector} was determined in the same 18 points of the sample area with the vector-based algorithm. Using the ortophoto-map the horizontal coordinates of the measurement points (in the Unified National Projection) can be determined. For the determination of the accurate elevation of the points we took into account the heights of the camera above the surface and the elevation of the surface from a DEM covering the area.

4. DIFFERENCES BETWEEN THE SVF VALUES
(EVALUATION AND EXPLANATION OF DIFFERENCES)

Firstly, we have compared visually the fish-eye photographs with the graphical results of the algorithm (*Fig. 5*). Based on this comparison we found minor deviations between the outlines of the buildings in the photos and the polygons, generated from the 3D building database with the SVF_{vector} algorithm.
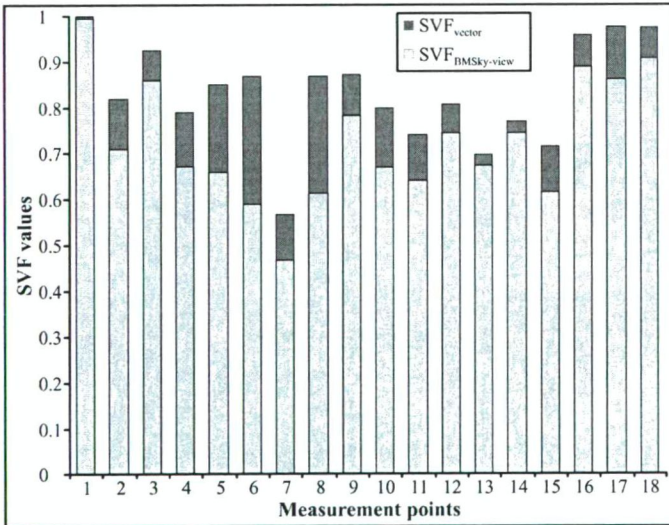
The vegetation is not included in the database therefore the border of the sky in the presented photographs does not always coincide with the border generated by the algorithm. Apart from the vegetation there are other reasons that can cause some differences in the SVF values calculated by the two methods. For example there are traffic signs with relatively large sky obstruction (*Fig. 5b*).

As the statistical comparison shows there is a relatively strong ($R^2 = 0.4452$) correlation between the SVF values if we use the linear $y = ax$ formula (*Fig. 7*). If the constant is included in the equation ($y = ax + b$) we get a closer connection ($R^2 = 0.7038$) and the constant (b) is 0.3176 in this case. The inclusion and the magnitude of the constant can be explained by the effect of the vegetation. Both coefficients of determination (R^2) are significant at the 1% level, however we have to note that these relationships are valid only for the range of the SVF values of our case (0.46 – 1).
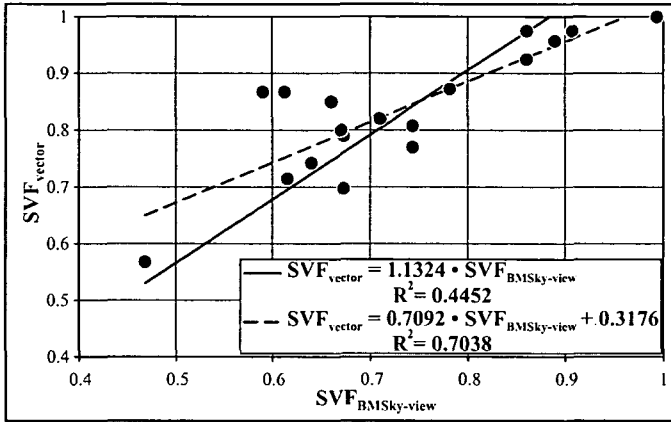
Fig. 7 Relationship between the SVF values calculated by the applied methods in the sample area (n = 18)

5. CONCLUSIONS

The derivation of a continuous image of SVF covering large urban areas is necessary to study the relationship between urban geometry quantified by SVF and intra-urban nocturnal temperature variations. It means thousands of SVF calculations in the selected urban area (*Unger*, 2007; *Gál et al.*, 2007). Only GIS-based methods are suitable for this kind of evaluation. In our study we presented a GIS method for the SVF calculation which is uses an urban 3D building database.

Before the application of this continuous SVF field for studying its relationship with the urban heat island field we had to check the errors of this method. The photographic technique is particularly well suited for urban environments and it is also a prevalent way of SVF determination. Thus the SVF values from one of the photographic methods (BMSky-view) are suitable for studying the errors of the vector-based method. In this study we presented field measurements to take fish-eye photographs and we applied the above-mentioned SVF calculation method based on these photos.

The comparison of the two methods showed that there are some differences between the obtained values. These differences are caused mainly by the presence of vegetation around the measurement sites. Apart from the vegetation there is a close connection between the values therefore the vector-based method is appropriate for the SVF calculation in urban environment.

With the vector-based method the calculation (without field measurements) of the continuous SFV field for an entire urban environment takes a few days if the building database is available. Applying a database of the intra-urban vegetation the error of the vector-based calculation could be decreased.

REFERENCES

Bärring, L., Mattsson, J.O. and Lindqvist, S., 1985: Canyon geometry, street temperatures and urban heat island in Malmö, Sweden. *J. Climatol. 5*, 433-444.

Bottyán, Z. and Unger, J., 2003: A multiple linear statistical model for estimating the mean maximum urban heat island. *Theor. Appl. Climatol. 75*, 233-243.

Brown, M.J., Grimmond, C.S.B. and Ratti, C., 2001: Comparison of methodologies for computing sky view factor in urban environment. *International Society of Environmental Hydraulics Conference*, Tempe, AZ. *Internal Report Los Alamos National Laboratory*, Los Alamos, NM. LA-UR-01-4107.

Chapman, L. and Thornes, J.E., 2004: Real-time sky-view factor calculation and approximation. *J. Atmos. Oceanic. Technol. 21*, 730-742.

Chapman, L., Thornes, J.E. and Bradley, A.V., 2002: Sky-view factor approximation using GPS receivers. *Int. J. Climatol. 22*, 615–621.

Chapman, L. Thornes, J.E., Muller, J-P. and McMurdoch, S., 2007: Potential applications of thermal fisheye imagery in urban environments. *IEEE Geoscience and Rem. Sens. Letters 4*, 56-59.

Eliasson, I., 1996: Urban noctural temperatures, street geometry and land use. *Atmos. Environ. 30*, 379-392.

Gál, T., Lindberg, H.E. and Unger, J., 2007: Computing continuous sky view factor using 3D urban raster and vector databases: comparison and an application for urban climate. *Theor. Appl. Climatol.* (in press)

Grimmond, C.S.B., Potter, S.K., Zutter, H.N., and Souch, C., 2001: Rapid methods to estimate sky-view factors applied to urban areas. *Int. J. Climatol. 21*, 903–913.

Gulyás, Á., Unger. J, and Matzarakis. A,, 2006: Assessment of the microclimatic and human comfort conditions in a complex urban environment: modelling and measurements. *Building and Environment 41*, 1713-1722.

Landsberg, H.E., 1981: *The urban climate*. Academic Press, New York.

Lindberg, F., 2005: Towards the use of local governmental 3-D data within urban climatology studies. *Mapping and Image Science 2*, 32-37.

Oke, T.R., 1981: Canyon geometry and the nocturnal urban heat island: comparison of scale model and field observations. *J. Climatol. 1*, 237-254.

Oke, T.R., 1982: The energetic basis of the urban heat island. *Quart. J. Roy. Meteorol. Soc. 108*, 1-24.

Oke, T.R., 1987: *Boundary layer climates*, Routledge, London and New York.

Oke, T.R., 1988: Street design and urban canopy layer climate. *Energy and Buildings 11*, 103-113.

Ratti, C., Raydan, D. and Steemers, K., 2003: Building form and environmental performance: archetypes, analysis and an arid climate. *Energy and Buildings 35*, 49-59.

Rzepa, M. and Gromek, B., 2006: Variability of sky view factor in the main street canyon in the center of Łódź. *Preprints Sixth Int. Conf. on Urban Climate*, Göteborg, Sweden. 854-857.

Souza, L.C.L., Rodrigues, D.S. and Mendes, J.F.G., 2003: The 3D SkyView extension: an urban geometry acces tool in a geographical information system. In *Klysik, K., Oke, T.R., Fortuniak, K, Grimmond, C.S.B. and Wibig, J.* (eds.): *Proceed Fifth Int Conf on Urban Climate*. Vol. 2. University of Lodz, Lodz, Poland. 413-416.

Steyn, D.G., 1980: The calculation of view factors from fish-eye lens photographs. *Atmosphere-Ocean 18*, 254-258.

Svensson, M., 2004: Sky view factor analysis – implications for urban air temperature differences. *Meteorol. Applications 11*, 201-211.

Unger, J., 1996: Heat island intensity with different meteorological conditions in a medium-sized town: Szeged, Hungary. *Theor. Appl. Climatol. 54*, 147-151.

Unger, J., 2006: Modelling of the annual mean maximum urban heat island with the application of 2 and 3D surface parameters. *Clim. Res. 30*, 215-226.

Unger, J., 2007: Connection between urban heat island and sky view factor approximated by a software tool on a 3D urban database. *Int. J. Environ. and Pollution* (in press)

Upmanis, H., 1999: The influence of sky view factor and land use on city temperatures. In *Upmanis, H.:* Influence of Parks on Local Climate. *Earth Sciences Centre, Göteborg University A 43, paper 3.*

www.esri.com, 2006

MAPPING THE ROUGHNESS PARAMETERS IN A LARGE URBAN AREA FOR URBAN CLIMATE APPLICATIONS

T. GÁL and Z. SÜMEGHY

Department of Climatology and Landscape Ecology, University of Szeged, P.O.Box 653, 6701 Szeged, Hungary
E-mail: tgal@geo.u-szeged.hu

Összefoglalás – A munkánk fő célja egy városi felszín érdesség térképezési eljárás bemutatása egy nagy szegedi vizsgálati területen. Ezzel a térképezési eljárással képesek vagyunk a ventilációs folyosók lehatárolására a városok területén. A feltételezett ventilációs folyosók fontos szerepet játszhatnak a városi hősziget cirkuláció kifejlődésében, ezáltal a légtér szennyezettségének csökkenését eredményezve a város központi részein. Ezek az eredmények fontos alapadatokat szolgáltathatnak a várostervezési munkákhoz. Eredményeink alapján lehatárolhatjuk azon területeket, amelyeknél a városvezetésnek célszerű lenne megőrizni a ventilációs folyosók humán komfort szempontból kedvező hatását a városklímára. Az érdességi paraméter számításaink 3D épület adatbázison alapulnak és részletesebbek, mint a legutóbbi hasonló munkák (e.g. *Bottema*, 1997; *Ratti et al*, 2006). Számításunk úgynevezett *lot area* poligonokon alapul, amely az általunk ismert publikációk alapján példanélküli megközelítés.

Summary – The overall purpose of this study is the presentation of an urban roughness mapping method in a large study area in Szeged. With this roughness mapping procedure we can locate the ventilation paths in the city. The supposed ventilation paths could play a significant role in the development of the urban heat island circulation and as a result in the reduction of air pollution in the inner part of the city. These results could provide important input data for urban planning procedures. Based on our results we can give a list of the areas where the city government should keep the advantages of the ventilation paths considering the human comfort aspects of the urban climate. The calculations of the roughness parameters are based on a 3D building database and they are more detailed than in other recent studies (e.g. *Bottema*, 1997; *Ratti et al*, 2006). Our calculation based on the lot area polygons is a new approach and according to our knowledge there are no similar examples in the literature.

Key words: urban roughness mapping, frontal area, roughness length, porosity, Szeged, Hungary

1. INTRODUCTION

In the settlements the primary geometry and surface characteristics have been changed compared to the original natural surfaces. Urban environments modify the water and energy balance which often results in higher urban temperature compared to the relatively natural surroundings (urban heat island – UHI). The effect of the urban surface on the air flow is also one of the most important differences.

The cities are about the roughest surfaces. Because of the roughness of the surface, wind speed decreases in urban areas. The average wind speed is lower in the cities than in rural areas (*Oke*, 1987).

In direct analogy with the well-known sea breeze system the cities generate a local air flow the so-called country breeze, which is based on the fact that the cities are commonly warmer than the rural background. For the development of the country breeze

the regional winds need to be very weak, so anticyclonal weather conditions are ideal for this flow system. This includes low-level breezes across the perimeter, which converge in the center. The vertical thermal differences are as important as the rural urban thermal differences (*Oke,* 1987). The vertical instability and the different heating distributions induce this 3 dimensional weak circulation (*Vukovich,* 1971). There is uplift in the centre of the city and there is also a counter-flow in the higher air layer (*Fig. 1*). Unlike in the case of the sea breeze there is no diurnal reversal because the city is usually warmer than the countryside. During the day the small horizontal thermal gradient is sufficient to drive this system. Due to the larger roughness of the surface the average wind speed is lower in the cities than in rural areas (*Oke,* 1987).

Owing to the high surface roughness of the city the development of the country breeze needs significant thermal difference between the urban and rural surface. During the day the country breeze can be observed above the roof level. At night the thermal difference is significant under the roof level therefore the country breeze can be found here. In summary, this is the urban heat island (-induced) circulation (UHIC) (*Eliasson and Holmer,* 1990).
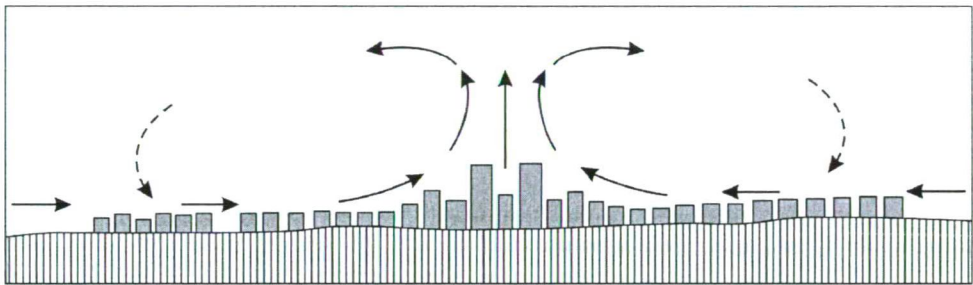
Fig. 1 The schematic shape of the urban heat island circulation

This meso-scale circulation could offer a potential for the improvement of the urban air quality (*Barlag and Kuttler,* 1990). The depth of the inflow in the UHIC system depends on the roughness of the surface. In the ventilation paths – where the roughness is lower than in other urban areas – the country breeze can reach the inner parts of the city and it decreases the pollution accumulated during the day.

For describing the roughness of the surfaces numerous parameters are known. The prevalent parameters are the zero-plane displacement height (z_d) and the roughness length (z_0) (*Lettau,* 1969; *Counihan,* 1975). Further known parameters are the plan area density (λ_p), frontal area density (λ_f), average height weighted with frontal area (z_H), depth of the roughness sublayer (z_r) (e.g. *Kutzbach,* 1961; *Raupach,* 1992; *Bottema,* 1997; *Grimmond and Oke,* 1999) and the effective height (h_{eff}) (*Matzarakis and Mayer,* 1992). The porosity of the urban canopy layer (P) can also be a useful tool for urban roughness mapping.

If we evaluate the roughness parameters in a large urban area we have the opportunity to find the potential ventilation paths which are essential for enhancing the efficiency of the country breeze. *Matzarakis and Mayer* (1992) summarize the main properties of the ventilation paths with the following points: a) aerodynamic surface roughness length lower than 0.5 m, b) negligible zero point displacement, c) sufficiently great length in one direction, at least 1000 m, d) sufficiently great width, minimum width is double to four times the height of the lateral obstacles, but et least 50 m, e) the edges of

ventilation paths should be comparatively smooth, f) the width of the obstacles in a ventilation path should not be greater than 10% of the width of the ventilation path, g) the height of the obstacle in a ventilation path should not be greater then 10 m, h) obstacles within a ventilation path should be oriented in such a way that their greatest width is parallel to the axis of the ventilation path, i) single obstacles within a ventilation path should have a ratio of height to horizontal distance between two successive obstacles of 0.1 for buildings and 0.2 for trees.

Based on these results there is an opportunity to give some advice for the local government on how to promote the intrusion of the cool and clean air and to decrease urban air pollution. *Barlag and Kuttler* (1990) summarized these advices in six points:

(a) almost straight free aisles must be kept to the centre of the city;

(b) surface roughness along these free aisles must be kept low;

(c) ventilation aisles into city centers must feature low-roughness vegetation to filter out pollution;

(d) surfaces in these areas should have a cooling effect on the 'thin-layered' air moving slowly towards the centre of the city;

(e) clearances to take air into the city centre should be designed to give directional stability to air flows;

(f) pollution should be minimized in the areas from which air moves to the city centre and along the ventilation aisles.

The overall purpose of this study is the presentation of an urban roughness mapping method in a large study area in Szeged. The specific objectives are (i) to describe the application of the roughness length calculation method in irregular building groups, (ii) to present the calculation of porosity in the urban canopy layer, and (iii) to find the potential ventilation paths in the study area using the calculated urban roughness parameters.

2. METHODS FOR THE DETERMINATION OF ROUGHNESS PARAMETERS

There are numerous ways for the z_0 and z_d calculation. There are two classes of these methods: (i) micrometeorological (or anemometric) and morphometric (or geometric) methods.

The prevalent micrometeorological method uses data of field observations of wind or turbulence for the roughness length and the zero plane displacement height computations based on the log-law:

$$\frac{\bar{u}(z)}{u_*} = \frac{1}{\kappa} \ln\left(\frac{z - z_d}{z_0}\right)$$

where $\bar{u}(z)$ is the time averaged wind speed in z height, u_* is the friction velocity and κ is von Karman's constant (*Counihan*, 1975). For this equation we need wind speed data from at least one height above the surface therefore this method is unsuitable for roughness mapping in urban areas.

There are several known morphometric methods which are based on surface morphology data. The simple ones use only the average heights and density of the roughness elements in the cities (e.g. *Counihan*, 1975; *Bottema*, 1997). The sophisticated methods include the computation of the frontal area index, which combines the mean

height, width and density of the roughness elements (*Grimmond and Oke*, 1999). The results of these methods mean more accurate approximations for the roughness parameters (e.g. *Lettau*, 1969; *Raupach*, 1992; *Macdonald et al.*, 1998).

The above-mentioned methods are based on regular building arrangement and there are only a few examples of their generalization. *Ratti at al.* (2006) calculate the λ_P, z_H, λ_F and z_0 from urban digital elevation model (DEM) however their computation is applied for small sample areas. *Bottema and Mestayer* (1998) present a method for urban roughness mapping. This method is based on a cadastral database (vector-based building database) and the spatial basis of the computation is the rugoxel (roughness pixel). The applied z_0 and z_d formulas are referring to these rugoxels and give average values.

2.1. Compution of the roughness length and the zero displacement height in irregular building groups

The basis of the roughness length computations is in accord with the method of *Bottema and Mestayer* (1998). His basic equation was designed for regular building groups:

$$z_0 = (h - z_d)\exp\left(-\frac{\kappa}{\sqrt{0.5 \cdot C_{Dh} \cdot \lambda_F}}\right) \qquad (2.1)$$

where h is the volumetrically averaged building height, z_d is the zero displacement height, κ is von Karman's constant (0.4), C_{Dh} is the isolated obstacle drag coefficient (0.8) and λ_F is the frontal area density.

The next computation formula of the zero displacement height gives an opportunity to use *Equation 2.1* for irregular building groups (*Bottema and Mestayer*, 1998):

$$z_d = h \cdot (\lambda_P)^{0.6} \qquad (2.2)$$

where λ_P is the plan area density. With this equation we can give an approximate value for z_d without taking the volume of the buildings and the recirculation zones into account.

For these equations we need some input parameters. *Fig. 2* shows these parameters for an irregular building group. The basis of the calculation of these input parameters is the building block; therefore the contiguous buildings were classified into blocks (*Fig. 2a*).

We divided the study area in polygon-shape areas (lot area) based on these blocks. Each polygon consists of the set of points closer to the central building block than to the other blocks. We defined the total surface or lot area (A_T) as the complete area of these polygons (*Fig. 2a*). The plan area of the roughness elements (A_P) is the sum of the surface areas of the buildings (A_{P1}, A_{P2}, A_{P3}, ..., A_{Pn}) are the areas of buildings. The plan area density is the ratio of the total plan area of the roughness elements and the total surface area ($\lambda_P = A_P / A_T$).

The computation of the volumetrically averaged building height needs the volumes (V_1, V_2, V_3, ..., V_n) and heights (h_1, h_2, h_3, ..., h_n) of each building (*Fig. 2a*) in each block:

$$h = \frac{\sum_{i=1}^{n} V_i \cdot h_i}{\sum_{i=1}^{n} V_i}$$

For the calculation of the frontal area density we have to compute the frontal area (A_F) of each building (*Fig. 2b*). This frontal area of a building block depends on the direction of the view (or direction of the airflow). In our calculations the frontal area density is defined as the ratio of the frontal area and the total surface area ($\lambda_F = A_F / A_T$).
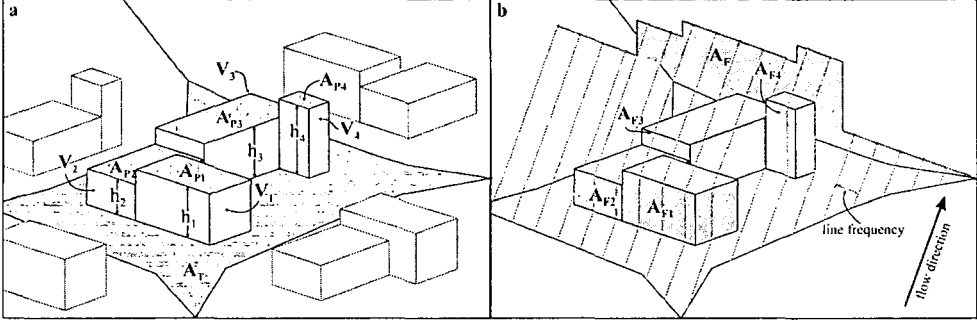
Fig. 2 (a) Input parameters for the roughness calculation for an irregular building group and *(b)* frontal area calculation with the parallel lines in a given direction

2.2. Calculation of the porosity in the urban canopy layer

Porosity could be a useful roughness parameter in the UHIC modeling because it quantifies the ratio of open air volume in the canopy layer. By definition it is the ratio of the volume of the open air and the volume of the entire urban canopy layer (UCL) referring to the same area. There are two possible ways to compute this parameter. The first is less precise however easy to evaluate for urban areas, the second is much more accurate but the computation is rather time-consuming.

Porosity ($P_{h\text{-}const}$) evaluation with the first method is based on the input parameters of building volumes, total surface area (lot areas) and the height of the UCL (h_{const}) which is defined as a constant. This constant value is based on the analysis of the buildings' heights in the entire study area. The principle is that the number of buildings higher than the UCL height has to be significantly low in the entire area. So the equation of this type of porosity of a spatial unit (lot area) is the following:

$$P_{h-const} = \frac{A_T \cdot h_{const} - V}{A_T \cdot h_{const}}$$ (2.3)

where V is sum of the building volumes located at the actual lot area.

The second method of porosity ($P_{h\text{-}var}$) computation is based on variable urban canopy layer heights by spatial units. For each spatial unit of the investigated area the height of the UCL (h_{UCL}) has to be computed. Based on these values the equation of this type of porosity of a spatial unit is the following:

$$P_{h-var} = \frac{A_T \cdot h_{UCL} - V}{A_T \cdot h_{UCL}}$$ (2.4)

3. ROUGHNESS MAPPING IN THE URBAN AREA OF SZEGED

3.1. Study area and the building database

Szeged (46°N, 20°E) is located in southeast Hungary, in the southern part of the Great Hungarian Plain at 79 m above sea level on a flat plain (*Fig. 3*). According to Trewartha's classification Szeged belongs to the climatic type D.1 (continental climate with longer warm season), similarly to the predominant part of the country (*Unger*, 1996). While the administrative area of Szeged is 281 km^2, the urbanized area is only around 30 km^2. The avenue-boulevard structure of the town was built to the axis of the river Tisza. Szeged is a medium-sized town and the number of the inhabitants is about 160,000.

In the earlier urban climate investigations the temperature measurements for identifying the UHI were taken in a 25,75 km^2 sized area of Szeged. Our study is partly based on the earlier results therefore we used the same study area (e.g. *Unger et al.*, 2000, 2001; *Bottyán and Unger*, 2003; *Unger*, 2006) (*Fig. 3*).
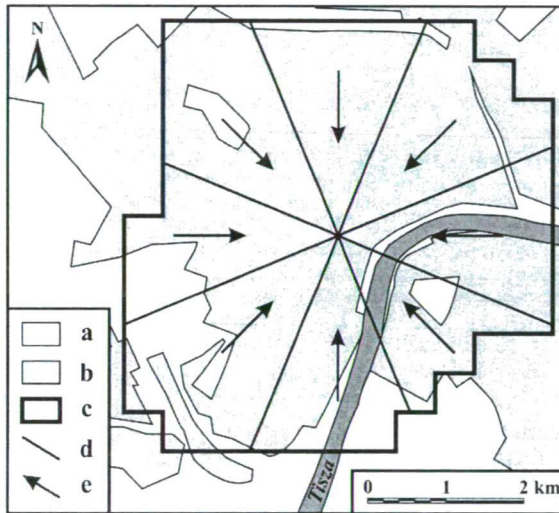
Fig. 3 Study area and the calculation zones for the frontal area (*a:* rural area, *b:* urban area, *c:* border of the study area, *d:* border of the frontal area calculation zone, *e:* direction of the frontal area computation)

From earlier projects there is a 3D building database available for the study area. This data source is based on local municipality data on building footprints and the individual building heights were evaluated by photogrammetric methods. This means more than 22,000 individual buildings with their main parameters (footprint area, building height). The creation of the database is described in details in *Unger* (2006, 2007).

3.2. Details of the roughness calculations

Fig. 4 summarises the main steps of roughness mapping in the study area. Firstly, we have aggregated the buildings in the database to building blocks, similarly to the work of *Ratti et al.* (2006). That resulted in more than 11,000 blocks in the study area, each containing the interlocking buildings. Based on these building blocks the determination of

the lot areas is achievable with ArcView 3.2 software by using the assign proximity function of the Spatial analyst module. All of the roughness parameter calculations were carried out for these lot area polygons (units) (*Fig. 5*).
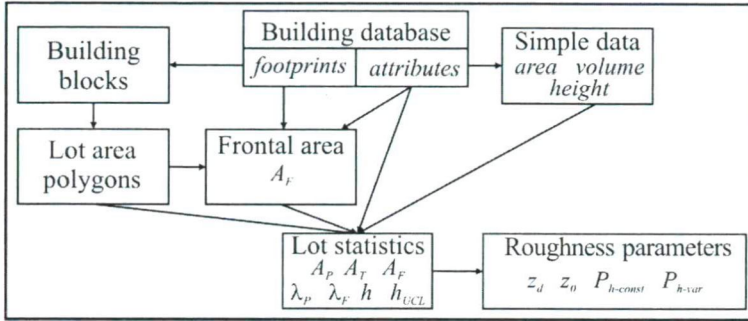
Fig. 4 Schematic description for the roughness mapping procedure

Fig. 5 As an example, some lot area polygons (units) in a part of the investigated area in Szeged
(*a*: building footprints, *b*: building blocks, *c*: lot area polygons)

The values of some roughness parameters depend on the wind direction. The calculation methods of these parameters are also direction-dependent because of the application of the direction-dependent frontal area (A_F) as an input. Generally these roughness parameters are computed for several directions and the obtained results are averaged giving the final value (*Ratti et al.,* 2006). As our main objective is the mapping of the ventilation paths which have conducive effect on the heat island circulation, we evaluated these roughness parameters in radial directions within each calculation zones (see *Fig. 3*).

The frontal area calculation in ArcView is a more complex task than the calculation of the footprint area, the volume and other simple parameters. Therefore we have constructed a simple Avenue script for this calculation. Before the evaluation a shape file needs to be created, containing lines parallel with the given radial direction and covering each frontal area calculation zone (see *Fig. 2b* and *Fig. 3*). The distance between the neighboring lines is 5 m. The algorithm is searching for the highest building elevation in

each lot using the line–building intersections for each line. Based on these elevation values and the line frequency (5 m) the frontal area is computable (see *Fig. 2b*).

With the frontal area calculation all of the input parameters for the z_0 and z_d calculation become available (*Equations 2.1* and 2.2). The obtained values refer to the lot area polygons of the investigated area.

The porosity values are calculated with *Equations 2.3* and 2.4. For the $P_{h-const}$ calculation we analyzed the heights of the buildings in the study area and defined h_{const} (P_{h-40}) as 40 m. For the P_{h-var} calculation we defined h_{UCL} as the height of the highest building within a given lot area (its maximum is 63.4 m and its mean is 6.59 m on the study area).

4. SPATIAL DISTRIBUTIONS OF THE CALCULATED PARAMETERS AND THE POTENTIONAL VENTILATION PATHS

As a result of our calculations we have got the values of the roughness parameters referring to the plot area polygons. Based on this database we can analyze the spatial distributions of these parameters in order to find the potential ventilation paths.

Fig. 6 shows the spatial distribution of z_0 as well as the supposed ventilation paths in the investigated area. We have located the ventilation paths with a method similar to the one used by *Matzarakis and Mayer* (1992). The analysis is based on this map only and we have not applied precise calculations with the z_0 and other values to find the locations of the ventilation paths.

We also examined the spatial distribution of the P_{h-40} (*Fig. 7a*) and P_{h-var} (*Fig. 7b*). Comparing the two figures we find that the spatial distribution of the first parameter is similar to the spatial distribution of the z_0. The shapes of the possible ventilation paths based on P_{h-40} values in *Fig. 7a* (not shown) would be similar to the shapes on *Fig. 6*.

If we examine *Fig. 7b* we can identify new areas which can take a part in the city ventilation. For instance, on the east side of the town there is an area with high blocks of flats and large green areas between them. Because of this special built-up style this area can also be regarded as a potential ventilation path disregarding the relatively high roughness length values.

5. CONCLUSIONS

We have calculated the main roughness parameters in the study area. This calculation is based on a 3D building database and it is more detailed than those in other recent studies in this topic (e.g. *Bottema*, 1997; *Ratti et al.*, 2006). The calculation based on the lot area polygons is a new approach and according to our knowledge there are no similar examples in the literature.

Based on the spatial distribution of the calculated parameters we can locate the potential ventilation paths. These ventilation paths could take an important role in the development of the urban heat island circulation and as a result in the reduction of air pollution in the inner part of the city.

Based on our results we can give a list of the areas where the city government should have to consider the six advices of *Barlag and Kuttler* (1990) to keep the advantages of the ventilation paths considering the human comfort aspects of the urban climate.
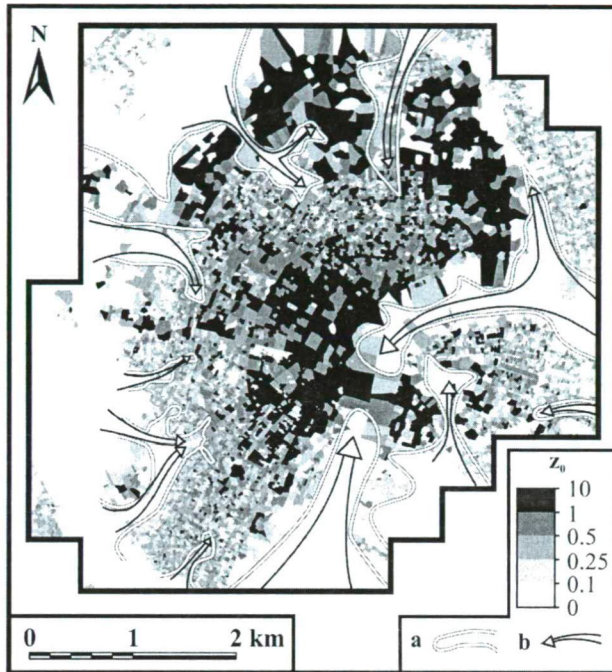
Fig. 6 Spatial distribution of the roughness length (z_0) values and the supposed ventilation paths in the investigated area (*a:* border of a continuous area with z_0 values lower than 0.5, *b:* supposed ventilation path)
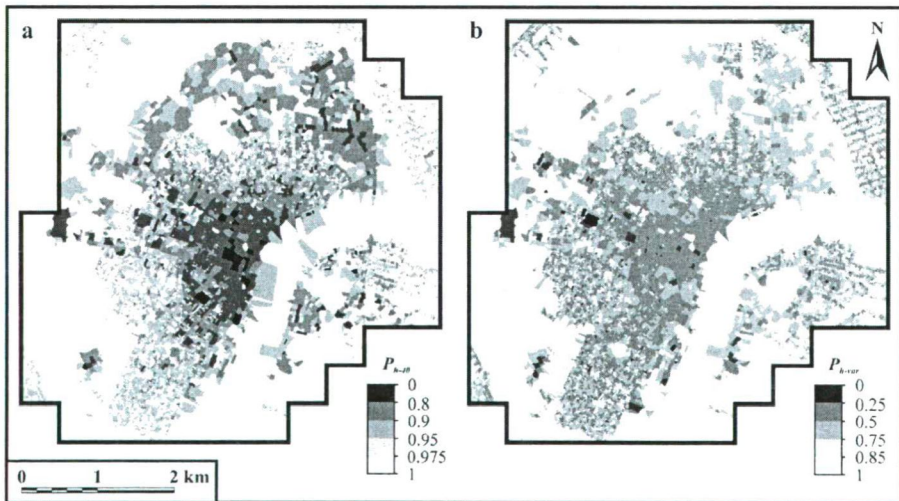
Fig 7. Spatial distribution of the porosity values in the investigated area (*a:* P_{h-40}, *b:* P_{h-var})

REFERENCES

Barlag, A.B. and Kuttler, W., 1990: The significance of country breezes for urban planning. *Energy and Buildings 15-16*, 291-297.

Bottema, M., 1997: Urban roughness modelling in relation to pollutant dispersion. *Atmos. Environ. 31*, 3059-3075.

Bottema, M. and Mestayer, P.G., 1998: Urban roughness mapping – validation techniques and some first results. *J. Wind Engineering and Industrial Aerodynamics 74-76*, 163-173.

Bottyán, Z. and Unger, J., 2003: A multiple linear statistical model for estimating mean maximum urban heat island. *Theor. and Appl. Climatology 75*, 233-243.

Counihan, J., 1975: Adiabatic atmospheric boundary layers: A review and analysis of data from the period 1880-1972. *Atmos. Environ. 9*, 871-905.

Eliasson, I. and Holmer, B., 1990: Urban heat island circulation in Göteborg, Sweden. *Theoretical and Applied Climatology 42*, 187-196.

Grimmond, C.S.B. and Oke, T.R., 1999: Aerodynamic properites of urban areas derived from analysis of surface form. *J. Appl. Meteorol. 34*, 1262-1292.

Lettau, H., 1969: Note on aerodynamic roughness-parameter estimation on the basis of roughness-element description. *Appl. Meteorol. 8*, 828-832.

Macdonald, R.W., Griffiths, R.F. and Hall, D.J., 1998: An improved method for estimation of surface roughness of obstacle arrays. *Atmos. Environ. 32*, 1857-1864.

Matzarakis, A. and Mayer, H., 1992: Mapping of urban air paths for planning in Munchen. Wiss Ber Inst. Meteorol. *Klimaforsch. Univ. Karlsruhe 16*, 13-22.

Oke, T.R., 1987: *Boundary layer climates*, Routledge, London and New York. 435 p.

Ratti, C., Di Sabatino, S. and Bitter, R., 2006: Urban texture analysis with image processing techniques: wind and dispersion. *Theor. and Appl. Climatol. 84*, 77-99.

Raupach, M.R., 1992: Drag and drag partition on rough surfaces. *Bound. Lay. Meteor. 60*, 375-395.

Unger, J., 1996: Heat island intensity with different meteorological conditions in a medium-sized town: Szeged, Hungary. *Theor. and Appl. Climatol. 54*, 147-151.

Unger, J., 2006: Modelling of the annual mean maximum urban heat island with the application of 2 and 3D surface parameters. *Clim. Res. 30*, 215-226.

Unger, J., 2007: Connection between urban heat island and sky view factor approximated by a software tool on a 3D urban database. *Int. J. Environment and Pollution* (in press)

Unger, J., Bottyán, Z., Sümeghy, Z. and Gulyás, Á., 2000: Urban heat island development affected by urban surface factors. *Időjárás 104*, 253-268.

Unger, J., Sümeghy, Z., Gulyás, Á., Bottyán, Z. and Mucsi, L., 2001: Land-use and meteorological aspects of the urban heat island. *Meteorol. Applications 8*, 189-194.

Vukovich, M.F., 1971: Theoretical analysis of the effect of mean wind and stability on a heat island circulation characteristic of an urban complex. *Monthly Weather Review 99*, 919-926.

SELECTED EXAMPLES OF BIOCLIMATIC ANALYSIS APPLYING THE PHYSIOLOGICALLY EQUIVALENT TEMPERATURE IN HUNGARY

Á. GULYÁS[1] and A. MATZARAKIS[2]

[1]Department of Climatology and Landscape Ecology, University of Szeged, P.O.Box 653, 6701 Szeged, Hungary
E-mail: agulyas@geo.u-szeged.hu
[2]Meteorological Institute, University of Freiburg, 79085 Freiburg im Breisgau, Germany

Összefoglalás – Cikkünkben bioklimatológiai elemzést végzünk az ún. Fiziológiailag Equivalens Hőmérséklet (PET) index felhasználásával először Magyarország egész területén (1 km-es felbontású bioklíma térkép segítségével). A bioklíma térképek a PET index térbeli eloszlását mutatják Magyarországon egy téli (február) és egy nyári (augusztus) hónapban. Majd két szinoptikai állomás (Szombathely és Sopron) 1996 és 1999 között rögzített adataiból számított PET értékek alapján részletes elemzésben hasonlítjuk össze a két város főbb bioklimatológiai jellegzetességeit.

Summary – In this study, maps were created that show the geographical distribution of Physiologically Equivalent Temperature (PET) values in February and August for the area of Hungary, with a resolution of 1 km. For the further analysis of the thermal bioclimate, data of the synoptical stations of Szombathely and Sopron, recorded from 1996 to 1999, has been used. This study provides a detailed analysis and comparison of the bioclimatic properties of these locations.

Key words: Physiologically Equivalent Temperature, thermal comfort, mapping, Hungary

1. INTRODUCTION

For the bioclimatic evaluation of a specific location or area not only a single meteorological parameter is required, but a complex evaluation of the effects of climate conditions and thermo-physiological values in order to describe the effects of the thermal environment on humans. Several models and indices were developed to calculate the extent of thermal stress during the last decades. The earlier bioclimatic indices (Discomfort Index, Windchill, thermohygrometric index-THI) consider only some meteorological parameters (*Thom, 1959; Steadman, 1971; Unger, 1999; Matzarakis et al., 2004*). Recent models, based on the human energy balance equation, produce so-called comfort indices - for example Predicted Mean Vote-PMV, Physiologically Equivalent Temperature-PET, Outdoor Standard Effective Temperature-OUT_SET* - to evaluate the thermal stress and thermal comfort on the human body (*Fanger, 1972; Jendritzky et al., 1990; Höppe, 1993, 1999; VDI, 1998; Matzarakis et al., 1999; Spagnolo and de Dear, 2003*). These indices can be applied in different time and spatial resolutions for recent climate and climate change projections (*Jendritzky et al., 1990; Matzarakis et al., 1999; Koch et al., 2005; Matzarakis, 2006*). For example, describing a small area (eg. the surroundings of a building, part of a street), with fine resolution can be useful for architects and urban designers (*Mayer and Matzarakis, 1998; Matzarakis, 2001*). Micro-scale studies (eg. bioclimatological

description of a town) provide data for urban planning (*Unger et al.*, 2005). Examining even larger areas (eg. a whole region or country) has not only scientific value: the results of these studies can form the basis of planning regional recreation and tourism development (*Mayer and Matzarakis*, 1997; *Matzarakis et al.*, 1999; 2004; 2007; Matzarakis, 2006).

The aim of this study is to present a bioclimatic analysis of Hungary by means of bioclimatic mapping with the aid of geo-statistical methods. The present study links geographical information (*Hastings et al.*, 1999) with climatological data (*New et al.*, 1999, 2000, 2002) in order to generate a spatial distribution of PET values of a region. The calculation of PET is performed with the application of the RayMan Model, which calculates the thermal indices mentioned above (*Matzarakis et al.*, 2000, 2007).

2. STUDY AREA AND METHODS

2.1. Study area

Although the original study was carried out for a larger area, this paper focuses on the description of bioclimatic properties in Hungary (the national border is marked with black line – *Fig. 1*).

Hungary is situated in the Carpathian Basin almost in the centre of Europe between the latitudes 45°48'N and 48°35'N, longitude 16°05'E and 22°58'E with an areas of 93,030 km^2.
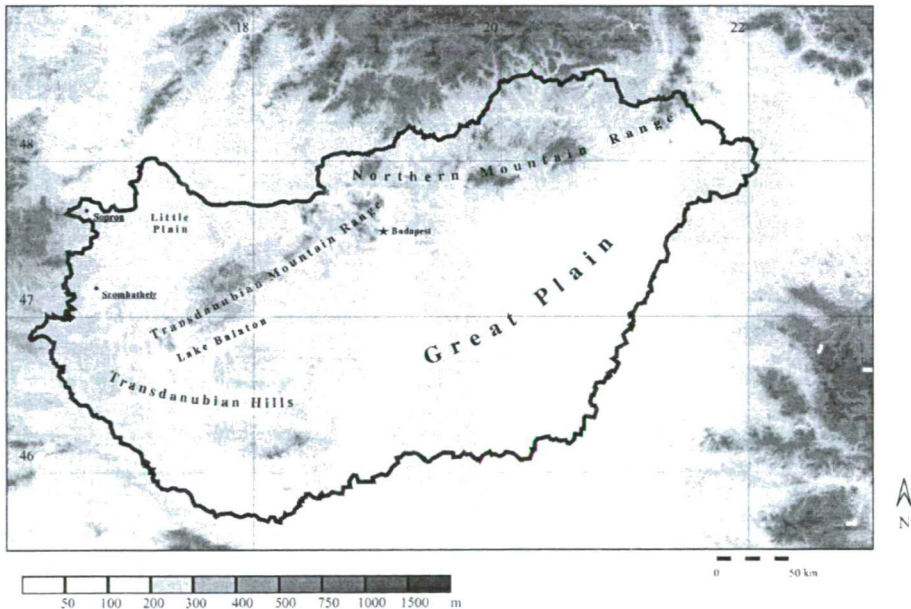
Fig. 1 Geographical location and topography of Hungary (the numbers are northern latitudes and eastern longitudes in degrees) and location of the two examined cities

As *Fig. 1* shows Hungary has three basic relief types: the low-lying regions (under 200 m above sea level) of the Great Plain in the east, centre and south-east, and of the Little

Plain in the north-west, which together cover the two-thirds of Hungary's territory. There is the Northern Mountain Range (Északi-középhegység); and the mountainous (Transdanubian Mountain Range - Dunántúli-középhegység) and hilly regions of Transdanubia in the west and south-west (Transdanubian Hills - Dunántúli-dombság).

The main characteristics of Hungary's climate and the frequent fluctuations in climatic factors are greatly due to the central position in Europe. Namely, Hungary is situated at the 'crossroads' of the East-European continental, the West-European oceanic and the subtropical Mediterranean climatic zones (*Pécsi and Sárfalvi*, 1964).

Using Köppen's classification, Hungary fits in the climatic region *Cf*, which is characterized by a temperate warm climate with a rather uniform annual distribution of precipitation. Its annual mean temperature is 10.4°C (in Budapest/Lőrinc); the amount of precipitation is 516 mm. These values show little variance across the country due to the limited variation in topography (*WMO*, 1996).

2.2. Applied bioclimatic index

In this study one of the most widely used bioclimatic indices, the PET is used, as it has a widely known unit (°C) as an indicator of thermal stress and thermal comfort (*Table 1*). This makes the results easily comprehensible for potential users. This is especially the case for planners, decision-makers, and even the public who might not be familiar with modern human-biometeorological terminology. PET evaluates the thermal conditions in a physiologically significant manner (*Höppe*, 1999; *Matzarakis et al.*, 1999).

Table 1 Physiologically Equivalent Temperature (PET) for different grades of thermal sensation and physiological stress on human beings (during standard conditions: heat transfer resistance of clothing: 0.9 clo internal heat production: 80 W) (*Matzarakis and Mayer*, 1996)

PET (°C)	Thermal sensation	Physiological stress level
	very cold	extreme cold stress
4	....	....
	cold	strong cold stress
8	....	....
	cool	moderate cold stress
13	....	....
	slightly cool	slight cold stress
18	....	....
	comfortable	no thermal stress
23	....	....
	slightly warm	slight heat stress
29	....	....
	warm	moderate heat stress
35	....	....
	hot	strong heat stress
41	....	....
	very hot	extreme heat stress

PET is defined as the air temperature at which the human energy budget for the assumed indoor conditions is balanced by the same skin temperature and sweat rate as under the actual complex outdoor conditions to be assessed.

PET enables various users to compare the integral effects of complex thermal conditions outside with their own experience indoors (*Table 1*). In addition PET can be

used throughout the year and in different climates (e.g. *Mayer and Matzarakis*, 1997; *Höppe*, 1999). Meteorological parameters influencing the human energy balance, such as air temperature, air humidity, wind speed and short- and longwave radiation, are also represented in the PET values. PET also considers the heat transfer resistance of clothing and the internal heat production (*VDI*, 1998).

2.3. The RayMan model

One of the recently used radiation and bioclimate models, RayMan, is well-suited to calculate radiation fluxes (e.g. *Mayer and Höppe*, 1987; *Matzarakis*, 2002; *Matzarakis et al.*, 2007), and thus, all our calculations for T_{mrt} and PET were performed using this model. The RayMan model, developed according to the Guideline 3787 of the German Engineering Society (*VDI*, 1998) calculates the radiation flux in simple and complex environments on the basis of various parameters, such as air temperature, air humidity, degree of cloud cover, time of day and year, the albedo of the surrounding surfaces and their solid-angle proportions.

The main advantage of RayMan is that it facilitates the reliable determination of the microclimatological modifications of different urban environments, since the model considers the radiation modification effects of the complex surface structure (buildings, trees) very precisely. Besides the meteorological parameters, the model requires input data on the surface morphological conditions of the study area and on personal parameters.

2.4. Data

The used climate data for this analysis was provided by the data collation program at the Climatic Research Unit (*New et al.*, 1999, 2000, 2002). The required data for the thermal bioclimate analysis – these are air temperature, relative humidity, sunshine and wind speed – are available at monthly resolution for the climate period 1961 to 1990 at ten minute spatial resolution for the specific area. The calculated PET grid values have been used as dependent variable. They have been recalculated into a higher spatial resolution (1 km) through the use of geo-statistical methods (independent variables were latitude, longitude and elevation). For this purpose the digital elevation data of the GLOBE data set (*Hastings et al.*, 1999) was used.

An additional analysis has been performed for two selected stations (Szombathely and Sopron) for the period 1996 to 1999 for 12 UTC in order to describe the thermal bioclimate conditions more analytically on a daily basis.

3. RESULTS

3.1. Spatial distribution of PET in Hungary

From the produced monthly and seasonal maps, only one for the winter period (February), and one for the summer period (August) are presented here. The statistical relationship is very high (r > 0.9) for all months and seasons.

The spatial distribution of the average PET in February for the period of 1961-1990 is shown in *Fig. 2*. The orographical situation of Hungary is not diverse: most of the country lies on plains below 200 m latitude, thus the bioclimatic conditions are relatively homogeneous. The whole country is categorised as being subject to extreme cold stress

levels. The regional differences are not more than 9°C. The lowest PET values (-9°C) can be observed in the areas with higher latitude, especially in the Northern Mountain Range. Due to the effect of the oceanic climatic zone, the winter is milder in Transdanubia. This is the main reason why the PET values are not so low (between -4 and -6°C) in the Transdanubian Mountain Range as in the Northern Mountain Range (between -6 and -9°C).

| ▓ > -2°C | ▓ -2 - -4°C | ▓ -4 - -6°C | ▓ < -6°C |
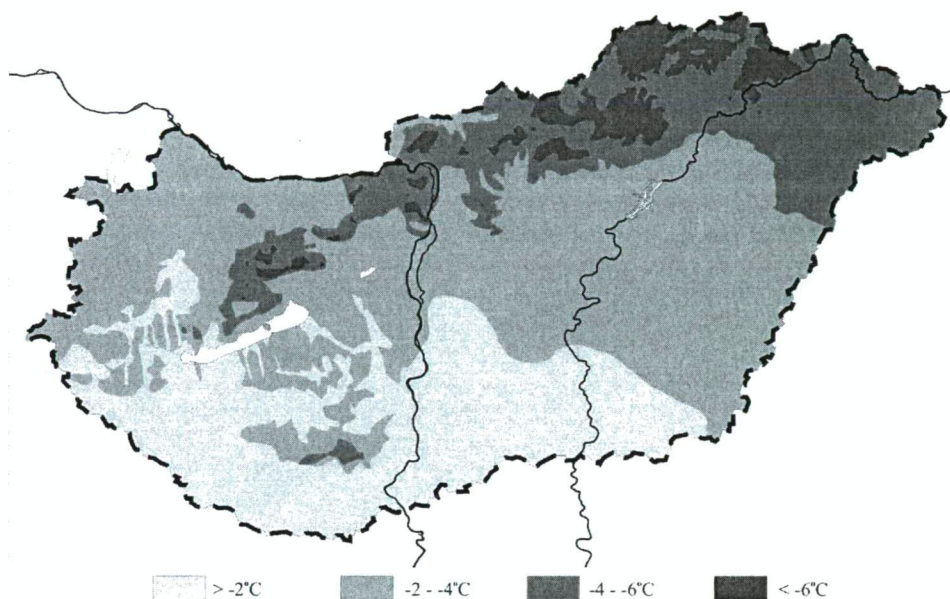
Fig. 2 Geographical distribution of PET for February

The cold stress in February is less pronounced in the southern part of the Great Plain and in the Transdanubian Hills, due to the mediterranean effect in case of the latter. Towards the eastern borders of the country, the PET values are decreasing due to the increasingly continental (and Carpathian) climate. The cold stress increases in the hill regions, and it has the lowest value in the Northern Mountain Range.

Fig. 3. shows the spatial distribution of the average PET values for August during the examined time frame. The ΔPET is higher in this month than in February (11–7°C) and covers three stress levels (*Table 1*). In August, however, the bioclimatic situation in the plains is more homogeneous than in February. There is a maximum PET value of 26°C, dominating the south-western part of the country, reaching upwards in the Duna, Tisza, and Dráva valley. Almost the whole country has average PET values, corresponding to the "slightly warm" category. The thermal sensation decreases below 23°C only in the hill regions, and further decreases by one physiological stress level at the higher altitudes (*Table 1.*). The PET values are decreasing in the mountains to the "slightly cool" thermal sensation (PETmin = 14°C).

It should be noted that the coastline of Lake Balaton, one of Hungary's most popular tourist destination, shows the lowest cold stress level in February. The situation is different in summer, when the heat stress is high around the lake, especially on the north-western

41

coast which is surrounded by mountains. This situation, which is caused by the southern exposure and the reflection from the water surface, creates ideal circumstances for water-based recreational activities.

■■■ < 20°C   ■■■ 20-22°C   ■■■ 22-24°C   □ > 24°C
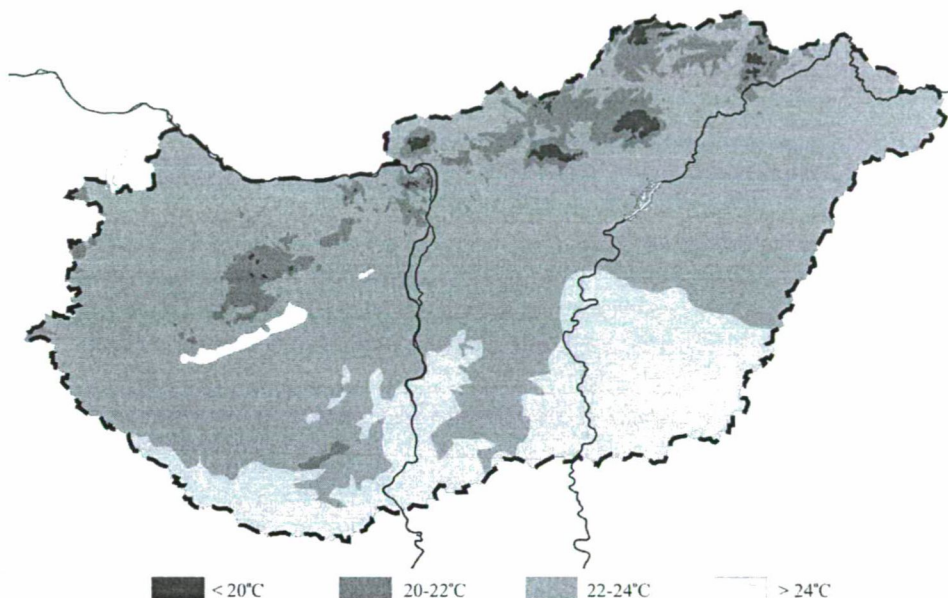
Fig. 3 Geographical distribution of PET for August

3.2. Selected stations

An additional analysis that has been performed with the PET index, based on daily meteorological values of a certain location, provides an opportunity for a more detailed analysis of the bioclimatic situation of the two selected areas. The chosen two meteorological stations (Szombathely and Sopron) are located close to the western border of the country in proximity to the Alps at about 210 m above the sea level, approximately 50 km from each other. Their climate conditions are strongly affected by the proximity of the Alps and characterised by the oceanic effect throughout the year.

The bioclimatic diagrams for the two places (*Fig. 4*) illustrate information on the percentages of different bioclimatic classes of PET, plotted in decas (10 days intervals) during the whole year, based on a four-year long data series for 12 UTC in the period of 1996-1999.

The diagram also shows the following values:
- mean PET value in the examined time period (PETa)
- maximum PET value in the examined time period (PETmax)
- minimum PET value in the examined time period (PETmin)
- amount of days for the examined period with PET < 0°C, 15°C < PET < 25°C and PET > 35°C.

The characteristics of the bioclimatic properties of the two examined cities are obviously similar but differences can be easily detected.
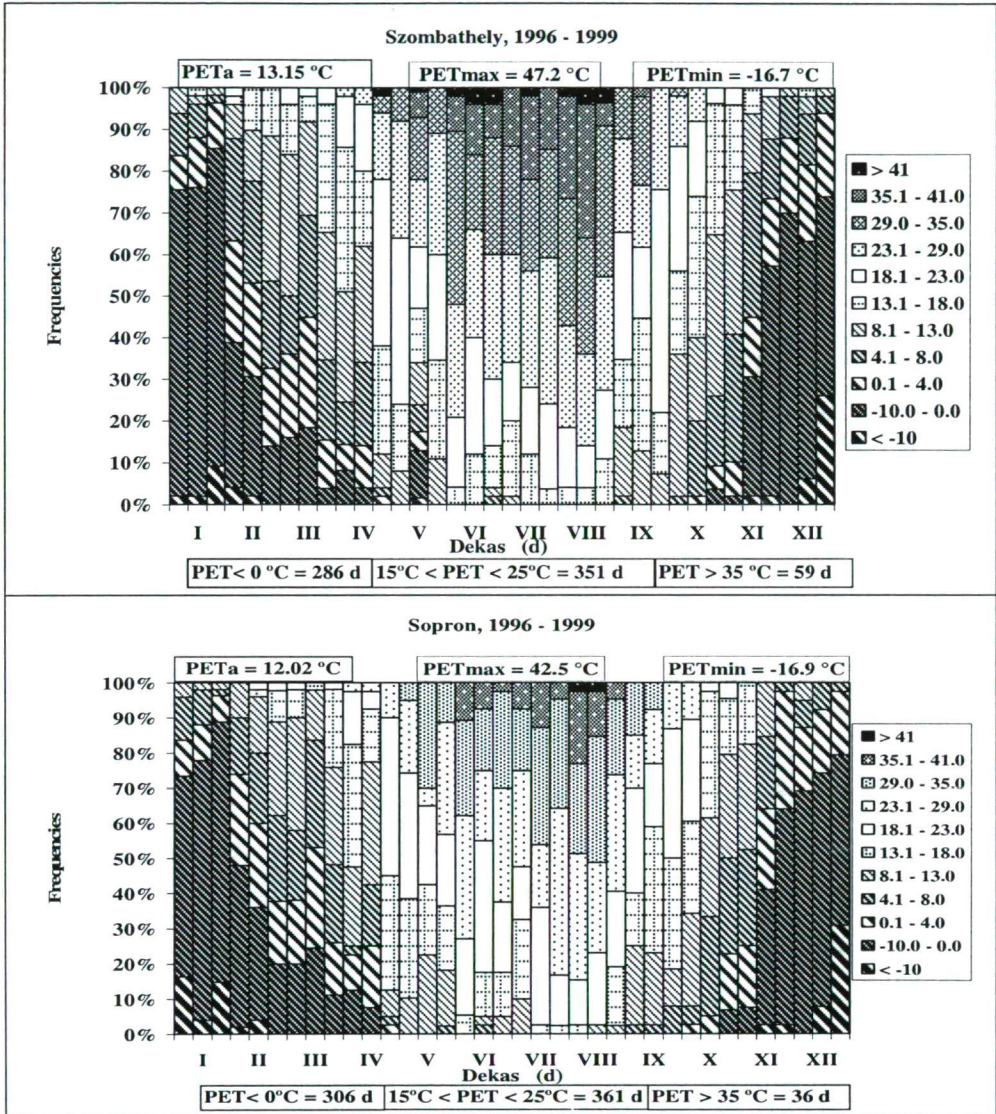
Fig. 4 Bioclimate diagram for Szombathely and Sopron for 1996 to 1999 for 12 UTC

The climate data obtained for Hungary show that January has the lowest average mean temperature (*WMO*, 1996). However, the lowest PET values (most extreme cold stress) were calculated with the highest probability in both cities in December and January. Despite that the PET values of the examined cities are nearly identical (PETmin$_{Szh}$: -16.7°C, PETmin$_{So}$: -16.9°C), the occurrence of PET > 0°C value is approximately 10% lower in Szombathely. Comfortable, heat stress-free periods occur at higher probability in the second half of April in both cities (again later in the second half of September). Interestingly, the frequency of the occurrence of these comfort periods was slightly lower in Szombathely than in Sopron (Szh = 351 days, So = 361 days), during the examined period.

The bioclimatic profile of Szombathely is warmer and shifted to the higher heat stress, compared to Sopron. Common feature is that the first days with moderate and strong heat stress (PET > 29°C) occurred in spring; heat stress becomes even more intense in May. (However, the occurrence of PET > 29°C value is approximately 30% higher in Szombathely, than in Sopron.) The possible reason for this phenomenon is the increasing continental effect that occurs in the Carpathian Basin, resulting in shortened transitional seasons (spring and autumn). This effect cannot be masked by the western location of the examined meteorological station. The frequency of the days with strong and extreme heat stress (PET > 35°C) is constantly increasing during the summer months and reaches the highest values in the first decas of August. In Szombathely, however, extreme heat stress days can be observed form the second half of April and the occurrence of these days is more frequent until the end of August than in Sopron. The amount of days with PET > 35°C for the examined period is in Szombathely 59 and in Sopron just 30, thus the number of days with extreme heat stress was nearly two times higher in Szombathely than in Sopron. The difference of the maximum of the PET values is higher than in the case of the minimum values (PETmax$_{Szh}$: 47.2°C, PETmax$_{Szh}$: 42.5°C). The bioclimatic data clearly show the presence of several days with comfortable thermal sensation in early autumn ("Indian Summer"). This "Indian Summer" is more pronounced in Szombathely than in Sopron: it is longer and has higher PET values.
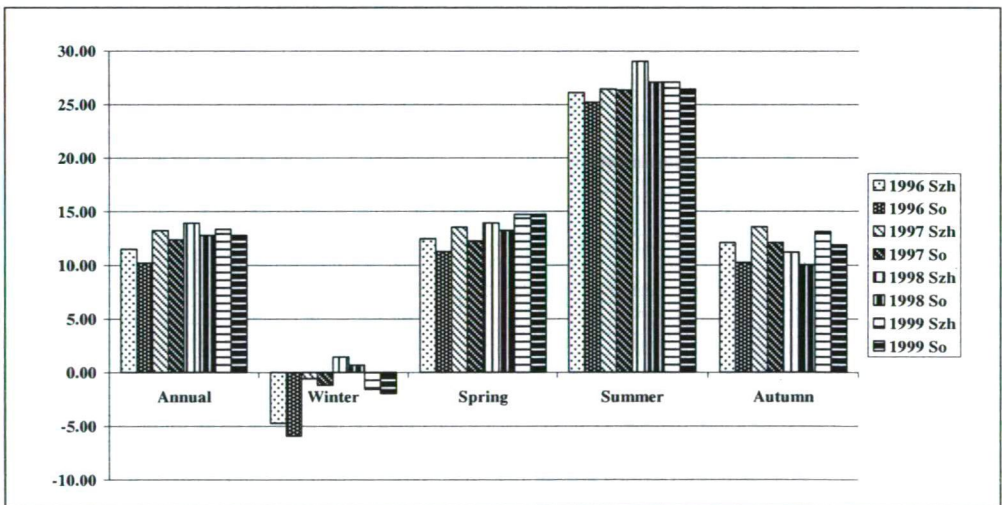
Fig. 5 Annual and seasonal average PET values in Szombathely (Szh) and Sopron (So) between 1996-1999, 12 UTC

The annual average PET value is higher by 1.13°C in the case of Szombathely than in Sopron. *Fig. 5* shows the annual and seasonal averages of the PET values.

Differences between the two examined locations, despite the close location and same elevation, can be observed. The main reason of this can be the stronger effect of the mountains in Sopron, which shifts its climate to a colder range in a bioclimatic sense.

4. CONCLUSIONS

Spatial data are required in order to describe and analyse the bioclimate of regions or areas. The methods exist, and the thermal indices based on the energy balance of humans present an appropriate method.

Bioclimate maps can be produced by using existing gridded data and geo-statistical methods of mesoscale and microscale resolution for a region. When applying a time resolution of several months, it is impossible to discover the whole range of thermal bioclimate conditions, especially in extreme events. Extreme conditions can be analysed through the use of data from synoptical or climatological networks.

Because of the used ten-day intervals, which are more detailed than monthly resolutions and also more relevant for recreation and tourism, the presented bioclimate diagram constitutes a highly effective method.

For the bioclimate of Hungary the produced maps present a first approach in the field of high resolution maps, which can be helpful for diverse issues like human health and tourism. Additionally, periods of extreme cold and heat waves can now be detected.

The climate becomes more continental towards north, north-east throughout the country. This is represented in the bioclimatic properties of the examined area: the thermal stress tends towards extremities both in summer and winter.

REFERENCES

Fanger P.O., 1972: *Thermal comfort.* New York, Mc Graw–Hill.
Hastings, D.A., Dunbar, P.K., Elphingstone, G.M., Bootz, M., Murakami, H., Maruyama, H., Masaharu, H., Holland, P., Payne, J., Bryant, N.A., Logan, T., Muller, J.-P., Schreier, G. and MacDonald, J.S., (eds.), 1999: The Global Land One-kilometer Base Elevation (GLOBE) Digital Elevation Model, Version 1.0. National Oceanic and Atmospheric Administration, National Geophysical Data Center, 325 Broadway, Boulder, Colorado 80303, U.S.A. Digital data base on the World Wide Web (*http://www.ngdc.noaa.gov/mgg/topo/globe.html*).
Höppe, P.R., 1993: Heat balance modelling. *Experientia 49*, 741-745.
Höppe, P.R., 1999: The physiological equivalent temperature – a universal index for the biometeorological assessment of the thermal environment. *Int. J. Biometeorol. 43*, 71–75.
Jendritzky, G., Menz, H., Schirmer, H. and Schmidt-Kessen W., 1990: Methodik zur raumbezogenen Bewertung der thermischen Komponente im Bioklima des Menschen (Fortgeschriebenes Klima-Michel-Modell). *Beitr. Akad. Raumforsch. Landesplan.* No. 114.
Koch, E., Marktl, W., Matzarakis, A., Nefzger, H., Rudel, E., Schunder-Tatzber, S. and Zygmuntowski, M., 2005: Klimatherapie in Österreich. *Broschüre zu den Potentialen der Klimatherapie in Österreich.* Bundesministerium für Wirtschaft und Arbeit.
Matzarakis, A., 2001: *Die thermische Komponente des Stadtklimas.* Ber. Meteorol. Inst. Univ. Freiburg Nr. 6.
Matzarakis, A., 2002: Validation of modelled mean radiant temperature within urban stuctures. *AMS Symposium on Urban Environment,* Norfolk, 7.3.
Matzarakis, A., 2006: Weather and climate related information for tourism. *Tourism and Hospitality Planning & Development 3, 99-115.*
Matzarakis, A. and Mayer, H., 1996: Another kind of environmental stress: Thermal stress. *WHO Newsletters 18,* WHO Collaborating Centre for Air Quality Management and Air Pollution Control, 7-10.

Matzarakis, A., Mayer, H. and Iziomon, M., 1999: Applications of a universal thermal index: physiological equivalent temperature. *Int. J. Biometeorol. 43*, 76-84.

Matzarakis, A., Rutz, F. and Mayer, H., 2000: Estimation and calculation of the mean radiant temperature within urban structures. In *de Dear, R.J., Kalma, J.D., Oke, T.R. and Auliciems, A.* (eds.): *Biometeorology and Urban Climatology at the Turn of the Millenium. Selected Papers from the Conference ICB-ICUC'99.* WCASP-50, WMO/TD No. 1026, Sydney 2000. 273-278.

Matzarakis, A., de Freitas, C. and Scott, D., 2004 (eds.): *Advances in tourism climatology.* Ber. Meteorol. Inst. Univ. Freiburg Nr. 12.

Matzarakis, A., Rutz, F. and Mayer, H., 2007: Modelling Radiation fluxes in easy and complex environments – Application of the RayMan model. *Int. J. Biometeorol. 51*, 323-334.

Mayer, H. and Höppe, P., 1987: Thermal comfort of man in different urban environments. *Theor. Appl. Climatol. 38*, 43-49.

Mayer, H. and Matzarakis, A., 1997: The urban heat island seen from the angle of human-biometeorology. *Proceed. Int. Symposium on Monitoring and Management of Urban Heat Island.* Fujisawa, Japan, 84-95.

Mayer, H. and Matzarakis, A., 1998: Human-biometeorological assessment of urban microclimates' thermal component. *Proceed. Int. Symposium on Monitoring and Management of Urban Heat Island.* Fujisawa, Japan. 155-168.

New, M., Hulme, M. and Jones, P., 1999: Representing twentieth century space-time climate variability. Part I: Development of a 1961–90 mean monthly terrestrial climatology. *J. Climate 12*, 829-856.

New, M., Hulme, M. and Jones, P., 2000: Representing twentieth century space-time climate variability. Part II: Development of 1901-1996 monthly grids of terrestrial surface climate. *J. Climate 13*, 2217-2238.

New, M., Lister, D., Hulme, M. and Makin, I., 2002: A high-resolution data set of surface climate over global land areas. *Climate Research 21*, 1-25.

Pécsi, M. and Sárfalvi, B., 1964: *The Geography of Hungary.* Budapest, Corvina Press. 299 p.

Spagnolo, J. and de Dear, R., 2003: A field study of thermal comfort in outdoor and semi-outdoor environments in subtropical Sydney Australia. *Building and Environment 38*, 721-738.

Steadman, R.G., 1971: Indices of windchill of clothed person. *J. Appl. Meteorol. 10*, 674-683.

Thom, E.C., 1959: The Discomfort Index. *Weatherwise 12*, 57-60.

Unger, J., 1999: Comparisons of urban and rural bioclimatological conditions in the case of a Central-European city. *Int. J. Biometeorol. 43*, 139-144.

Unger, J., Gulyás, Á. and Matzarakis, A., 2005: Eltérő belvárosi mikrokörnyezetek hatása a humán bioklimatikus komfortérzetre. [Effects of the different inner city micro-environments on the human bioclimatological comfort sensation. (in Hungarian)]. *Légkör 50/1*, 9-14.

VDI, 1998: *Methods for the human-biometeorological assessment of climate and air hygiene for urban and regional planning. Part I: Climate.* VDI guidline 3787. Beuth, Berlin.

WMO, 1996: Climatological normals (CLINO) for the period 1961-1990. WMO/OMM-No. 847, Geneva.

HUMAN BIOCLIMATOLOGICAL EVALUATION WITH OBJECTIVE AND SUBJECTIVE APPROACHES ON THE THERMAL CONDITIONS OF A SQUARE IN THE CENTRE OF SZEGED

N. KÁNTOR, J. UNGER and Á. GULYÁS

Department of Climatology and Landscape Ecology, University of Szeged, P.O.Box 653, 6701 Szeged, Hungary
E-mail: Kantor.Noemi@geo.u-szeged.hu

Összefoglalás – A vizsgálat egy szegedi belvárosi tér humán bioklimatológiai értékelését tűzte ki célul. 2006 nyarának végén (augusztus 17, 22, szeptember 12) az Aradi vértanúk terén felállított mikrometeorológiai állomás segítségével mértük az emberek termikus komfortérzetét befolyásoló meteorológiai tényezőket, melyekből azután a RayMan modell segítségével termikus indexeket számítottunk. A kapott eredményeket összevetettük a mérésekkel egyidejűleg, kérdőívek felhasználásával nyert információkkal, melyek a területen tartózkodó emberek szubjektív véleményét tükrözik, hogy meghatározhassuk az emberek szabadtéri tartózkodását és termikus komfortérzetét leginkább befolyásoló tényezőket. Eredményeinket összevetettük a hasonló körülmények között végzett svéd és japán vizsgálatok eredményeivel.

Summary – The aim of the present study was the human bioclimatological assessment of a square in the centre of Szeged. We measured the meteorological factors influencing people's thermal comfort level on the Aradi square at the end of the summer of 2006 (17th, 22nd August, 12th September) with the help of a micro-meteorological station. Using these observational data we calculated the thermal indices with the RayMan model. We compared these (objective) results with the information derived from simultaneously filled questionnaires that reflected the subjective opinion of the people staying in the area, in order to determine the factors, which most likely influence the people's outdoor staying and sensation of thermal comfort. Our results were compared with results of Swedish and Japanese investigations with similar conditions.

Key words: urban square, thermal comfort, objective methods (meteorological measurements, modelling), subjective methods (social survey)

1. INTRODUCTION

Due to the increasing urbanization, people spend less and less time in the open air, and therefore the city parks and squares of appropriate qualities and quantities could play an important role in the recreation and outdoor activities of the city-dwellers. Up to now several comfort indices were created, which describe the thermal conditions of indoor or outdoor areas in the terms of human bioclimatology. Our long-term aim is to help the development of a universal thermal comfort index, which can be applied independently of the climatic zones (*Spagnolo and de Dear*, 2003), and of which the usage makes possible the evaluation of both indoor and outdoor areas. For this purpose, a thorough examination of the factors behind the – especially outdoor – thermal sensation is necessary; particularly the psychological reactions triggered by the area (*Nikolopoulou and Steemers*, 2003, *Nikolopoulou and Lykoudis*, 2006, *Thorsson et al.*, 2004). Moreover, the examination of the different reactions of people living in different geographical regions/cultures for similar thermal conditions is also highly important (*Knez and Thorsson, 2006*).

The goal of the present study is the human bioclimatological evaluation of a square in the centre of Szeged using objective and subjective methods. We measured meteorological factors with a meteorological station and we calculated thermal indices (*PET* and *PMV*, see in *Section 2.2.1*) from these. Then we compared these (objective) results with simultaneously gathered information, derived from a social survey and reflecting the subjective opinion of the people staying in the area at the time. We did that in order to determine the factors that most likely influence people's attitude of staying outdoors and their sensation of thermal comfort.

2. MATERIAL AND METHODS

2.1. Study area

We took our examinations in Aradi square at the end of the summer of 2006 (17th, 22nd August, 12th of September) in Szeged. Based on large-scale climatic classification the region belongs to the Köppen *Cf* (warm-temperate with even distribution of precipitation) or the Trewatha *D.1* (continental climate with longer warm season) climate zone (*Unger and Sümeghy*, 2002).
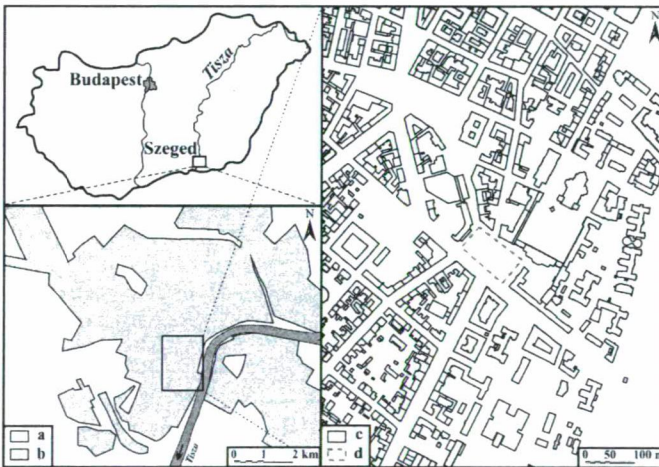
Fig. 1 Location of Szeged in Hungary, as well as the location of the study area in Szeged: (a) open area, (b) built-up area, (c) buildings, (d) border of the investigated square

The area of the Aradi square (*Figs. 1 and 10*) is about 7300 m^2, and it is divided by tram rails from south to north. Its west side is covered by pavements and grass courts, while the east side is dominated by asphalt cover. There are plenty of deciduous and some coniferous trees on both sides of the square, which offer shadow for people in the warm period.

2.2. Methods

We applied objective and subjective methods in order to get an appropriate picture of the thermal conditions of the area. The objective approach is based on thermal indices calculated from measured meteorological parameters with the help of one of the comfort-models (RayMan). The basis of the subjective method was the investigation of the people's

opinion visiting the area in the form of questionnaires. The two approaches have been applied simultaneously in order to compare the obtained results with each other.

2.2.1. Objective method

The two human bioclimatological indices we used are the *PMV* (Predicted Mean Vote) and the *PET* (Physiological Equivalent Temperature). *PMV* predicts the mean assessment of the thermal environment for a large sample of human beings by values according to the seven-point (from -3 to +3) ASHRAE comfort scale (*Table 1*) (*Mayer and Höppe*, 1987). In real (extreme) weather situations *PMV* can be higher than +3 or lower than -3.

Table 1 Comparison of *PMV* (Predicted Mean Vote) and *PET* (Physiological Equivalent Temperature) ranges for different human sensations and thermal stress level by human beings. (Internal heat production: 80 W, heat transfer resistance of the clothing: 0.9 clo) (*Matzarakis et al.*, 1999)

PET (°C)	PMV	Human sensation	Thermal stress level
4		very cold	extreme cold stress
	-3	cold	strong cold stress
8			
	-2	cool	moderate cold stress
13			
	-1	slightly cool	slight cold stress
18			
	0	comfortable	no thermal stress
23			
	1	slightly warm	slight heat stress
29			
	2	warm	moderate heat stress
35			
	3	hot	strong heat stress
41		very hot	extreme heat stress

PET is based on the Munich Energy Balance Model for Individuals (MEMI), and is defined as the air temperature at which the energy balance for assumed indoor conditions is balanced with the same mean skin temperature and sweat rate as calculated for the actual outdoor conditions (*Mayer and Höppe* 1987). A *PET* value of around 20°C is characterised as comfortable, higher values indicate increasing probability of heat stress, and lower values indicate increasing probability of cold stress (*Table 1*).

The meteorological data have been obtained by a HWI type mobile meteorological station with Vaisala and Kipp&Zonen sensors, which was placed in a point of the area (*Fig. 3*), where it was exposed to direct radiation during the whole day. *Table 2* contains the characteristics of the sensors for air temperature (T_a), relative humidity (RH), wind velocity (v) and global radiation (G). The ten-minute averages of the parameters were recorded by a data logger, in the first two occasions from 8.00 a.m. to 7.00 p.m., and in the 12th of September from 8.00 a.m. to 6.00 p.m.

Using the measured parameters we calculated comfort indices *PMV* and *PET* with the help of the RayMan model, developed according to guideline 3787 of the German Engineering Society (*VDI* 1998), which calculates the radiation fluxes within urban structures based on parameters including air temperature, air humidity, degree of cloud cover, air transparency, time of day and year, albedo of the surrounding surfaces, and their solid angle proportions (*VDI* 1994). *Fig. 2* shows the picture of the investigated area, generated with RayMan.

Table 2 Measured meteorological parameters, instruments and accuracy

Parameter	Instrument	Accuracy
T_a (°C)	Vaisala	± 5 %
RH (%)	Vaisala	± 5 %
v (ms^{-1})	Vaisala	± 5 %
G (Wm^{-2})	Kipp&Zonen	± 1-3 %
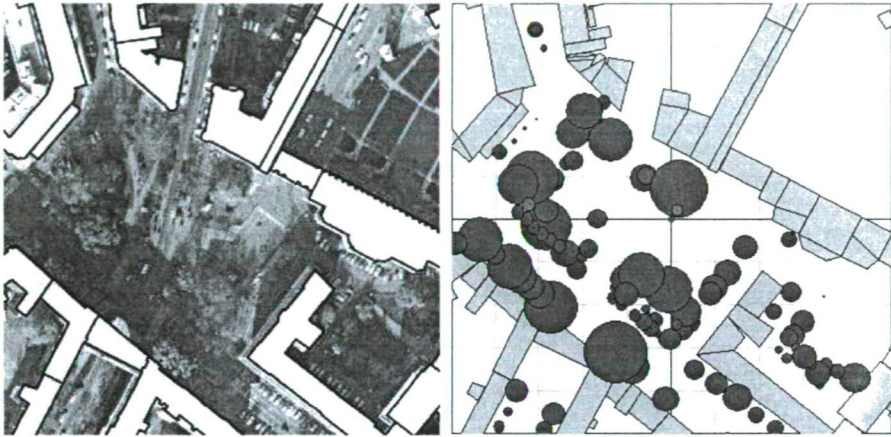
Fig. 2 Aerial view of the Aradi square (the buildings are stressed) (left), and the simplified picture of the square generated by RayMan (right). The place of the measuring station is marked by red.

Especially during sunny weather, the mean radiant temperature (T_{mrt}) is the most important input parameter for the energy balance – thus also for RayMan – therefore the recent comfort-indices include it. T_{mrt} is defined as the uniform temperature of a surrounding surface giving off blackbody radiation (emission coefficient = 1) which results in the same energy gain of a human body as the prevailing radiation fluxes (*Höppe*, 1992). T_{mrt} may be an input parameter for RayMan as well as an output provided the above mentioned parameters are known.

2.2.2. Subjective method

In order to find the psychological factors behind the attendance of the outdoor areas and the thermal comfort sensation which emerges there, we made a social survey with structured interviews simultaneously with the meteorological measurements. Altogether 844 questionnaires were filled by the answers of the randomly selected people during the 3 days mentioned above. Each interview took about 2-3 minutes, and the questioner recorded the time of the beginning of the interview. According to an earlier arrangement – with a few minor modifications – we used the questions already used by *Knez and Thorsson* (2006) in their investigation in Sweden and Japan.

At the beginning of the interview we recorded the subject's position (whether he/she is on the sun or in shadow; sitting / standing / walking), and his/her clothes as well. The data on clothes were converted into the clo-unit typical of summer clothes (*Spagnolo and de Dear*, 2003). Demographic variables, such as age, sex and whether the subject works or lives near the square were recorded, too.

First the following simple questions were asked from the interviewed persons:

- *"How often do you come here?"* (daily; plenty times a week; few times a week; few times a month; rarely; it is the first time)
- *"What is your main reason for being here?"* We were curious whether the area was only on the subject's way going home / school / etc., or he/she purposely came to the place in order to walk / be in the open-air / meet somebody / etc., or both of them.
- *"How long have you been in the open air, and in this area?"* The time was measured in minutes.

Then they were asked to answer the following questions by responding to scales ranging from 1 to 5:

- *"What do you think about today's weather?"* (a) cold/warm; (b) calm/windy; (c) dry/humid and (d) bad/good for outdoor activity.
- *"What do you think about the momentary conditions of the square?"* (a) cold/warm; (b) calm/windy; and (c) dry/humid; (d) unpleasant/pleasant
- *"How do you feel yourself in the square at the moment?"* (a) tired/fresh; (b) gloomy/glad; (c) nervous/calm.

Participants also estimated their thermal comfort by responding to a 9-point scale ranging from very cold (-4) to very hot (+4), with a score of 0 rating as comfortable (*Knez and Thorsson*, 2006). This vote is referred to as *ASV (Actual Sensation Vote)* and it is a subjectively perceived value reflected one's thermal sensation-level.

We asked the participants about what they thought the actual temperature was This is the *estimated temperature (T_{est})*. The estimation was helped by 9 temperature grades.

The questionnaire also measured the participants' *urban vs open-air person attitude* on a 5-point scale ranging from 1 (mostly urban person) to 5 (mostly open-air person) related to the question: "How much of an urban person (find pleasure in street life, shops, the amusements of the city) and open-air person (find pleasure in the sea, the woods, nature) are you?".

With the help of the questionnaires we can clearly get a lot of information, which cannot be achieved by the "traditional" estimation using indices that are relevant only in thermo-physiological terms.

3. RESULTS AND DISCUSSION

The results are discussed in the next steps:
- Presentation of the daily variation of the measured parameters and the indices.
- Analysis of the data from the structured interviews.
- Comparison of the calculated (objective) data and the people's subjective opinions.
- Comparison of the information obtained from the questionnaires belonging to the comfortable *PET*-range with the earlier published (*Knez and Thorsson*, 2006) Swedish and Japanese results gained in similar circumstances.

3.1. Evaluation of the objective measurements

Fig. 3 shows the daily variation of different indices on the first day. According to it, the running of the *PET* can be compared rather with the T_{mrt}, than with the T_a. The variation of the *PMV* was almost the same as that of the *PET* (not shown). This indicates one of the

most important characteristics of RayMan: the significant role of the radiation conditions during the calculation of the indices; namely the people's thermal comfort sensation is mainly determined by the amount of radiation they are exposed in a given place.
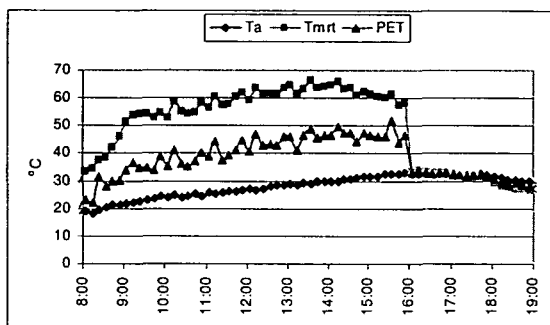
Fig. 3 Daily variation of T_a, T_{mrt} and *PET* on the Aradi square in Szeged (17th August 2006)

3.2. Evaluation of the subjective measurements

During the three days the majority of the interviewed persons were young, preferred to stay in the shade, and attended the square daily (sometimes more than one occasion). Most of the people found the weather warm, dry and calm (and so they thought about the momentary weather conditions, too), and a remarkable majority found it appropriate for open-air activities (*Fig. 4*).
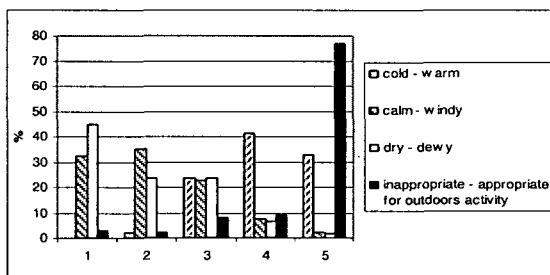
Fig. 4 Frequency of the answers for the current days in 5-degree scales

In order to know if there is any difference between the answers of the people with "urban vs. open-air attitude", how this characteristic effects the answers, and which answers are affected the most, the originally 5-degree scale was simplified to a 3-degree (so 1 and 2 were the "urban", 3 was the "neutral", 4 and 5 were the "open-air" category) one. This operation was performed for other opinions with 5-degree scales too. Apart from the question for tiredness and the *ASV* relating to the comfort sensation we found no connection with the "urban vs. open-air" attitude. The people with "open-air" attitude are usually more tired than the ones with "urban" attitude (*Fig. 5*) and the "neutral" ones find most likely comfortable the actual conditions of the square (*Fig. 6*).

The explanation for the more tired mood of the "open-air" people is that although they would have more gladly spent their times in nature, somehow they had to stay in the town, of which the crowdedness and noise-level influence affects that kind of people more

negatively. However, they found the place as much comfortable as the people with "urban" attitude *(Fig. 6)*, which is more likely due to the fact that the design of the square is very reminiscent of a park (which counterbalances the inconvenience of the urban environment to a certain extent).
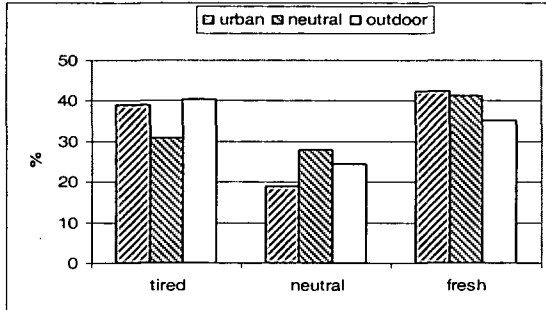
Fig. 5 Frequency of the actual tiredness of the interviewed persons according to the "urban–open-air" attitude
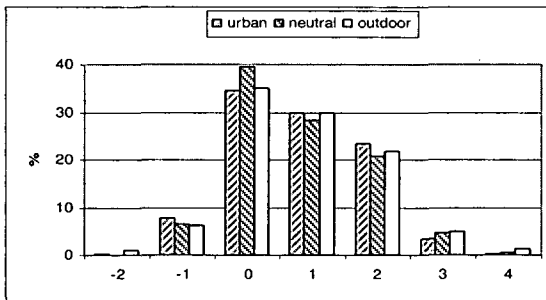
Fig. 6 Frequency of the *ASV*-values relating the people's actual comfort sensation according to the "urban-open-air" attitude

3.3. Comparison of the two different approaches

Comparing the *ASV* relating to the human thermal sensation with the *PMV* calculated with the model, we realized that the vote number reflecting the people's subjective opinion in comparison with the *PMV* occurs more likely in the 'comfortable' domain and those that border, and rarely occurs in the categories indicating extreme stress-level *(Fig. 7)*.

The explanation of the phenomenon is the following: people prepare themselves for much more extreme conditions during their staying in the open-air, which leads to the widening of 'comfortable' and its neighbouring domains. However, the applied indices relate to the indoor reference-conditions, and they were developed in connection with the comfort zones typical of indoor areas. These zones are much narrower, because of the thermal conditions expected in buildings are artificially maintained near the comfortable level. With this it can be also explained that some of the calculated *PMV* values exceed the limits of the expanded (from -4 to +4) scales *(Fig. 7)*. So in the light of the results it is inappropriate to apply the indoor comfort zone without modifying its limits in outdoor examinations.
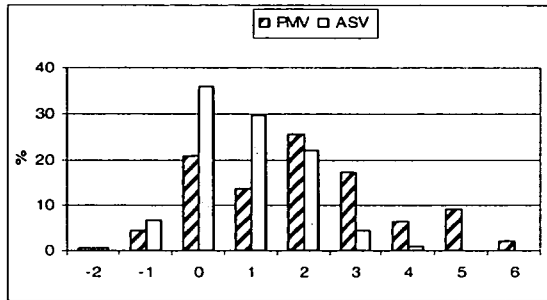
Fig. 7 Frequency of the calculated *PMV* and the interviewed *ASV* values

If one spent more time in the area of examination, the difference was substantially smaller between the *ASV* given by the person and the actual *PMV* (*Fig. 8*). According to this the RayMan model and similar models can give a real outcome in the case of long-term exposure, thus they are appropriate only in a limited way for the evaluation of the sensation of people with a short-time exposure.
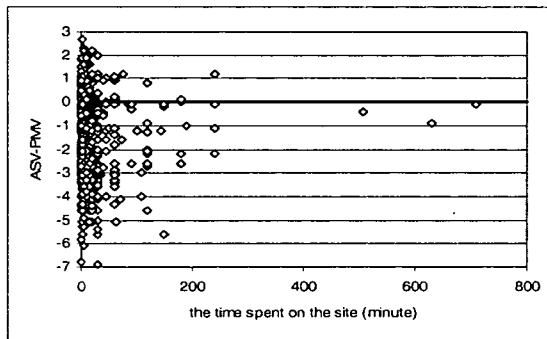
Fig. 8 Differences between the *ASV* values of the interviewed people and the *PMV* values in the time of the interview, as a function of the time spent in the area
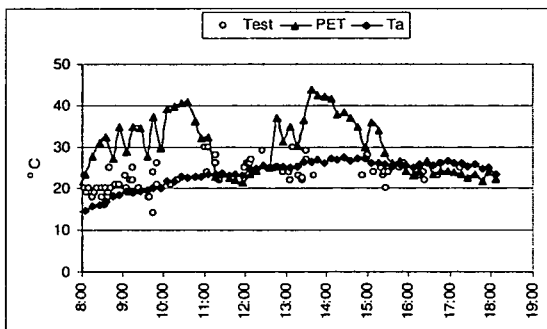
Fig. 9 Diurnal course of T_a, *PET* and T_{est} (indicating the values estimated by the people staying in sun) on 12th September

Fig. 9 shows the diurnal variation of the measured T_a, the calculated *PET* and the subjective T_{est} parameter during the third day. The figure contains only the T_{est} values

estimated by the people sitting or standing in the sun, because these people's positions were the most comparable with the position of the meteorological station. The variation of T_{est} is more similar to the measured air temperature, than to the calculated *PET* values. It can be explained by the people's long- and short-term experiences (see *Thorsson et al.*, 2004; *Nikolopoulou and Steemers*, 2003). During one day with weather conditions not unusual at the season people can estimate the temperature appropriate for the season more precisely, especially when the thermal conditions were the same in the preceding days. Since the investigated days occurred in a time period, of which the days were very similar regarding the weather conditions, people did not encounter with suddenly changed air temperature or sun radiation values, so they could estimate more precisely the temperature typical of those days.

3.4. International comparison

Now we compare our data within the comfortable *PET*-range (only 63 questionnaires from the 844!) with the recently published Swedish and Japanese data obtained at similar conditions (*Knez and Thorsson*, 2006). The two squares of the already published studies are typical for the medium sized Swedish and Japanese cities (*Fig. 10*). *Table 3* contains some data related to the study areas and the examinations made there.

Fig. 10 Photos of the Hungarian, Swedish and Japanese squares: Aradi square (Szeged), Gustav Adolfs torg (Göteborg), Matsudo Station Square (Matsudo)

According to *Fig. 11* the square in Szeged is visited most frequently, and in case of the question on the reason for being there most answers were the same ("The area was only in the way").

Comparing the answers on 5-degree scales, the Japanese participants found the similar thermal conditions (comfortable according to the *PET*) much warmer than the others (*Table 4*). It can be explained by the differences between the cultures (see *Knez and Thorsson*, 2006), but it is more likely, that the explanation lies in the design of the areas.

In the Hungarian square the vegetation is more abundant that makes the area more evocative and aesthetical. Moreover, the trees provide shade on a significant part of the area (see *Fig. 10*), which makes the thermal conditions of the square more comfortable during the warm and hot (summer) periods. The area – due to its design – increases the chance of the physical and psychical adaptation (*Thorsson et al.*, 2004) by offering different microclimatological conditions that permit staying there for a long time. In contrast, the Swedish and Japanese squares have a great extent of paved surface, and there is negligible or no vegetation. Without shading the amount of solar radiation people are exposed to increases and it produces a more unpleasant sensation during the warm periods. The Japanese square has the least vegetation and the largest ratio of pavement with large albedo,

which explains the above mentioned inconveniences and the greatest difference from 0 (or the comfortable condition) at *ASV*.

Table 3 Information related to the Hungarian, Swedish and Japanese study areas and examinations

		Hungary	Sweden	Japan
Geography	Country	Hungary	Sweden	Japan
	City	Szeged (46°15'N, 20°16'E)	Göteborg (57°42'N, 11°58'E)	Matsudo (35°78'N, 139°90'E)
	Population	160,000	500,000	500,000
Climate	General	warm-temperate	martime	temperate
	Summer	warm, dry	cool	warm, humid
	Winter	mild, dry	mild, humid	mild, dry
	Mean annual temp.	11°C	7.6°C	15.6°C
Study area	Name	Aradi square	Gustav Adolfs torg	Matsudo Station Sq.
	Size	7300 m^2	6000 m^2	2000 m^2
	Surface cover	grass, concrete	different cobblestones	light coloured clinkers
	Vegetation	grass, deciduous and coniferous trees	a few deciduous trees	none
Examination	Time of the study	Aug., Sept. 2006	April 2004	March 2004
	Time of the day	from morning to evening (8.00-19.00)	at noon (11.00-15.00)	at noon (11.00-15.00)
	Number of persons questioned (at comfort PET level)	63	43	63
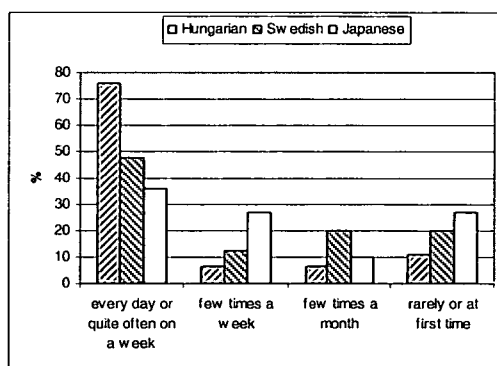
Fig. 11 Frequency of the interviewed persons in the Hungarian, Swedish and Japanese squares regarding how frequently they visit the area

We can draw a parallel between the interviewed people's mood (gloomy-glad) and the answers of how pleasant they felt the actual conditions of the area (*Table 4*). The Japanese participators seemed to be less happy, and they felt themselves the least pleasantly in their environment. In contrast, for both of the questions the Hungarian achieved the

greatest average values. According to this one can suppose some relationship between people's comfort and their judgement on the studied urban area. A person in a less good mood will likely find her actual place more unpleasant and the actual thermal conditions as well. The phenomenon works vice versa: the mood can be influenced easily by the aesthetical experience of their surroundings and the surroundings that give appropriate (comfortable) thermal sensation are predominantly the consequence of the design of the area.

Table 4 Average values of the answers of people visiting the Hungarian, Swedish or Japanese areas on 5-degree and 9-degree scales, which relate to the evaluation of the areas and the people's actual sensation

	Hungarian	Swedish	Japanese
Cold-Warm [1 – 5]	3.35	3.40	4.15
Unpleasant-Pleasant [1 – 5]	4.65	4.20	3.50
Nervous-Calm [1 – 5]	3.95	4.25	3.75
Gloomy-Glad [1 – 5]	3.85	3.78	3.25
ASV [(-4) – (+4)]	0.3	0.2	0.8
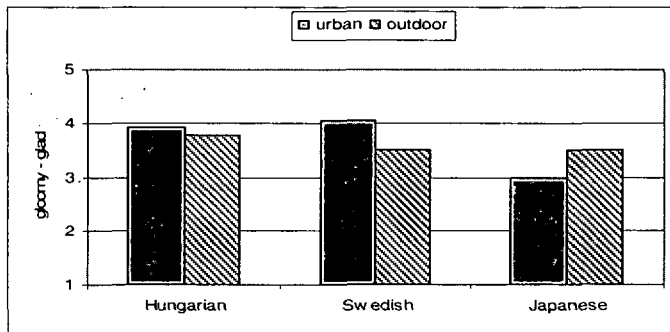
Fig. 12 Average values of the answers for the question "How do you feel yourself at the moment?" on a 5-degree scale by the interviewed persons' nationality and "urban–open-air" attitude

Fig. 12 also relates to the socio-cultural differences. While the difference in the answers of the Hungarian participants were not so large between the people with "urban" and "open-air" attitudes, in the cases of the other two nations the differences were more remarkable. Moreover, in contrast to the Swedish and Hungarian results, the Japanese people with "urban" attitude were in the worse mood.

4. CONCLUSIONS

Our examinations showed some differences between the values based on subjective estimation (*ASV*, T_{est}) and on the common human bioclimatological indices (*PMV, PET*). On one hand, the phenomenon can be explained with the fact that the models similar to RayMan are unable to examine the short-term (temporary) exposition; on the other hand, it is explicable with the application of indoor methods for outdoor comfort examination – without the modification of the comfort-zone limits. The similarity between the people's answers and the air temperature emphasizes the short- and long-term experiences with the thermal environment.

The study intends to draw attention to the importance of the vegetation. First, the trees can modify the radiation conditions to a great extent, and they can provide great alleviation with their shades during particularly during the hot periods. Besides, the green areas within a certain city structure can influence the mood and way of sensation of the people staying in the area to a great extent by their location, size and condition, and so incidentally influence the thermal estimation of the area. Based on the results some connection can be established between the judgement of the areas (comfortable-uncomfortable) and the mood and thermal sensation of people.

The difference between the answers of people of different cultures (Hungarian, Swedish and Japanese) and "urban–open-air" attitudes draws the attention for the further necessity for investigation of socio-cultural factors. This direction could have particular importance in the adjustment of comfort and discomfort indices developed in the future, based on uniform principles, since people with different cultures and accustomed to different climate can react in different ways to the same thermal conditions.

There is a need for similar examinations in a great quantity and in areas in diverse climate-zones as well, in order to develop a universally applicable comfort-model and index, which can be modified according to the area of use (or rather the people and culture typical to the area).

REFERENCES

Höppe, P., 1992: Ein neues Verfahren zur Bestimmung der mittleren Strahlungstemperatur im Freien. *Wetter und Leben 44*, 147-151.

Knez, I. and Thorsson, S., 2006: Influences of culture and environmental attitude on thermal, emotional and perceptual evaluations of a public square. *Int. J. Biometeorol. 50*, 258-268.

Matzarakis, A., Mayer, H. and Iziomon, M., 1999: Applications of a universal thermal index: physiological equivalent temperature. *Int. J. Biometeorol. 43*, 76-84.

Mayer, H. and Höppe, P., 1987: Thermal comfort of man in different urban environments. *Theor. Appl. Climatol. 38*, 43-49.

Nikolopoulou, M. and Lykoudis, S., 2006: Thermal comfort in outdoor urban spaces: Analysis across different European countries. *Building and Environment 41*, 1455-1470.

Nikolopoulou, M. and Steemers, K., 2003: Thermal comfort and psychological adaptation as a guide for designing urban spaces. *Energy and Buildings 35*, 95-101.

Spagnolo, J. and de Dear, R., 2003: A field study of thermal comfort in outdoor and semi-outdoor environments in subtropical Sydney, Australia. *Building and Environment 38*, 721-738.

Thorsson, S., Lindqvist, M. and Lindqvist, S., 2004: Thermal bioclimatic conditions and patterns of behaviour in an urban park in Göteborg, Sweden. *Int. J. Biometeorol. 48*, 149-156.

Unger, J. and Sümeghy, Z., 2002: *Környezeti klimatológia. Kisléptékű éghajlatok, városklíma. [Environmental climatology. Small-scale climates, urban climate.* (in Hungarian)] SZTE TTK, JATEPress, Szeged, 202 p.

VDI, 1994: *VDI guideline 3789*, Part 2: Environmental Meteorology, Interactions between Atmosphere and Surfaces; Calculation of the short- and long wave radiation. Beuth, Berlin. 52 p.

VDI, 1998: *VDI guideline 3787*, Part 1: Environmental Meteorology, Methods for the human biometeorological evaluation of climate and air quality for urban and regional planning. Beuth, Berlin. 29 p.

GLOBAL SURFACE TEMPERATURE TIME SERIES CHARACTERISTICS FOR THE EARTH, IN RELATION TO CO$_2$ PERTURBATIONS

L. MAKRA[1], T. KŐVÁGÓ[1] and D. OLIVIE[2]

[1]*Department of Climatology and Landscape Ecology, University of Szeged, P.O.B. 653, 6701 Szeged, Hungary*
E-mail: makra@geo.u-szeged.hu
[2]*METEO-FRANCE / CNRM / CAIAC, 42 Avenue Gaspard Coriolis, 31057 Toulouse, France*

Összefoglalás – A tanulmány célja a globális felszínhőmérséklet idősor néhány statisztikai jellemzőjének tanulmányozása. A lineárisi trendanalízis nem mutatott ki hosszú tartamú szignifikáns trendeket. Az esetleges rövid tartamú (legfeljebb hatelemű) trendek a legnagyobb gyakorisággal a D(QTH, QTM) globális felszínhőmérséklet differencia idősor középső harmadában fordulnak elő. A vizsgált idősorra alkalmazzuk a Makra-tesztet, mely a kétmintás próba egy új interpretációja. A próba alapkérdése: kimutatható-e szignifikáns különbség a vizsgált idősor egy tetszőleges részmintájának, illetve a teljes idősornak az átlagai között. A próba alkalmas arra, hogy szignifikáns töréseket mutassunk ki az idősorban, meghatározva annak erősségét, hosszát és tartamát, azaz kezdő és záró időpontját. A Makra-próba segítségével meghatároztuk a D(QTH, QTM) globális felszínhőmérséklet differencia idősor szignifikáns részperiódusait. Két szignifikáns részperiódust mutattunk ki: Pozitív törést 1861-1900 között, míg negatív törést 1881-1958 között tapasztaltunk. További célunk az volt, hogy tanulmányozzuk a megnövekedett CO$_2$ szint hatását a globális felszínhőmérséklet változásaira. A D(QTH, QTM) idősor legjobb görbeillesztései az adatsor varianciájának (teljes négyzetes hiba = total squared error) jelentős részét megmagyarárzzák: R^2 > 80 %; RMSE (becsült szórás) < 0.5. Az RMSE értéke igen hasonló a referencia szimulációra kapott RMSE értékhez. Az adatsorhoz illesztett görbék futása az időszak elején növekvő, majd 10-15 éves futást követően eléri maximumát, s később fokozatosan csökken. Ugyanakkor az illesztett görbék számos esetben emelkedő tendenciát jeleznek a vizsgált 100 éves periódus végén, mely meglehetősen leronthatja a hosszútávú előrejelzéseket.

Summary – The aim of the study was to analyse some statistical characteristics of the global surface temperature time series. Linear trend analysis did not reveal any significant long-range trends. Significant sporadic short term trends (with not more than 6 elements) can only be observed with higher frequency in the middle third of the D(QTH, QTM) temperature difference times. The Makra-test, as a new interpretation of the two-sample test, was also applied to the global surface temperature time series. The basic question of this test is whether or not a significant difference can be found between the mean of an arbitrary sub-sample of a given time series and that of the whole series. This test is suitable to detect breaks in the data set, along with their strength, length and time interval, namely their starting and ending date. With the help of the Makra-test two significantly different sub-periods in the global temperature difference time series of D(QTH, QTM) were detected. In the here-mentioned data set a significant positive break were found between 1861-1900 and a significant negative break relating to the term around 1881-1958. A further aim was to study the effect of the increased CO$_2$ level on the changes of the global temperature. The curves best fitting to the D(QTH, QTM) global surface temperature difference time series explain changes (total squared error) of the data set in fairly high ratios. The value of the R-square generally exceeds 80 %. The estimated standard deviations (RMSE) are rather low, mostly below 0.5. These RMSE values are very similar to those of standard deviation in the reference simulation. The fitted curves adjusted to the data show an increasing tendency in the first period; then, after 10-15 years run reaches its maximum and later is gradually decreasing. However, the fitted curves in several cases indicate slight increasing tendencies at the end of the 100-year period, which may rather ruin long-range forecasts.

Key words: QTM simulation, QTH simulation, D(QTH, QTM) global surface temperature difference time series, linear trend analysis, Makra-test, curve fittings

1. INTRODUCTION

The aim of the study was to analyse some statistical characteristics of surface temperature time series; namely, to perform linear trend analysis, as well as to show the Makra-test, as a new interpretation of the two-sample test with its application to the global surface temperature times series. The basic question of this test is whether or not a significant difference can be found between the means of an arbitrary sub-sample of a given time series and the whole sample (*Makra et al.*, 2002, 2005).

A further aim was to study the effect of the increased CO_2 level on the changes of the temperature of the Earth and its separate regions. The data of three simulations, concerning a 100-year long period, were used in the analysis. Among them the first one was a reference simulation, for which the background data were adjusted on the basis of a period preceding industrialization. The original temperature data set was distorted by the supposed high level of CO_2 the effect of which gradually decreased by 20-year periods from the beginning till the end of the time series.

2. DATABASE

The original data come from the research team CAIAC (Atmospheric Chemistry and its Interactions with Climate), METEO-FRANCE, CNRM (Centre National de Recherches Météorologiques, Toulouse, France. They were derived from a simulation of 100 years. Each year contains 12-monthly mean fields. There are data for the unperturbed run and the pulse perturbations of CO_2. The pulses started at January 1st 1860 and the relaxation time was 20 years. The results of the simulation were stored in netCDF format. NetCDF (network Common Data Form) is an interface for array-oriented data access and a library that provides an implementation of the interface. The netCDF library also defines a machine-independent format for representing scientific data. The interface, library and format together support the creation, access and sharing of scientific data. The netCDF User's Guide and the Interface Guides (*http://www.unidata.ucar.edu/software/netcdf/docs/*) were most useful in the course of our work.

The database can be divided in two parts:

The first part contains the surface air temperature at 2 m height, with monthly mean values for the years from 1860 till 1959. Every file contains one three-dimensional field with the following dimensions: longitude (128) latitude (64) and months (12). The surface air temperature fields are given on a Gaussian grid with 128 x 64 points, 128 longitudes and 64 latitudes. A Gaussian grid is one where each grid point can be uniquely accessed by one-dimensional latitude and longitude arrays (i.e. the coordinates are orthogonal). The longitudes are equally spaced, while the latitudes are unequally spaced according to the Gaussian quadrature. Gaussian grids do not have points at the poles. Typically, the number of longitudes is twice the number of latitudes (i.e. 128 longitudes and 64 latitudes). A MATLAB function Gauss2lats can be useful to compute the latitude coordinates. The function determines the Gaussian latitudes by finding the roots of the ordinary Legendre polynomial of degree NLAT using Newton's iteration method. The only input required is the number of latitude lines in the Gaussian grid. The outputs are Gaussian latitudes, latitude spacing and cosine of latitude. The land-sea mask is given as a two-dimensional array of 128 x 64 values, (= 1 if land; = 0 if sea). However we have to admit that the mask

and the grid with the atmospheric data are not identical to the grid used during the simulations. The grid used during the simulation is a "reduced" Gaussian grid with 128 x 64 points, while the grid with the results is a Gaussian grid with 128 x 64 points. So there is already an interpolation step. However, during this interpolation, the influence of the different masks has been accounted for.

The second part contains the ocean temperature monthly mean values for the years from 1860 till 1959. Every file contains one four-dimensional field with the following dimensions: longitude (182), latitude (152), level (31) and month (12). This data is given on an irregular grid of 182 x 152 x 31: 182 longitude, 152 latitude, and 31 levels. In the southern hemisphere, this grid is in fact still regular, but in the northern hemisphere it is irregular. The latitude grid is given as a Gaussian grid. The 1st and 2nd longitudes are identical to the 181st and 182nd longitudes: in fact there are only 180 distinct longitudes. The longitudes vary between 90° and 450°.The vertical grid is described by the following fields: depth is a one-dimensional array (31) of the depth below the oceanic surface of the centre of the layer, and bounds (2 x 31) is a two-dimensional array (2 x 31) of the depth below the oceanic surface of the upper and lower bound of the layer. The mask of the ocean is described by a three-dimensional field (182 x 152 x 31), where 1 means that the given grid is ocean.

There were two different simulations: The QTM simulation is a simulation with ordinary pre-industrial climate conditions, i.e. the CO_2 concentration is constant at 282.6 ppbv that can be used as a reference run. This simulation starts at 1 December 1859 and goes on for 50 years. The QTH (CO2_20Y) simulation also starts at 1 December 1859, where from 1 January 1860 the CO_2 concentration is multiplied by 6.5. This perturbation then also fades away with a relaxation time of 20 years. This simulation goes on for 100 years.

3. SIMULATIONS

On the basis of the original land-sea mask, another file converted to continents was prepared. The co-ordinates of the original mask-file were calculated on the basis of a "Gaussian grid". For each grid it was checked whether land or sea was found in the place of the co-ordinate belonging to the centre of the grid, and also which continent the land belonged to. If land was found on the given co-ordinate, then the number belonging to the adequate continent was written into the mask-file. On the other hand, if sea was found on the given co-ordinate, then 0 was written in the given grid in the database. Seven continents were distinguished, namely Europe, Africa, Asia, Australia, North-America, South-America and the Antarctic. America, together with North- and South-America, was also considered. Then it was looked up in GoogleEarth, whether, on the basis of the position of the middle of the grids, a given point was land or sea.

3.1. The differences of the simulations

A netCDF database was prepared from the surface temperature files for the period, which comprises yearly averages for each co-ordinates and a global mean value for the database over the lands, which were computed with the help of the land-sea mask.

The reference simulations have also been examined by continents and, they seem to run fairly horizontal. From this, we conclude that at the end of the period the difference

between data of the pulse and the reference simulations mainly shows the residual response and that is not the result of long term variability. For this reason the method was changed, according to which the difference of the pulse simulations is to be considered in relation to the 50-year average of the reference simulation.

3.2. The curve-fitting

In a second step curves were fitted to the data. The suggested curve corresponds (to some extent) with a simple model of the atmosphere. The following curves were fitted to the time series:

Those curves were tried to be fit to the data sets that contain only one exponential component: one with a decay time of 20 years:

$$a \cdot e^{-\frac{x-1859.5}{20}} \qquad \text{("exp")}$$

one with an unknown decay time:

$$a \cdot e^{-\frac{x-1859.5}{b}} \qquad \text{("exp2")}$$

and one with a linear factor:

$$a \cdot (x-1859.5) \cdot e^{-\frac{x-1859.5}{20}} \qquad \text{('tau')}$$

At these fittings a weighting factor was used and the weight of the first 20 years was defined as 0.

Then the curves were tried to be fit to the database with the difference of two exponential components: one with a decay time of 20 years and another one with an unknown decay time. The first curve "2dvar" was a simple difference:

$$a \cdot \left(e^{-\frac{x-1859.5}{20}} - e^{-\frac{x-1859.5}{b}} \right) \qquad \text{("2dvar")}$$

The second curve "3dvar" contains a constant factor:

$$a \cdot \left(e^{-\frac{x-1859.5}{20}} - c \cdot e^{-\frac{x-1859.5}{b}} \right) \qquad \text{("3dvar")}$$

The next curve, namely "3dvarlin" has a linear component:

$$a \cdot \left(e^{-\frac{x-1859.5}{20}} - e^{-\frac{x-1859.5}{b}} + c \cdot (x-1859.5) \right) \qquad \text{("3dvarlin")}$$

The curve "4dvarlin" combines the previous two curves and contains a constant factor and a linear component, too:

$$a \cdot \left(e^{-\frac{x-1859.5}{20}} - c \cdot e^{-\frac{x-1859.5}{b}} + d \cdot (x - 1859.5) \right) \qquad \text{("4dvarlin")}$$

The "5dvarlin" curve adds a constant component to the previous formula:

$$a \cdot \left(e^{-\frac{x-1859.5}{20}} - c \cdot e^{-\frac{x-1859.5}{b}} + d \cdot (x - 1859.5) + e \right) \qquad \text{("5dvarlin")}$$

The last two formulas have an unknown offset, namely the "6dvarlin" with one unknown decay time:

$$a \cdot \left(e^{-\frac{x-f}{20}} - c \cdot e^{-\frac{x-f}{b}} + d \cdot (x - f) + e \right) \qquad \text{("6dvarlin")}$$

and "7dvarlin" with two unknown decay times:

$$a \cdot \left(e^{-\frac{x-f}{g}} - c \cdot e^{-\frac{x-f}{b}} + d \cdot (x - f) + e \right) \qquad \text{("7dvarlin")}$$

The number of free parameters to fit varies from 1 to 7. Some of these parameters have to be initialized for the fit to converge: giving the correct sign is generally enough; sometimes other parameters also need a starting value.

3.3. The goodness of the curve-fitting statistics

After using graphical methods to evaluate the goodness of fit, some goodness-of-fit statistics were examined, namely, the Sum of Squares Due to Error statistics, R-Square statistics, adjusted R-square statistics and the Root Mean Squared Error statistics (*http://www.mathworks.com/access/helpdesk/help/pdf_doc/curvefit/curvefit.pdf*).

4. RESULTS

4.1. Linear trends

It was examined whether or not linear trends of the 100-year long temperature difference time series of D(QTH, QTM) were significant, considering all three-element sub-periods, for all four-, five-, ... , 98- and at last 99-element sub-periods. Student's t-distribution was considered to be the basis of the significance analysis, which was performed at the 1% probability level and with a degree of freedom of $n - 2$ (where n is the element number of the time series).

The D(QTH, QTM) time series show very few significant trends with not more than 6-element sub-periods. Relatively high frequency of significant trends can be observed between 1877-1914, a 38-year period in the D(QTH, QTM) data set (14 of all the 20 significant trends: 70.0%); however, they are distributed rather sporadically in the data sets. Higher frequency of the significant trends indicates higher variability of the time series for the period and region examined. Nevertheless, no clear tendencies of the temperature difference time series have been experienced.

4.2. Significant sub-periods (breaks) (Makra-test)

With the help of the Makra-test significant sub-periods in the global surface temperature difference time series of D(QTH, QTM) were detected (*Figs. 1-4*).

The time series examined shows two significant breaks with the highest significant value of the probe statistics. Namely, between 1861 and 1893 there is a 33-element significant positive sub-period, while between 1895 and 1958 a 64-element significant negative one (first-type two-dimensional figure, *Fig. 1*).

Though the second-type two-dimensional figure (*Fig. 2*) does not indicate the strength of the significant sub-periods (that is to say the difference of their means from the whole sample mean); however, it shows all the significant breaks, either distinct or overlapping) (positive breaks: light-grey block, lower part of the figure; negative breaks: dark-grey block, upper part of the figure, *Fig. 2*).
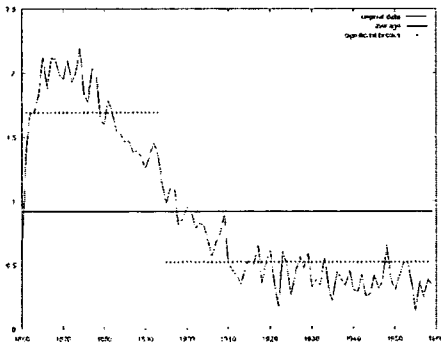
Fig. 1 Significant breaks in the D(QTH, QTM) temperature difference time series, 1860-1959, Earth, first-type two-dimensional presentation
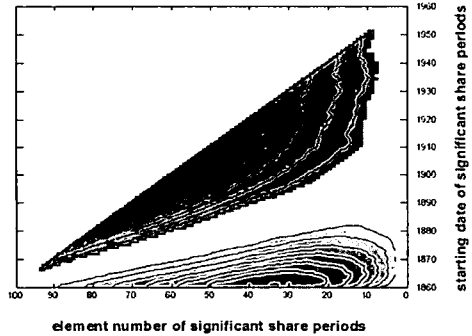
Fig. 2 Sub-periods of which the means differ significantly from that of the D(QTH, QTM) temperature difference time series, 1860-1959, Earth, second-type two-dimensional presentation

The three-dimensional figure (*Fig. 3*) comprises the most complete information on the significant breaks in the data set examined. Namely it consists of all the significant sub-periods with their (1) time interval, namely their starting and ending date (axis x); (2) element number (axis y); and (3) strength.

The maximum and minimum values of the significant probe statistics concerning all the sub-periods (the highest value belonging to the 32-element sub-period, while the lowest one to the 62-element sub-period), as well as frequency of the significant breaks with

different element number (maximum frequencies belong to the 11-element significant positive and the 12-element significant negative breaks) were also computed (*Fig. 4*).
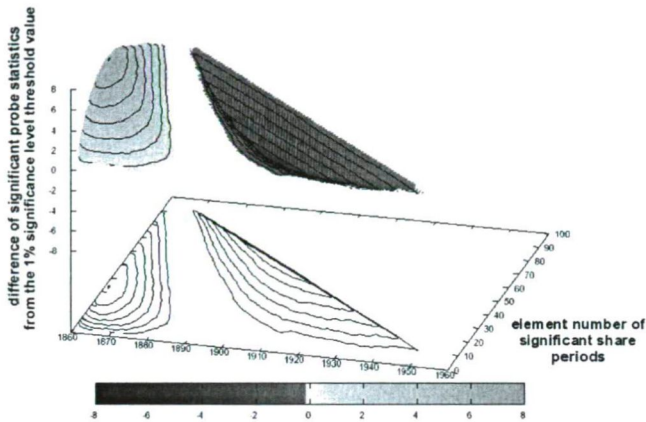
Fig. 3 Sub-periods of which the means differ significantly from that of the D(QTH, QTM) temperature difference time series, 1860-1959, Earth, three-dimensional presentation
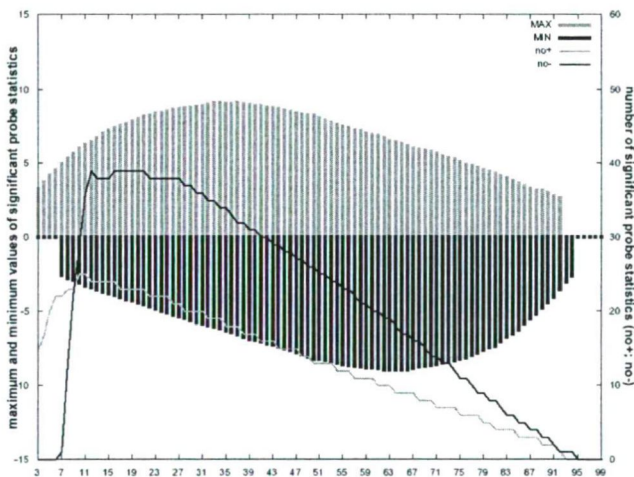
Fig. 4 Sub-periods of which the means differ significantly from that of the D(QTH, QTM) temperature difference time series, 1860-1959, Earth, values and number of significant probe statistics

4.3. Curve-fitting

In order to characterise the differences in the data sets of the simulations, curve-fittings were made. The curves to be fitted were generated on the basis of an exponential function or the difference of two exponential functions (the latter ones seem to be more useful) and different numbers of freely variable parameters were used in the formulas.

Among the curve-fittings applied, generally those of "4dvarlin", "5dvarlin" and "6dvarlin" proved to be the best ones; hence, their analysis will be emphasized in the

following. The first six curve-fittings ("exp", "exp2", "tau", "2dvar", "3dvar", "3dvarlin") comprised only a few parameters; consequently, they were not very good. Adding a new parameter to the curve-fitting of "7dvarlin" did not result in a clear improvement compared to that of "6dvarlin". Generally, the values of SSE and R-square statistics in curve-fitting are nearly identical or even better than those of "6dvarlin". On the other hand, values of the adjusted R-square and the RMSE statistics did not indicate improvement.

4.3.1. QTH global surface temperature time series fits

The curve-fitting of "6dvarlin" seemed to be the best one for this data set. It shows better values for each statistics than those of "4dvarlin" and "5dvarlin". Still out of these latter two fittings "4dvarlin" is better; the adjusted R-square and the RMSE statistics also indicate this. Nevertheless the other two statistics do not show important differences (SSE, R-square) (*Figs. 5-6*).
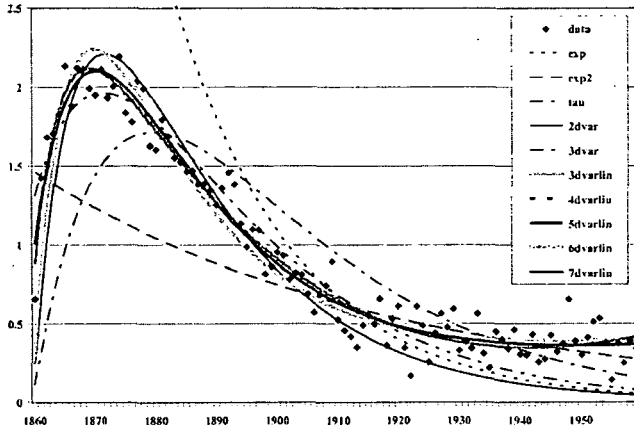
Fig. 5 Curve-fittings, QTH global surface temperature time series1860-1959
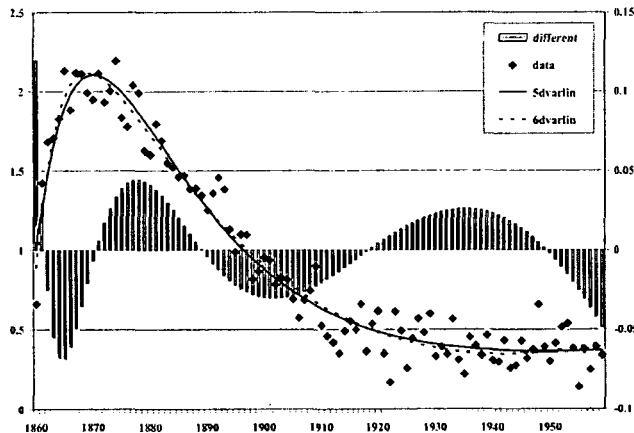
Fig. 6 Comparison of the two best curve-fittings, QTH global surface temperature time series, 1860-1959. Vertical axis on the left shows the original values of the data set; while vertical axis on the right indicates the D(6dvarlin; 5dvarlin) difference

5. CONCLUSION

The more detailed trend analysis applied to all the possible sub-periods of the data sets did not detect any long-range significant trends for the regions examined. The short term significant trends (with not more than 6 elements) can only be observed with higher frequency in the middle third of the D(QTH, QTM) temperature difference times series and in the last fifth of the D(QTK, QTM) times series. The linear trends received can be considered sporadic ones, which are mostly due to the higher variability of the data compared to the temperature anomalies between the simulations. In this way, decreasing tendency in the data sets could not be detected by the trend analysis.

The Makra-test makes it possible to determine whether or not significant differences can be found between the means of two non-independent time series. At a global level the highest significant value of the probe statistics belongs to a 33-element significant positive sub-period between 1861 and 1893, while the lowest significant value refers to a 64-element significant negative one between 1895 and 1958. According to the Makra-test, the difference of the temperature time series proved to be significantly higher at the beginning of the period examined (around 1861-1900), while this effect substantially decreased by the end of the term (around 1881-1958). This near-uniform distribution of the significant breaks in each region considered assumes that the effect of increased CO_2 concentration (QTH) and solar perturbation (QTK) have similar time interval.

The curve-fittings presented in the paper represent the data sets fairly well; however, the best fittings could neither be determined for each case and formula nor could be found to produce definitely the best result for each data set. The curve-fittings found best explain changes (total squared error) of the data sets in fairly high ratios. In some cases, the value of R-square reaches approximately 95%, and its value is generally 80% or so; while its lowest value, only in a few cases, is about 70%. The estimated standard deviations (RMSE) are rather low. They rarely exceed the value of 0.5; in some cases, their values are even below 0.2. These RMSE values are very similar to those of standard deviation in the reference simulation. The run of the fitted curves adjusts to the data: it is increasing in the first period; then, after 10-15 years it reaches its maximum and later is gradually decreasing. However, it should be noted that the fitted curves in several cases indicate slight increasing tendencies at the end of the 100-year period. Therefore, they may rather ruin long-range forecasts. The temperature differences of the simulations should disappear with time, since effects resulting in temperature-increase decline. On the basis of the above results, curve-fittings applied in the paper can be considered fairly good ones; however, better fittings might also be found for long-range forecast.

REFERENCES

Makra, L., Horváth, Sz., Pongrácz, R. and Mika, J., 2002: Long term climate deviations: an alternative approach and application on the Palmer drought severity index in Hungary. *Phys. Chem. Earth B - Hydrology, Oceans and Atmosphere 27,* 1063-1071.

Makra, L., Mika, J. and Horváth, Sz., 2005: 20th century variations of the soil moisture content in East-Hungary in connection with global warming. *Phys. Chem. Earth 30,* 181-186.

http://www.mathworks.com/access/helpdesk/help/pdf_doc/curvefit/curvefit.pdf

http://www.unidata.ucar.edu/software/netcdf/docs/

INTRA-REGIONAL AND LONG-RANGE RAGWEED POLLEN TRANSPORT OVER SOUTHERN HUNGARY

L. MAKRA and S. PÁLFI

Department of Climatology and Landscape Ecology, University of Szeged, P.O.Box 653, 6701 Szeged, Hungary
E-mail: makra@geo.u-szeged.hu

Összefoglalás – A tanulmány célja, hogy a hosszú távú parlagfü pollen szállítás szerepét elemezze Szeged fölött, Délmagyarország térségében a napi pollenkoncentrációk 15 éves (1989-2003) adatbázisa alapján.. A szállított és a helyi eredetű parlagfü pollen szemeket oly módon választottuk szét, hogy a helyi parlagfü virágzása előtt mért parlagfü koncentrációkat nem helyi eredetűnek tekintettük. Ezt követően elemeztük egyrészt a helyi parlagfü virágzása előtti időszak három legnagyobb pollenterhelésű napjának, másrészt a vizsgált időszak három legnagyobb átlagos pollenterhelésű napjának három- és hétnapos, időben visszafelé számított (backward), trajektóriáit. A fenti kiválasztott napokra alkalmaztuk a HYSPLIT-modellt azon célból, hogy kiszámítsuk a parlagfüpollen szemek trajektóriáit, s meghatározzuk azok forrásterületeit. A kapott trajektóriák azt mutatják, hogy amikor nincs helyi pollenszórás Délmagyarország térségében, akkor a Rhône-völgyéből (Franciaország), Észak-Olaszországból és Horvátországból érkezhet parlagfü pollen Délmagyarország fölé. Másrészről, a három legsúlyosabb átlagos pollenterhelésű nap mindegyikének a trajektóriái áthaladnak a Duna-Tisza köze fölött, ami parlagfüvel és pollenjével az egyik leginkább fertőzött területnek számít Magyarországon. Következésképp, a legsúlyosabb pollenterhelésű napokon a szállított pollen tovább emelheti Délmagyarország fölött a levegő pollenkoncentrációját.

Summary – The aim of the study was to analyse the role of long-range transport of ragweed pollen over Szeged City, Southern Hungary on the basis of the daily pollen levels for the 15-year period between 1989-2003. Transported and local pollen grains were separated; ragweed pollen levels measured before the blooming of local ragweed were considered to be of transported origin. Then, 3-day and 7-day backward trajectories belonging partly to the three days having the highest pollen levels before the blooming period of ragweed and partly belonging to the three days having the highest average peak concentrations in the period were examined. For the days selected above, the HYSPLIT model was applied in order to calculate trajectories of airborne ragweed pollen grains, as well as to detect their source areas. The resulting trajectories show that when there is no release of ragweed pollen grains in Szeged and its surroundings, then ragweed pollen may come over the Szeged region from the Rhône-valley (Southern France), Northern Italy and Croatia. On the other hand, each of the trajectories, belonging to the three days having in average the three highest pollen levels during the 15-year period examined (1989-2003), passes through the region between the rivers Danube and Tisza, considered to be one of the areas most polluted with ragweed pollen in Hungary. Hence, transported pollen on the most heavily polluted days can further raise the airborne ragweed pollen concentrations over Southern Hungary.

Key words: HYSLPIT model, trajectory, ragweed pollen grains, source area, days before blooming, days with heaviest pollen load

1. INTRODUCTION

Dust and other aerosols have been applied several times as air mass tracers both in studying atmospheric transport processes and in paleoclimatological analyses (*Biscaye et al.*, 1997; *Kahl et al.*, 1997; *Bory et al.*, 2002). Some of the researchers used bioaerosols to trace air masses. Concerning the long-range transport of airborne pollen grains, many

studies have already been published (*Hjelmroos*, 1991; *Franzen et al.*, 1994; *Hjelmroos and Franzen*, 1994; *Cabezudo et al.*, 1997; *Campbell et al.*, 1999; *Bourgeois et al.*, 2000, 2001). Further proofs of transported pollen are reported in works of e.g. *Smith et al.* (2005); *Gassmann and Perez* (2006), *Hicks and Isaksson* (2006) and *Lorenzo et al.* (2006). Trajectory models, no matter whether they are backward or forward in time, show that pollen transport is a fairly complex process: it comprises both extended vertical changes of the air masses and long distances covered by them from the source area during a short time interval. It was *Rousseau* (*Rousseau et al.*, 2003, 2004, 2005), who firstly deduced a complete trajectory of the whole movement of the air masses responsible for the transportation of airborne pollen grains to Southern Greenland, released over the eastern part of North-America.

According to the literature, no study has been published so far on long-range pollen transport over Southern Hungary. The aim of this paper is to detect transported pollen over the region examined, to determine the direction of the transport and potential source areas of the transported pollen; furthermore, to calculate its potential role on the three days having the highest pollen levels before the blooming period of ragweed and also on the three days having the highest average peak concentrations in the period examined. With the help of the HYSPLIT model, trajectories of ragweed (*Ambrosia*) pollen grains were determined, their source areas were indicated and the air masses concerned were established.

2. DATA

2.1. Pollen database

The pollen concentration over Szeged has been measured with a high volume Hirst-type pollen trap (Lanzoni VPPS 2000) since 1989 (*Hirst*, 1952). The air sampler is placed on the roof of the building of the Faculty of Arts, University of Szeged, at a height of 20 m above the urban surface. The building itself is one of the highest in the downtown. Daily pollen data were calculated in the way suggested by *Käpylä and Penttinen* (1981). The data indicate the number of ragweed pollen grains in 1 m^3 of air. The database consists of daily ragweed pollen grain concentrations for the 15-year period between 1989-2003. Firstly, those three days were examined, which showed the three highest ragweed pollen levels before the blooming period. These days were 21 June, 1993; 3 July, 2000 and 6 July, 2003, when 3, 4 and again 4 ragweed pollen grains were found on the sampling site, respectively. Secondly, three days were selected in this term, of which the average ragweed pollen levels were the highest; namely, in decreasing order: 27 August, 1991 (2,003 ragweed pollen grains); 28 August, 1994 (1,899) and 24 August, 1992 (1,658).

2.2. Meteorological database (Global Re-Analyses)

The meteorological database applied is jointly operated by the National Center for Environmental Prediction (NCEP) and the National Center for Atmospheric Research (NCAR) in the United States, comprising data from the period between 1948-2005. The basic surface for the database is the Gauss sphere, from which the projection takes place, in our case into the Mercator cylindrical projection. This database can be reached from ARL (Atmospheric Research Laboratory, USA) in a format suitable for performing calculations

for transport and dispersion with the HYSPLIT model. The database applies meteorological parameters for modelling. For this aim, the Global Re-Analysis comprises data of several Hungarian and European meteorological stations as well.

3. METHODS

3.1. Google Earth

Google Earth (*http://www.earth.google.com/*) service can be downloaded and used freely. It represents a virtual Earth with high resolution satellite pictures. By applying Google Earth, 3D graphics and broad band „streaming" technology, the users can practically enlarge picture scales free, and their elaboration is set automatically to the actual height of sight by the programme.

3.2. Mercator cylindrical projection

The major advantage of this map is that it is free from longitudinal distortion along each meridian and, therefore, the determination of the points of the compass is simple at any location of the map. Namely, the north-south and east-west directions are parallel with the vertical and horizontal sides of the rectangle; hence, geographical co-ordinates of various locations and air pressure formations can easily be determined with the help of the spaces indicated on the rectangle both horizontally and vertically (and, if required, by making linear interpolation). The only drawback of its use is that the background map becomes longer at higher latitudes in east-west direction.

3.3. Description of the HYSPLIT model

The HYSPLIT-4 model (HYbrid Single Particle Lagrangian Integrated Trajectories) (*http://www.arl.noaa.gov/ready/hysplit4.html*) was developed in the National Oceanic and Atmospheric Administration (NOAA) and in the Atmospheric Research Laboratory (ARL), USA (*Draxier and Hess*, 1998). Its first version was prepared in 1982 and its latest, the fourth, was published in 2004 after persistent development,. The model is a complete system, able to calculate simple trajectories as well as to run complex simulations for dispersion and deposition either for one particle or for a big amount of emission.

HYSPLIT-4 is a Lagrangian trajectory model that estimates particle movement in both forward and backward directions. Lagrangian methods are favoured when point source emissions are restricting computations to a few grid points. Lagrangian models compute advection and dispersion components individually. The HYSPLIT-4 model available on the web applies archive meteorological data, by which the movement of any pollutant, either coming from a source area, or arriving to a given region, can be detected. Hence, considering a point with its geographical coordinates, we could determine that from which direction the pollutant arrived there, or to which direction it moved on further. Results can be presented on three different projections (polar plain, Lambert plain, or Mercator cylindrical). In this paper Mercator cylindrical projection was used.

During an average run, the HYSPLIT model calculates trajectories for given time intervals, starting from the point given by the user. In this case we receive long temporal series of trajectories. Namely, by running a mere model, e.g. a trajectory starting in every three hours can be calculated for a one-month period. Each trajectory of the series comes

from the same starting point and, of course, more than one starting points can also be defined. In this way, since the trajectories can overlap one another in time, several trajectories starting from the same point can be received.

4. RESULTS

4.1. Pollen transport on peak days before the blooming period

In this paper, using the geographical coordinates of Szeged, the HYSPLIT-4 model was used to investigate the long-range transport of airborne ragweed pollen over Southern Hungary. The figures show three different trajectories, separated by the streaming height of the air masses, come over Szeged. Air currents taking part in long-range pollen transport move between the heights of 500 m and 3,000 m (*Rousseau*, 2004, 2005). In order to cover this vertical range, trajectories of the pollen transport were examined at heights of 500 m, 1,500 m and 3,000 m, respectively. The model was run for a one-week period and, in favour of better visibility, for a three-day term, too. The model calculates trajectories in every six hours, which are indicated by points, triangles and squares on the figures. On each figure, trajectories of different heights are indicated with the following colours: 500 m – red; 1,500 m – blue and 3,000 m – green.

Consider the first selected day: 21 June, 1993 (*Fig. 1*). On this day 3 pollen grains were collected by the pollen trap. The figure clearly shows that all the three air masses departed from over the Atlantic Ocean and crossing the southern part of the British Isles reached Northern Italy through France. Northern Italy seems to be polluted with ragweed pollen. This region is characterised by long, warm and dry summers and shorter and rainy autumn and winter seasons. In this climate, warmer compared to that in Southern Hungary, the blooming of ragweed begins earlier. The climatic differences of different geographical positions appear in the pollination period of ragweed as well. In the Mediterranean the release of ragweed pollen starts as early as the end of June or the beginning of July.

According to *Fig. 1*, air masses moving at the height of 1,500 m and 3,000 m reach the Szeged region through Croatia. However, in our case air currents moving at the height of 500 m are of special importance, since they run at a lower height over the pollen-loaded region. These air currents arrive over Szeged through Switzerland and Austria, crossing Northwestern Hungary and the region between the rivers Danube and Tisza. The role of air currents moving at lower heights seems to be more important, since over a pollen-loaded region the height that a pollen grain can reach depends on the speed of the upwelling. Air currents, passing through a region at a lower height, can take up pollen grains with higher chance.

On the 2nd day examined (3 July, 2000) 4 pollen grains were collected (*Fig. 2*). Air currents arrived over the Szeged region from southwestern direction passing through Northern Italy. All the three trajectories went through Croatia, which indicates a mediterranean climate impact. This country shows similarly severe ragweed pollen load in the air as Hungary. Air currents moving at the heights of 500 m and 1,500 m pass through the Dinari Mountains, then cross the productive regions of ragweed pollen and transport pollen over Hungary including the region of Southern Hungary (*Fig. 2*).

The last day examined before the pollination period of ragweed was 6 July, 2003. Though this date is close to the blooming of ragweed in Hungary the 4 ragweed pollen grains found in the pollen trap this day and the pollen-free period of the following three

days indicate transported pollen (*Fig. 3*). According to the map (*Fig. 3*), trajectories of air currents moving at the height of 500 m and 1,500 m are near to each other, they run almost along a parallel curve and pass through France over the Rhône-valley, then after crossing Northern Italy and Northern Austria they turn southeast and reach the Szeged region. Both air masses moved at lower heights; therefore, presumably both might have transported pollen in the given period, since both passed over pollen releasing regions. Besides Northern Italy the Rhône-valley, which passes for the third area most seriously loaded with ragweed pollen in Europe, can also be considered as a source area (*Fig. 3*).
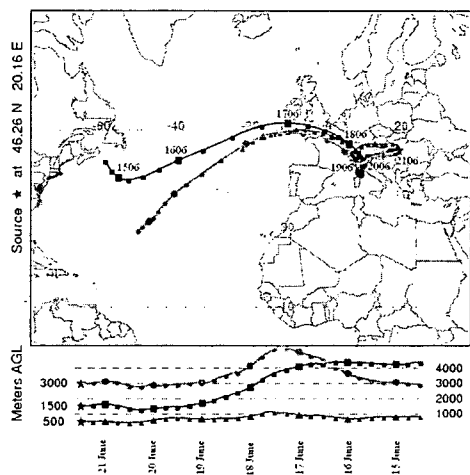
Fig. 1 7-day trajectories belonging to one of the three days having the highest pollen levels before the blooming period, 21 June, 1993
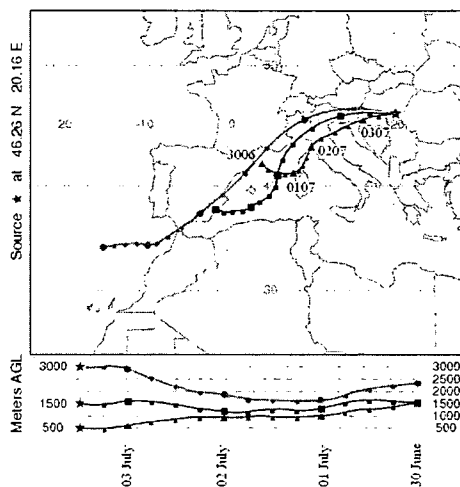
Fig. 2 3.5-day trajectories belonging to one of the three days having the highest pollen levels before the blooming period, 3 July, 2000

On the three days examined there was no precipitation; hence, there was no wet deposition either. The hot and dry weather experienced then was ruled by an anticyclone. Namely, pollen grains deposited on the pollen trap during a high pressure system, with the contribution of descending air currents.

4.2. Pollen transport on peak days within the blooming period

Those three days that were in average the most seriously loaded with ragweed pollen, were selected from the 15-year period examined.

Among the 4-day trajectories belonging to the day having in average the highest pollen level, the air current at the height of 3,000 m comes from the British Isles, while that at the height of 1,500 m arrives from the temperate belt Atlantic region and both cross Southern Germany and Austria. However, the trajectory at the height of 500 m is more important and it covers a very simple and short path within the Carpathian Basin. A common characteristic is that all the three trajectories pass through the region between the rivers Danube and Tisza before reaching Southern Hungary (*Fig. 4*).
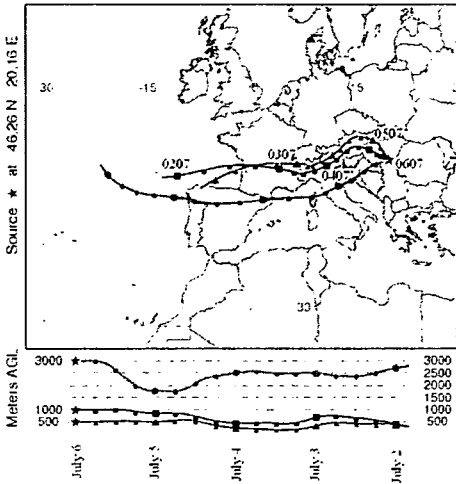
Fig. 3 4-day trajectories belonging to one of the
three days having the highest pollen levels
before the blooming period, 6 July, 2003
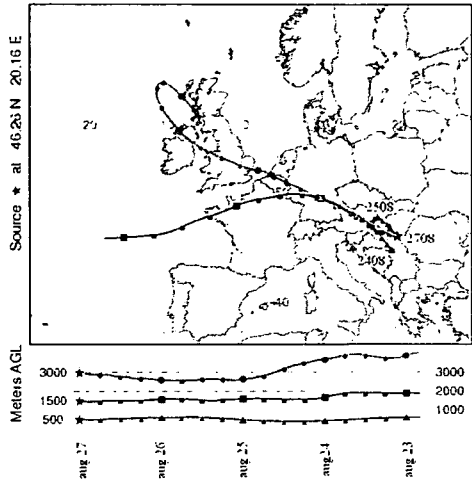
Fig. 4 4-day trajectories belonging to the day
having in average the highest pollen level
during the 15-year period examined
(1989-2003), 27 August, 1991
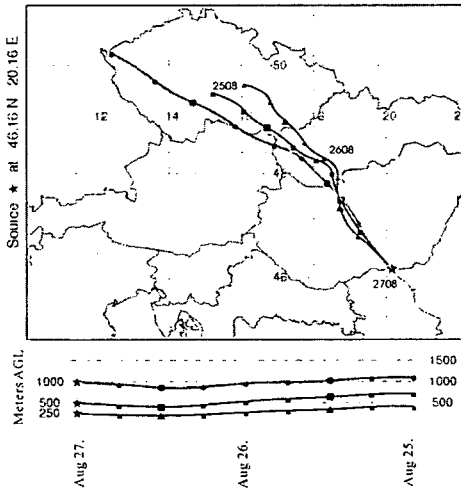
Fig. 5 2-day trajectories belonging to the day
having in average the highest pollen level
during the 15-year period examined
(1989-2003), 27 August , 1991
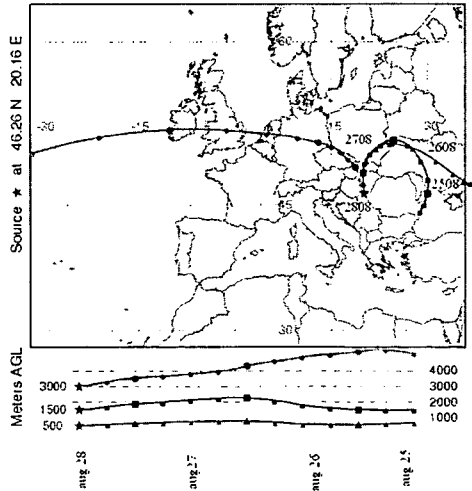
Fig. 6 4-day trajectories belonging to the day
having in average the 2nd highest pollen level
during the 15-year period examined
(1989-2003), 28 August, 1994

Among the 2-day trajectories calculated for 27 August, 1991 (*Fig. 5*), the air current
moving at the height of 500 m started from the middle part of the Czech Republic, then
passed through southwest Slovakia (Csallóköz) and the region between the rivers Danube
and Tisza, when at last it arrived over Szeged (Southern Hungary). All of the areas listed
above have ragweed and its pollen levels are especially high over the latter two regions. On
28 August, 1994 (*Fig. 6*) air masses arrived over Southern Hungary both from northwest

and northeast. With their contribution, ragweed pollen grains might have arrived over Szeged from Slovakia. However, similarly to the earlier case, the area between the rivers Danube and Tisza can be considered to be the primary and basic source of ragweed pollen over Szeged at this time (*Figs. 6-7*).
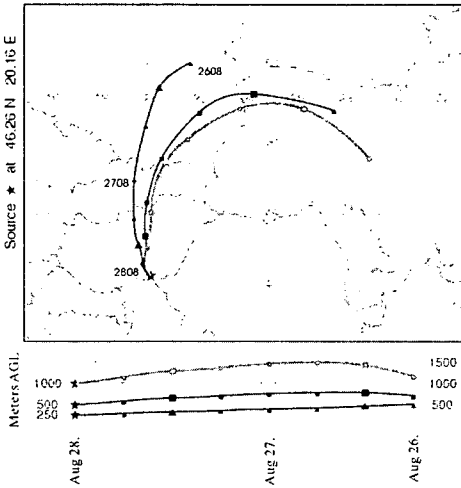
Fig. 7 2-day trajectories belonging to the day having in average the 2nd highest pollen level during the 15-year period examined (1989-2003), 28 August, 1994
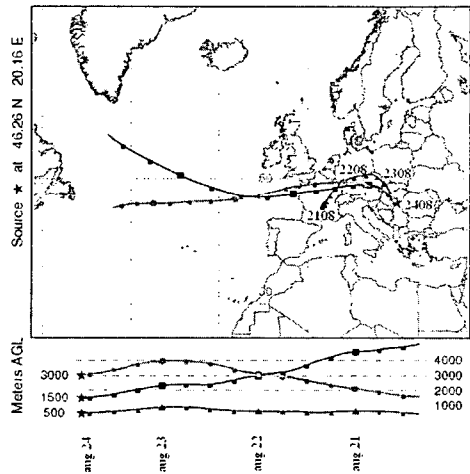
Fig. 8 4-day trajectories belonging to the day having in average the 3rd highest pollen level during the 15-year period examined (1989-2003), 24 August, 1992

In average, the 3rd highest pollen level during the 15-year period examined occurred in Szeged on 24 August, 1992 (*Figs. 8-9*). Among the three trajectories, air masses moving at the height of 500 m can mainly be responsible for pollen transport. This trajectory crosses the eastern part of France, partly the Rhône-valley, then passes through the Czech Republic, Eastern Slovakia and the middle part of Hungary *Figs. 8-9*).

According to *Figs. 3-4, 6 and 8*, all the trajectories pass through the region between the rivers Danube and Tisza, which is supposed to be the main source of transported pollen. Although less important, ragweed pollen can be derived from the Rhône-valley, Csallóköz (Southwestern Slovakia), as well as from the south, namely from Vojvodina (Northern Serbia). However, the latter area is less realistic in the cases examined.
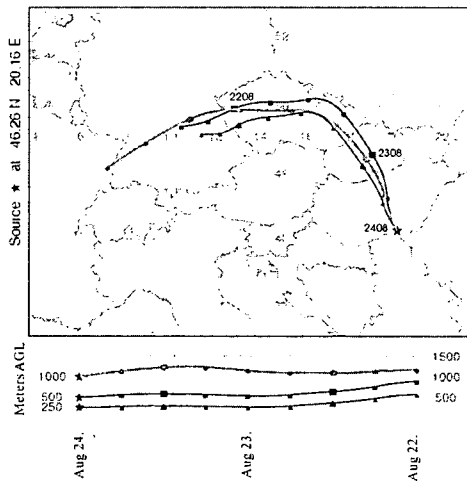
Fig. 9 2-day trajectories belonging to the day having in average the 3rd highest pollen level during the 15-year period examined (1989-2003), 24 August, 1992

Then the peak days of pollen release were coupled to the 2-day trajectories for the heights of 250 m, 500 m and 1,000 m, passing through the region between the rivers Danube and Tisza, in order to refine further the spatial scales of the transport. The results received for low elevations, being within the boundary layer, confirm those related to the higher levels. Pollen levels of all the three days having the highest pollen release over Szeged are influenced by transported pollen from the region, which is one of the most polluted over Hungary.

5. CONCLUSIONS

Since the blooming period of ragweed begins in Southern Hungary at the middle of July, airborne pollen grains collected in this region before this period might have arrived from long distances over this area. Three days having the highest pollen levels before the blooming were examined. The resultant trajectories showed that pollen grains can be originated from the Rhône-valley (France), Northern Italy and Croatia. The climate of the regions listed above, according to the Köppen climate classification, is mediterranean (Cs), which is characterised by warm-temperate climate with winter precipitation and summer drought. As the increasing temperature and decreasing humidity favours pollen formation (*Makra et al.*, 2004, 2005); hence, the pollination period of ragweed with its blooming begins earlier in the above regions than in Southern Hungary. This makes possible detecting ragweed pollen over Szeged before the blooming period.

Furthermore, it was also revealed that on each of the three days with the highest pollen release of the 15-year period examined, air currents arrived over Southern Hungary crossing the region between the rivers Danube and Tisza.

There is a significant relation between the daily pollen number and wind speed with both positive and negative signs. This seems to explain both high and low pollen concentrations as a consequence of high wind speed. This fact might hint at the ambivalent role of wind speed (*Makra et al.*, 2004). Since air currents mainly determine trajectories and, at the same time, pollen transport, study of the latter one is worth of distinguished attention.

As a result, it can be established that ragweed pollen concentrations measured at Szeged are partly of non-local origin. Long-range pollen transport contributes to the extreme pollen levels over Southern Hungary, which produces serious health decay of patients concerned in ever increasing ratio. Transported pollen has an apparent role in local pollen levels; however, precise calculations of both its concentration and the ratio of local and transported pollen grains need further analysis.

REFERENCES

Biscaye, P.E., Grousset, F.E., Revel, M., Van der Gaast, S., Zielinski, G.A., Vaars, A. and Kukla, G., 1997: Asian provenance of glacial dust (Stage 2) in the Greenland Ice Sheet Project 2 Ice Core, Summit, Greenland. *J. Geophysical Research-Oceans 102(C12)*, 26765-26781.

Bory, A.J.M., Biscaye, P.E., Svensson, A. and Grousset, F.E., 2002: Seasonal variability in the origin of recent atmospheric mineral dust at NorthGRIP, Greenland. *Earth and Planetary Science Letters 196(3-4)*, 123–134.

Bourgeois, J.C., Koerner, R.M., Gajewski, K. and Fisher, D.A., 2000: A holocene ice-core pollen record from Ellesmere Island, Nunavut, Canada. *Quaternary Research 54(2)*, 275-283.

Bourgeois, J.C., Gajewski, K. and Koerner, R.M., 2001: Spatial patterns of pollen deposition in arctic snow. *Journal of Geophysical Research-Atmospheres 106(D6)*, 5255-5265.

Cabezudo, B., Recio, M., SanchezLaulhe, J.M., Trigo, M.D., Toro, F.J. and Polvorinos, F., 1997: Atmospheric transportation of marihuana pollen from North-Africa to the southwest of Europe. *Atmos. Environ. 31(20)*, 3323-3328.

Campbell, I.D., McDonald, K., Flannigan, M.D. and Kringayark, J., 1999: Long-distance transport of pollen into the Arctic. *Nature 399(6731)*, 29-30.

Draxier, R.R. and Hess, G.D., 1998: An overwiew of the HYSPLIT_4 modelling system for trajectories, dispersion and deposition. *Australian Meteorol. Magazine 47(4)*, 295-308.

Franzen, L.G., Hjelmroos, M., Kallberg, P., Brorstromlunden, E., Juntto, S. and Savolainen, A.L., 1994: The yellow-snow episode of Northern Fennoscandia, March-1991. A case-study of long-distance transport of soil, pollen and stable organic-compounds. *Atmos. Environ. 28(22)*, 3587 –3604.

Gassmann, M.I. and Perez, C.F., 2006: Trajectories associated to regional and extra-regional pollen transport in the southeast of Buenos Aires province, Mar del Plata (Argentina). *Int. J. Biometeorol. 50(5)*, 280-291.

Hicks, S. and Isaksson, E., 2006: Assessing source areas of pollutants from studies of fly ash, charcoal, and pollen from Svalbard snow and ice. *J. Geophysical Research-Atmospheres 111 (D2)*, Art. No. D02113

Hirst, J.M., 1952: An automatic volumetric spore trap. *Annales of Applied Biology 39*, 257-265.

Hjelmroos, M., 1991: Evidence of long-distance transport of Betula pollen. *Grana 30*, 215-228.

Hjelmroos, M. and Franzen, L.G., 1994: Implications or recent long-distance pollen transport events for the interpretation of fossil pollen records in Fennoscandia. *Review of Palaeobotany and Palynology 82(1–2)*, 175–189.

Kahl, J.D.W., Martinez, D.A., Kuhns, H., Davidson, C.I., Jaffrezo, J.L. and Harris, J.M., 1997: Air mass trajectories to Summit, Greenland: A 44-year climatology and some episodic events. *J. Geophysical Research-Oceans 102(C12)*, 26861-26875.

Käpylä, M. and Penttinen, A., 1981: An evaluation of the microscopial counting methods of the tape in Hirst-Burkard pollen and spore trap. *Grana 20*, 131-141.

Lorenzo, C., Marco, M., Paola, D.M., Alfonso, C., Marzia, O. and Simone, O., 2006: Long distance transport of ragweed pollen as a potential cause of allergy in central Italy. *Annals of Allergy, Asthma and Immunology 96(1)*, 86-91.

Makra, L., Juhász, M., Borsos, E. and Béczi, R., 2004: Meteorological variables connected with airborne ragweed pollen in Southern Hungary. *Int. J. Biometeorol. 49*, 37-47.

Makra, L., Juhász, M., Béczi, R. and Borsos, E., 2005: The history and impacts of airborne Ambrosia (Asteraceae) pollen in Hungary. *Grana 44*, 57-64.

Rousseau, D.D., Duzer, D., Cambon, G., Jolly, D., Poulzen, U., Ferrier, J., Schevin, P. and Gros, R., 2003: Long distance transport of pollen to Greenland. *Geophysical Research Letters 30 (14)*, p. 1766.

Rousseau, D.D., Duzer, D. Etienne, J.L., Cambon, G., Jolly, D., Ferrier, J. and Schevin, P., 2004: Pollen record of rapidly changing air trajectories to the North Pole. *J. Geophysical Research-Atmosphere 109(D6)*, D0616

Rousseau, D.D. Schevin, P. Duzer, D. Cambon, G. Ferrier, J. Jolly, D. and Poulsen, U., 2005: Pollen transport to southern Greenland: new evidences of a late spring long distance transport. *Biogeosciences Discussions 2*, 829-847.

Smith, M., Emberlin, J. and Kress, A., 2005: Examining high magnitude grass pollen episodes at Worcester, United Kingdom, using back-trajectory analysis. *Aerobiologia 21(2)*, 85-94.

http://www.arl.noaa.gov/ready/hysplit4.html

http://www.earth.google.com

OBJECTIVE ANALYSIS AND RANKING OF HUNGARIAN CITIES, WITH DIFFERENT CLASSIFICATION TECHNIQUES, PART 1: METHODOLOGY

L. MAKRA and Z. SÜMEGHY

Department of Climatology and Landscape Ecology, University of Szeged, P.O.Box 653, 6701 Szeged, Hungary
E-mail: makra@geo.u-szeged.hu

Összefoglalás – A tanulmány célja, hogy a magyarországi városokat és megyéket környezetminőségük és környezeti tudatosságuk szintje alapján osztályozza. Ahhoz, hogy ezt a feladatot megoldjuk, kiszámítottuk a „Green Cities Index", illetve a „Green Counties Index" értékeket, melyek alapján a városokat és a megyéket 7 különböző kategória 19 környezeti indikátora segítségével rangsoroltuk. Ezt követően azt a célt tűztük ki, hogy összehasonlítsuk a különböző clusterező eljárásokat a városok és megyék osztályozásában. Az SPSS szoftver segítségével elvégzett clusteranalízis mind a városokra, mind a megyékre 6-6 homogén csoportot eredményezett. Az R-nyelv segítségével végrehajtott clusteranalízis az *agnes*, a *fanny* és a *pam* algoritmusok felhasználásával történt.

Summary – The aim of the study was to rank and classify Hungarian cities and counties according to their environmental quality and level of environmental awareness. To accomplish this task, „Green Cities Index" and „Green Counties Index" were calculated that rank cities and counties on the basis of seven different categories of 19 environmental indicators. Furthermore, our aim was to compare different methods in classifying cities and counties. Cluster analysis using SPSS software resulted in 6 homogenous groups for both the cities and the counties. Clustering with R-language was carried out using algorithms *agnes*, *fanny* and *pam*.

Key words: environmental indicators, Green Cities Index, Green Counties Index, factor analysis, clustering, SPSS-software, R-language; algorithms: agnes, fanny, pam

1. INTRODUCTION

In Hungary, 236 cities accounting for 65.7 % of the country's population were registered on January 1, 2001. Environmental factors in cities such as housing, transportation, air quality and public green space, etc., are important for the quality of life (*Kerényi*, 1995). But which cities have cleaner air, more urban parkland, or more pleasant climate? Which do a better job at organising traffic systems, waste management or public sanitation? Which cities are wasteful in their use of water or energy? To answer these questions, at least at a preliminary level, the so-called "Green Cities Index", which ranks cities on several environmental criteria, was developed (*Cutter*, 1992).

In this study, 25 environmental indicators were initially considered for each of the 236 Hungarian cities. Indicators, which were not available for all cities, were subsequently omitted. The cities were ranked by population and population density as well. However, these two parameters were not included for ranking according to the Green Cities Index, since larger and more densely populated cities do not necessarily have poorer environmental quality. Because environmental regulations in many cities have become

increasingly more stringent, part of the data used in this study may be out of date by the date of publication. Consequently, Green Cities Index rankings should be viewed as a measure of environmental quality and concern at a given time.

The data basis for the study is drawn partly from the statistical yearbooks of Hungarian counties and Budapest for the year 2000 (*HCSO*, 2000a, 2000b) and partly from *Vaskövi* (2000).

2. OBJECTIVES

The aim of the study is to rank and classify Hungarian cities and counties according to their environmental quality and level of environmental awareness. A further aim of the study is to compare results received after performing hierarchical, agglomerative clustering techniques of both the SPSS software and the R-language. Besides, the spatial distribution of clusters received is also compared and their connection with the planning-statistical regions of Hungary is evaluated.

The different clustering techniques are found in most statistical softwares. These algorithms are represented by using the R-language.

3. METHODS

3.1. Environmental indicators

Seven different categories of environmental indicators ranging from water consumption to air quality were included in the Green Cities Index. Specific measures within each category were selected on the basis of data availability. Some related measures were combined to yield new, composite measures. Altogether 25 indicators were considered initially but only 19 were retained with 7 categories and their 19 indicator elements (*Table 1*). In *Table 1*, air quality is based on the average of the non-heating half-year (April 1, 2000 – September 30, 2000) and the average of the heating half-year (October 1, 2000 – March 31, 2001). Heating (cooling) degree-days are defined as the number of days when the mean temperature is above (below) 18°C, with each day weighted by the number of degrees above (below) 18°C. This parameter can be used as a measure of energy use for space heating (cooling) (Cutter, 1992). 18°C is considered the optimum temperature.

Data on all 19 indicators are available for only 88 of the 236 cities in the data base. Hence, further analyses are based on those 88. Though these indicators are neither perfect nor exhaustive, they enable an overall comparison among the relevant cities.

3.1.1. The Green Cities Index

The Green City Index is derived as follows
(a) The statistics for each indicator for each city were compiled from the yearbooks.
(b) Each indicator element was represented with a serial number (1 – 19).
(c) For each indicator element, cities were ranked from the most environmentally friendly
    (1) to least friendly (88) based on their statistics as determined in step (a). These
    ranks represent city scores on each indicator.

(d) The rank scores achieved by each city over the 19 indicator elements were averaged. The resulting figure is the Green City Index.

(e) Finally, the Green City Indices were ranked to yield the Final Sequence. The Final Sequence (FS) places the cities in rank order from the best (1) to the worst (88) based on step (d). FS is a rank of ranks.

Table 1 Categories and indicators used for compiling the Green Cities Index for the cities and counties

Categories	Indicators		
	Serial No.	Elements	Units
Water Consumption	1	Water use	m³ / capita / year
Energy Consumption	2	Gas consumption	m³ / household / year
	3	Electric energy consumption	kWh / household / year
	4	Degree days	sum of heating and cooling degree days
Public Utilities Supply	5	Ratio of households connected to gas network	percent
	6	Ratio of dwellings connected to drinking water network	percent
	7	Ratio of dwellings connected to public sewage system	percent
	8	Public sewage system	m / km drinking water conduit
Traffic	9	car supply	inhabitants per car
Waste management	10	Total drained-off waste water	m³ / capita / year
	11	Total waste removed	m³ / capita / year
	12	Ratio of dwellings connected to regular waste removal system	percent
Settlement amenities factors	13	Public green area	m² / capita
	14	Ratio of constructed inner roads	percent
	15	Ratio of constructed public surfaces cleaned regularly	percent
	16	Housing	occupants / dwelling

Table 1 (cont.)

Categories	Indicators		
	Serial No.	Elements	Units
Air Quality*	17	Average concentration of particulates deposited	g / m² / 30 days
	18	Average concentration of sulphur-dioxide	µg / m³
	19	Average concentration of nitrogen-dioxide	µg / m³

It is to be noted that the indicator elements were not weighted to reflect their relative importance to environmental quality or overall contribution to making a city liveable. Rather, they illustrate how each city fares when compared to others.

Human activities are the greatest source of contaminants in the environment. Thus, population and population density might be important environmental factors. But their implications to environmental quality are frequently contradictory since increases in the size of either variables or both do not automatically indicate a tendency towards poorer environmental quality. For example, compact and highly centralised cities with high population densities have the advantage of decreasing passenger car traffic between the city centre and the suburbs thus contributing to lower air pollution loads. However, such advantage may be countered by more concentrated sources of pollution and waste, and more congestion. On the other hand, cities that sprawl and are dispersed, resulting in lower population densities, may have a difficulty providing mass transit, but they may have more open space. On balance, large centralised cities tend to have greater difficulty achieving the same level of environmental quality than smaller cities. To test the impact of population and population density on the Green Index, a second set of Final Sequence (modified sequence) based on 21 indicator elements – the nineteen original ones, plus population and population density – was derived.

3.1.2. The Green Counties Index

The 19 Hungarian counties were also ranked from the most environment- friendly to the worst. The same environmental indicators as the ones used for the cities were applied. The so-called Green Counties Index values are the average of the scores achieved by all cities within the county. The Green Counties Index, similar to the Green Cities Index, is effectively a rank of ranks. Low numbers indicate better environmental quality.

3.2. Factor analysis

In order to reduce the dimensionality of the above-mentioned meteorological data sets and thus to explain the relations among the 19 variables (environmental indicators), the multivariate statistical method of factor analysis is used. The main object of factor analysis is to describe the initial variables X_1, X_2, ... , X_p in terms of m linearly independent indices ($m < p$), the so called factors, measuring different *"dimensions"* of the initial data set. Each variable X can be expressed as a linear function of the m factors, which are the main contributors to the climate of Szeged:

$$X_i = \sum_{j=1}^{m} \alpha_{ij} F_j \qquad\qquad (1)$$

where α_{ij} are constant called factor loadings. The square of α_{ij} represents the part of the variance of X_i that is accounted for by the factor F_j.

One important stage of this method is the decision for the number (m) of the retained factors. On this matter, many criteria have been proposed. In some studies, the *Guttmann criterion* or *Rule 1* is used, which determines to keep the factors with eigenvalues > 1 and neglect those ones that do not account for at least the variance of one standardised variable X_i. Perhaps the most common method is to specify a least percentage (80 % in this paper) of the total variance in the original variables that has to be achieved (*Jolliffe*, 1993; *Sindosi et al.*, 2003). Extraction was performed by *Principal Component Analysis* (*k*th eigenvalue is the variance of the *k*th principal component). There is an infinite number of equations alternative to Eq. 1. In order to select the best or the desirable ones, the so-called "*factor rotation*" is applied, a process, which either maximises or minimises factor loadings for a better interpretation of the results. In this study, the "*varimax*" or "*orthogonal factor rotation*" is applied, which keeps the factors uncorrelated (*Jolliffe*, 1990, 1993; *Bartzokas and Metaxas*, 1993, 1995).

Factor analysis was applied on the tables of the initial data consisting, in the first case, of 19 columns (environmental indicators) and 88 rows for cities and, in the second, the same 19 columns (environmental indicators) and 19 rows for counties.

3.3. Cluster analysis

Clustering is an organizational methodology dating back to the Ancient Greeks. Aristotle was the first great classifier. He attempted to understand the essence of subgroups of the population. Observing that dolphins have a placenta, Aristotle reasoned that dolphins are mammals, not fish. This insight was greeted with almost uniform derision for nearly two thousand years. The fortunes of taxonomists have barely improved in the interim (*Gould*, 1996).

Objective classification of the cities and counties examined was achieved with the help of cluster analysis. The aim was to group cities and counties objectively based on their similarity in environmental conditions. The basis for the classification is to maximise the homogeneity of cities and counties within the clusters and maximise the heterogeneity among them. The database for the analysis consisted of city (county) scores in each of the 19 environmental indicators measured in 2000.

Cluster analysis is applied to the factor scores time series in order to objectively group days with similar weather conditions. The aim of the method is to maximize the homogeneity of objects within the clusters and also to maximize the heterogeneity between the clusters. Each observation (day) corresponds to a point in the *m*-dimensional space and each cluster consists of those observations, which are "*close*" to each other in this space.

3.3.1. Grouping procedures in R-language

Generally speaking, cluster analysis methods are of either of two types:

Partitioning methods: algorithms that divide the dataset into *k* clusters, where the integer *k* needs to be specified by the user. Typically, the user runs the algorithm for a range

of k-values. For each k, the algorithm carries out the clustering and also yields a „*quality index*", which allows the user to select a value of k afterwards.

Hierarchical methods: algorithms yielding an entire hierarchy of clustering of the dataset. Agglomerative methods start with the situation where each object in the dataset forms its own little cluster, and then successively merge clusters until only one large cluster remains which is the whole dataset. Divisive methods start by considering the whole dataset as one cluster, and then split up clusters until each object is separate.

Algorithms *Pam* and *fanny* of the partitioning type as well as algorithms *Agnes* and *mona* of the hierarchical type are considered in this paper.

3.3.1.1. Partitioning methods

Partitioning Around Medoids: function „pam"

The function *pam* is based on the search for k representative objects, called medoids, among the objects of the dataset (*Kaufman and Rousseeuw*, 1990). These medoids are computed so that the total dissimilarity of all objects to their nearest medoid is minimal: i.e. the goal is to find a subset $\{m_1,\ldots,m_k\} \subset \{1,\ldots,n\}$ which minimizes the objective function:

$$\sum_{i=1}^{n} \min_{t=1,\ldots,k} d(i,m_t)\cdot \tag{2}$$

Each object is then assigned to the cluster corresponding to the nearest medoid. That is, object i is put into cluster v_i when medoid m_{v_i} is nearer to i than any other medoid m_w, or

$$d(i,m_{v_i}) \leq d(i,m_w) \text{ for all } w = 1,\ldots,k\cdot \tag{3}$$

Finally *pam* provides a novel graphical display, the *silhouette plot* (*Rousseeuw*, 1986), and a corresponding *quality index* allowing to select the number of clusters. Let us first explain the silhouette plot. For each object i we denote by A the cluster to which it belongs, and compute

$$a(i) := \frac{1}{|A|-1} \sum_{j \in A, j \neq i} d(i,j)\,, \tag{4}$$

namely, $a(i)$ measures average dissimilarity of i to all other objects of A.

Now consider any cluster C different from A and put

$$d(i,C) := \frac{1}{|C|} \sum_{j \in C} d(i,j)\,, \tag{5}$$

namely, $d(i,C)$ measures average dissimilarity of i to all other objects of C.

After computing $d(i;C)$ for all clusters $C \neq A$, we take the smallest of those:

$$b(i) := \min_{C \neq A} d(i, C). \tag{6}$$

The cluster B which attains this minimum [that is, $d(i;B) = b(i)$] is called the neighbour of object i. This is the second-best cluster for object i.

The silhouette value $s(i)$ of the object i is defined as:

$$s(i) = \frac{b(i) - a(i)}{\max\{a(i), b(i)\}}. \tag{7}$$

Clearly, for $s(i)$: $-1 \leq s(i) \leq 1$. The value $s(i)$ may be interpreted as follows:

$s(i) \approx 1 \Rightarrow$ object i is well classified (in A);
$s(i) \approx 0 \Rightarrow$ object i lies intermediate between two clusters (A and B);
$s(i) \approx -1 \Rightarrow$ object i is badly classified (closer to B than to A).

The silhouette of the cluster A is a plot of all its $s(i)$, ranked in decreasing order. The entire silhouette plot shows the silhouettes of all clusters below each other, so the quality of the clusters can be compared: a wide (dark) silhouette is better than a narrow one.

The quality index mentioned earlier is the overall average silhouette width of the silhouette plot, defined as the average of the $s(i)$ over all objects i in the dataset.

In general *pam* is proposed to run several times, each time with a different k, and to compare the resulting *silhouette plots*. The user can then select that value of k yielding the highest average silhouette width, over all k, which is called the silhouette coefficient. Experience has led to the subjective interpretation of the silhouette coefficient (*SC*). This interpretation does not depend on the number of objects (*Table 2*).

Table 2 Interpretation of the silhouette coefficient (*SC*) for partitioning methods

SC	Proposed interpretation
0.71-1.00	A strong structure has been found
0.51-0.70	A reasonable structure has been found
0.26-0.50	The structure is weak and could be artificial, try additional methods
≤ 0.25	No substantial structure has been found

Fuzzy Analysis: function „fanny"

The functions *pam* is a „*crisp*" clustering method. This means that each object of the dataset is assigned to exactly one cluster. For instance, an object lying between two clusters will be assigned to one of them. However, a fuzzy method spreads each object over the various clusters. For each object i and each cluster v there will be a membership u_{iv} which indicates how strongly object i belongs to cluster v. Memberships have to satisfy the following conditions:

$$u_{iv} \geq 0 \text{ for all } i = 1, \ldots, n \text{ and all } v = 1, \ldots, k .$$

$$\sum_{v=1}^{k} u_{iv} = 1 = 100 \% \text{ for all } i = 1, \ldots, n .$$

We will focus on the method *fanny* (*Kaufman and Rousseeuw*, 1990), where the memberships u_{iv} are defined through minimization of the objective function:

$$\sum_{v=1}^{k} \frac{\sum_{i,j=1}^{n} u_{iv}^2 u_{jv}^2 d(i,j)}{2\sum_{j=1}^{n} u_{jv}^2} . \tag{8}$$

In this expression, the dissimilarities $d(i; j)$ are known and the memberships u_{iv} are unknown. The minimization is carried out numerically by means of an iterative algorithm, taking into account the side constraints on memberships by means of Lagrange multipliers.

Compared to other fuzzy clustering methods, *fanny* has the advantage that it can handle dissimilarity data, since Eq. 8 uses only inter-object dissimilarities and does not involve any averages of objects (*Rousseeuw*, 1995). Also, *fanny* is rather robust to the assumption of spherical clusters since the $d(i; j)$ in (0.5) are not squared.

For any fuzzy clustering, such as the one produced by *fanny*, one can consider the nearest crisp clustering. The latter assigns each object i to the cluster v in which it has the highest membership u_{iv}. This crisp clustering can then be represented by a silhouette plot.

3.3.1.2. Hierarchical methods

Agglomerative Nesting: function „agnes"

The function *agnes* is of agglomerative hierarchical type, hence it yields a sequence of clustering. In the first clustering each of the n objects forms its own separate cluster. In subsequent steps clusters are merged, until (after $n - 1$ steps) only one large cluster remains. Many such methods exist. In *agnes*, the group average method is taken, based on arguments of robustness, monotonicity and consistency. Also four other well-known methods are available in *agnes*, namely single linkage, complete linkage, Ward's method, and weighted average linkage. These five methods can be described in a unified way (*Lance and Williams*, 1966).

The *agglomerative coefficient* (AC) (*Rousseeuw*, 1986) measures the clustering structure of the dataset. For each observation i, denote by $d(i)$ its dissimilarity to the first cluster it is merged with, divided by the dissimilarity of the merger in the last step of the algorithm. AC is then defined as the average of all $1 - d(i)$. It can also be seen as the average width (or the percentage filled) of the banner plot. Note that the AC tends to increase with the number of objects, unlike the average silhouette width. Because it grows with the number of observations, this measure should not be used to compare datasets of very different sizes.

The AC derived by *agnes* measures the goodness of the analyzed hierarchy.

The hierarchy obtained from *agnes* can be graphically displayed in two ways: by means of a *clustering tree* or by a *banner*.

Agglomerative tree: A tree in which the leaves represent objects. The vertical coordinate of the junction of two branches is the dissimilarity between the corresponding clusters. An agglomerative clustering tree is a rotated version of a dendrogram (*Anderberg*, 1973).

Agglomerative banner: The banner shows the successive mergers from left to right. (Imagine the ragged flag parts at the left, and the flagstaff at the right.) The objects are listed vertically. The merger of two clusters is represented by a horizontal bar which

commences at the between-cluster dissimilarity. The banner thus contains the same information as the clustering tree. Note that the agglomerative coefficient (*AC*) defined above can be seen as the average width (the percentage filled) of the banner.

In this study *Ward's* method is used, since it does not depend on extreme values, besides it produces more realistic groupings (*Anderberg*, 1973; *Kalkstein et al.*, 1987; *Hair et al.*, 1998; *Sindosi et al.*, 2003). The database was standardized with the "stand" option of *agnes* before calculating the dissimilarities. In this case the characterization of a distance between two observations *k* and *l* as *"close"* or *"far"* is determined by the square of their Euclidean distance:

$$D_{kl}^2 = \sum_{i=1}^{m}(x_{ki} - x_{li})^2 \tag{9}$$

where x_{ki} is the value of the *i*th factor for the *k*th day and x_{li} is the value of the *i*th factor for the *l*th day.

Monothetic analysis: function „mona"

The function *mona* is a different type of divisive hierarchical method, which operates on a data matrix with binary variables. For each split *mona* uses a single (well-chosen) variable, which is why it is called a monothetic method. Most other hierarchical methods (including *agnes*) are polythetic, i.e. they use all variables simultaneously.

The output of the function *mona* facilitates evaluating a divisive banner, which is defined as follows. Divisive banner: The banner shows the successive mergers from left to right. (Imagine the ragged flag parts at the right, and the flagstaff at the left.) The objects are listed vertically. The merger of two clusters is represented by a horizontal bar which commences at the between-cluster dissimilarity.

Introduce the following notations:

$$E_v = \sum_{\substack{c \in C \\ v(c)=1}} 1 \quad \text{and} \quad N_v = \sum_{\substack{c \in C \\ v(c)=0}} 1 \tag{10}$$

where *C* is an optional group, while v is a contingency table of any v_i and v_j variables:

	N_{v_j}	E_{v_j}
N_{v_i}	$a(v_i, v_j)$	$b(v_i, v_j)$
E_{v_i}	$c(v_i, v_j)$	$d(v_i, v_j)$

Mark

$$con(v_i, v_j) = a(v_i, v_j)d(v_i, v_j) - b(v_i, v_j)c(v_i, v_j), \tag{11}$$

relation of the variables v_i and v_j. The total association of a variable v is defined by the following formula:

$$\sum_{i=1}^{|v|} con(v, v_i), \tag{12}$$

87

where *V* is the set of variables. The variable used for splitting a cluster is the variable with the maximal total association to the other variables, according to the observations in the cluster to be splitted.

A cluster is divided into one cluster with all observations having value 1 for that variable, and another cluster with all observations having value 0 for that variable.

The clustering hierarchy constructed by *mona* can also be represented by means of a divisive banner. The length of a bar is now given by the number of divisive steps needed to make that split. Inside the bar, the variable is listed which was responsible for the split. A bar continuing to the right margin indicates a cluster that cannot be split.

All statistical computations were performed with SPSS (version 9.0) and R softwares.

REFERENCES

Anderberg, M.R., 1973: *Cluster Analysis for Applications.* Academic Press, New York. 353 p.

Bartzokas, A. and Metaxas, D.A., 1993: Covariability and climatic changes of the lower troposphere temperatures over the Northern Hemisphere. *Nouvo Cimento della Societa Italiana di Fisica C Geophysics and Space Physics 16C*, 359-373.

Bartzokas, A. and Metaxas, D.A., 1995: Factor Analysis of Some Climatological Elements in Athens, 1931-1992: Covariability and Climatic Change. *Theor. and Appl. Climato. 52*, 195-205.

Cutter, S.L., 1992: Green Cities. Ranking major cities by environmental quality reveals some surprises. In: *Hammond, A.* (ed.): *Environmental Almanac.* World Resources Institute – Houghton Mifflin Company, Boston. 169-186.

Gould, S.J., 1996: *Full house: The spread of excellence from Plato to Darwin.* Harmony, New York. 38-42.

Hair, J.F., Anderson, R.E., Tatham, R.L. and Black, W.C., 1998: *Multivariate data analysis.* 5th ed. Prentice Hall, New Jersey. 730 p.

HCSO, 2000a: Budapest Statisztikai Évkönyve, 2000. [*Statistical Year Book of Budapest, 2000.* (in Hungarian)] HCSO, Budapest.

HCSO, 2000b: *Megyei Statisztikai Évkönyvek, 2000. [Statistical Year Books of the Hungarian Counties, 2000.* (in Hungarian)] HCSO, Budapest.

Jolliffe, I.T., 1990: Principal component analysis: A beginner's guide – I. Introduction and application. *Weather 45*, 375-382.

Jolliffe, I.T., 1993: Principal component analysis: A beginner's guide – II. Pitfalls, myths and extensions. *Weather 48*, 246-253.

Kalkstein, L.S., Tan, G. and Skindlov, J.A., 1987: An evaluation of three clustering procedures for use in synoptic classification. *Journal of Climate and Applied Meteorology 26*, 717-730.

Kaufman, L. and Rousseeuw, P.J., 1990: *Finding Groups in Data: An Introduction to Cluster Analysis.* Wiley-Interscience, New York. (Series in Applied Probability and Statistics). 342 p. ISBN 0-471-87876-6

Kerényi, A., 1995: *Általános környezetvédelem. Globális gondok, lehetséges megoldások. [General Environmental Protection. Global concerns, possible solutions.* (in Hungarian)] Mozaik Educational Studio, Szeged. 383 p. ISBN 963 8024 75 5

Lance, G.N. and Williams, W.T., 1966: A general theory of classificatory sorting strategies: 1. Hierarchical systems. *Computer Journal 11*, 195.

Rousseeuw, P.J., 1986: A Visual Display for Hierarchical Classification. In: *Diday, E., Escoufier, Y., Lebart, L., Pages, J., Schektman, Y. and Tomassone, R.* (eds.): *Data Analysis and Informatics 4*. North-Holland. 743–748.

Rousseeuw, P.J., 1995: Fuzzy Clustering at the Intersection. *Technometrics 37*, 283–286.

Sindosi, O.A., Katsoulis, B.D. and Bartzokas, A., 2003: An objective definition of air mass types affecting Athens, Greece; the corresponding atmospheric pressure patterns and air pollution levels. *Environmental Technology 24*, 947-962.

Vaskövi, B., 2000: Országos levegőminőségi (immissziós) adatok 2000. április- szeptember, nem fűtési félév. [National air quality (immission) data 2000 April - September, non-heating half-year. (in Hungarian)] *Egészségtudomány 44(4)*, 366-377.

OBJECTIVE ANALYSIS AND RANKING OF HUNGARIAN CITIES, WITH DIFFERENT CLASSIFICATION TECHNIQUES, PART 2: ANALYSIS

L. MAKRA and Z. SÜMEGHY

Department of Climatology and Landscape Ecology, University of Szeged, P.O.Box 653, 6701 Szeged, Hungary
E-mail: makra@geo.u-szeged.hu

Összefoglalás – A tanulmány célja, hogy a magyarországi városokat és megyéket környezetminőségük és környezeti tudatosságuk szintje alapján osztályozza. Bemutatjuk a magyarországi városok és megyek rangsorát azok „Green Cities Index", illetve a „Green Counties Index" értékeinek összevetésével. Az 1. részben (*Makra and Sümeghy*, 2007) bemutatott módszertan szerint a városokat, illetve megyéket eltérő klasszifikációs technikák szerint osztályoztuk, s elemeztük az osztályozás hatékonyságát. Azonban ezek egyike sem adott elfogadható eredményt sem a városokra, sem a megyékre. E három algoritmus paraméterei alapján egyik clusterezési eljárás során sem találtunk elfogadható cluster-szerkezetet. A *fanny* algoritmus alkalmazásával kapott clusterek – jóllehet gyenge a szerkezetük – kiterjedt és jól körülhatárolható térségeket jeleznek Magyarországon, melyek adott földrajzi objektumokkal jól körülírhatók.

Summary – The aim of the study was to rank and classify Hungarian cities and counties according to their environmental quality and level of environmental awareness. The rankings of the Hungarian cities and counties are based on their „Green Cities Index" and „Green Counties Index" values. According to the methodology presented in Part 1 (*Makra and Sümeghy*, 2007), cities and counties were grouped with different classification techniques and the efficacy of the classification was analysed. However, these did not give acceptable results for the cities, nor for the counties. According to the parameters of the here-mentioned three algorithms, no reasonable structures were found in any clustering. Clusters received applying the algorithm *fanny*, though having weak structure, indicate large and definite regions in Hungary, which can well be circumscribed by geographical objects.

Key words: environmental indicators, Green Cities Index, Green Counties Index, ranking, factor analysis, clustering, SPSS-software, R-language; algorithms: agnes, fanny, pam

1. RESULTS

1.1. Ranking

1.1.1. Cities

The final sequence of the cities shows some surprising results (*Table 2*). Nagykanizsa, near the Hungarian-Croatian border, is the highest-ranked city. It is followed by settlements around Lake Balaton: Balatonföldvár (2), Balatonboglár (3) and Balatonlelle (4). Among the major cities, Szombathely (5), Zalaegerszeg (7) and Kaposvár (8) stand out (*Table 2*).

Mosonmagyaróvár (88), Mór (87) and Balassagyarmat (86) are the worst ranked cities (*Table 2*) in spite of their relatively good rank in a number of indicators. Summing up, no city is found consistently either at the top or the bottom half of the rankings on all

environmental indicators. All cities in Hungary are characterised by a mix of favourable and less favourable environmental quality.

The environmental quality of Hungarian cities is best in the western and southern parts of Transdanubia, where Green Cities Index values are smallest. There are no clear regional patterns in the rest of the country (*Fig. 1*).
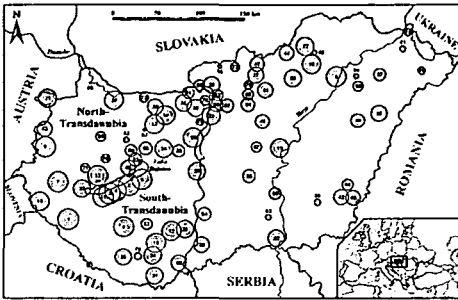
Fig. 1 Environmental quality of cities according to their Green Cities Index
[High values (circles with large area) = favourable; Low values (circles with small area) = disadvantageous]. The numbers indicate the final sequence of the cities
(1 = best, 88 = worst).
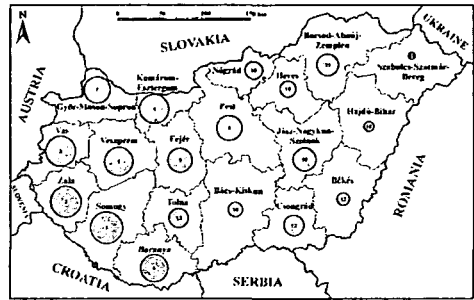
Fig. 2 Environmental quality of counties according to their Green Counties Index
[High values (circles with large area) = favourable; Low values (circles with small area) = disadvantageous]. The numbers indicate the final sequence of the counties
(1 = best, 19 = worst).

1.1.1.1. Potential impact of population on the Green Cities Index

The possible consequence of including population and population density in the Green Index was examined by comparing the rankings obtained with the inclusion of the two variables (modified Final Sequence) and those calculated without them (original Final Sequence). The Spearman's rank correlation coefficient, which was utilized for this purpose, yielded a value of 0.94 significant at the 99.9% confidence level. This means that there is a significant connection between the original and modified groups of indicators. We would be in error once in 1000 cases. Hence, the original final sequence is not substantially influenced by not considering population and population density. This result indicates that, although not perfect, the Green Cities Index, as calculated, is a reasonably fair method of providing an environmental rating for cities in Hungary.

1.1.2. Counties

According to the final rank order of the counties (*Table 1*), Somogy is the greenest county of Hungary. Though it is almost the most wasteful in water consumption (ranked 18) and average in waste removal (13), its favourable ranking in public green area total (1), average sulphur dioxide concentration (1), energy requirement and electric energy consumption (2 and 4, respectively), regularly cleaned constructed public surfaces (3) and average concentration of particulates deposited (3) make it the most environment-friendly county in the country. Somogy is followed by Zala and Vas respectively. Both Zala and Vas score well in environmental factors related to infrastructural and social developments and to a lesser extent, in physical factors such as air quality and green areas. The Green

Counties Index is a good measure of the general level of development of the counties. It well reflects the fact that the western part of the country, namely Transdanubia, is much more environment-sensitively developed than eastern Hungary.

The seven best counties are all found in Transdanubia (Somogy, Zala, Vas, Komárom-Esztergom, Veszprém, Baranya and Győr-Moson-Sopron), while the worst five all in the Great Hungarian Plain: Szabolcs-Szatmár-Bereg, Hajdú-Bihar, Békés, Bács-Kiskun and Heves. However Szabolcs-Szatmár-Bereg, Hajdú-Bihar and Békés do well in some indicators.

Table 1 Average of rankings of the environmental indicators considered, namely the Green Counties Index, and the final sequence of the counties (1 = best, 19 = worst; the numbers indicate the counties)

County	Final sequence	Green Counties Index
Somogy	1	6.32
Zala	2	6.79
Vas	3	7.21
Komárom-Esztergom	4	8.79
Veszprém	5	9.26
Baranya	6	9.53
Győr-Moson-Sopron	7	10.00
Pest	8	10.05
Fejér	9	10.16
Jász-Nagykun-Szolnok	10	10.16
Borsod-Abaúj-Zemplén	11	10.42
Csongrád	12	10.47
Tolna	13	10.79
Nógrád	14	11.00
Heves	15	11.21
Bács-Kiskun	16	11.47
Békés	17	11.58
Hajdú-Bihar	18	11.89
Szabolcs-Szatmár-Bereg	19	12.32

Like in the case of cities, there is no county found consistently at either the top or the bottom half of the rankings, in all indicators. In general, Transdanubian counties have better ranks than counties in eastern Hungary (*Fig. 2*).

1.2. Clustering procedures

1.2.1. Cluster analysis using SPSS-software

After performing factor analysis, cluster analysis is applied to the factor scores time series in order to objectively group cities and counties according to their similar characteristics. In this paper, the agglomerative hierarchical technique, *Ward's* method is applied.

1.2.1.1. Cities

After performing cluster analysis, the 88 cities were divided into 6 groups, considered to be the most homogenous. The groups received do not form a comprehensive (contiguous) spatial system (*Fig. 3*). All the 14 cities of Group 1 are found either in eastern or northern Hungary, indicating considerable dispersion. Group 2 consists of 6 Transdanubian settlements, 4 are located in the southwestern part of Transdanubia, while the other two are far from them. The 30 cities of Group 3 also exhibit considerable spatial dispersion. Here, two distinct sub-groups are found; one in the southern part of Transdanubia and the other in the northern part. Four cities in Group 4 are found around Lake Balaton, while the other two are in the southern part of the Great Hungarian Plain. All the 4 cities of Group 5 are found around Budapest. Though settlements belonging to Group 6 (28 cities) show density junctions in the middle part of Transdanubia, south of Budapest and Northern Hungary they are considerably dispersed (*Fig. 3*).

Table 2 Average of rankings of the environmental indicators considered namely, the Green Cities Index, and the final sequence of the cities (1 = best, 88 = worst) City

City	Final sequence	Green Cities Index	City	Final sequence	Green Cities Index	City	Final sequence	Green Cities Index
Nagykanizsa	1	29.89	Siklós	31	42.26	Esztergom	61	47.74
Balatonföldvár	2	30.58	Szeged	32	42.32	Göd	62	47.78
Balatonboglár	3	30.68	Vác	33	42.47	Dombóvár	63	48.16
Balatonlelle	4	32.11	Dorog	34	42.74	Békés	64	48.37
Szombathely	5	32.89	Debrecen	35	42.84	Lőrinci	65	48.84
Tiszaújváros	6	33.00	Szigetvár	36	42.88	Nagymaros	66	50.00
Zalaegerszeg	7	33.16	Bátonyterenye	37	43.00	Cegléd	67	50.74
Kaposvár	8	33.32	Baja	38	43.26	Hajdúnánás	68	50.84
Siófok	9	34.32	Tata	39	43.32	Pápa	69	51.05
Százhalombatta	10	34.63	Mohács	40	43.95	Szentendre	70	51.14
Fonyód	11	34.74	Gyöngyös	41	44.05	Sümeg	71	51.32
Bonyhád	12	34.79	Békéscsaba	42	44.21	Szécsény	72	51.42
Tapolca	13	35.95	Kőszeg	43	44.37	Komárom	73	51.47
Tatabánya	14	36.26	Ózd	44	44.53	Ajka	74	51.58
Miskolc	15	36.84	Gyula	45	44.63	Pásztó	75	51.63
Komló	16	37.16	Balatonfüred	46	44.79	Mátészalka	76	51.74
Oroszlány	17	37.21	Salgótarján	47	44.89	Budaörs	77	52.00
Lenti	18	37.68	Jászberény	48	45.00	Záhony	78	52.11
Szolnok	19	38.26	Hajdúszoboszló	49	45.05	Szentlőrinc	79	52.37
Győr	20	38.58	Dunakeszi	50	45.47	Orosháza	80	53.16
Sopron	21	39.05	Hatvan	51	45.63	Kisvárda	81	53.26
Kazincbarcika	22	39.37	Veresegyház	52	46.00	Zirc	82	54.16
Budapest	23	39.74	Balatonalmádi	53	46.21	Kistelek	83	54.26
Székesfehérvár	24	39.89	Kalocsa	54	46.27	Tiszavasvári	84	55.89
Szekszárd	25	39.91	Várpalota	55	46.58	Sajószentpéter	85	56.79
Pécs	26	40.00	Kecskemét	56	46.74	Balassagyarmat	86	58.05
Keszthely	27	40.32	Nyíregyháza	57	46.95	Mór	87	58.68
Eger	28	40.74	Gárdony	58	47.21	Mosonmagyaróvár	88	59.21
Dunaújváros	29	41.21	Csongrád	59	47.26			
Pilisvörösvár	30	41.63	Veszprém	60	47.42			

1.2.1.2. Counties

The grouping of counties using cluster analysis separated regions more clearly. The southern part of the Great Hungarian Plain (Bács-Kiskun, Csongrád and Békés counties) is well defined. The middle part of the Great Hungarian Plain and Northern Hungary (Jász-Nagykun-Szolnok, Hajdú-Bihar, Nógrád, Heves, Borsod-Abaúj-Zemplén and Szabolcs-

Szatmár-Bereg counties) stand out as well. Zala, Somogy and Fejér counties form a distinct region as do regions representing Vas, Veszprém and Komárom-Esztergom counties; Baranya and Tolna; Győr-Moson-Sopron and Pest (*Fig. 4*).

Fig. 3 Spatial distribution of cities, with symbols of their 6 clusters, using cluster analysis, agglomerative method, after performing factor analysis, SPSS.
[Right and down the sign, serial number of the cluster and the number of cities in the cluster (in parentheses) are found.]

Fig. 4 Spatial distribution of counties, with symbols of their 6 clusters, using cluster analysis, agglomerative method, after performing factor analysis, SPSS.
[Right and down the sign, serial number of the cluster and the number of cities in the cluster (in parentheses) are found.]

1.2.2. Cluster analysis using R-language

When applying the agglomerative method, the goodness of clustering is indicated by the agglomerative coefficient (*AC*). The higher the *AC*, the better the clustering is. However, it should be emphasized again, that the *AC* tends to increase with the number of objects.

The application of classification techniques did not result in strong structure either for the cities or the counties. The silhouette coefficient (*SC*) of methods *fanny* and *pam* shows values between 0.00 and 0.50. Among them the only highest ones were retained. In spite of this, they refer to the weak structure of the database (*SC* is between 0.26 and 0.50) (see *Table 2* in *Chapter 3.3.1.1.* in *Makra and Sümeghy* (2007)).

1.2.2.1. Cities

Firstly the algorithm *agnes* was applied to the database comprising 19 variables for each city. As a result of this analysis 7 clusters were received (*Fig. 5*). Spatial distribution of the cities with symbols of their 7 clusters does not indicate any clearly homogenous regions. However, definite subregions of cities belonging to cluster 1 can be observed in South-Transdanubia and, along a SW-NE axis, in North-Transdanubia. Furthermore, cities of cluster 5 are predominant in Western Transdanubia (*Fig. 5*).

Afterwards, factor analysis was used on the original database (to the 19 environmental indicators of the 88 cities) and then the algorithm *agnes* was applied to the seven factor score time series received. Altogether 7 clusters were established (*Fig. 6*). The spatial distribution of the cities with symbols of their 7 clusters also shows homogenous subregions. They are as follows: South Transdanubia with cities of cluster 7, SW Transdanubia with cities belonging to cluster 6 and Lake Balaton region with cities of

cluster 5. Smaller homogenous regions are North Transdanubia with cities of cluster 7, North Hungary with cities of cluster 1 and the southern part of the Great Hungarian Plain with cities of cluster 5 *(Fig. 6)*.
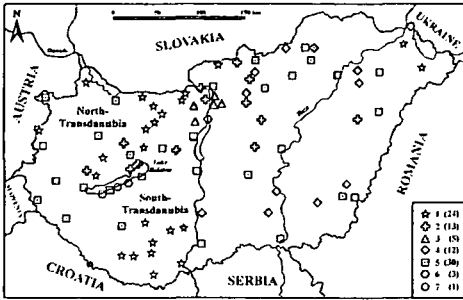

Fig. 5 Spatial distribution of cities, with symbols of their 7 clusters using agnes algorithm based on the 19 environmental indicators.
[Right and down the sign, serial number of the cluster and the number of cities in the cluster (in parentheses) are found.] (AC = 0.80)

Fig. 6 Spatial distribution of cities, with symbols of their 7 clusters, using agnes algorithm, after performing factor analysis, SPSS.
[Right and down the sign, serial number of the cluster and the number of cities in the cluster (in parentheses) are found.] (AC = 0.84)

Algorithms *agnes, fanny* and *pam* did not give acceptable results ($SC \leq 0.25$) neither for the database comprising 19 variables of the 88 cities, nor for their application to the seven factor score time series after performing factor analysis.

1.2.2.2. Counties

Firstly, the algorithm *agnes* was applied to the database including 19 variables for each county. This analysis resulted in 8 clusters *(Fig. 7)*. Spatial distribution of the counties with symbols of their 8 clusters indicates definite regions with similar characteristics. They are counties of cluster 2, which cover all Eastern and Northern Hungary, furthermore counties of cluster 5 which are found in Southern and NNW Transdanubia. However, it should be mentioned that clusters 1, 4, 7 and 8 include only one county each *(Fig. 7)*.

Then, factor analysis was used on the original database (to the 19 environmental indicators of the 19 counties) and after that the algorithm *agnes* was applied to the seven factor score time series received. Altogether 8 clusters were established *(Fig. 8)*. Spatial distribution of the counties with symbols of their 8 clusters shows different homogenous regions. The largest of them with four counties of cluster 5 is found in the middle part of the Great Hungarian Plain and in NE Hungary. Though cluster 3 comprises altogether 6 counties, it is divided into three two-county subregions. Moreover, clusters 1, 5, 7 and 8 include only one county each *(Fig. 8)*.

Algorithms *agnes, fanny* and *pam*, similarly to the case of the cities, did not give acceptable results ($SC \leq 0.25$) neither for the database including 19 variables of the 19 counties, nor for their application to the seven factor score time series after performing factor analysis.

Thereafter, algorithm *mona* was applied to the database including the 19 variables. The banner belonging to this analysis is found on *Fig. 9*. It indicates 15 clusters; hence, this result is omitted from further consideration. Furthermore, the banner shows that the

algorithm classified the whole database using 8 variables. This result gave an idea to use the algorithms *agnes*, *fanny* and *pam* on these 8 variables. Then, factor analysis was applied to these 8 variables. According to the *Guttmann criterion* 3 factors were retained, for which algorithms *agnes*, *fanny* and *pam* were performed again.
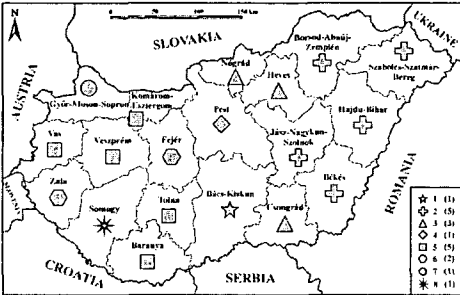
Fig. 7 Spatial distribution of counties, with symbols of their 8 clusters, using agnes algorithm based on the 19 environmental indicators.
[Right and down the sign, serial number of the cluster and the number of cities in the cluster (in parentheses) are found.] (AC = 0.61)

Fig. 8 Spatial distribution of counties, with symbols of their 8 clusters, using agnes algorithm, after performing factor analysis, SPSS.
[Right and down the sign, serial number of the cluster and the number of cities in the cluster (in parentheses) are found.] (AC = 0.58)
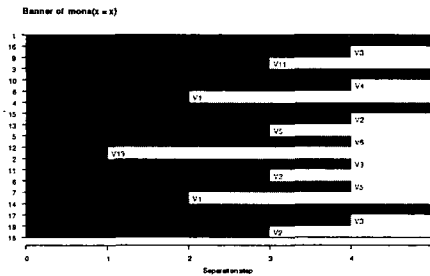
Fig. 9 Banner of function *mona* based on the 19 environmental indicators, counties
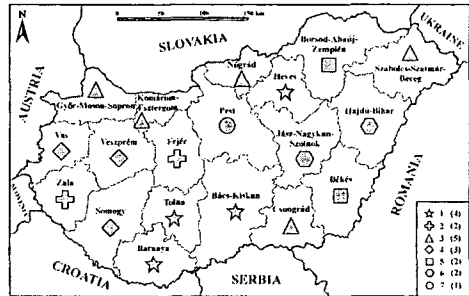
Fig. 10 Spatial distribution of counties, with symbols of their 7 clusters, using agnes algorithm, after performing mona algorithm.
[Right and down the sign, serial number of the cluster and the number of cities in the cluster (in parentheses) are found.] (AC = 0.65)

The analysis using algorithm *agnes*, after performing algorithm *mona* resulted in 7 clusters (*Fig. 10*). The largest region belongs to cluster 1 comprising three uniform counties in Southern Hungary, while the fourth county belonging to cluster 1 is found in North Hungary. Clusters 3 and 4 are divided into 4 and 2 subregions, respectively (*Fig. 10*). Thereafter, algorithm *agnes* was used after performing algorithm *mona* and then factor analysis was performed to the three factor score time series retained. As a result of this analysis, 5 clusters were received (*Fig. 11*). The spatial distribution of the counties with

symbols of their 5 clusters indicates a large uniform region in Eastern Hungary with five counties of cluster 3. Another extended region is characterized by cluster 5; however, it is divided into two parts: a three-county subregion in North Transdanubia and a two-county subregion in North Hungary (*Fig. 11*).

Algorithm *fanny*, which was applied to the database comprising 8 variables, did not give acceptable clustering. The analysis applied to the three retained factors resulted in only one clustering, namely for k = 5, for which $SC > 0.25$ (*Fig. 12*). As a result of the analysis, 4 clusters were received only. Spatial distribution of the counties with symbols of their 4 clusters indicates large and definite regions in Hungary. Eastern Hungary is characterized by five counties of cluster 3, South Transdanubia by four counties of cluster 2, North Transdanubia by three counties of cluster 4 and Northern Hungary by three counties of cluster 1 (*Fig. 12*).

Fig. 11 Spatial distribution of counties, with symbols of their 5 clusters, using agnes algorithm after performing mona algorithm and then factor analysis.
[Right and down the sign, serial number of the cluster and the number of cities in the cluster (in parentheses) are found.] (AC = 0.83)
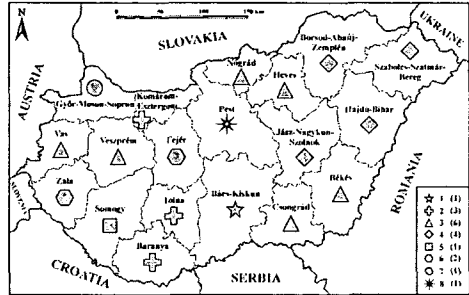
Fig. 12 Spatial distribution of counties, with symbols of their 4 clusters, using fanny algorithm (with k = 5) after performing mona algorithm and then factor analysis.
[Right and down the sign, serial number of the cluster and the number of cities in the cluster (in parentheses) are found.]
[Average silhouette width (ASW) = 0.32]

Applying algorithm *pam* to the database comprising 8 variables did not give acceptable clustering ($SC \leq 0.25$). Algorithm *pam* applied to the three factor score time series after performing factor analysis to the 8 variables, gave acceptable results only for the cases k = 5 (*Fig. 13*), k = 7 (*Fig. 14*) and k = 8 (*Fig. 15*) ($SC > 0.25$). The spatial distribution of counties with symbols of their 5 clusters shows two large uniform regions. The largest one is found in Eastern Hungary with five counties of cluster 3. However, one county in the middle part of Transdanubia also belongs to this cluster.

The other important region is that of cluster 4, which is divided into two parts: North Transdanubia with four counties and Northern Hungary with two counties (*Fig. 13*). The uniform regions indicated by counties with symbols of their 7 clusters become smaller. Regions in Middle and East Hungary with three counties of cluster 3 and North Transdanubia with four counties of cluster 6 are the most characteristic (*Fig. 14*). Spatial distribution of counties with symbols of their 8 clusters shows smaller uniform regions than that for k = 7. The largest uniform regions are found in Middle and East Hungary with three

counties of cluster 3 and in North Transdanubia with also three counties of cluster 6 (*Fig. 15*).

Fig. 13 Spatial distribution of counties, with symbols of their 5 clusters, using pam algorithm (with k = 5) after performing mona algorithm and then factor analysis.
[Right and down the sign, serial number of the cluster and the number of cities in the cluster (in parentheses) are found.]
[Average silhouette width (*ASW*) = 0.33]

Fig. 14 Spatial distribution of counties, with symbols of their 7 clusters, using pam algorithm (with k = 7) after performing mona algorithm and then factor analysis.
[Right and down the sign, serial number of the cluster and the number of cities in the cluster (in parentheses) are found.]
[Average silhouette width (*ASW*) = 0.37]

Fig. 15 Spatial distribution of counties, with symbols of their 8 clusters, using pam algorithm (with k = 8) after performing mona algorithm and then factor analysis.
[Right and down the sign, serial number of the cluster and the number of cities in the cluster (in parentheses) are found.]
[Average silhouette width (*ASW*) = 0.35]

2. CONCLUSION

The aim of the study was to rank and classify Hungarian cities and counties according to their environmental quality and level of environmental awareness.

The top 5 most environmentally friendly cities are, in descending order, Nagykanizsa, Balatonföldvár, Balatonboglár, Balatonlelle and Szombathely. The bottom

five are, starting with the worst, Mosonmagyaróvár, Mór, Balassagyarmat, Sajószentpéter and Tiszavasvári. Cities situated in the western and southwestern part of Transdanubia have the best environmental quality. In the rest of the country, cities with either favourable or unfavourable positions are mixed, forming no comprehensive regional patterns.

The top 3 counties are Somogy, Vas and Zala; Szabolcs-Szatmár-Bereg, Hajdú-Bihar and Békés counties are the most disadvantaged. The most environment-friendly counties can be found in Transdanubia, clearly separated from the least environment-friendly ones found in eastern Hungary.

Clustering was performed with cluster analysis using both SPSS software and R-language. Cluster analysis with the application of SPSS software resulted in 6 most homogenous groups of cities, which did not form comprehensive spatial patterns. The classification of the counties according to cluster analysis determined also 6 clear groups of them.

Cluster analysis using R-language was carried out with different procedures. Algorithms *agnes*, *fanny* and *pam* did not give acceptable results ($SC \leq 0.25$) neither for the database of the cities, nor for the counties. The silhouette coefficient did not exceed the value 0.5 in either case, which means that a reasonable structure was found. Clusters received applying algorithm *fanny*, though having weak structure, indicate large and definite regions in Hungary, which can be circumscribed by clear geographical objects. The *agglomerative coefficient* (*AC*), which measures the goodness of the clustering of the dataset, shows the highest values when (1) clustering cities with 7 clusters, using algorithm *agnes* (*AC* = 0.80; *Fig. 5*), (2) clustering cities with 7 clusters, using algorithm *agnes* after performing factor analysis, SPSS (*AC* = 0.84; *Fig. 6*) and (3) clustering counties with 5 clusters, using algorithm *agnes* after performing algorithm *mona* and then factor analysis (*AC* = 0.83; *Fig. 11*).

REFERENCES

Makra, L. and Sümeghy, Z., 2007: Objective analysis and ranking of Hungarian cities, with different classification techniques, Part 1: Methodology. *Acta Climatologica et Chorologica Univ. Szegediensis 40-41 (this issue)*, 79-89.

A NEWLY DEVELOPED MODEL FOR THE SPATIAL ALLOCATION OF WIND ENERGY UTILIZATION

K. RÓZSAVÖLGYI

Department of Climatology and Landscape Ecology, University of Szeged, P.O.Box 653, 6701 Szeged, Hungary
E-mail: rozsavolgyi@geo.u-szeged.hu

Összefoglalás – Kutatásunk célja a szélenergia hasznosításának területi allokációja. Ezt egy saját fejlesztésű klímaorientált modellel KMPAM (Komplex Multifaktoros Poligenetikus Adaptív Modell) kívánjuk megvalósítani. Ennek a modellnek a legfontosabb eleme a szélmező modellezés melyre a legtöbb energiát fordítottuk munkánk során, de más tényezőket is számításba vettünk. Ez a szélmező modellezés geostatisztikai, légkör fizikai és GIS számításokon, módszereken és egy Szekvenciális Gaussi Szimuláción (sGs) alapszik. A magyarországi szimulációkhoz a bemenő adatokat Radics (2004) WAsP 10 méter magasságra készített modellezési vizualizációjából vettük, melyet geokorrigáltunk. Feltáró variográfiát és az sGs-t használva elkészítettük a modellezett terület – Magyarország – feletti szimulációs térképeinket, különböző magasságokra, melyek közül bemutatunk néhányat. A különböző magasságokra kapott szimulációs eredményeket összefoglaltuk illetve készítettünk egy vertikális szélprofilt leíró exponenciális regresszív függvényt is. A KMAPM komplex elemzései közül a 100m-es magasságra kapott eredményeket tartalmazza az utolsó térkép, mely alapján meghatározható több lehetséges helyszíne a szélenergia felhasználásnak.

Summary – Our research is on the spatial allocation of possible wind energy usage. We would like to carry this out with a self-developed model (Complex Multifactoral Polygenetic Adaptive Model = CMPAM), which basically is a climate-oriented system, but other kind of factors are also considered. The wind field modelling core is mainly based on sGs (sequential Gaussian simulation) hence geostatistics, but atmospheric physics and GIS are used as well. For the application developed for Hungary we used WAsP visualization from Radics (2004) at 10 m height as input data, the geocorrection of which was performed by us. Using optimized variography and sequential Gaussian simulation, our results were applied for Hungary in different heights. Simulation results received for different heights are summarized; furthermore, an exponential regressive function describing the vertical wind profile was also established. From the complex analyses of CMPAM, results received to the 100 m height were also included, on the basis of which several possible sites for the utilization of wind energy can be selected, under given conditions.

Key words: wind field modelling, complex modelling, Sequential Gaussian Simulation, expected value of wind speed, uncertainty of expected value of wind speed, wind profile

1. INTRODUCTION

Due to the ever increasing anthropogenic environmental pollution and the worldwide energy claim, the research and exploitation of environment-friendly renewable energy sources become more and more important. Developed countries, especially the European Union, support systems based on renewable energies, the exploitation of wind energy among them. Moreover, they inspire profit oriented ventures based on these. Besides economic incentives, the most extensive and most accurate scientific results are

required in order to provide regional planning with the possibility of selecting geographical coordinates for optimal exploitation of renewable energy sources.

In this project a climate oriented model (Complex Multifactoral Polygenetic Adaptive Model = CMPAM) has been developed, which facilitates to select those regions where the exploitation of the available wind energy would yield profit. The model consists of several sub-modules, the most important one of them is the wind field modelling part (CMPAM/W) (W in the abbreviation denotes to Wind field modelling). Our research focuses mainly on this sub-module. The other sub-modules (e.g. those of landscape ecology, administration and physical geography) are declared in a much more general way in the model.

2. WIND FIELD MODELLING

This wind field modelling comprises methods and calculations of atmospheric physics, geostatistics and GIS and its aim is to supply information on wind field for system planning and economic efficiency calculations, which can not or can hardly be provided by using other techniques. Resolution of the CMPAM/W grid system is 4 km^2 and supplies the following information for each grid: (1) expected value of the wind speed, (2) uncertainty of the wind speed (width of the probability interval) and (3) wind potential value.

All of this information is ensured mainly by geostatistics, since this field of science, contrary to mathematical statistics, uses regionalized variables with structural and erratic features and works with dependent sampling methods. On the other hand, mathematical statistics uses probability variables and works with independent sampling. Geostatistics deals with the spatial structure of the data; it is able to measure variability and heterogeneity in this structure and to use these in estimating the values of grid points.

3. INPUT DATA FOR WIND FIELD MODELLING AND THE SAMPLING METHOD

Our basic input data come from *Radics's* (2004) 10 meters height wind field modelling visualization, which was compiled by the Wind Atlas Analysis and Application Program (WAsP) using wind speed data of 29 Hungarian meteorological stations for a 6-year period (1997 – 2002). After performing polynomial geometric correction (transformation into geographic EOV projection) on this WAsP result, a so-called K – type randomized sampling algorithm was applied in order to get sampling points (150) for further processing (*Fig. 1*). These new sampling points received the appropriate wind speed data by GIS processes. Then two GIS functions were used to determine the proper geographic coordinates of the sampling points. These newly gained sampling points constituted the basis of further calculations and simulations.

4. DATA PROCESSING AND MODELLING

Our newly developed wind field model was prepared using calculations and methods of atmospheric physics, geostatistics and GIS. The core of our simulation is a Sequential Gaussian Simulation (sGs) (*Deutsch et al.,* 1998). The variogram surface, which is the

visualisation of the spatial anisotropy of the phenomenon examined, was made of the z-score transformation of wind speed data coming from random sampling. Furthermore, segments of the variogram surface in different directions, namely the semi-variograms (which are measures of spatial continuity) were also prepared from our newly gained data. Variogram models, required for further simulations (sGs), were prepared on the basis of these semi-variograms. Each of these variogram models, comprising three structures (two spherical and a Gaussian ones), are nested models (*Pannatier,* 1996). They were used to the Sequential Gaussian Simulation for all of the modelled altitudes (10 m, 30 m, 60 m, 80 m, 100 m, 120 m, 140 m above ground level). The final results were received after the normal score back-transformation of the grid data.
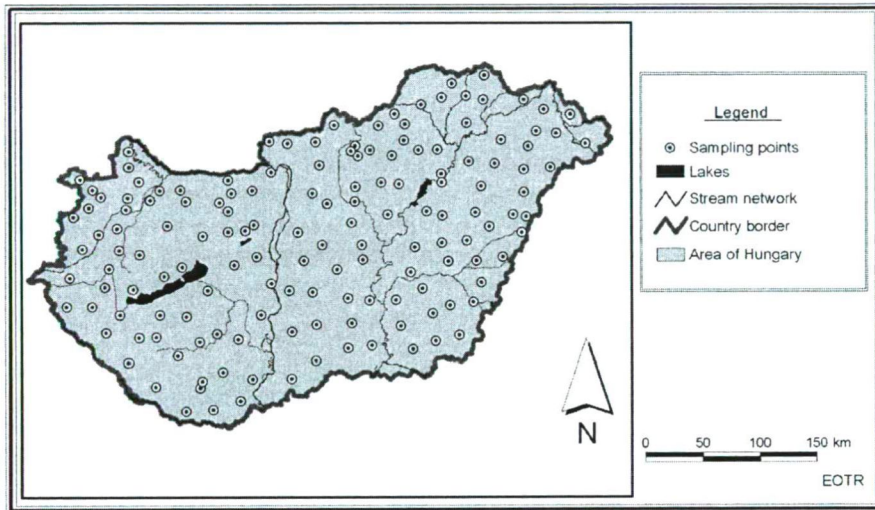
Fig. 1 Spatial distribution of sampling points for our simulation

Extrapolation of the vertical wind speed was performed using sampling points on the basis of the Hellmann exponent formula (*Molly,* 1990):

$$\frac{v_2}{v_1} = \left(\frac{h_2}{h_1}\right)^{\alpha},$$ (1)

where $\alpha = 1/\ln(10/z_0)$; α characterizes the roughness of the surface, and z_0 is the aerodynamic roughness height. The value of α was determined by GIS methods.

5. DISCUSSION

When preparing the simulations, 100 different realizations with the same probability level were made for each simulation altitude. Results of the simulation, modelling and grid system of 1 km^2 resolution can not be evaluated, due to the special combination of small-scale heterogeneity and noise. But after increasing the grid resolution to 4 km^2, acceptable results could be achieved. The spatial variability was preserved in a better way on this

scale. When performing the sGs simulations, the results of each altitude for all of their 100 realizations can be analyzed and displayed on maps. However, the mean of these 100 realizations represents a good approximation of the expected value of the wind speed (*Figs. 2-3*). According to the results, in the height of 10 m above ground level, the Transdanubian Mountain Range shows high wind potential, including the Bakony Mountain, Marcal Basin and the plain in Northwestern Hungary. On the other hand, some parts of the Great Hungarian Plain (mouths of the Rivers Maros and Körös as well as Nagy-Sárrét and Kis-Sárrét) have higher than average wind potential, and thus may be of good use (*Fig. 2*). Concerning the spatial pattern, similar results achieved by using significantly different methods have already been published (*Wantuchné*, 2005). So these can be regarded as the verification of each other.

Fig. 2 Average values of the simulations realizations for wind speed and gross wind potential, 10 meter above ground level

Summarizing the results of wind field modelling for higher levels (from 10 meters to 140 meters above ground level), on large scale a spatial homogeneity appeared in the wind field structure, while on small scale heterogeneity of the expected values of wind speed are indicated. This is a very interesting dual feature of the wind field (*Fig. 3*). The possible reason of the large scale homogeneity of the wind field in the Inner Boundary Layer (IBL) is that the surface roughness is not as significant at higher altitudes as at low levels (*Baranka et al.*, 2001). That is, the wind field becomes more and more homogenous at higher altitudes. According to our simulation outcomes it can be stated that at the altitude of 60 meters above ground level or higher, the surface objects do not have significant influence on the wind field (*Wieringa*, 1976, 1983; *Kircsi*, 2004).
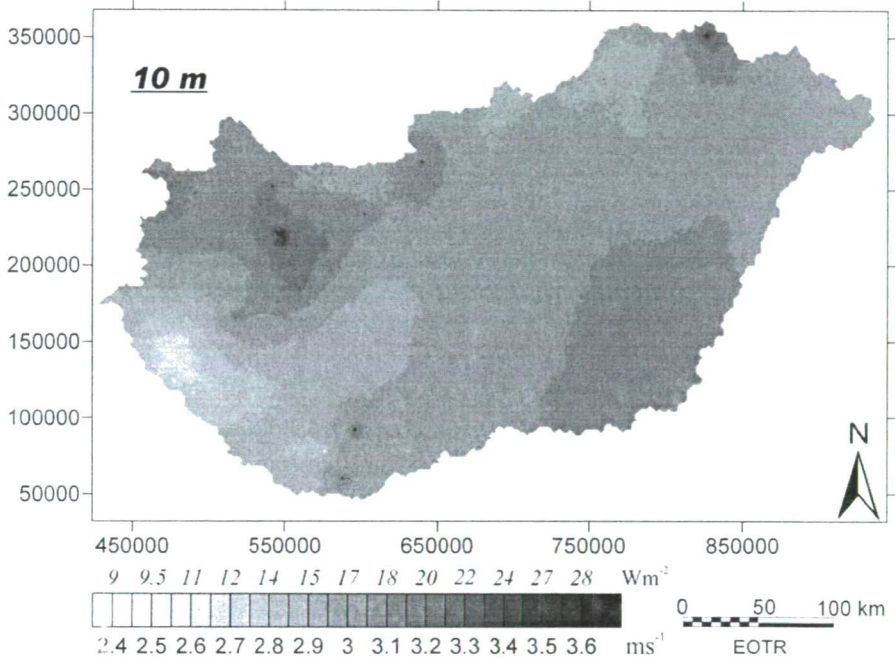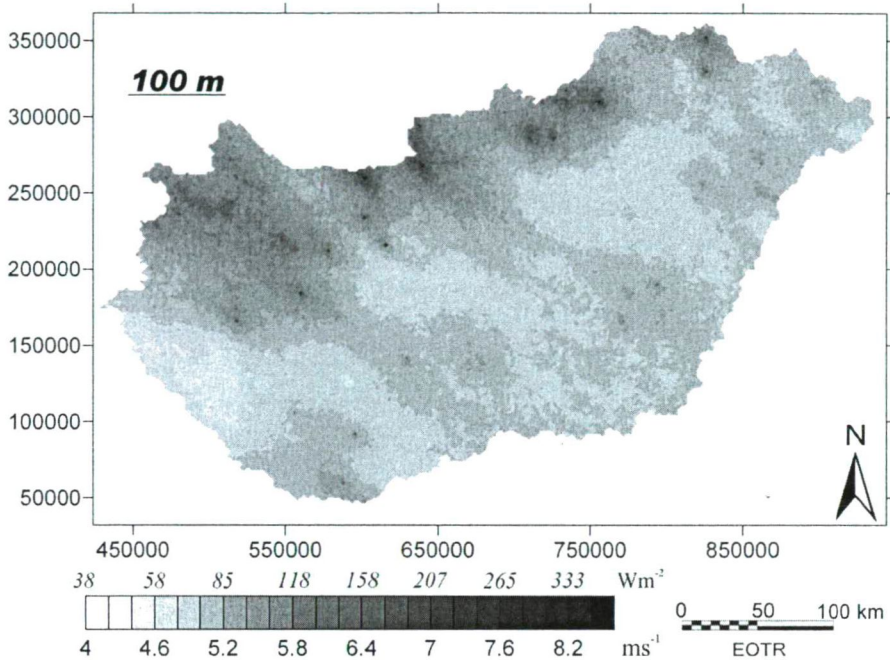
Fig. 3 Average values of the simulations realizations of wind speed and gross wind potential, 100 meter above ground level

In one-variable mathematical statistics it is evident to compute confidence interval when estimating the expected value. At the first step of the geostatistical analysis, standard normal transformation of the input data was performed. Consequently, surfaces belonging to the lower and upper limit of the confidence intervals can be determined (*Geiger and Mucsi, 2005*). The tighter this confidence interval, the more stable the estimation of the expected values is. Consequently, the width of the probability (confidence) interval can be interpreted as the uncertainty in assessment of the expected value at every grid. Thus this can be interpreted as an uncertainty map (*Figs. 4-5*)

Hence, the uncertainty maps are spatial extensions of the confidence intervals of the expected values, belonging to each simulation grid.

All of the uncertainty values according to the above definition have been classified into some equidistance scale between the minima and maxima of the uncertainty. Naturally these intervals can be expressed in a verbal scale, as well. This idea is demonstrated on *Fig. 4* and *5* with intervals and the corresponding verbal categories. It is very important to emphasize that uncertainty is not equal to error.

On the basis of our simulations a multiple regression function was established that describes the vertical wind profile for the modelled territory. This function was found to be suitable for vertical extrapolation of wind speed from 10 m to 140 m height above ground level, but this function seems to be applicable for higher altitudes, as well. This function is as follows:

$$y = 1,7437 \cdot x^{0,2353} \quad (R^2 = 0,9998) \tag{2}$$

where y is the wind speed (ms^{-1}) and x is the height (m).
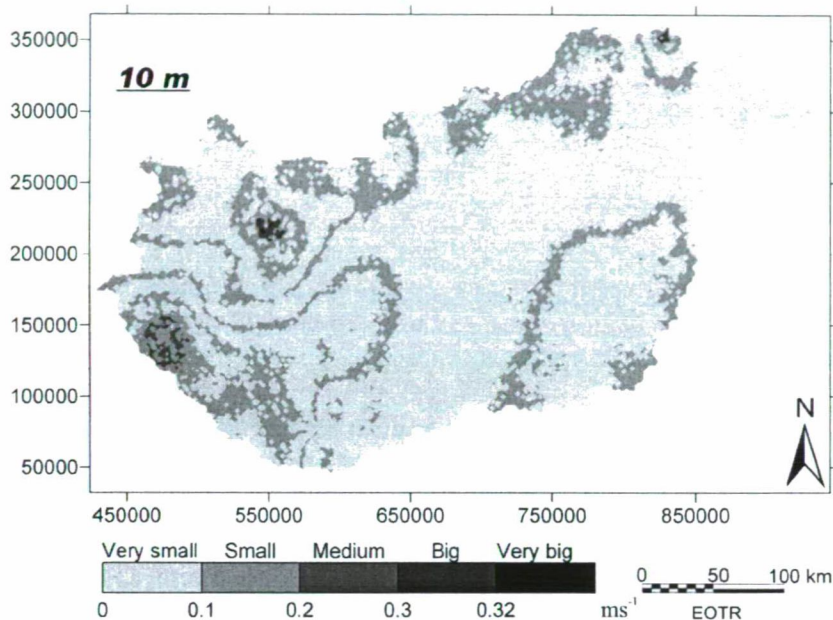
Fig. 4 Uncertainty of the expected values of wind speed, 10 m height above ground level
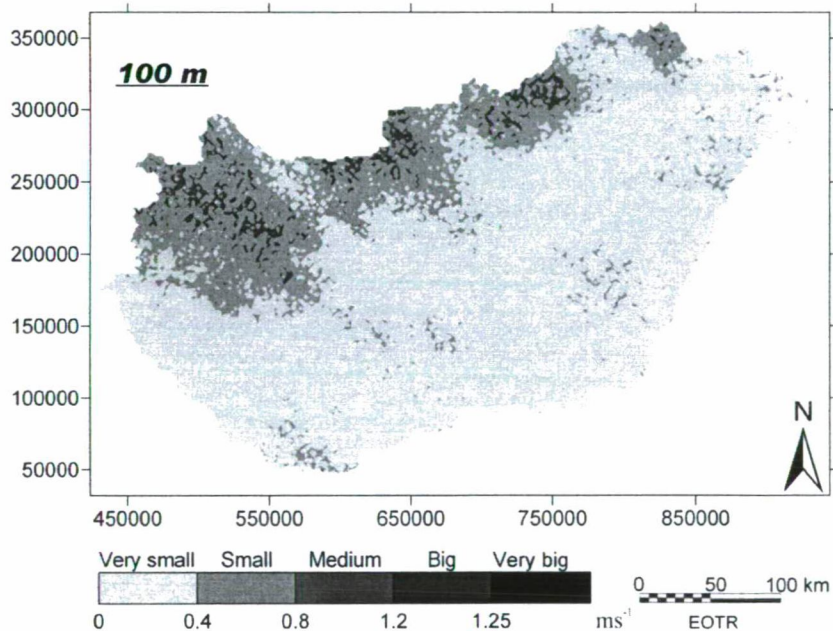
Fig. 5 Uncertainty of expected values of wind speed, 100 m height above ground level

The advantage of this function over other extrapolation functions (*Molly*, 1990; *Dobesch and Kury*, 1999) is that it was created from our wind field simulations on the

characteristics of the modelled territory, so it is more suitable for vertical wind speed extrapolation for Hungary.

Results of the simulations are summarized in *Table 1* and *2*. *Table 2* consists of regional ratios (percentage) of each category in Hungary. According to these tables we can conclude that Hungary belongs to moderately windy regions. Other authors received similar results (*Tar et al.*, 2001; *Radics*, 2004). However, as our maps indicate, Hungary has economically utilizable wind energy. *Table 1* and *2* shows some mathematical statistical characteristics of the Hungarian wind climate. Nevertheless, researches dealing with the spatial distribution of wind speed have great importance, since mathematical statistical parameters do not inform us about the spatial structure of wind speed, therefore they are not sufficient for the planning of a possible wind power plant project. Hence, analysis of the spatial distribution of climatological and energetic components of wind parameters is of vital importance.

Table 1 Statistics of the results of the simulations calculated to different levels

Height (m)	Wind speed (ms^{-1})				
	Min	*Max*	*Mean*	*Modus*	*Variance*
10	2.4	3.6	3.00	3	0.005437
30	3.08	5.43	3.88	3.86	0.009207
60	3.72	6.92	4.56	4.52	0.023178
80	3.87	7.66	4.88	4.839	0.03931
100	4.12	8.28	5.14	5.09	0.04609
120	4.27	8.83	5.37	5.31	0.071292
140	4.4	9.31	5.61	5.5	0.174398
mean between 10 -140	*3.7*	*7.14*	*4.63*	*4.59*	*0.052702*

Table 2 Regional statistics of results of simulations calculated to different levels

Ratios of regional distribution of simulation results in Hungary (%)								
Wind speed (ms^{-1})	Wind potential (Wm^{-2})	Height (m)						
		10	*30*	*60*	*80*	*100*	*120*	*140*
2.4 – 3.0	8 – 17	**73.38**	~0	0	0	0	0	0
3.1 – 3.5	17 – 26	26.6	10	~0	0	0	0	0
3.6 – 4.0	26 – 39	~0	77	1.4	~0	0	0	0
4.1 – 4.5	39 – 56	0	12.7	44.4	1.7	~0	~0	0
4.6 – 5.0	56 – 77	0	~0	51	78	37.6	2	~0
5.1 – 5.5	77 – 102	0	0	3	19.1	**51.25**	75	54.5
5.6 – 6.0	102 – 132	0	0	~0	1.5	9.8	16.35	28
6.1 – 6.5	132 – 168	0	0	0	~0	1.3	5.4	10
6.6 – 7.0	168 – 210	0	0	0	0	~0	1.1	6.5
7.1 – 7.5	210 – 258	0	0	0	0	0	~0	~0
7.6 – 8.0	258 – 314	0	0	0	0	0	0	0

6. CMPAM IN PRACTICE

In the course of planning and developing CMPAM, not only the scientific but also the practical applicability of the model was of high priority.

Suppose that a firm would like to establish a wind power plant system in Hungary. They would like to know, which sites would be the best ones for wind turbines having the following parameters: height = 100 m and impulse speed = 5.5 ms^{-1}. *Fig. 6* indicates a countrywide analysis of CMPAM for 100 m height, where three sub-modules of CMPAM were used. *The wind field modelling sub-module* (CMPAM/W) was run with the condition that the expected value of the wind speed is at least 5.5 ms^{-1}. In this way, regions appropriate to settle a wind power plant system are defined from the climatologic aspect. The next one is *the administration sub-module*, comprising administration regions of towns, villages and farms. The third one is *the landscape ecology sub-module*, consisting of the regions of Natura 2000 and bird conservation regions (according to the edict no. 275/2004 X. 08, completing the Conservation Law no. 1996/53), as well as regions of wells, springs, wetlands, rivers and their 50 m zones, furthermore lakes and their 100 m ranges and last but not least specially protected natural conservation regions and national parks. The last two sub-modules represent those regions, which are not suitable to perform such projects. Practical utilization and importance of CMPAM is well demonstrated by *Fig 6*. On this example it can be understood that a mere climatological analysis is not sufficient, since the regions with the best the climatic conditions will not necessarily be the ones suitable for the establishment of a wind power station.
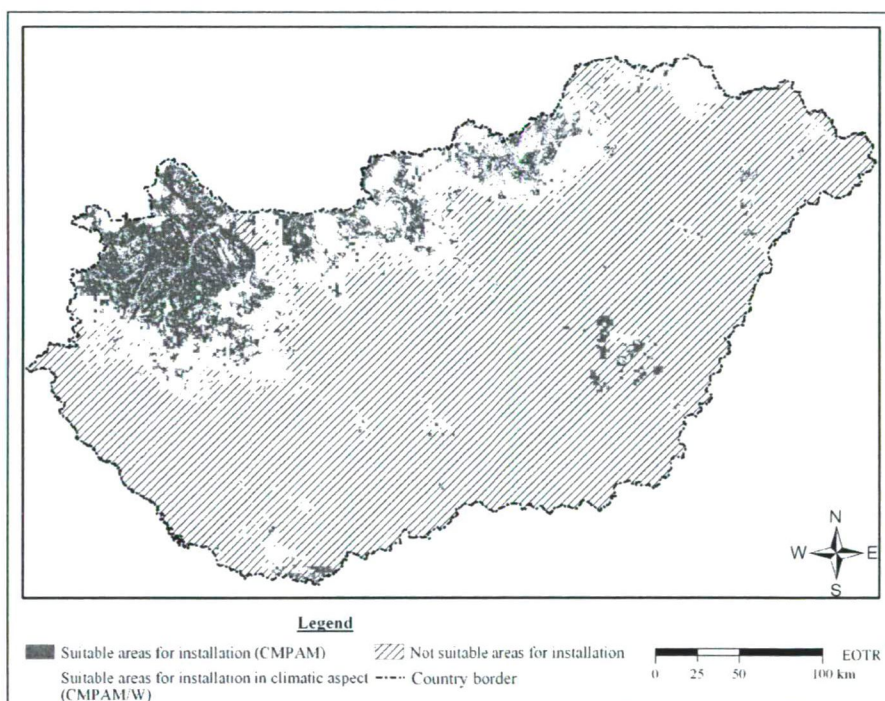

Fig. 6 Practical use of CMPAM in the planning of a speculative wind power plant project, in 100 m height

REFERENCES

Baranka, Gy., Weidinger, T., Mészáros, R., Mikó, R. and Kovács, R., 2001: A planetáris határréteg szerkezete, szél- és hőmérsékleti profiljai. A légköri erőforrások hasznosíthatásának meteorológiai alapjai. [Structure of the Boundary Layer, its wind and temperature profiles. Meteorological basis of utilization of atmospheric resources. (in Hungarian)] *Meteorológiai Tudományos Napok kiadványa,* 109-119.

Deutsch, C.V. and Journel A., 1998: *GSLIB. Geostatistical Software Library and User's Guide.* Oxford University Press, New York. 369.

Dobesch, H. and Kury, G. 1999: Basic meteorological concepts and recommendations for exploitation of wind energy in the atmospheric boundary layer. Central Institute for Meteorolgy and Geodinamics, Vienna. 46-48.

Geiger, J. and Mucsi, L., 2005: A szekvenciális sztochasztikus szimuláció előnyei a talajvízszint kisléptékű heterogenitásának térképezésében. [Advantages of the sequential, stochastic simulation in mapping of small scale heterogeneity of the ground water level. (in Hungarian)] *Hidrológiai Közlöny 85/2,* 37-47.

Kircsi, A. 2004: Szélsebesség adatok területi extrapolációja – lehetőségek és nehézségek. [Regional extrapolation of wind speed data – possibilities and difficulties. (in Hungarian)] *A megújuló energiák kutatása és hasznosítása az Észak-Alföldi régióban. A Magyar Szélenergia Társaság kiadványai 2,* 71 - 78.

Molly, J.P. 1990: Windenergie. In *Müller, C.F.* (ed.) *Theorie and Praxis.* Karlsruhe. 270-289.

Pannatier, Y., 1996: *VARIOWIN: Software for Spatial Data Analysis in 2D.* Springer, New York. 91. p.

Radics, K. 2004: *Szélenergia hasznosításának lehetőségei Magyarországon: Hazánk szélklímája, a rendelkezésre álló szélenergia becslése és modellezése.* [*Utilization possibilities of wind energy in Hungary: Wind climate of Hungary, assessment of wind energy being at disposal and modelling.* (in Hungarian)] PhD Thesis (manuscript). Eötvös Lóránd Tudományegyetem, Meteorológiai Tanszék, Budapest.

Tar, K., Makra, L., Horváth, Sz. and Kircsi, A., 2001: Temporal change of some statistical characteristics of wind speed in the Great Hungarian Plain. *Theor. and Appl. Climatol. 69/1-2,* 69-76.

Wantuchné Dobi, I., 2005: A megújuló energiaforrások felhasználási lehetőségeinek meteorológiai vonatkozásai. [Meteorological concerns of utilization of renewable energy sources. (in Hungarian)] In *OMSZ beszámoló a 2005. évi tevékenységről.* OMSZ, Budapest. 135-141.

Wieringa, J., 1976: An objective exposure correction method for average wind speeds measured at shelted location. *Quart. J. Roy. Meteorol. Soc. 102,* 241-253.

Wieringa, J. 1983: Description requirments for assassment of non-ideal wind stations – for example Aachen. *J. Wind Engineering and Industrial Aerodynamics 11,* 121-131.

LANDSCAPE REPRESENTATION AND THE URBAN-RURAL DICHOTOMY IN EMPIRICAL URBAN HEAT ISLAND LITERATURE, 1950–2006

I. D. STEWART

Department of Geography, University of British Columbia, 1984 West Mall, Vancouver, Canada V6T 1Z2
E-mail: stewarti@interchange.ubc.ca

Összefoglalás – A városi hősziget (UHI) mérésével kapcsolatos irodalom áttekintése széleskörű ellentmondásokat tár fel a hősziget erősségének számszerűsítéséhez felhasznált városi és külterületi mérési helyeknek az értelmezésében és osztályozásában. Bizonyított, hogy ezeknek az eltéréseknek a gyökere a városklimatológia tér-osztályozási rendszerében régóta fennálló paradigmában, a városi-külterületi kettősségben keresendő. Kidolgozatlan természetének és különösen annak a szerepének köszönhetően, amely a bizonytalanná teszi az UHI irodalomban a városok közötti hősziget-összehasonlításokat, felvetődik a kérdés a városi-külterületi kettősség módszertanával kapcsolatban. Ez a dolgozat egy kezdeti lépést jelent abban az irányában, hogy a többdimenziós helyi léptékű tájosztályozási rendszer jobban illeszkedjen a különböző városokban és régiókban megjelenő UHI-t jellemző felszíni klímatípusok változatosságához. A kapcsolódó történeti irodalom áttekintése és a városföldrajz rokon szakterületének vele párhuzamos fejlődése ösztönzést ennek a rendszernek a kialakítására és fejlesztésére.

Summary – A review of observational urban heat island (UHI) literature uncovers widespread discrepancies in the representation and classification of so-called urban and rural measurement sites defining heat island magnitude. It is argued that the root of this discrepancy is urban climatology's long-standing paradigm for space classification, the urban-rural dichotomy. Due to its crude and amorphous nature, and more specifically for its role in generating unsubstantiated inter-city heat island comparisons in UHI literature, the heuristic value of the urban-rural dichotomy is brought into question. This paper initiates movement toward a multidimensional, local-scale landscape-classification scheme better suited to the complexity of surface climates characterising UHI in cities and regions worldwide. The design and development of this scheme has found impetus in historical literature review and through parallel advancements in the cognate field of urban geography.

Key words: urban heat island, urban-rural dichotomy, landscape classification, field methodology, literature review

1. INTRODUCTION

As the world's population shifts to an urban majority for the first time in human history, our towns, cities, and megacities, and the spaces that surround them, are becoming increasingly complex and interactive. Driven by a half-century of rapid population growth, massive rural-urban migration, and a globalizing economy, this urban "revolution" has triggered a spectacular surge in empirical urban heat island (UHI) literature. City climate investigations of the modern era, dating from *Sundborg's* (1951) classic study of Uppsala, Sweden, have observed and documented the heat island effect at every level of the settlement hierarchy, from agrarian village to post-industrial supercity. This voluminous literature remains coherent in its aim and is impressive in its geographic purview—urban climatology is indeed fortunate to have such diversity of place represented in its ground observations of UHI. However, in looking more critically at the foundations of this

literature, we uncover a less coherent, and consequently more concerning, dimension to our representation of urban and rural space.

Essentially a nocturnal phenomenon, the canopy-layer UHI is defined as the region of screen-level warmth created by a city; the surrounding countryside, by comparison, is relatively cool (*Oke*, 1976). The primary causes of the UHI effect are well described in urban climate literature. The thermal, moisture, aerodynamic, and radiation properties of a city are dramatically different from those of the country, due primarily to the replacement and vertical screening of natural surfaces with perpendicular structures and building materials of high heat capacity and low permeability (*Oke*, 1982). Pollutant emissions and anthropogenic heat discharge into the urban atmosphere also contribute to an artificially warm city environment.

The magnitude, or "intensity," of the canopy-layer UHI effect invokes a seemingly intuitive testing procedure of synchronous screen-level air temperature differences between pairs of *in situ* "urban" and "rural" climate stations, or among purposively selected "urban" and "rural" measurement sites along a mobile traverse route. Denoted universally as $\Delta T_{u\text{-}r}$, this testing procedure has been the backbone of UHI field methodology since *Luke Howard's* (1833) pioneering observations of the London heat island nearly two centuries ago. Despite the timeless and universal appeal of $\Delta T_{u\text{-}r}$ as an empirical test of urban impact on thermal climate, the very landscapes (i.e., urban and rural) that give meaning and method to the heat island effect have not been defined in clear, objective, or climatologically germane terms.

A cursory review of modern UHI literature from 1950 to 2006 exposes an alarming diversity of "urban" and "rural" measurement sites characterising UHI. The apparent simplicity behind urban-rural site classification is obscuring the complex array of surfaces and near-surface climates that actually define UHI magnitude; in turn, the tendency of UHI investigators to overlook the micro- and local-scale peculiarities of these surfaces has generated untenable and unconfirmed inter-city comparisons of UHI magnitude in empirical climate literature. This paper invites compelling arguments for a reassessment of the urban-rural dichotomy and its critical role in UHI field methodology.

2. UHI OBSERVATION AND THE URBAN-RURAL DICHOTOMY

Like all branches of natural science, the empirical study of urban heat islands is bound by an experimental method of observation, measurement, analysis, and classification of the "facts" behind the "phenomenon." Beneath this rubric, each case study of UHI embodies a distinct blend of geographic, topographic, and cultural controls on its observed patterns. Not surprisingly, the micro- and local-scale settings of the measurement sites chosen to quantify the UHI effect are remarkably diverse in their exposure and surface characteristics. In describing these sites and their screen-level temperature regimes with such overarching constructs as "urban" and "rural," our investigations of UHI are presupposing the efficacy of this grossly simplified and poorly understood dichotomy.

Table 1 provides a sample of "urban" and "rural" sites used in estimating the magnitude of UHI in modern heat island literature. Although the studies differ slightly in their specific aims, they have common purpose insofar as each seeks an estimate of canopy-layer UHI magnitude based on an "urban-rural" temperature difference from fixed weather stations or mobile temperature surveys. The problem highlighted by *Table 1* relates not to the variety or number of sites classified as "urban" or "rural," but to the representation of

sites by an ambiguous and inclusive taxonomy. The geometry, surface materials, and anthropogenic heat flux of a street canyon, for example, are radically different from a botanical garden or a rail station, yet, ironically, all of these settings correspond with "urban" in UHI literature. Likewise, a range of agricultural and undisturbed landscapes are captured by a single (rural) class, while their surface and exposure properties are nothing alike. And perhaps most concerning is the widespread use of airports, college campuses, and meteorological observatories and institutes to represent either "urban" or "rural." This overlap in landscape representation has led to confusion and indiscretion surrounding the classification of measurement sites—especially those on the urban periphery—defining UHI magnitude, and now underscores a need for breakdown and re-examination of the urban-rural dichotomy and its heuristic value to urban climatology.

Table 1 "Urban" and "rural" sites representing T_u and T_r in UHI literature, 1950–2006.

URBAN	RURAL	URBAN *AND* RURAL*
botanical garden (*Syrakova and Zaharieva*, 1998)	paddy fields (*Sakakibara and Matsui*, 2005)	airports (U: *Adebayo*, 1991; R: *Klysik and Fortuniak*, 1999)
city square (*Unger*, 1996)	experimental farm (*Bohm*, 1988)	
building rooftop (*Lee*, 1979)	grain fields (*Stewart*, 2000)	college campuses (U: *Parry*, 1956; R: *Chandler*, 1961)
shipyard (*Moreno-Garcia*, 1994)	fruit farm (*Tso*, 1996)	
rail station (*Mukherjee and Daniel*, 1976)	rubber plantation (*Emmanuel and Johansson*, 2006)	school yards (U: *Hisada et al.*, 2006; R: *Okoola*, 1980)
city park (*Gedzelman et al.*, 2003)	desert (*Hedquist and Brazel*, 2006)	
shopping centre (*Landsberg and Maisel*, 1972)	ecological preserve (*Jauregui*, 1997)	meteorological institutes (U: *Robaa*, 2003; R: *Tumanov et al.*, 1999)
housing estate (*Giridharan et al.*, 2005)	farming village (*Sakakibara and Owa*, 2005)	
street canyon (*Eliasson*, 1994)	tropical rainforest (*Chow and Roth*, 2006)	weather observatories (U: *Figuerola and Mazzeo*, 1998; R: *Zhou*, 1990)
hospital (*Tumanov et al.*, 1995)	ranchland (*Norwine*, 1976)	
fire station (*Yudcovitch*, 1966-7)	moorland (*Lyall*, 1977)	
golf course (*Jonsson*, 2004)	pine flatwoods (*Yow and Carbone*, 2006)	
parking lot (*Bowling and Benson*, 1978)	Arctic tundra (*Hinkel et al.*, 2003)	

*U: "urban" reference; R: "rural" reference.

To illustrate the micro- and local-scale surroundings of typical UHI measurement points such as those listed in *Table 1*, photographs of so-called urban and rural sites have been assembled in *Fig. 1*. Pictured here are data-collection sites-classified by the investigators themselves as "urban" and "rural" of modern UHI studies in European, North American, and Asian cities. The "urban" photographs in particular expose the heterogeneity of instrument sitings found in a city environment, from a sheltered town-square (*Unger*,

1996) to a featureless airstrip (*Hedquist and Brazel*, 2006). The "rural" photographs, although less contrasting, also reveal landscapes of distinct character, as seen in *Yow and Carbone's* (2006) native pine forest and *Böhm's* (1998) experimental farm.

"URBAN" SITES		UCZ*	"RURAL" SITES		UCZ*
Goteborg SWEDEN (*Eliasson*, 1994)		2	Vienna AUSTRIA (*Böhm*, 1998)		6
Hong Kong (*Giridharan et al.*, 2005)		1	Lodz POLAND (*Klysik and Fortuniak*, 1999)		6
Phoenix USA (*Hedquist and Brazel*, 2006)		NC	Orlando USA (*Yow and Carbone*, 2006)		NC
Szeged HUNGARY (*Unger*, 1996)		2	Szeged HUNGARY (*Unger*, 1996)		NC
Regina CANADA (*Stewart*, 2000)		1	Singapore (*Chow and Roth*, 2006)		NC
Vienna AUSTRIA (*Böhm*, 1998)		2	Wroclaw POLAND (*Szymanowski*, 2005)		7

UCZ* 1: Intensely developed, detached high-rise buildings; 2: Intensely developed, attached low-rise buildings; 3: Highly developed, medium density; 4: Highly developed, low density; 5: Medium development, low-density suburban; 6: Mixed use with open landscapes; 7: Semi-rural development; NC: Site can not be classified.

Fig. 1 "Urban" and "rural" reference sites used in estimating UHI magnitude in observational heat island literature. Each site is classified according to *Oke's* (2004) Urban Climate Zone (UCZ) scheme.

The site locations displayed in *Fig. 1* have been carefully selected by the investigators to ensure, first, that the instruments are secure, and, second, that the immediate surroundings are representative of the local-scale setting. Paradoxically,

conventional UHI methodology prescribes these sites, along with countless others in the literature, as universally "urban" or "rural," when in fact the sites have no identical match in any other city. Without aid of photographs, maps, site sketches, and other important metadata, the detailed character of these sites is lost behind a seemingly opaque urban-rural taxonomy. Studies of UHI must therefore report site-specific properties such as surface roughness, extent of impermeable cover, sky view, soil moisture, and artificial heat; otherwise, generalisations and cross-study comparisons of UHI have little or no basis. Indeed, abstracting UHI relationships from among cities and countrysides so diverse in form, function, and setting is made difficult by the fact that the heterogeneity of these landscapes precludes the direct transfer of results from one region to another.

UHI investigators must, then, consider to what extent the micro-scale properties of their selected sites are representative of the larger local-scale setting. If the aim of a UHI investigation is to induce generalisations from the temperature data of specific sites, it is crucial that the temperatures be representative of the thermal conditions across a wider area; if the temperatures are not representative, then subsequent estimates of UHI magnitude are likely to be erroneous. Here, again, we are reminded that the inclusion of detailed metadata with observational UHI studies is essential to meaningful exchange and public understanding of experimental results. The representativeness of a UHI measurement site can only be assessed in the context of its micro- and local-scale properties of surface geometry (sky view factor, height-to-width ratios, roughness class), cover (percentage of built material, albedo, thermal admittance), and artificial heat (space heating/cooling, traffic density). Topographic and climatic influences at both scales must also be documented for all sites. *Oke* (2004) provides a useful template for recording these and other metadata describing the local- and micro-scale environment of a climate station.

3. A PROBLEM OF DEFINITION

Definitions are an important feature of scientific inquiry: they give basis to our hypotheses and sharpen our experimental tests. Despite the long history of UHI observation, urban climate literature has yet to impart a thorough and systematic explanation, from a climate science perspective, of the terms "rural" and "urban." In contrast, literature on urbanisation theory historically distinguishes "urban" from "rural" by population size and density, territorial limits, type of local government, and by various forms of material culture, all of which change by state and region (*Gugler*, 1997). Common to all accounts is that "rural" traditionally denotes a cultural landscape of predominantly agrarian-based employment or peasant-based production. Urban climatologists have yet to translate this basic interpretation into concepts of relevance to natural science. Our definition of UHI as an "urban-rural" temperature difference (ΔT_{u-r}) is therefore flawed because its constituent terms have no operational grounding.

Investigations of UHI consistently define "urban" and "rural" through narrative descriptions, and occasionally through provision of appropriate metadata. The latter is imperative because conventional narratives alone tend to incite tautological, or circular, accounts of site surroundings. Throughout UHI literature we find clumsy definitions and redundant use of synonyms portraying so-called urban and rural spaces: "*rural* measurements were carried out in *open surroundings* typical of the *countryside*," for example, or "*urban* temperatures are representative of the *built-up* environment of the *city*."

Regardless of how intuitive the terms "urban" and "rural" may be, the reader in these cases is not remotely apprised of the micro- and local-scale surface conditions known to influence screen-level air temperatures.

ΔT_{u-r} has given rise to a host of methodological interpretations of its testing procedure. The most basic of these interpretations invokes a temperature difference between pairs of single-point measurements, often at airports and downtown observatories (eg., *Moreno-Garcia*, 1994), although any combination of so-called urban and rural points is possible. A second interpretation invokes a maximum temperature difference between any two points (usually, but not always, an "urban-rural" pair) along a linear traverse route or within a spatial network of stations (eg., *Chandler*, 1961). *Lowry* (1977) provides a different interpretation of ΔT_{u-r} as an urban-preurban temperature anomaly ("preurban" here denoting an undisturbed, natural landscape beyond the average urban-affected area, or existing prior to urban development). Preurban sites are difficult to locate because undisturbed landscapes scarcely exist in or near most towns and cities; some investigators have, nevertheless, identified preurban landscapes in their study area (eg., *Yow and Carbone*, 2006). And finally, ΔT_{u-r} is often construed as a temperature difference between spatial averages of several "urban" and several "rural" points along a traverse (eg., *Sundborg*, 1951) or within a fixed station network (eg., *Hinkel et al.*, 2003). In all cases, the choice of sites for quantifying ΔT_{u-r} is balanced on criteria of representativeness, known temperature regimes, *in situ* station networks, access to land and data, and instrument safety.

If each of the above interpretations of ΔT_{u-r} is tested in the same city, at the same time, estimates of that city's UHI magnitude will disagree completely. One can only imagine, then, the scatter of results ensuing from a test of all methodological interpretations of ΔT_{u-r} across the continuum of micro-scale settings found in any given city. This prospect alone undermines the validity with which inter-study comparisons of UHI can be made. More fundamentally, it demonstrates a need for increased rigour and standardisation in UHI field methodology.

4. A NEW SCHEME FOR UHI LANDSCAPE CLASSIFICATION

The studies depicted in *Fig. 1* have made valuable contributions to our understanding of city climates, each one describing the time and space patterns of UHI for a particular geographic and cultural milieu. Yet as a community of scientists we are not communicating the findings of these and countless other studies as best we can. The urban-rural dichotomy – our long-standing paradigm for space classification – is diverting attention away from the specific methods, assumptions, definitions, landscapes, and temperature regimes embodied in each study. In turn, we are creating a false impression that all UHI investigations observe a similar combination of "urban" and "rural" climates, and each combination is therefore amenable to inter-city comparison. This impression was confronted by *Parry* (1967) in his discussion of the heat island effect in Reading, England. He correctly warns of the danger in failing to identify micro-scale features of UHI:

> Consideration of the diverse ways in which information has been gathered regarding urban "heat islands" compels one to doubt if the same feature has been measured in all cases... The conditions of exposure at fixed recording stations are ... highly significant and the dangers of unrepresentative siting are stressed. A

plea is made for the recognition of the essentially micro-climatic character of the so-called "urban climate."

Chandler (1962) also addresses issues of scale in his description of the London heat island:

> Local urban morphologies are almost certainly dominant over larger-scale considerations in determining the [urban-rural] temperature anomaly. This may well be true of all occasions, the local heat island intensity being more dependent on the geography of the immediate environment than on the size of the whole urban complex.

The insightful words of *Parry* and *Chandler* some four decades ago give hint of discordance among the "regional-scale" urban-rural dichotomy, the "local-scale" urban heat island phenomenon, and the "micro-scale" influences on our instruments readings. In reconciling these differences of scale, urban climatology must adopt an analytical, multidimensional site characterisation scheme that accommodates the complexity of surface types found in cities and hinterlands around the world (*Stewart and Oke*, 2006). The scheme should be referenced not by the subjective and overly simplistic assessment of landscapes as either "urban" or "rural," but by quantitative, objective measures of surface climate impact. Shifting our experiments into a framework of this nature will guarantee proper assessment and communication of UHI estimates.

No direct attempts have been made at developing a classification system specifically for use in ground-based UHI studies. *Auer* (1978) proposed a scheme for identifying "meteorologically significant" land uses in urban areas. Although some features of his classification system are useful to UHI field methodology, such as the percentage of vegetative cover in a given land-use type, his portrayal of urban and rural land use is less informative because it relates more to land function than to surface form. *Ellefsen* (1990/1) devised a detailed classification system of urban morphological units based on building geometry and materials, and *Davenport et al.* (2000) categorized the aerodynamic roughness of various urban and rural landscapes based on surface form. Neither of these schemes, however, takes account of the urban fabric and its thermal, radiative, and moisture properties. Most recently, *Oke* (2004) blended elements of each of the above schemes into a simple classification of Urban Climate Zones (UCZ). His schematic model divides urban areas into discrete, homogenous units, or "zones," defined only by their ability (in terms of surface geometry and cover) to modify the local surface climate. Each of his seven UCZs is assigned a representative roughness class, aspect ratio, and percentage of impermeable cover. The zones are intended for use at the local scale and as a general guide for the siting and exposure of urban climate stations.

The sites depicted in *Fig. 1* have each been classified according to *Oke's* (2004) UCZ model. Metadata to appropriately classify the sites were obtained from the original studies and through site visitations. Superimposing *Oke's* model on the settings represented in *Fig. 1* quickly exposes the inadequacy of the urban-rural dichotomy. For the most part, the "urban" sites fall into Zones 1 and 2, depending on the general cover and geometry of the local area (<1 km^2) surrounding each site. But on the "rural" side the scheme is much less effective, as only two of the six sites correspond to UCZs, while the remainder can not be classified based on their known site properties. It must be remembered that *Oke's* scheme is not intended for rural site classification, and therefore it specifies only the amount of natural surface cover at a site and not the thermal nature of that cover. Furthermore, *Oke's* (2004) and *Ellefsen's* (1990) schemes are modeled on the built forms of modern, industrialized cities, and thus their application to ancient or underdeveloped

settlements is awkward. Nevertheless, the UCZ template provides an ideal framework on which to construct a universal definition of, and measurement protocol for, UHI magnitude. Although not designed specifically for heat island assessment, *Oke's* climate zones can be adapted to this purpose with a complementary and expanded set of agricultural and undisturbed zones. *Stewart and Oke* (2006) have commenced this effort.

In pursuit of a local-scale climate-zone model with universal appeal, climatologists have much to learn from urban theorists and cultural geographers. Substantive literature points to increasingly complex and dispersed metropolitan forms in both the developed and developing worlds: poly-nucleated, decentralized, and dispersed cities have become definitive features of global urbanization (*Lo and Yeung*, 1998). Meanwhile, the urban-rural distinction has become ever more ambiguous. In fact, decades ago social scientists abandoned the urban-rural dichotomy as a policy paradigm in the developing world. It was argued that the space economy in peri-urban regions could no longer be distinguished by a clear city-country divide (*McGee and Robinson*, 1995). Urban theorists now contend that the spatial demarcation between "urban" and "rural" is artificial, and that this relation is better described as a continuum, or a dynamic, rather than a dichotomy: on the urban periphery of the developing world, *in situ* population densities are extremely high; traditional (i.e., small-holder agriculture) and non-traditional land uses co-exist; and people, capital, commodities, and information flow continuously between city and countryside. Urban geographers reject these peripheral spaces as universally "urban" or "rural," and instead adopt expressions like "development corridors," "growth triangles," and "extended metropolitan regions" (*Chu-Sheng Lin*, 1994). In dramatic contrast, the outskirts of localised North American and European cities are open, sparsely settled, and effectively detached from the city. Far from absolute, our interpretations of "urban" and "rural" are profoundly nuanced in culture, geography, and history.

5. CONCLUSION

As the corpus of empirical UHI studies continues to swell, unconfirmed comparisons of city climate are becoming increasingly difficult to tolerate. The need for a structured, unified, and comparative view of UHI findings is now crucial. It has been argued in this paper that a new landscape classification scheme must supersede the traditional urban-rural dichotomy as a basis for comparison and communication of canopy-layer climate observations over surfaces of particular character (such as those in cities and countrysides). The new model will dislodge our instinctive tendency to assess landscapes as crudely "urban" or "rural," and instead embody appropriate physical measures of surface climate impact. Embedded in such a model will be a multidimensional UHI testing implication better suited to the continuum of landscapes shaping city regions worldwide. Our estimates of UHI magnitude can then be anchored to a framework of generalised and standardised surface-climate zones applicable to any city and to any combination of surface types.

The immediate aim of the new classification scheme is to eclipse urban climatology's obstructive and distracting fixation with "urban" and "rural" site designations, and in the process to curtail baseless cross-study comparisons of UHI behaviour. The intent is not, incidentally, to encourage repeated (and redundant) case studies of UHI. Urban climate literature is overstocked with descriptive and confirmatory

cases of UHI, each retesting and restating in predictable fashion what has been known for decades of the heat island effect. In spite of their often elaborate and extensive measurement programs, these investigations are primarily of local interest.

The new climate-zone model will steer critical experiments toward sharp, provocative, and novel disclosures of canopy-layer climates and their underlying causes. This prospect bears important implications for climate studies of a much larger context that require intimate understanding of local-scale surface types, especially those of the city and its environs. Attempts to remove urban bias from long-term climate trends, for example, must find improved techniques. Traditional approaches have used surrogate measures of urbanisation, such as population (e.g., *Kukla et al.*, 1986) and satellite night-light data (eg., *Peterson*, 2003), to separate "urban" and "rural" temperature series. Future studies must instead take into consideration the structural and climatological character of individual measurement sites. The proposed scheme described in this paper will provide the initial steps toward more definitive assessments of urban impact on regional and global climates.

In closing, there are historical lessons to be learned from urban theorists who contend that the urban-rural divide has collapsed altogether in many parts of the world, and that its heuristic value as a policy paradigm has greatly diminished. Arguably, historical developments in urban geography give impetus to climatologists uprooting this same dichotomy as an operational testing procedure of urban impact on thermal climate. Landscape classification, whether "urban," "rural," or otherwise, is fundamental to UHI definition, experimentation, and explanation. Thought should therefore be given to the progress made in cognate fields before dismantling a shared tradition of space classification.

REFERENCES

Adebayo, Y.R., 1991: "Heat island" in a humid tropical city and its relationship with potential evaporation. *Theor. Appl. Climatol. 43*, 137-147.

Auer, A.H., 1978: Correlation of land use and cover with meteorological anomalies. *J. Appl. Meteorol. 17*, 636-643.

Böhm, R., 1998: Urban bias in temperature time series. A case study for the city of Vienna, Austria. *Climatic Change 38*, 113-128.

Bowling, S., and C. Benson, 1978: Study of the Subarctic heat island at Fairbanks, Alaska. *Env. Protection Agency Report*, EPA-600/4-78-027, North Carolina.

Chandler, T.J., 1961: The changing form of London's heat island *Geography 46*, 295-307.

Chandler, T.J., 1962: Temperature and humidity traverses across London. *Weather 17*, 235-241.

Chow, W. and Roth, M., 2006: Temporal dynamics of the urban heat island of Singapore. *Int. J. Climatol. 26*, 2243-2260.

Chu-Sheng Lin, G., 1994: Changing theoretical perspectives on urbanization in Asian developing countries. *Third World Planning Review 16*, 1-23.

Davenport, A.G., Grimmond, S.B., Oke, T.R. and Wieringa, J., 2000: Estimating the roughness of cities and sheltered country. Proceedings, *12th Conference on Applied Climatology*, Asheville, North Carolina, American Meteorological Society.

Eliasson, I., 1994: Urban-suburban-rural air temperature differences related to street geometry. *Physical Geography 15*, 1-22.

Ellefsen, R., 1990/91: Mapping and measuring buildings in the urban canopy boundary layer in ten US cities. *Energy and Buildings 15-16*, 1025-1049.

Emmanuel, R., and Johansson, E., 2006: Influence of urban morphology and sea breeze on hot humid microclimate: The case study of Colombo, Sri Lanka. *Clim. Res. 30*, 189-200.

Figuerola, P.I. and Mazzeo, N.A., 1998: Urban-rural temperature differences in Buenos Aires. *Int. J. Climatol. 18*, 1709-1723.

Gedzelman, S.D., Austin, S., Cermak, R., Stefano, N., Partridge, S., Quesenberry, S. and Robinson, D.A., 2003: Mesoscale aspects of the urban heat island around New York City. *Theor. Appl. Climatol. 75*, 29-42.

Giridharan, R., Lau, S. and Ganesan, S., 2005: Nocturnal heat island effect in urban residential developments of Hong Kong. *Energy and Buildings 37*, 964-971.

Gugler, J. (ed.), 1997: *Cities of the Developing World: Issues, Theory and Policy*. Oxford University Press, Oxford.

Hedquist, B.C. and Brazel, A.J., 2006: Urban, residential, and rural climate comparisons from mobile transects and fixed stations: Phoenix, Arizona. *J. Arizona-Nevada Acad. Sci. 38*, 77-87.

Hinkel, K.M., Nelson, F., Klene, A.E. and Bell, J.H., 2003: The urban heat island in winter at Barrow, Alaska. *Int. J. Climatol. 23*, 1889-1905.

Hisada, Y., Matsunaga, N. and Ando, S., 2006: Summer and winter structures of heat island in Fukuoka metropolitan area. *JSME Int. J. 49B*, 65-71.

Howard, L., 1833: *The Climate of London*. Dalton, London.

Jauregui, E., 1997: Heat island development in Mexico City. *Atmos. Environ. 31*, 3821-3831.

Jonsson, P., 2004: Vegetation as an urban climate control in the subtropical city of Gaborone, Botswana. *Int. J. Climatol. 24*, 1307-1322.

Klysik, K. and Fortuniak, K., 1999: Temporal and spatial characteristics of the urban heat island of Lodz, Poland. *Atmos. Environ. 33*, 3885-3895.

Kukla, G., Gavin, J. and Karl, T.R., 1986: Urban warming. *J. Appl. Meteorol. 25*, 1265-1270.

Landsberg, H.E. and Maisel, T.N., 1972: Micrometeorological observations in an area of urban growth. *Bound. Lay. Meteorol. 2*, 365-370.

Lee, D.O., 1979: Contrasts in warming and cooling rates at an urban and rural site. *Weather 34*, 60-66.

Lo, F. and Yeung, Y. (eds.), 1998: *Globalization and the World of Large Cities*. United Nations University Press, New York.

Lowry, W.P., 1977: Empirical estimation of the urban effects on climate: A problem analysis. *J. Appl. Meteorol. 16*, 129-135.

Lyall, I.T., 1977: Some local temperature variations in north-east Derbyshire. *Weather 32*, 141-145.

McGee, T. and Robinson, I.M. (eds.), 1995: *The Mega-Urban Regions of Southeast Asia*. University of British Columbia Press, Vancouver.

Moreno-Garcia, M.C., 1994: Intensity and form of the urban heat island in Barcelona. *Int. J. Climatol. 14*, 705-710.

Mukherjee, A.K. and Daniel, C., 1976: Temperature distribution over Bombay during a cold night. *Indian J. Met. Hydrol. Geophys. 27*, 37-41.

Norwine, J., 1976: City size and the urban heat island: Observed effects at small cities in a subtropical environment. *The Texas J. Sci. 27*, 383-396.

Oke, T.R., 1976: The distinction between canopy and boundary-layer urban heat islands. *Atmosphere 14*, 269-277.

Oke, T.R., 1982: The energetic basis of the urban heat island. *Quart. J. Roy. Met. Soc. 108*, 1-24.

Oke, T.R., 2004: Initial Guidance to Obtain Representative Meteorological Observations at Urban Sites. *IOM Report 81*, World Meteorological Organization, Geneva.

Okoola, R.E., 1980: The Nairobi heat island. *Kenya J. Sci. Tech. 1A*, 53-65.

Parry, M., 1956: Local temperature variations in the Reading area. *Quart. J. Roy. Met. Soc. 82*, 45-57.

Parry, M., 1967: The urban "heat island." *Biometeorology 2*, 616-624.

Peterson, T.C., 2003: Assessment of urban versus rural in situ surface temperatures in the contiguous United States: No difference found. *J. Climate 16*, 2941-2959.

Robaa, S.M., 2003: Urban-suburban/rural differences over Greater Cairo, Egypt. *Atmosfera 16*, 157-171.

Sakakibara, Y. and Matsui, E., 2005: Relation between heat island intensity and city size indices/urban canopy characteristics in settlements of Nagano Basin, Japan. *Geographical Rev. Japan 78*, 812-824.

Sakakibara, Y. and Owa, K., 2005: Urban-rural temperature differences in coastal cities: Influence of rural sites. *Int. J. Climatol. 25*, 811-820.

Stewart, I.D., 2000: Influence of meteorological conditions on the intensity and form of the urban heat island effect in Regina. *The Canadian Geographer 44*, 271-285.

Stewart, I.D. and Oke, T., 2006: Methodological concerns surrounding the classification of urban and rural climate stations to define urban heat island magnitude. Preprints, *Sixth International Conference on Urban Climate*, Goteborg, Sweden, 431-434.

Sundborg, A., 1951: Climatological studies in Uppsala with special regard to the temperature conditions in the urban area. *Geographica 22.* Geographical Institute of Uppsala, Sweden.

Syrakova, M. and Zaharieva, M., 1998: Sofia heat island – diurnal and seasonal variations. Part I: Frequency distribution of hourly temperature differences. *Bulgarian J. Met. Hydrol. 9*, 210-219.

Szymanowski, M., 2005: Interactions between thermal advection in frontal zones and the urban heat island of Wrocław, Poland. *Theor. Appl. Climatol. 82*, 207-224.

Tso, C.P., 1996: A survey of urban heat island studies in two tropical cities. *Atmos. Environ. 30*, 507-519.

Tumanov, S., Stan-Sion, A., Lupu, A., Soci, C. and Oprea, C., 1995: Local and mesoscale influences of the metropolitan areas on some meteorological parameters and phenomena. Application to the city of Bucharest. *Romanian J. Met. 2*, 1-18.

Tumanov, S., Stan-Sion, A., Lupu, A., Soci, C. and Oprea, C., 1999: Influences of the city of Bucharest on weather and climate parameters. *Atmos. Environ. 33*, 4173-4183.

Unger, J., 1996: Heat island intensity with different meteorological conditions in a medium-sized town: Szeged, Hungary. *Theor. Appl. Climatol. 54*, 147-151.

Yow, D.M. and Carbone, G.J., 2006: The urban heat island and local temperature variations in Orlando, Florida. *Southeastern Geographer 46*, 297-321.

Yudcovitch, N., 1966-7: Factors influencing the temperature variation in Calgary. *The Albertan Geographer 3*, 11-19.

Zhou, S., 1990: Five islands effects of Shanghai urban climate. *Science in China 33B*, 67-78.

FOREST STRUCTURE STUDIES IN AGGTELEK NATIONAL PARK (HUNGARY)

E. TANÁCS, A. SAMU and I. BÁRÁNY-KEVEI

*Department of Climatology and Landscape Ecology, University of Szeged, P.O.Box 653, 6701 Szeged, Hungary
Email: nadragulya@geo.u-szeged.hu*

Összefoglalás – Vizsgálatunk célja a Haragistya-Lófej erdőrezervátumban a faállomány jelenlegi állapotának fel-
térképezése, és a 212 felhasznált mintapont kategóriákba sorolása volt. A vizsgálathoz az egyes mintapontokra ki-
számítottunk néhányat a leggyakrabban alkalmazott szerkezeti és diverzitási mutatók közül. Megvizsgáltuk ezek
térbeli eloszlását a mintaterületen, valamint egymással való kapcsolatukat. Kiválasztottunk négyet (Shannon in-
dex, variációs koefficiens, körlapösszeg/ha, állománymagasság) és ezek alapján hierarchikus klaszter-analízis se-
gítségével csoportosítottuk a mintapontokat. Az eredmény alapján elmondható, hogy a faállomány-szerkezetet je-
lentősen befolyásolja a termőhely, különösen a domborzat.

Summary – Our measurements were carried out in the Haragistya-Lófej forest reserve, in Aggtelek karst. The aim
of our investigation was to describe the present state of the forests in our study area and to define groups with the
help of structural and compositional indices. We have chosen some of the most commonly used indices and
calculated them for 212 plots. Out of these we chose a set that were not strongly correlated with each other while
each described a range of other related variables. These were the Shannon Index, the coefficient of variation (dbh),
the basal area/ha and the stand height. On the basis of these 4 variables we divided the area's forests in 6 classes.
The groups are much affected by the production site; the role of elevation seems especially important. The buffer
zone and the core area of the reserve also differ, especially in terms of tree size and distribution.

Key words: forestry, stand structure, Aggtelek National Park, karst, Haragistya

1. AIMS AND OBJECTIVES

The aim of designating forest reserves in Hungary was to provide places where
research can be carried out in order to better understand the natural processes of forest
ecosystems. (*Temesi*, 2002) Researching stand structure is one of the practical ways of
approaching the concept of biodiversity, which has recently become increasingly important
for stake-holders.

Generally speaking, diversity means the inner variability of the structures and
elements of a system (*Haeupler*, 1982). Ecological diversity means the variability in the
spatial and temporal patterns and the relationships of populations along with their
structures. This diversity describes the physical structure deriving from the spatial
distribution of species, age groups and growth forms (*Standovár and Primack*, 2001).

Besides being related to the diversity of the forest wildlife, stand structure can also
provide an explanation to its spatial patterns. (*McElhinny et al.*, 2005) Analysing the
patterns of stand-level structural and compositional indices has a great practical
significance, the stand being the basis of forest management and thus the possibility of
direct human interference is highest at that level. The knowledge of both spatial and

temporal patterns may serve as a basis for sustainable management aiming to keep a broad range of forest goods and services. (*Spies*, 1998)

The forests of the karst plateau called Haragistya (Aggtelek Mts.) have been seriously affected by anthropogenic activity in the last centuries. After much of the area had been designated a forest reserve in the 1990's active forest management has declined. The aim of this study is to describe the area's forests by analysing the spatial distribution of some common structural and compositional indices. The present forest structure in the area is a result of long-term human impact and a spatially very varied natural environment. Thus, after examining the correlations we also define a set of basic indices suitable for categorising the sampling points. The resulting groups are then compared in terms of both production site and management history in order to understand the development of the area's forests.

2. MATERIALS AND METHODS

2.1. The study area

The Haragistya-Lófej forest reserve is situated in the north-western corner of Aggtelek National Park, surrounded by the Slovakian border. Except for a part of its buffer zone in the south, the area is under strict protection. The Haragistya bears all the hallmarks of a typical karst plateau; its surface is dry and highly varied, covered by series of dolines and dry valleys. The sample area is situated in the south-eastern part of the plateau (*Fig. 1*). Its main features are two N-S direction dry valleys (Hosszú-valley in the east and the other is referred to as Dry valley), two mountains (Mt. Ocsisnya in the west and Mt. Káposztás in the east) and a ridge between the valleys. The northern boundary is a series of dolines in E-W direction.
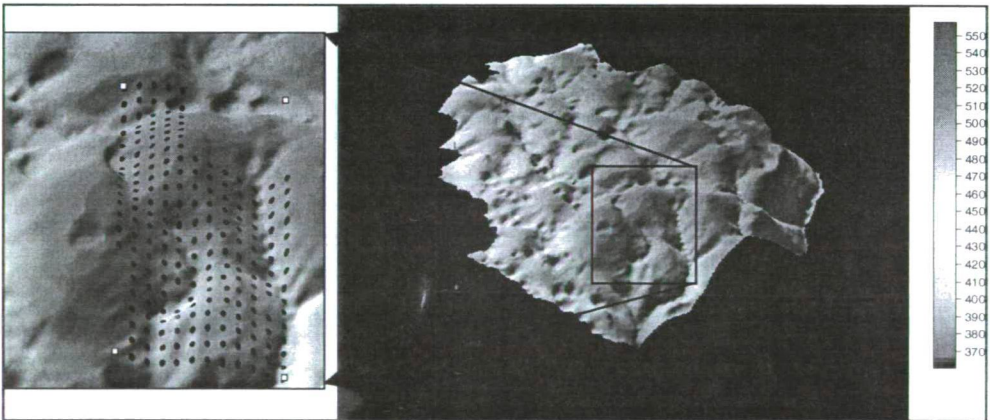
Fig. 1 The study area and the sampling points

The bedrock is rather homogenous; light grey limestone and dolomite of the Wetterstein Formation vary. However, in the bottom of hollows (dolines, valleys and slope curves) Cretaceous red clay sediments (*Jakucs*, 1977; *Beck and Borger*, 1999) have accumulated. The bedrock essentially defines soil type distribution; on the tops, ridges and slopes different types of hollow rendzina soils are characteristic while in the above-mentioned hollows deeper red clayey rendzinas and brown forest soils can be found. The

development of the soil profiles is rather disturbed; traces of either erosion or accumulation appear in most cases.

The vegetation is a mosaic of dry thermophilous oak forests, dominated by *Quercus pubescens*, oak-hornbeam forests and beech-hornbeam forests in smaller patches in the valleys and on northern slopes. The most common species are *Carpinus betulus, Quercus petraea, Quercus pubescens, and Fagus sylvatica*, often accompanied by *Acer campestre* and *Sorbus torminalis (Fig. 2)*.

According to the forest management plan made in 1993 the age of the forests in the sample area varies between 50 and 110. However, archive plans show slightly higher ages; according to these even the youngest forests have been regenerated in the mid-thirties and are therefore approximately 70 years old. The oldest forests can be found in the series of dolines in the northern parts of the study area *(Fig. 3)*. Management activity mostly consisted of thinning. In some parts of the area, there's no written evidence of cuttings since 1935; much of the area has not been managed for the last 40 years. However in some sections thinnings took place in the 80's and the last cutting occurred in 1997 in a single section in the reserve's buffer zone *(Fig. 4)*.

2.2. Data and methods

We have started our measurements in the Haragistya-Lófej forest reserve in April 2006. We have recorded the position, diameter at breast height (dbh), species and social position (according to the Kraft-classification) of every living or dead tree exceeding a dbh of 5 cm or a height of 5 m in 10 m-radius permanent plots, situated in a 50 m-resolution grid. In the present study we use the data of 212 such plots. About half of these are situated in the core area of the reserve while the rest are in the buffer zone. No detailed measurement has been carried out in

Fig. 2 The main species of the area

Fig. 3 The age of forests

the area before; however there are available archive forest management plans dating back until 1935. The spatial resolution of these is rather lower than the variety of the karst surface and consequently that of the forest but still they represent a valuable information source concerning past management activities and the state of the forest.
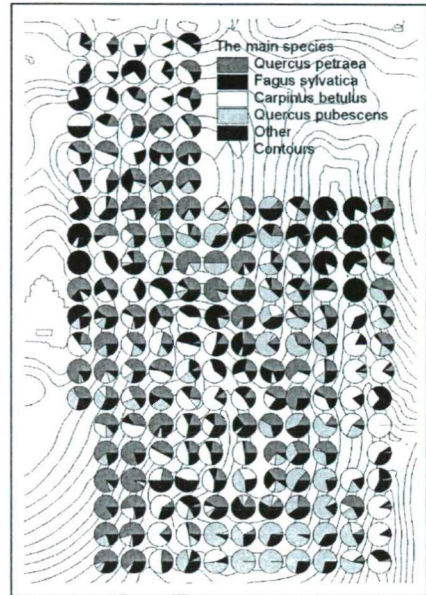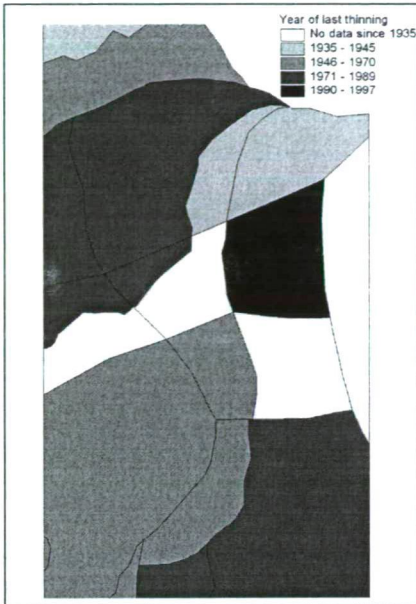
Fig. 4 Year of last thinning

In order to describe the present state of the forests we have chosen some of the most commonly used structural and compositional indices after *McElhinny et al.* (2005) and *Neumann and Starlinger* (2001) and calculated them for every plot. We looked at the spatial distribution in general and the upper and lower 10 % of the values in order to outline areas where the indices are extremely different from the expected value. In the case of the Cox Index, we used the categories defined by *Cox* (1971).

Structural indices: These indices mostly describe the diversity of forms in space. Some of the most typical indices included in this category are the diameter distribution, the number of tree species, the horizontal distribution of individuals and the vertical structure of the crown layer (*Dylla and Krätzner*, 1986). We have computed most of them including the living trees and the dead standing trees (snags), not taking into account the data of shrub species.

The number of stems/ha is a widely used measure of density (*Nagel*, 2001).

Average dbh: This index increases with age and in different forest types it was successfully used for discriminating successional stages (*McElhinny et al.,* 2005)

Standard deviation of dbh: This index is related to the presence of different-aged individuals in the plot and thus reflects naturalness.

Coefficient of variation (dbh): This index is calculated as the quotient of the standard deviation and the mean dbh.

Basal area/ha is a widely used index in forestry for expressing tree volume and biomass in an area.

The number and proportion of snags: The ecological importance of snags, apart from their effects on recruitment, is more similar to that of living trees than logs. Although seedlings in most cases cannot grow on the snag directly it offers favourable places for regeneration at the root collar (*Bauer,* 2002). In case of undisturbed forests the number of snags and their proportion can refer to the successional stage. However their main importance lies in their role as bird habitat; they are an important source of tree hollows (*McElhinny et al.,* 2005).

Stand height (modelled): In order to define stand height we used a height map derived from a Digital Terrain Model as described in *Zboray and Tanács* (2005).

Cox Index: This index serves to characterise the horizontal distribution of trees (*Cox,* 1971). It is calculated on the basis of smaller sample areas (in our case each 10 m circle was divided in 52 squares in a 2.5*2.5 m grid) as $K = s^2/x$ where s^2 is the variance and x is the mean of the sample plots. The Cox Index defines the proportion of usage within each sample plot and whether this value has a Poisson distribution. If it does, the distribution of the trees follows no pattern (*Fröchlich,* 1993). If it is not significantly different from 1, which means it does follow a Poisson distribution, then the trees are randomly distributed in the stand. If $K<1$ the pattern is regular while if $K>1$ the trees are aggregated. If K exceeds

5, the trees are highly aggregated (*Cox*, 1971). When calculating the Cox Index, we did not include shrub species, such as *Cornus mas, Cornus sanguinea, Crataegus monogyna, Crataegus laevigata* and *Coryllus avellana.*

Compositional indices: according to *Kimmins* (1987) the notion of diversity should always include species diversity and dominance. Several indices were developed in order to measure diversity; these indices are considered to be very important indicators. Generally the diversity of a community is higher if the number of species is higher and the individuals are more equally divided between species. Only those indices are suitable to measure biodiversity that include both the number of species and the distribution of individuals among the species (*Mühlenberg*, 1993). From among these we chose the widely used *Shannon-Weaver* (1949) diversity index. The advantage of this index is that it takes into account both the number and evenness of the species. Its value is increased either by having more unique species, or by having a greater species evenness (*Pielou*, 1977).

$$Hsh = \sum_{i=1}^{n} pi \cdot \ln pi$$

Where p_i is the relative abundance of each species, in this case calculated as the proportion of the basal area of individuals of a given species to the total basal area of individuals in the plot and n is species richness. When computing the Shannon Index, we also included shrub species.

We then analysed the spatial distribution of each, using ArcView 3.3 software. We examined their relationship with the help of SPSS 11 software and defined a set of indices that were not strongly correlated with each other while each described a range of other related variables. These were the Shannon Index, the coefficient of variation (dbh), the basal area/ha and the stand height.

After choosing the appropriate indices the values were standardised and hierarchical cluster analysis was applied on the selected variables. 6 classes were created. We then examined each class in terms of site and management history to see the reasons behind their differences.

3. RESULTS AND DISCUSSION

3.1. The spatial distribution of the indices in the study area

The mean stem number/ha is 997. Generally this value is lower in the valleys and dolines where *Carpinus betulus* and *Fagus sylvatica* are the dominant species (*Fig. 5a*) and higher on the slopes. The low values of the valleys can partly be explained by former and still existing roads. Also these sections have not been thinned for 40 years in average. There are 3 areas with especially high values: a southeast-facing slope besides Hosszú-valley, the south-eastern slope of Mt. Ocsisnya and some scattered points on the east-facing slope of the upper part of Hosszú-valley. The year of last thinning in these 3 areas varies from 1986 to the 1950's. On the southeast-facing slopes the dominant species is mainly *Quercus pubescens*, accompanied by *Quercus petraea, Carpinus betulus, Acer campestre* and *Sorbus torminalis (Fig. 2).*

The mean dbh of the plots is 19.35 cm, the highest values appear on the north-facing slopes of Mt. Ocsisnya. *(Fig. 5b)* There the last production occurred in 1989. The dominant species are *Carpinus betulus* and *Fagus sylvatica*, along with *Quercus petraea,*

accompanied by *Cerasus avium* and *Sorbus torminalis*. The dolines north of this area also hold relatively high values; this section was last thinned in 1964. Besides *Carpinus betulus* and *Fagus sylvatica*, *Tilia cordata* and *Ulmus glabra* can also be found. In the southern part, in the buffer zone of the reserve there are only a few small patches with high values; mainly in Dry valley.
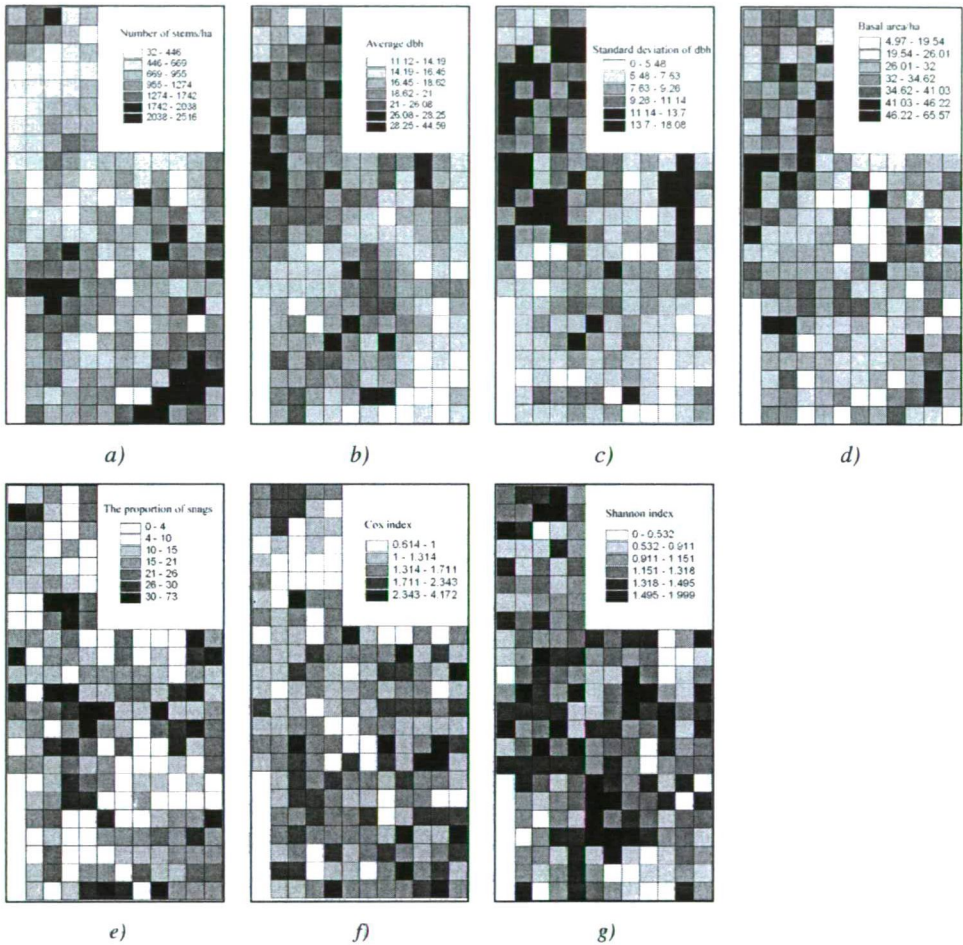
Fig. 5 The spatial distribution of structural and compositional indices in the study area

The mean value of the dbh standard deviation in the area is 8.82 cm. The sampling points with small values are all situated in the buffer zone; their dominant species are usually *Quercus* species with *Carpinus betulus*, *Sorbus torminalis*, *Acer campestre* and *Fraxinus excelsior*. The areas with higher values are situated in the core area, mainly on north- or west-facing slopes or ridges (*Fig. 5c*) where *Quercus petraea*, *Carpinus betulus* and *Fagus sylvatica* dominate the crown layer along with *Tilia platyphyllos*, *Quercus cerris* and *Cerasus avium*.

The mean basal area/ha (*Fig. 5d*) in the study area is 30.64 m². This index shows high values mainly in the northern part of the area and the saddle between Mt. Ocsisnya and

Káposztás where *Quercus petraea* and *Carpinus betulus* are most frequent. The basal area is also high on the east-facing slope in the northern part of Hosszú-valley (*Fagus sylvatica*) and the southern part where *Quercus pubescens* and *Carpinus betulus* dominate. Small values characterise the reforesting clearings on the ridge south of Mt. Káposztás. Average values occur in the sampling points dominated by *Carpinus betulus* in the bottom of the valleys.

The proportion of snags in the sampling points is rather varied (*Fig. 5e*); there are no major consistent patches. The mean of the sampling points is 16.78%. There are 3 areas with higher values: the south-east-facing slopes of Mt. Ocsisnya, a small patch west of Mt. Káposztás and the northern part of Hosszú-valley. This value is very small (0-10%) on the ridge south of Mt. Káposztás and the slope north of it. These sampling points are usually characterised by a varied species composition, mainly with *Carpinus betulus, Fraxinus excelsior* and *Quercus petraea.*

Examining the spatial distribution of the Cox Index (*Fig. 5f*) in the study area we found no sampling points with a very high aggregation value (K<5). Most of the area is characterised by an average level of aggregation while on the north-facing slopes of Mt. Káposztás the horizontal distribution of the trees is regular. The characteristic species in these stands are *Carpinus betulus, Fagus sylvatica* and *Quercus petraea* and the last thinning occurred in 1989. The same tendency can be seen in the middle parts of Dry valley, in a stand with the same species, last thinned in the 1960's.

The Shannon Index (*Fig. 5g*) shows a high variability in the area. However, highest are its values on the north-facing slope of the northern dolines, on the saddle between Mt. Ocsisnya and Káposztás, in the southern part of Dry valley and the middle part of Hosszú-valley. These forests have not been managed in the last 40-60 years and the high diversity reflects that well. We found the lowest values in the *Fagus sylvatica*-dominated northern part of Hosszú-valley, the *Quercus pubescens*-dominated southern slopes of Mt. Káposztás and in the northern dolines.

3.2. Relationship between the different indices

According to the one-sample Kolmogorov-Smirnov test, the basal area/ha, the proportion of snags in the plots, the coefficient of variation, the Shannon Index and the stand height have a normal distribution. *Table 1* shows their Pearson correlations. *Fig. 6a* shows the relationship between dbh-related indices and stem number/ha. The well-known allometric relationship between stem number and mean dbh can be clearly seen. There is also a positive non-linear relationship between mean dbh and diameter standard deviation, which shows that in the older forests gap dynamics have started and the originally even-aged stands are turning into uneven-aged ones. Since the coefficient of variation shows a positive linear relationship with the standard deviation of dbh it can be used to express naturalness among the variables chosen for the classification. It is also correlated to the proportion of snags in the plots.

Fig. 6b shows the relationship between snag characteristics, basal area/ha and stem number/ha. Out of these variables we have chosen basal area/ha to include in the classification. We have added stand height since it reflects site quality, being related to soil depth. To a lesser extent, it also refers to the species composition (*Fig. 6c*). It is positively correlated with the proportion of *Fagus sylvatica* in the plot and negatively with the proportion of *Quercus pubescens. Fig. 6d* shows that there is no correlation between the

finally chosen four variables: the Shannon Index, the coefficient of variation (dbh), the basal area/ha and the stand height.
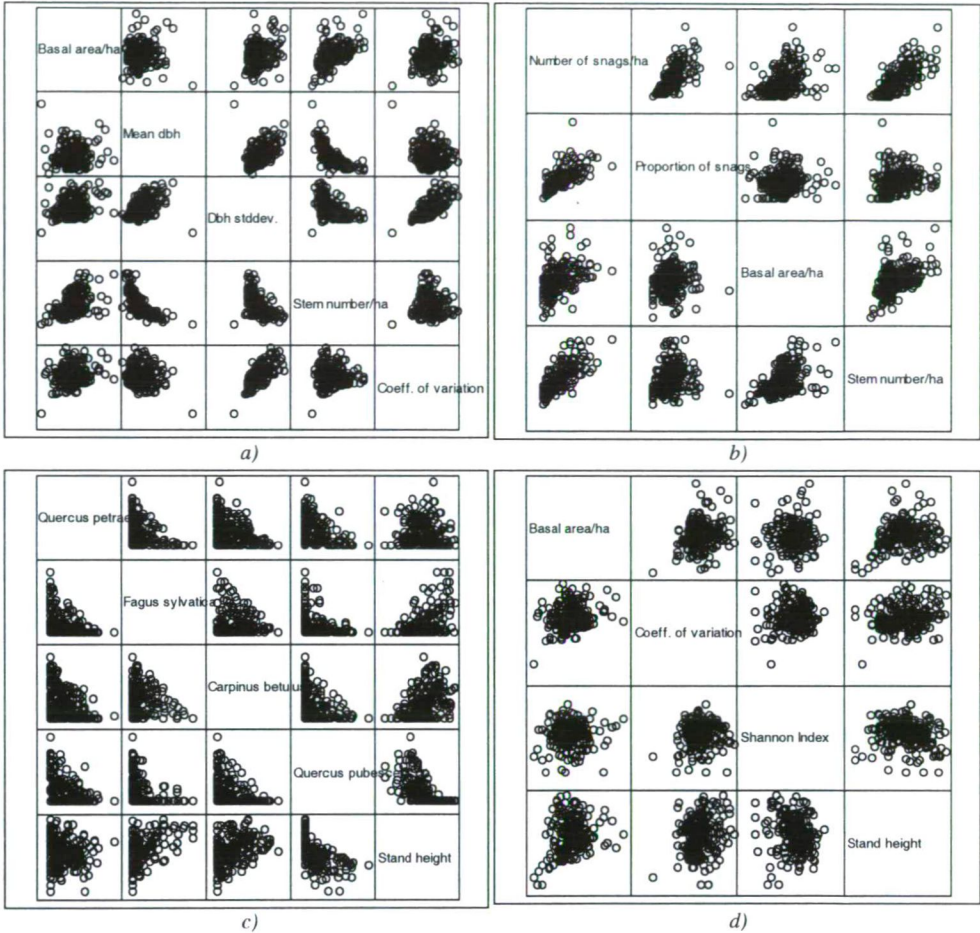
Fig. 6 Scatterplots of structural indices

Table 1 Pearson correlations of the variables with normal distribution

	B. area/ha	P.of snags	Coeff. of variation	Shannon Index
Basal area/ha	1			
Proportion of snags	0.099	1		
Coefficient of variation	0.186**	0.575**	1	
Shannon Index	0.020	0.031	0.031	1
Stand height	0.226**	0.071	0.193**	-0.188**

**Correlation is significant at the 0.01 level (2-tailed).

Fig. 7 shows one possible result of the hierarchical cluster analysis. In this case we used squared Euclidean distance and between-groups linkage. Choosing the optimal classification method will need further investigation; however this version summarizes the

result of the individual indices and also our field experiences well. Comparing the location of the sampling points in each group to the boundaries of forest management units and the contours it seems that the groups are distributed mainly according to the production site and not so much according to management history. However by defining the age of the forests and the species composition, the latter also plays an important part in forming the present structure.

Fig. 8 shows the boxplots of some chosen indices in the 6 categories. Group 1 is mainly situated on the lower parts of slopes along the valleys and is characterised by the dominance of *Quercus petraea* and *Carpinus betulus*. All the indices show rather high values, although never the highest. Stand height is about 22 meters. Group 2 is situated on the (mainly east-facing) slopes and includes the sampling points with the highest species diversity. Mean stand height is about 15 m but the basal area/ha is rather high, possibly because

Fig. 7 The groups identified by the cluster analysis

of a high stem density. The coefficient of variation (and consequently the diversity of age groups) is rather low. Group 3 represents the points in the older forests in the north and the valley heads, mainly dominated by *Fagus sylvatica*. The coefficient of variation is highest in these areas and the basal area is also rather high. The horizontal distribution of trees is close to regular while species diversity is rather lower. The average stand height is about 25 m. Group 4 is mainly situated on the ridge south of Mt. Káposztás, and the most characteristic species is *Quercus pubescens*. These stands generally show lower values; average stand height is around 10 m and both basal area and coefficient of variation are low. Species diversity however is very high and the stands are moderately aggregated. Group 5 represents the clearings in the ridge, so basal area is very low at these points and species diversity is not too high either. *Quercus pubescens, petraea* and *robur* dominate these points. A high median of the coefficient of variation refers to the natural reforestation processes occurring at these points. Group 6 consists of a single point in Hosszú-valley with rather low values in the case of all the indices, except height.

SUMMARY

In general we can conclude that there are several well-identifiable groups of sampling points in the Haragistya-Lófej forest reserve; the groups are much affected by the

production site; the role of elevation seems especially important. The buffer zone in the south and the core area of the reserve also differ especially in terms of tree size and distribution. From several widely used structural and compositional indices we managed to define a set that were not strongly correlated with each other while each described a range of other related variables. These were the Shannon Index, the coefficient of variation (dbh), the basal area/ha and the stand height. On the basis of these 4 variables we divided the area's forests in 6 classes, which can later be used in the analysis of changes.
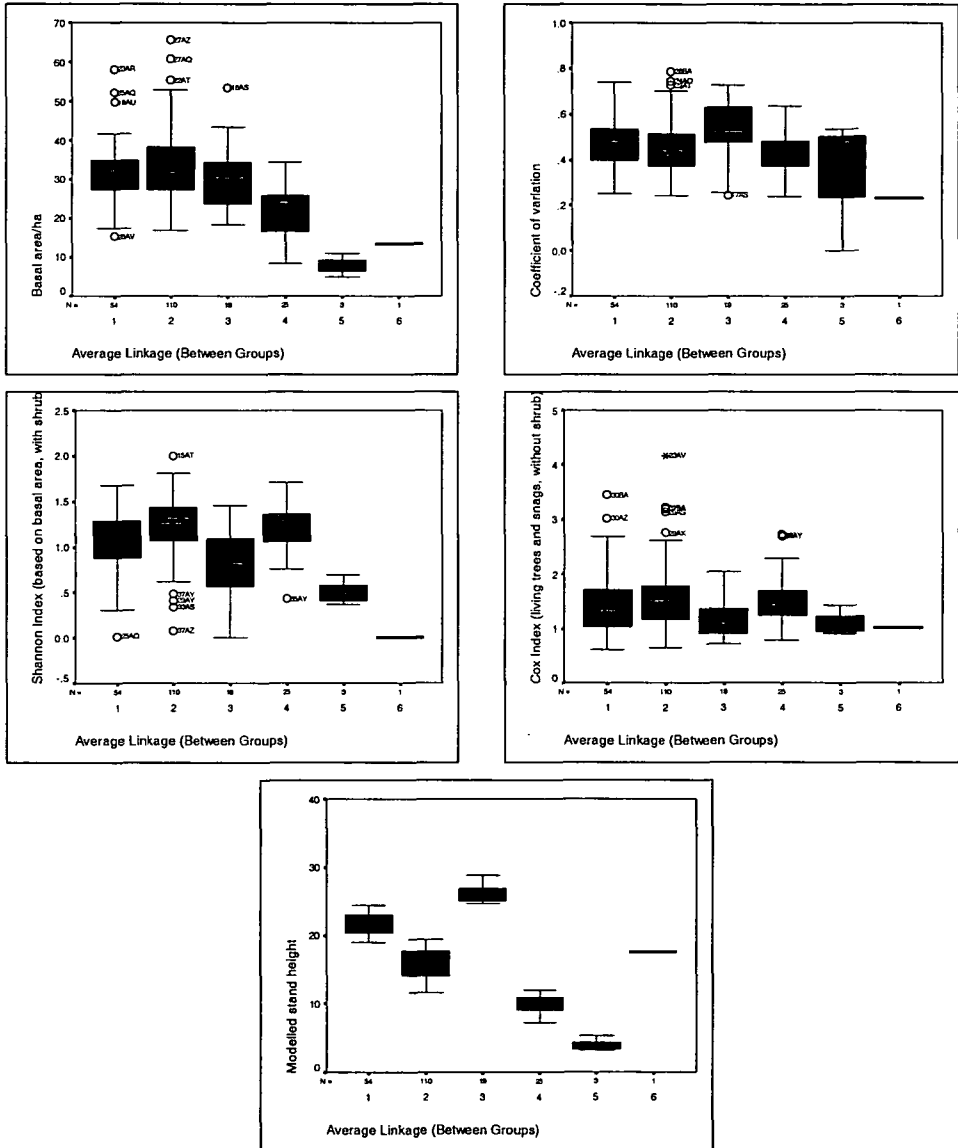
Fig. 8 Structural indices in the groups

REFERENCES

Bauer, M.L., 2002: Walddynamik nach Borkenkäferbefall in den Hochlagen des Bayerischen Waldes – Dissertation

Beck, R.K. and Borger, H., 1999: Soils and relief of the Aggtelek Karst (NE Hungary): A record of the ecological impact of paleoweathering effects and human activity. Essays in the ecology and conservation of karst. *Acta Geographica Szegediensis 36 (Special issue)*, pp. 13-30.

Cox, F., 1971: Dichtebestimmung und Strukturanalyse von Populationen mit Hilfe von Abstandsmessungen. Diss. Universität, Göttingen. 182 p.

Dylla, K. and Krätzner, G., 1986: *Das ökologische Gleichgewicht in der Lebensgemeinschaft Wald.* Quelle und Mayer Verlag, Heidelberg - Wiesbaden.

Fröchlich, M., 1993: Statistische Methoden zur Analyse der Verteilungsmusters von Naturverjüngungspflanzen im Bergmischwald. Unveröffentl. Diplomarbeit, Forstwissenschaft. Fakultät, Ludwig-Maximilians-Universität, München. 35 p.

Haeupler, H., 1982: Evenness als Ausdruck der Vielfalt in der Vegetation. Dissertationes Botanicae, Band 65, J. Cramer, 268.

Jakucs, L., 1977: Genetic Types of Hungarian Karst. *Karszt és Barlang (Special Issue)*, 3-18.

Kimmins, J.P., 1987: *Forest Ecology.* Macmillan Publishing Company, New York. 531 p.

McElhinny C. Gibbons P, Brack C, and Bauhus J., 2005: Forest and woodland stand structural complexity: Its definition and measurement. *Forest Ecology and Management 218*, 1–24.

Mühlenberg, M., 1993: *Freilandökologie.* 3 Aufl. Heidelberg, Wiesbaden, UTB: 511 p.

Nagel, J., 2001: Skript Waldmesslehre. (*http://wwwuser.gwdg.de/~jnagel/wamel.pdf*)

Neumann M. and Starlinger F., 2001: The significance of different indices for stand structure and diversity in forests. *Forest Ecology and Management 145*, 91-106.

Pielou, E.C., 1977: *Mathematical Ecology*, John Wiley & Sons, New York. 385 p.

Shannon, C. E. and Weaver, W., 1949: *The mathematical theory of communication.* University of Illinois Press, Urbana.

Spies T.A., 1998: Forest Structure: A Key to the Ecosystem. *Northwest Science, Vol. 72 (special issue No. 2).*

Standovár, T. and Primack, R., 2001: *A természetvédelmi biológia alapjai [Essentials of Conservation Biology* (in Hungarian)] Nemzeti Tankönyvkiadó, Budapest.

Temesi, G., 2002: Az erdőrezervátumok fenntartásának általános irányelvei. [General guidelines of managing forest reserves. (in Hungarian)] In *Horváth, F. and Borhidi, A.* (eds.): *A hazai erdőrezervátum-kutatás célja, stratégiái és módszerei. [The aims, strategies and methods of Hungarian forest reserve research.* (in Hungarian)] TermészetBúvár Alapítvány Kiadó, Budapest. 38-45.

Zboray, Z. and Tanács, E., 2005: An investigation of the growth type of vegetation in the Bükk Mountains by the comparison of Digital Surface Models *Acta Climatologica et Chorologica Universitatis Szegediensis 38-39*, 163-169.

THE RELATION OF METEOROLOGICAL ELEMENTS AND BIOLOGICAL AND CHEMICAL AIR POLLUTANTS TO RESPIRATORY DISEASES

SZ. TOMBÁCZ[1], L. MAKRA[1], B. BÁLINT[2], G. MOTIKA[3] and T. HIRSCH[4]

[1]Department of Climatology and Landscape Ecology, University of Szeged, P.O.Box 653, 6701 Szeged, Hungary
E-mail: szintmail@freemail.hu
[2]Thorax Surgery Hospital, Csongrád County, Alkotmány u. 36., 6772 Deszk, Hungary
[3]Environmental and Natural Protection and Water Conservancy Inspectorate of Lower-Tisza Region,
P.O.Box 1048, 6701 Szeged, Hungary
[4]Hungarian Meteorological Service, P.O.Box 38, 1525 Budapest, Hungary

Összefoglalás – A dolgozat a Kárpát-medence fölött, a téli hónapokban (december, január és február), valamint elsősorban a parlagfű pollinációjához köthető nyári – kora őszi időszakban (július 15. – október 15.) előforduló jellegzetes időjárási típusok és a fennállásuk során megfigyelt biológiai [Ambrosia (parlagfű) pollen] és kémiai légszennyezők (fő légszennyező anyagok) feldúsulásakor mérhető koncentrációi közötti összefüggések feltárásával, illetve mindezeknek a légúti betegségekre gyakorolt hatásával foglalkozik. A dolgozat adatbázisa 13 meteorológiai elem, 8 légszennyező paraméter, továbbá a légúti betegségek 9 BNO kódjának napi értékeit tartalmazza az 1999-2003 közötti ötéves periódusra vonatkozóan. A jellegzetes időjárási típusok objektív definiálása a faktoranalízis és a clusteranalízis módszereinek alkalmazásával történt. Eredményeink azt mutatják, hogy a nyári – kora őszi időszakban az összes betegszám a középhőmérséklettel, a maximum hőmérséklettel és a minimum hőmérséklettel arányosan változik, ugyanakkor a légúti megbetegedések gyakrabban fordulnak elő alacsony relatív nedvesség mellett. A téli hónapokban viszont nincs kapcsolat a meteorológiai változók és a betegszámok között. A nyári – kora őszi időszakban az összes betegszám csökken, ha alacsonyak a PM_{10}-, NO-, NO_2 és O_{3max} koncentrációk, és növekszik, ha azok magasak. A téli hónapokban – csakúgy, mint a nyári - kora őszi periódusban – az alacsony NO-koncentráció esetén az összes betegszám kisebb, míg magas NO-koncentráció alkalmával az megnövekszik. A nyári – kora őszi periódusban az összes betegszám a 7. és 8. időjárási típusokban volt a legmagasabb. A legalacsonyabb összes betegszám a 2. típus idején mutatkozott. Megjegyzendő, hogy a parlagfű pollenszórása augusztus 15. – szeptember 15. között kulminál, s ez lényeges szerepet játszik a 2. típus alacsony betegszámában.

Summary – This paper determines the relationship of the characteristic weather types of the Carpathian Basin in the summer – early autumn period (July 15 – October 15) and the winter months (December, January and February) with the levels of chemical (CO, NO, NO_2, NO_2/NO, O_3, O_{3max}, SO_2, PM_{10}) and biological (Ambrosia - ragweed pollen) air pollutants, and their effect on respiratory diseases. The database comprises daily values of thirteen meteorological parameters; furthermore, those of eight chemical and one biological pollutants for the period 1999-2003. The objective definition of the characteristic weather types was carried out by using Factor and Cluster Analysis. In the winter months there is no relation between the meteorological variables and the number of patients. In the summer – early autumn period the total number of patients decreases, if levels of PM_{10}, NO, NO_2, O_{3max} and ragweed pollen are low and it increases if these concentrations are high. At the same time, the total number of patients decreases both with high and low values of NO_2/NO. In winter only one important result was received: the total number of patients is proportional to the levels of NO. In the summer – early autumn period the total number of patients was the highest, when the weather types 7 and 8 were found over the Carpathian Basin. The lowest total number of patients occurred during weather type 2. Pollen release of ragweed culminates between August 15 – September 15 and this fact is important in the low patient numbers of weather type 2.

Key words: weather types, Ambrosia pollen, chemical air pollutants, asthma, rhinitis, BNO-code, Lorenz diagram, factor analysis, cluster analysis, ANOVA weather classification, Tukey-test

1. INTRODUCTION

Recently, in the U.S. 11.7% of the population have seasonal hay-fever allergies and about 6.7% suffer from asthma [in 2004: 6%; in 1980: 3% (*U.S. Center for Disease Control and Prevention, Atlanta*)]. *Rimpela et al.* (1995) describes a three-fold increase of physician-diagnosed asthma and allergic rhinitis among Finnish adolescents in the period 1977-1991. Studies indicate that asthma and allergic conditions are most prevalent in the UK, Australia and New Zealand. High rates have also been reported for Chile. Concerning Europe, intermediate prevalence rates are seen in Southern Europe (*Lundback*, 1998). Though *Lundback* (1998) gives an account of the lowest rates of asthmatic diseases from Central Europe (*Lundback*, 1998); however, in the Carpathian Basin it is not the case (*Makra et al.*, 2004; 2005). In Hungary, about 30% of the population has some type of allergy, 65% of them have pollen-sensitivity, and at least 60% of this pollen-sensitivity is generated by the pollen of ragweed *(Ambrosia)* (*Járai-Komlódi*, 1998). 50-70% of the patients suffering from allergy are sensitive to ragweed pollen (*Mezei et al.*, 1992). It is a shocking fact that the number of patients with registered allergic illnesses has doubled and the number of cases of allergic asthma has become four times higher in Southern Hungary by the late 1990s over the previous 40 years (*Mezei et al.*, 1992; *Farkas et al.*, 1998). Based on the period 1990-1996, *Ambrosia* pollen comprises about half (47.3%) of the total pollen number of the different species over Southern Hungary (*Makra et al.*, 2004). Though this ratio depends substantially from the values of the meteorological elements year by year (in year 1990: 35.9%, while in year 1991: 66.9%), *Ambrosia* is considered the most important aeroallergen species in Hungary (*Juhász*, 1995; *Makra et al.*, 2004, 2005; *Béres et al.*, 2005). Nevertheless, we have to remember that the diagnosis of asthma has also certainly developed significantly during this period (*Rimpela et al.*, 1995; *Makra et al.*, 2004).

Respiratory diseases can frequently result in the death of adults. The roles of meteorological or environmental factors in the development of respiratory diseases have already been proved by popular observations and medical practice as well as medical reports since the age of Hyppocrates. General characteristics of the weather, such as temperature, atmospheric humidity, wind directions and air pollution can influence the development of respiratory diseases. Although interesting results were received for children (*Jaklin et al.*, 1971; *Fielder*, 1989; *Beer et al.*, 1991) and adult populations (*Goldstein*, 1980), when studying the effect of meteorological parameters on respiratory diseases, the joint effect of meteorological parameters, chemical and biological air pollutants on the development of respiratory diseases have not yet been studied.

The influence of the weather elements on mortality, as well as the connection of meteorological parameters and respiratory diseases have already been widely studied in the related literature. At the same time, the relationship of weather types and respiratory diseases have yet scarcely been analysed (e.g. *Danielides et al.*, 2002).

One of the main aims of the study is to determine an objective, reliable classification system of weather types ruling the region over Szeged, Southern Hungary during the summer and winter months, by applying multivariate statistical methods. Then, for each weather type, characterised by homogeneous temperature and humidity relations, concentrations of *Ambrosia* pollen grains and those of the main chemical air pollutants; furthermore, the frequency of respiratory diseases are assessed. Afterwards, the spatial distribution of the mean sea level pressure fields and the levels of the chemical and biological air pollutants as well as the frequency of the respiratory diseases in the area of Szeged have been calculated for the different weather types for the North-Atlantic –

European region in order to reveal the possible relations between the prevailing weather conditions,. Thereafter, the significance of the differences in the concentration and frequency values of the specific weather types is established.

2. TOPOGRAPHY OF SZEGED REGION

The city of Szeged, the largest settlement in SE Hungary (20°06'E; 46°15'N) is located at the confluence of the Tisza and Maros Rivers. The area is characterised by an extensive flat landscape with an elevation of 79 m a.s.l. The built-up area covers a region of about 46 km^2 with approx. 155,000 inhabitants.

3. DATABASE

The air pollution monitoring station is located in Szeged's downtown in a crossroad with heavy traffic. Sensors, measuring the concentrations of the chemical air pollutants, are placed 3 m above the surface.

The database, containing the meteorological parameters and the chemical pollutants, consists of the 30-minute averages of the five-year period 1999 – 2003 for the summer – early autumn period (July 15 – October 15) and the winter months (December, January and February). As for the biological pollutants, the daily counts of *Ambrosia* pollen grains were considered for the summer – early autumn period of the above five-year term.

3.1. Meteorological parameters

The 13 meteorological parameters used are: mean temperature (T_{mean}, °C), maximum temperature (T_{max}, °C), minimum temperature (T_{min}, °C), diurnal temperature range ($T_{range} = T_{max} - T_{min}$, °C), day-to-day change in mean temperature (ΔT_{mean}), day-to-day change in maximum temperature (ΔT_{max}), day-to-day change in minimum temperature (ΔT_{min}), mean relative humidity (RH, %), day-to-day change in relative humidity (ΔRH, %), mean atmospheric pressure at sea level (P, mb), day-to-day change in mean atmospheric pressure (ΔP, mb), mean water vapour pressure (VP, hPa), day-to-day change in mean vapour pressure (ΔVP, hPa). Considering humidity parameters, water vapour pressure is the most important in assessing the effect of humidity to human body, since it involves the total amount of water in the air.

Daily sea-level pressure fields measured at 00 UTC come from the ECMWF (European Centre for Medium-Range Weather Forecasts) Re-Analysis ERA 40 project. The investigated area is in the North-Atlantic – European region between 30°N–70.5°N latitudes and 30°W–45°E longitudes. The grid network is established with a density of 1.5°x1.5°, which indicates 28x51 = 1428 grid points for the region.

3.2. Air pollutants

3.2.1. Chemical air pollutants

The elements considered are the daily average mass concentrations of CO, NO, NO_2, SO_2, O_3 and PM_{10} ($\mu g \cdot m^{-3}$), the daily ratios of NO_2/NO and the daily maximum mass concentrations of O_3 ($\mu g \cdot m^{-3}$).

3.2.2. Biological air pollutants

In Szeged, the pollen content of the air has been examined with the help of a "Hirst-type" pollen trap (*Hirst*, 1952) (Lanzoni VPPS 2000) since 1989. The air sampler is located on top of the building of the Faculty of Arts, University of Szeged (20 m above the city surface). Daily pollen data were obtained by counting *Ambrosia* pollen grains on four longitudinal transects (*Käpylä and Penttinen*, 1981).

3.3. Parameters of the respiratory diseases

The rest of the database, namely the daily number of patients registered with asthma and rhinitis for the period examined, comes from the Thorax Surgery Hospital, Csongrád County, Deszk, Southern Hungary. Altogether 9 groups of symptoms of respiratory diseases and their cumulative occurrences were taken into account. In the summer – early autumn period altogether 26,703 patients, while in the winter months 14,507 patients were registered with respiratory diseases (*Table 1a-b*). Most of the patients live in Szeged or in the neighbouring villages.

The Thorax Surgery Hospital, Csongrád County, Deszk is situated about 10 km from the monitoring station in Szeged downtown, from where the data of the meteorological elements and those of the chemical air pollutants are originated. Most of the patients were treated as out-patients, only a fraction of them were registered as in-patients. For studying relation of respiratory diseases to meteorological parameters and air pollutants, the regsitration date of the patients was used.

4. METHODS

The relationship between the incidence of partly the respiratory diseases and partly the meteorological parameters as well as the chemical and biological air pollutants was assessed by using (a) Pearson's χ^2-test, the most commonly used procedure for testing the independence of row and column classification in an unordered contingency table; (b) factor analysis (FA), which reduces the dimensionality of a large data set of p correlated variables, expressing them in terms of m ($m < p$) new uncorrelated ones: the factors (*Jolliffe*, 1986; *Danielides et al.*, 2002); and cluster analysis (CA), which classifies a series of n observations into different, characteristic homogeneous groups: the clusters (*Anderberg*, 1973; *Hair et al.*, 1998).

Table 1a Parameters of patients registered with respiratory diseases, summer – early autumn period (July 15 – October 15)

Patient			Age			
Sex	Number	%	Average	S.d.*	Min.	Max.
Women	15,480	58.0	44.4	15.3	8	90
Man	11,223	42.0	40.7	16.6	6	84
Total	26,703	100.0	42.8	16.0	6	90

*S.d. = Standard deviation

Table 1b Parameters of patients registered with respiratory diseases, winter months
(December, January and February)

Patient			Age			
Sex	Number	%	Average	S.d.*	Min.	Max.
Women	8,396	57.9	49.4	15.7	8	93
Man	6,111	42.1	45.4	18.0	10	93
Total	14,507	100.0	47.7	16.8	8	93

*S.d. = Standard deviation

When determining the synoptic types, only meteorological parameters are taken into account, excluding pollution data. Hence, the differences of the mean pollution levels calculated for each synoptic type need further statistical evaluation. This is performed by the method of one-way Analysis of Variance (ANOVA) for each pollutant. By using the method, significant differences in pollutant concentrations and frequency of the respiratory diseases of the different synoptic types (clusters) can be determined. Finally, Tukey's honestly significant difference test is applied in order to quantitatively compare the mean air pollution levels and the frequency of the respiratory diseases between each pair of synoptic type (pairwise multiple comparisons) (*Sindosi et al.*, 2003; *Makra et al.*, 2006).

For each objective weather type, average daily isobar maps on the basis of daily sea-level pressure data calculated at each grid point of the investigated region were constructed by applying the Surfer 7.00 software.

All statistical computations were performed with SPSS (version 9.0) software.

5. RESULTS

5.1. The meteorological and pollution parameters and the total number of patients

The values of the meteorological and pollution parameters were classified into 5-5 quintiles, so that the first quintile comprised the lowest 20% of the ranked data of the given variable, while the fifth quintile comprised the highest 20% of them. Then, the frequencies of the meteorological and pollution parameters were calculated in the given quintiles. In this way, contingency tables were prepared for each meteorological and pollution parameter in the summer – early autumn period and the winter months. Pearson's χ^2-test was applied partly to the contingency tables of the 13 meteorological and 9 pollution parameters in the summer – early autumn period and to those of the 13 meteorological and 8 pollution parameters in the winter months. Then the 0-hypothesis of independence was tested between the parameters' quintiles and the total number of patients. If the independence is true, it means that the meteorological and pollution parameters do not influence the total number of patients; while, in reverse case, relation can be indicated between them. The reason to apply contingency tables instead of Pearson's correlation was that the distribution of the total number of patients was not normal. As a result of the χ^2-test, among the 13 meteorological variables in the summer – early autumn period 4 variables (T_{mean}, T_{max}, T_{min}, RH), while in the winter months 0 variable show statistically significant relation to the total number of patients (namely, the independence is not fulfilled at $p = 0.01$ significance level). In the winter months day-to-day change of the maximum temperature (ΔT_{max}) and the mean atmospheric pressure (P) influence mainly the total number of patients; however,

this relation is not significant in either case. On the basis of the χ^2-test, in the summer – early autumn period 5 (PM_{10}, NO, NO_2, NO_2/NO, O_{3max}) of the 8 chemical pollutants as well as the biological pollutant (*Ambrosia* pollen), while in the winter months only NO (only at the 5% significance level) shows significant relations to the total number of patients (probability of independence is higher than 1% but lower than 5%).

The relationships of the total number of patients and the meteorological and pollution parameters indicating significant connection are represented with Lorenz curves. Only the Lorenz curves of those meteorological elements are analysed, which show significant relation to the total number of patients. The total number of patients decreases if mean temperature is low, since on these days (quintiles 1 and 2) the gradient of the Lorenz curve is the lowest; furthermore, its gradient increases with the increasing mean temperature. T_{max} and T_{min} covary highly with T_{mean}; hence, low values of these parameters also decrease chances of the illness. At the same time, respiratory diseases frequently occur during low relative humidity (the gradient of the Lorenz curve is the highest in the first quintile) (*Fig. 1*). In the winter months there are no significant relations between the total number of patients and the meteorological elements; hence, the Lorenz curves are not analysed in this case.
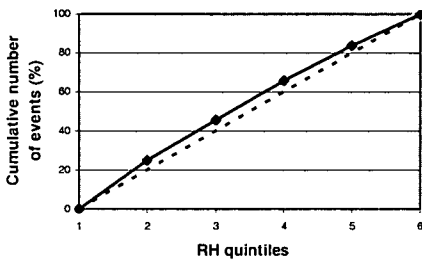
Fig. 1 Lorenz curve of relative humidity and the total number of patients, summer – early autunmn period (July 15 – October 15)
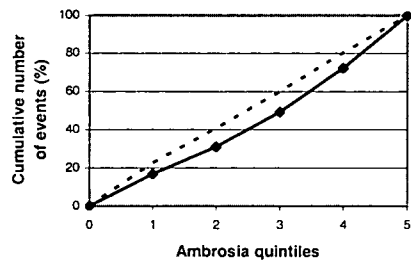
Fig. 2 Lorenz curve of *Ambrosia* pollen and the total number of patients, summer – early autunmn period (July 15 – October 15)

The total number of patients decreases if concentrations of PM_{10}, NO, NO_2 and O_{3max} are low and, in turn, it increases if they are high. In the case of NO_2/NO the situation is a bit different: the total number of patients decreases either with low, or with high value of the ratio. Low ratio of NO_2/NO is basically determined by low NO_2 level while high ratio of NO_2/NO is resolved by low NO level. At the same time, it has been presented that the total number of patients decreases with both low NO_2 concentrations and low NO levels. On the other hand, the total number of patients changes parallel to *Ambrosia* pollen levels: low (high) patient number is related to low (high) pollen levels (*Fig. 2*). Since in the winter months significant relation can only be detected between NO concentrations and the total number of patients, Lorenz diagram of only these two variables are analysed. In the winter months, similarly to the summer – early autumn period, the total number of patients is low (high) when NO levels are low (high).

5.2. *Factor and Cluster Analysis*

5.2.1. *Summer – early autumn period (July 15 – October 15)*

The application of factor analysis to the meteorological variables resulted in 5 factors, which explained 86.71% of the total variance. Then, cluster analysis was applied to the five-factor factor score time series (465 factor scores = 465 days) in order to classify them objectively into groups of days with characteristic weather types. Cluster analysis resulted in eight weather types (clusters) (*Fig. 3*). Each cluster contained at least 5.6% of all the days examined. Through all the summer only two main pressure systems rule the weather of the Carpathian Basin: the Icelandic low and the Azores high. The difference between these pressure systems is fairly small both in terms of the mean values of the parameters examined and in the spatial distribution of the atmospheric pressure. After that, daily mean sea level pressure fields of the eight weather types (clusters) and 30-day frequencies of the days of types were determined. Furthermore, mean values of meteorological and pollution parameters, as well as the patient numbers were calculated.

In order to decide whether the total number of patients depends on the weather types on a statistical basis, Pearson's χ^2-test was applied. If the 0-hypothesis of independence is fulfilled, then patient numbers do not depend on the weaher types; while, in the opposite case, relation can be detected between them. As a result, we received that the probability of independence is *0*; namely, patient numbers are in close relation to the weather types. The total number of patients was the highest in weather types *7* and *8*. These types are high pressure systems with high temperature and low relative humidity and occur almost exclusively between July 15 – September 15. The lowest values appeared during weather type 2. This is also a high pressure system with high temperature and low relative humidity and basically occurs between July 15 – August 15. It should be noted that the pollen release of ragweed culminates only following this period, and this is an important fact in the low patient numbers of type 2.

In order to decide whether the mean sea level pressure fields of the eight main types (clusters) of the North-Atlantic – European region differ significantly from each other, χ^2-test was applied with the assumption of independence (*0*-hypothesis). As a result, mean sea level pressure fields for half of the possible 28 cluster pairs; namely, for those of pairs *1-2, 1-5, 1-7, 1-8, 2-4, 2-7, 2-8, 3-6, 3-8, 4-6, 4-8, 6-7, 6-8* and *7-8* can be considered independent, while in the other half of cluster pairs independence is not fulfilled.

Then, an analysis of the inter-weather type comparison of concentrations of the chemical and biological pollutants and that of the patient numbers with different disease types was performed by means of analysis of variance (ANOVA). Inter-weather type differences of CO, PM_{10}, NO, NO_2, O_3, O_{3max}, SO_2, (daily mean concentrations), *Ambrosia* (daily concentrations) and those of total number of patients (frequency) are significant at 1% significance level for the following asthmatic and allergic diseases with their BNO codes: J3010 [allergic rhinitis from pollen (allergic hay-fever)], J3020 (other seasonal allergic rhinitis) and J3030 (other allergic rhinitis), while those of total number of patients for the respiratory disease J3040 (allergic rhinitis, without specifcation) at 2% significance level.

Performing pairwise comparisons (Tukey's difference tests), significant differences were found at both 5% and 1% significance levels. There are no two weather types, for which each parameter, indicating significant inter-weather type differences (13 of 19 parameters), differ significantly. The highest inter-weather type difference can be

experienced for the daily values of seven parameters in the following pairwise comparisons: types *1-7*, *3-7* and *4-7*. On the other hand, types *4-5* and *4-6* (no significant difference in the daily values of any parameter) as well as types *1-5*, *2-8*, *3-6* and *5-6* (significant difference in the daily values of 1 parameter) are mostly similar. Pairwise multiple comparisons indicated significant differences in the daily values of at least 6 (of the 13) parameters for the following cluster pairs: types *1-3* (6 parameters: CO, PM_{10}, NO, NO_2, O_{3max} and SO_2); types *1-7* (7 parameters: CO, PM_{10}, NO_2, O_3, O_{3max}, SO_2 and J3030); types *2-3* (6 parameters: CO, NO, O_3, O_{3max}, SO_2 and *Ambrosia*); types *3-7* (7 parameters: NO, O_3, O_{3max}, J3010, J3020, J3030 and Pat. no. = total number of patients); types *3-8* (6 parameters: CO, NO, O_3, SO_2, J3010 and J3040); furthermore, types *4-7* (7 parameters: PM_{10}, NO_2, O_3, O_{3max}, J3010, J3030 and Pat. no. = total number of patients). The daily pollen levels of *Ambrosia* show significant differences only between weather types *2-3*. Among the 28 pairs of types formed from the 8 weather types (clusters) received, 9 pairs (types *1–7*, *2-7*, *2-8*, *3-5*, *3-7*, *3-8*, *4-7*, *4-8* and *5-7*) show significant differences in the daily frequencies of some of the respiratory diseases and in the total number of patients.

Fig. 3 Frequency of the patients registered with respiratory diseases in the eight weather types (clusters) received, summer – early autumn period (July 15 – October 15)

On the whole, in decreasing order, weather types *7* and *3* differ mostly from the others, since pairwise multiple comparisons showed significant differences for the daily values of the most parameters between them and the other types. This is mainly due to macrocirculation reasons. During type *3*, an anticyclone centre pressure system is found over the Carpathian Basin, with the highest atmospheric pressure, lowest temperature and clear and calm weather. During type *7*, the Azores high pressure system penetrates over Ukraine, through the Carpathian Basin. In this case daily temperature parameters are the highest and relative humidity is the lowest. Besides, weather is also clear and calm. The ultimate reason might be that these weather types differ substantially in the temperature parameters and relative humidity. Type *5* and *6* can be considered as transitional ones, since they indicate the least significant pairwise differences for the variables examined.

5.2.2. Winter months (December, January and February)

The application of the factor analysis to the time series of the meteorological elements resulted in 5 factors, which explained 85.39% of the total variance. Afterwards, cluster analysis was applied to the five-factor factor score time series, as a result of which 9

homogeneous clusters of the days were determined and their main characteristics were established (*Fig. 4*). The clusters received comprise at least 6% of the days examined. Since in the winter months ITCZ draws southward, Middle-Europe becomes the running field of the weather fronts. The nine characteristic clusters involve the main weather types (*Fig. 4*), for which mean values of the meteorological and pollution parameters as well as mean frequency values of the total number of patients were calculated.

The dependence of the total number of patients from the weather types was calculated by using the Pearson's χ^2-test. If the *0*-hypothesis of independence is fulfilled, it means that total number of patients does not depend on the weather types and in reverse case there is a relation between them. As a result, the probability of the *0*-hypothesis of independence is very high: 0.7210. Hence, in the winter months there is no relation between the weather types and the patient numbers. The low variability of the total number of patients belonging to the nine weather types confirms the above result. The highest patient numbers are found in the weather types *3* and *4*, while the lowest numbers in the type *8*. Since there is no statistical relation between the weather types and the total number of patients the synoptic background and meteorological characteristics of the weather types comprising extreme patient numbers are not analysed in detail.

In order to determine whether sea level pressure fields of the nine clusters classified for the North-Atlantic European region differ significantly from each other, χ^2-test was applied with the assumption of independence as *0*-hypothesis. On the basis of our calculations, sea level pressure fields of clusters *1-4, 1-8, 2-5* and *8-9* are considered independent from each other. At the same time for 32 of the total 36 cluster pairs independence is not fulfilled.

For calculating the effect of the individual weather types on the pollution levels and the total number of patients, the ANOVA of the variables examined was performed. According to the analysis of variance, the daily mean concentrations of the chemical pollutants (with the exception of NO_2/NO) and the daily frequency values of the respiratory disease with the BNO-code J3020 (other seasonal allergic rhinitis) show significant difference between the individual weather types at 1% significance level.

Since significant differences were found in the above-mentioned mean concentrations and frequencies Tukey's honestly significant difference test was applied in order to receive pairwise multiple assessment of the differences mentioned. Statistically significant differences are detemined at 5% and 1% signifiance levels, respectively. It can be established that between weather types *3-8, 3-9, 5-6* and *5-7* daily mean concentrations of five pollutants (in fact, the most pollutants) show significant differences. Clusters *2-9, 3-4* and *5-9* (with no significant difference in the daily value of any parameter) and clusters *1-8, 1-9, 7-9* and *8-9* (with significant difference in the daily value of 1 parameter) are mostly similar. The daily frequency values of the respiratory disease BNO-code J3020 (other seasonal allergic rhinitis) show significant difference in 4 (of the total 36) cluster pairs formed of the nine weather types. Weather types *3* and *6* differ most from the others, since their pairwise multiple comparisons to the other types showed significant differences in the daily values of most parameters. During type *3*, cyclonic pressure patterns rule the Carpathian Basin with high temperature and humidity parameters and low atmospheric pressure. On the other hand, during type *6* an anticyclone ridge situation is found over the Carpathian Basin, with high atmospheric pressure, temperature and humidity parameters. Type *9* can be considered transitional, since this one shows the least significant differences

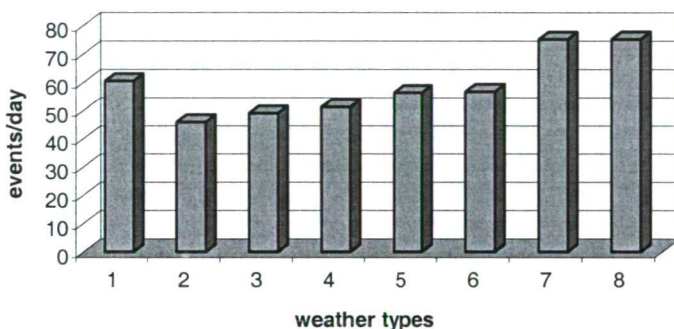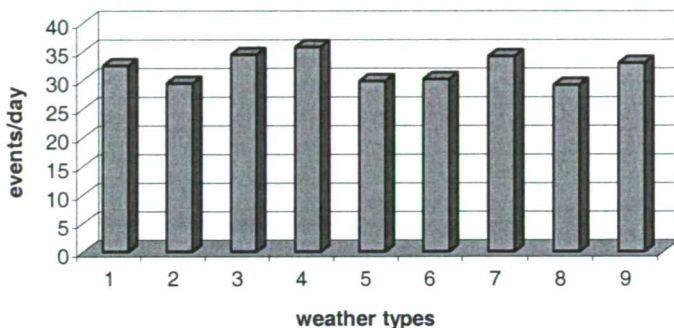in the daily values of the parameters considered in the pairwise multiple comparisons of the weather types.

Fig. 4 Frequency of the patients registered with respiratory diseases in the nine weather types (clusters) received, winter months (December, January and February)

6. CONCLUSIONS

The paper analyses the relationship of daily values of meteorological parameters, chemical and biological air pollutants and the daily frequency values of respiratory diseases for Szeged, Southern Hungary, during characteristic sea level pressure systems. Specific weather types determined by these pressure systems were defined both for the summer – early autumn period and the winter months, which play an important role in separating daily pollutant levels and daily frequency values of respiratory diseases. According to the results, 4 variables (T_{mean}, T_{max}, T_{min}, RH) show statistically significant relationship to the total number of patients. Namely, total number of patients changes proportionally to the mean temperature, maximum and minimum temperatures; on the other hand, respiratory diseases occur more frequently during low relative humidity. At the same time, in the winter months there is no relation between the meteorological variables and the total number of patients.

In the summer – early autumn period the total number of patients decrease if PM_{10}, NO, NO_2 and O_{3max} concentrations are low and increase if they are high. At the same time, the total number of patients decreases either with low or with high ratio of NO_2/NO. *Ambrosia* pollen levels are the most sensitive of all the variables to the total number of patients and their relation is characterised by direct proportionality. In the winter months, similarly to the summer – early autumn period, low NO levels go with low total number of patients, while in case of high NO concentrations the total number of patients increases.

In the summer – early autumn period, the total number of patients was highest in weather types 7 and 8. These types are of high pressure patterns with high temperatures and low humidity and they occur almost exclusively between July 15 – September 15. The lowest total number of patients appears during type 2. This is also a high pressure formation with high temperature and low humidity and occurs mostly between July 15 – August 15. Pollen release of ragweed reaches its peak values after this period, which plays an important role in the low patient numbers of type 2.

In the summer – early autumn period, weather types *2, 3* and *4* have a basic role in separating frequency values of respiratory diseases indicated with their BNO-codes of J3010, J3020, J3030 and Pat. No. (= total number of patientss). During all the three weather types the Carpathian Basin is ruled by high pressure systems. Furthermore, types *2* and *3* have an important role in classifying chemical air pollutants, too. In the winter months, types *3* and *5* have a determinative role in separating levels of chemical air pollutants. Type *3* is characterised by zonal cyclonic air currents over the Carpathian Basin, while type *5* is an anticyclone ridge situation.

The meteorological and pollutant parameters, their variation and covariation indicate strong relation to respiratory diseases. Hence, the above results might serve as important information for illness preventive actions.

REFERENCES

Anderberg, M.R., 1973: *Cluster Analysis for Applications.* Academic Press, New York. 353 p.

Beer, S.I., Kannai, Y.I. and Waron, M.J., 1991: Acute exacerbation of bronchial asthma in childern associated with afternoon weather changes. *American Review of Respiratory Diseases 144*, 31-35.

Béres, I., Novák, R., Hoffmanné Pathy, Zs. and Kazinczi, G., 2005: Az ürömlevelű parlagfű (*Ambrosia artemisiifolia* L.) elterjedése, morfológiája, biológiája, jelentősége és a védekezés lehetőségei. [Distribution, morphology, biology, importance and weed control of common ragweed (*Ambrosia artemisiifolia* L.). (in Hungarian)] *Gyomnövények, Gyomirtás 6/1*, 1-48.

Danielides, V., Nousia, C.S., Patrikakos, G., Bartzokas, A., Lolis, C.J., Milionis, H.J. and Skevas, A., 2002: Effect of meteorological parameters on acute laryngitis in adults. *Acta Oto-Laryngologica 122/6*, 655-660.

Farkas, I., Erdei, E., Magyar, D. and Fehér, Z., 1998. Anti-ragweed campaign in Hungary in the frame of the National Health Action Programme. In *Spieksma, F.Th.M.* (ed.): *Ragweed in Europe. Satellite Symposium Proceedings of 6th International Congress on Aerobiology.* Perugia, Italy. Alk–Abelló A/S, Horsholm, Denmark. 46.

Fielder, C.P., 1989: Effect of weather conditions on acute laryngotracheitis. *J. Laryngology and Otology 103*, 187-190.

Goldstein, J.F., 1980: Weather patterns and asthma epidemics in New York City and New Orleans. *Int. J. Biometeorol. 24*, 329-339.

Hair, J.F., Anderson, R.E., Tatham, R.L. and Black, W.C., 1998: *Multivariate data analysis.* Prentice Hall (5th edition), New Jersey. 730 p.

Hirst, J.M., 1952: An automatic volumetric spore trap. *Annals of Applied Biology 39*, 257-265.

Jaklin, R.H., Bender, S.W. and Becker, F., 1971: Environmental factors, in croup syndrome. *Zeitschrift für Kinderheilkunde 111*, 85-94.

Járai-Komlódi, M., 1998: Ragweed in Hungary. In *Spieksma, F.Th.M.* (ed.): *Ragweed in Europe. Satellite Symposium Proceedings of 6th International Congress on Aerobiology.* Perugia, Italy. Alk–Abelló A/S, Horsholm, Denmark. 33-38.

Jolliffe, I.T., 1986: *Principal component analysis.* Springer-Verlag, New York.

Juhász, M., 1995: New results of aeropalynological research in Southern Hungary. *Publications of the Szegedi Regional Committee of the Hungarian Academy of Sciences 5*, 17-30.

Käpylä, M. and Penttinen, A., 1981: An evaluation of the microscopial counting methods of the tape in Hirst-Burkard pollen and spore trap. *Grana 20*, 131-141.

Lundback, B., 1998: Epidemiology of rhinitis and asthma. *Clinical and Experimental Allergy 28, Suppl. 2*, 3-10.

Makra, L., Juhász, M., Borsos, E. and Béczi, R., 2004: Meteorological variables connected with airborne ragweed pollen in Southern Hungary. *Int. J. Biometeorol. 49*, 37-47.

Makra, L., Juhász, M., Béczi, R. and Borsos, E., 2005: The history and impacts of airborne *Ambrosia* (Asteraceae) pollen in Hungary. *Grana 44*, 57-64.

Makra, L., Mika, J., Bartzokas, A., Béczi, R., Borsos, E. and Sümeghy, Z., 2006: An objective classification system of air mass types for Szeged, Hungary with special interest to air pollution levels. *Meteorology and Atmospheric Physics 92/1-2*, 115-137.

Mezei, G., Járai-Komlódi, M., Papp, E. and Cserháti, E., 1992: Late summer pollen and allergen spectrum in children with allergic rhinitis and asthma in Budapest. *Pädiatrie Pädologie 27/3*, 75.

Rimpela, A.H., Savonius, B., Rimpela, M.K. and Haahtela, T., 1995: Asthma and allergic rhinitis among Finnish adolescents in 1977-1991. *Scandinavian Journal of Social Medicine 23/1*, 60-65.

Sindosi, O.A., Katsoulis, B.D. and Bartzokas, A., 2003: An objective definition of air mass types affecting Athens, Greece; the corresponding atmospheric pressure patterns and air pollution levels. *Environmental Technology 24*, 947-962.

U.S. Center for Disease Control and Prevention, Atlanta

ANTHROPOGEOMORPHOLOGIC IMPACTS OF ONSHORE AND OFFSHORE WINDFARMS

T. TÓTH and S. SZEGEDI

Department of Meteorology, University of Debrecen, P.O.Box 13, 4010 Debrecen, Hungary
E-mail: tamas.toth1@gmail.com

Összefoglalás – A szélerőművek építése során kisebb-nagyobb mértékben átalakítjuk a berendezés közvetlen környezetét. A mesterségesen létrehozott formák és az esetlegesen kiváltott folyamatok azonban a telepítés helyszínétől függően különbözőek lesznek. Az onshore szélparkok létesítése több évtizedes múltra tekint vissza. Nagy körültekintéssel, a lehető legkisebb környezeti beavatkozással végzett telepítések antropogeomorfológiai hatásai elhanyagolhatók. A szélenergia hasznosítás másik, egyre jelentősebb szerepet betöltő helyszínei a selfterületek lesznek. Az offshore telepítési körülmények természetesen különböznek a szárazföldön tapasztaltaktól. A tengeri szélparkok környezetre gyakorolt hatásairól még kevés információáll rendelkezésre, hiszen ezek telepítése a közelmúltban indult meg. A tanulmányban felvetett kérdések időszerűek, mert a következő évtizedekben az offshore parkok jelentős növekedése várható.

Summary – During the establishment of wind farms their close environment can become more or less altered. Artificial forms and processes triggered by the construction and operation of wind turbines can be different depending on the site. There is a several decades-long history of the operation of onshore wind farms, so many studies have dealt with their effects on landscape evolution. Anthropogeomorphologic issues of well-planned and appropriately carried out projects are insignificant. Continental shelf areas are sites with increasing importance for the establishment of wind farms today. The conditions for offshore projects are different from those of continental ones. There is not much information on the environmental effects of offshore wind farms, since their establishment has begun just recently. Questions raised in this paper have a growing importance together with the growing investments in this field.

Key words: wind turbines, establishment of wind farms, anthropogeomorphology, onshore and offshore wind farms, reef development

1. INTRODUCTION

The importance of renewable energy sources, thus wind energy is increasing in the energy strategy of the World today. In the EU the number of wind farms has been multiplied in the past ten years. Wind energy utilization is popular, since it is clear, abundant and easy to use.

Opponents of wind energy utilization criticize the effects of wind turbines on birds, on the landscape and the noise of the turbines. However, contrary to those opinions, many studies have proved that the noise loads of wind turbines are under the threshold limits, there is no mass loss of birds, and the effects on landscape are subjective issues. On the other hand there's much less research carried out on the anthropogenic forms created by the installation of wind turbines and their impacts on the surface.

To declare that wind energy utilization is really one of the most environment-friendly technologies, every factors should be taken into consideration which can be important from the aspect of the effects of wind farms on their living and inanimate environment.

This paper focuses on the theoretical examination of geomorphologic forms and processes connected to the construction and operation of onshore (built on the land) and offshore (built on the continental shelves) wind turbines and experimental hybrid systems.

2. DISCUSSION

2.1. Forms and landscape evolution processes connected to the construction and operation of onshore wind turbines

In the planning phase of the wind farms, the impacts of the turbines on the soil must be taken into account first, since during the construction there are significant mass movements. The most time-consuming part of the construction is the groundwork, the preparation of the area and the laying of foundations for the turbines. A solid base is required in order to resist the most severe storms. The first step is the excavation of the pit of the foundation, when special care is taken to save the upper, fertile layer of the soil. The excavated surplus of soil is carried away, or it is used for road building or levelling the ground. Significant amount of artificial materials are put into the foundation during the steel-concrete fitting, formworks and concrete works (*Fig. 1*). The actual amount depends on the size of the turbine (capacity of the turbine and height of the tower). In the case of a 0.6 MW turbine the volume of the fundamentals can reach 500 m^3.
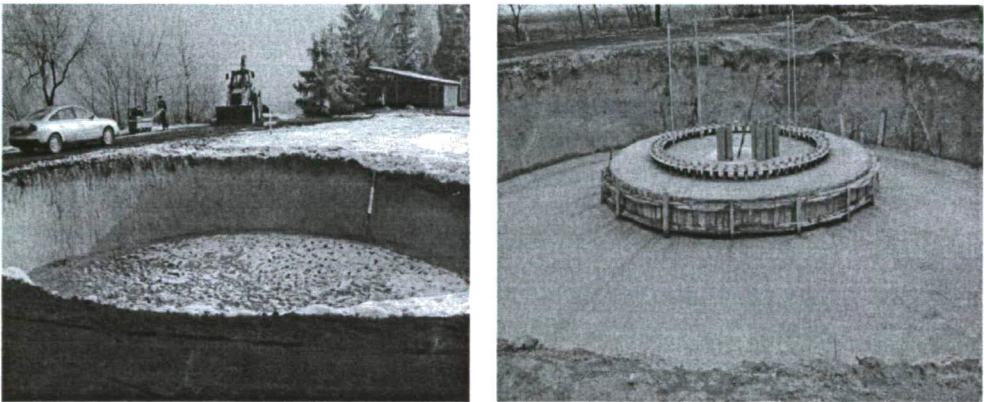
Fig. 1 Phases of laying the foundations for the wind turbine at Kulcs
(source: *www.winfo.hu*)

Although fundamentals do not reach the groundwater and streamlets, it is incontestable that they have certain impacts on the flows of ground waters. It still does not pose a threat in the case of the individual turbines or the whole farm, since due to the diffuse spacing of the turbines groundwater is not banked up, but flows around the concrete bodies of the fundamentals.

The soil suffers slight disturbances during the laying of the ground cables. Electricity generated by the turbines is fed into the public electric network via converters

and ground cables. Cables are laid into a depth between 1.5 and 5 meters according to the licence, this way they will not be visible in the landscape (*Horváth*, 2005). When turbines are connected to the public electricity network soil horizons are disturbed in the zone of the cable laying and in the vicinity of those zones. Soil becomes more compacted due to treading.

Before the establishment of a wind farm, the infrastructure of the area must be surveyed. Important factors are the availability of the aforementioned public electric network, the accessibility of the area and the quality of its roads. For the excavators and bulldozers any kind of roads are suitable, but the heavy trailers, which transport the elements of the turbine towers, nacelles and blades and the heavy duty cranes require good-quality, paved roads and hardened unpaved roads. The site is often not accessible on paved roads, because in Hungary those areas are banned, where there are public roads and electric cables within the range of falling (the total height of the tower and the vertical blade) of the turbine (*Fegyverneky*, 2004). As a consequence of this, for the transportation and construction of the turbine the hardening of an existing unpaved road or building of a paved road is necessary in almost every case. Although impacts and landscape forms created by road building are not connected directly to the operation of the turbines, they must be considered as "by-products" of the establishment of wind farms. In the sides of unpaved roads hardened by crushed gravel, asphalt paving, or rarely clinkers, gullies can form due to runoff, while on the lower surfaces along the roads accumulation forms can be established. In the case of paved roads the strong runoff can lead to more marked forms. The size of the forms and the activity of the landscape evolution processes are determined by the type of the pavement, the geological and pedological conditions, the height above sea level and the relief.

The time demand of the preparation of the area for the construction depends on the infrastructure. It usually does not mean a long time, since the accessibility and availability of the public electricity network are important factors in the selection of the site. The installation of the turbine takes only a few days; during the operation, practically, there are no significant changes in the environment of the turbine tower till its removal. During the removal of the turbine cranes, trailers and other vehicles use the roads built for the construction; therefore, there is no further landscape forming.

Built-in blast holes in the fundamentals make the demolition of the base of the tower much easier. Parts of the turbine like the tower trunk and the blades are made of recyclable materials. These, together with the debris of the tower base can be used again. After the removal of artificial materials only the pit of the tower base is left behind, which will be filled and the fertile upper soil layer will be replaced. In this phase the area can be reclaimed for agricultural (or actually any other) use. After the recultivation the paved roads, which became part of the road network of the area, are the only reminders of the former wind farm.

In the case of wind turbines in Hungary the hill of the fundamental is under the ground level and completely covered with grass or crushed gravel; therefore, there are no positive forms except the tower. Only a narrow concrete ring is visible from the fundamentals along the tower base. The extent of artificial surface cover is insignificant even if compared to the area of the fundamentals; therefore runoff will not increase to a degree that would lead to the formation of erosion forms.

The wind turbine of Kulcs, which operates since 2001, is a slightly different case. There the fitting ring of the tower and the fundamental are both visible, but the result is not a level surface rather a small negative form, characteristic of this turbine only in Hungary.

The soil was replaced onto the fundamental there as well, but the road, built for the construction lies higher than the base of the tower. As it was one of the first operating wind turbines in Hungary a conference and exhibition room was built near the tower and the hardened unpaved road, and the yard was paved later in order to make the site easily accessible. The higher, well-ordered surface emphasizes the almost entirely closed small basin with the trunk of the tower, which can be accessed via a few steps. Water from precipitation is drained westward (*Fig. 2b*).

The fundamental became covered with grass quite early, so it protected the soil already in the phase of the construction (*Fig. 2a*). In the second year of the operation there were no visible signs of material movement processes during our field observations, therefore there were no measurements carried out. During the six years operation time of the wind turbine of Kulcs (which means the quarter of the planned operating time), there were no signs of material movements; therefore it is probable that there won't be any mass movement processes in the future either.

a   b   c
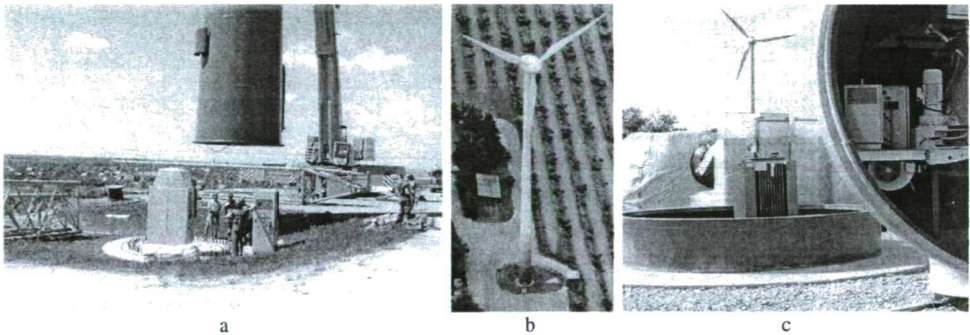
Fig. 2 The wind turbine of Kulcs and Újrónafő
(source: *www.winfo.hu, www.szelenergia.lap.hu*)

In connection with the onshore establishment of wind turbines it can be stated that the primary form created during the appropriate construction of the turbine does not trigger the formation of any secondary forms, new landscape evolution processes, nor does it modify the working processes significantly. The base hills of the wind turbines are small positive or negative forms; for this reason, classic geomorphic features like fluvial forms, gullies, etc. can occur on them rarely. It can be explained partly by the small size of these forms (*Fig. 2c*). In addition the soil is covered with grass or crushed gravel, which protects them from wind and water erosion. The possibility of mass movement processes caused by the weight of the turbines can be excluded, because the construction can only be licensed in statically stable sites.

2.2. Forms and landscape evolution processes connected to the construction and operation of offshore wind turbines

Recently in the establishment of wind farms in coastal countries there has been a tendency of moving from the land out onto the continental shelves. In Europe in 2005 the capacity of offshore wind turbines reached only 680 MW (less than 2%) within the 40 500 MW total installed wind power capacity, but, according to the EWEA (European Wind Energy Association), their ratio can reach 30% by 2020 and even 50% by 2030 (*ec.europa.eu*).

The main reason for the investments in the field is the higher effectiveness and profit rate of offshore wind turbines. The better wind profile originating from the low roughness over the sea surface provides 40 percent more energy. There are other advantages of offshore wind farms over onshore ones: the area of individual wind farms is not limited; and the environmental protection licence procedure is simpler than in the case of onshore wind farms.

Although the establishment of offshore wind farms is advantageous from the aspect of energy production, they can cost more by up to 60 percent. Higher costs are not originated from laying the foundations or the construction itself, but from the more complicated process of laying the submarine cables. Higher losses of electric power during long range transportation must also be taken into account.

Besides economic possibilities it must be taken into consideration as well that the sea bed does not remain undisturbed under offshore wind farms. Offshore wind turbines need much stronger fundamentals, since, due to its higher density, moving sea water exerts much higher pressure on the trunks of the towers of wind turbines than the flowing air. Different conditions require different building technologies; stronger concrete structures have to be used (*Fig. 3a-b*).

In order to decrease costs, out of the way sites with water depths between 5-10 meters are preferred, although it is possible to lay the fundamentals and cables for the turbines even into 40 meter deep waters. In the case of most of the planned German wind farms in the North Sea, water depths are between 20-40 meters, which causes high additional costs. In waters shallower than 10 meters, the base for the wind turbines is made of concrete, while in deeper waters, due to its weight, the base is made of steel. It is advantageous, since it can be put together on the land and it is adjustable to any types of sea beds. Nevertheless, it is still necessary to prepare the site: divers have to clear deposits from the seabed and a gravel bed has to be laid before the construction (*www.windpower.org*).

The huge steel-concrete base hill is much more a positive form on the sea bed, than in the case of onshore wind turbines. For the crane that lifts the elements of the turbine a stable platform is required on the seabed. For this reason, the sea bed is disturbed not just under the fundamentals of the turbines, but under the platforms of the cranes either (*Fig. 3c*). However, the strongest disturbances of the sea bed are caused by laying the submarine cables for the turbines.

a   b   c
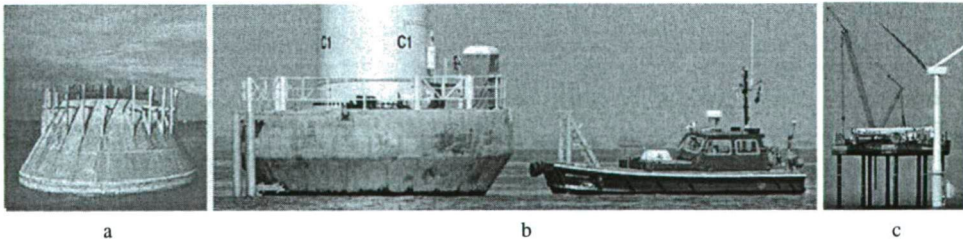
Fig. 3 Main phases of the establishment of offshore windparks
(source: *www.windpower.org, www.windpowerphotos.com*)

The process of the construction of offshore wind turbines does not create significant new geomorphic forms or processes. On the other hand – in the authors' opinion – installing the fundamental structures of the wind turbines into the sea bed can affect the surface evolution processes in the shallow water environment and can lead to the creation of new forms.

The towers and, depending on the depth of the water, even the base hills of the turbines can alter the dynamics of waves. On the sides of the towers of turbines facing the waves, processes characteristic of abrasion shorelines occur: waves break on the vertical concrete and steel bodies of the towers. The breaking of the waves results in much smaller "microforms" than in the case of abrasion shorelines forming at the base of the towers on the sea bed. Their small size is a consequence of the relatively small surface of the tower trunk under sea level and the diffuse spacing of the towers.

The basement embedded into the sea bed can have a significant impact on the mass movements on the sea floor. These artificial bodies do not alter the flows of the water directly but they behave as obstacles for the currents.

Coarse material rolled on the sea floor can be trapped at the base of the tower directly; or indirectly, it can lose most of its kinetic energy in the collision with the tower body so it will be deposited in the front and along the sides of the tower. Due to water movements from the opposite direction (the soog) from the shores deposition of coarse grains can occur behind the tower as well (*Fig. 4*). Microforms of the abrasion terrace will not affect the developing form strongly, since material transport towards the shores evens the roughness of the sea bed. The size of the new form and the time of its development are determined mainly by the amount of deposits.
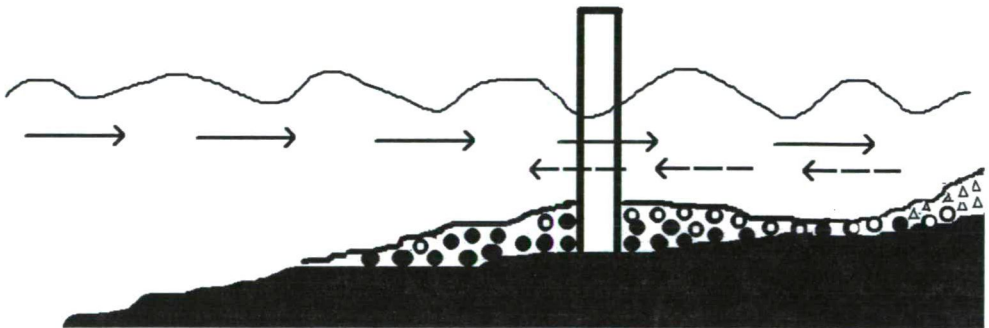
Fig. 4 Developement of accumulation forms in the environment of a wind turbine.

Along the coastline of North Germany the depth of water exceeds 10 meters at a distance of several hundred meters from the coast only. Some 10 meters wide, moving underwater bars run parallel with the coast on the abrasion terrace there. Under permanent and even winds and waves, they move towards the coast, but in a strong storm they withdraw towards the deeper waters due to the violent soog. The process of their development is not clear in every detail, but it can be assumed that they form due to the collusion of the coastward and seaward currents (*Borsy*, 1992).

It is a hard task to determine the shape of the reef formed on the sea bed on a purely theoretical base. If the strength of the two currents equals, the shape will be symmetric. However it is clear from the aforementioned facts that the strength of the currents is different, so the shape of the accumulation form will be deformed in one direction.

The role of underwater moving bars should be taken into consideration, since the towers of wind turbines mounted on abrasion terraces can alter those unique interactions between the currents there. If there is a visible and measurable effect of the base hills and tower trunks within a short period of time, it is necessary to take into consideration that the planned life span of those objects in the seabed is 50 years.

Without field measurements and experiments it is impossible to determine the parameters of the developing forms, but on the basis of the aforementioned facts it seems quite probable that in the environment of the wind turbines rather special accumulation forms can develop. Those reefs can be interesting not just because of the special way of their development, but because of their potential effect on navigation. Although (anthropo-) geomorphologic concerns of this "impact assessment" are not based on measurements, but they are merely hypotheses, the authors believe that they can emphasize the importance of the issue, triggering further investigations into the topic which can prove or disprove the hypotheses.

In countries which have huge wind farms, the relatively old low-capacity turbines have been being replaced by new high-capacity ones, which can produce several times more energy in the same area. The cables, the fundamentals and the towers are left in the sea; new turbines are installed on the former structures. That way, investors spare the costs of laying submarine cables, building fundamentals and towers. At the same time, the number of new offshore wind farms increases dynamically as well, together with the increasing popularity of renewable energy utilization.

The first offshore wind farms were established in Denmark in the early 1990-s. The establishment of huge, high capacity offshore wind farms, like Horns Rev (80 turbines, 160 MW), or Nysted (72 turbines, 165.5 MW) have taken place since 2002. Further establishment of huge wind farms is also expected in the future, since there are plans for the establishment of 4,000 WM offshore capacity by 2030 in Denmark alone (*www.windpower.org*). There are similar plans in Germany too: the establishment of 27,820 MW of total capacity is planned on the German seas. Most of it (25,242.5 MW) will be situated on the North Sea. The greatest wind farm will have 980 turbines with a total capacity of 4,720 MW. At the same time more there are moderate plans for the Baltic Sea, where 2,577.5 MW of total capacity is planned (*www.offshore-wind.de*).

Those areas are suitable for offshore wind farms that are situated outside of the National Parks, navigation lines and military areas. In Denmark most of these territories are situated within 7-40 kilometres off the coasts, while the aforementioned German wind farms (mainly in the North Sea) are situated at a distance between 70-100 kilometres from the coasts. The infrastructure for the transportation of electric power is very expensive and there are significant losses during the transportation. An additional problem for laying the submarine and ground cables is that many coastal areas belong to national parks.

The establishment of offshore wind farms is of high importance, because in the land a wind farm with 25 turbines and 50 MW of capacity, cannot get licence due to environmental and landscape protection causes if its area exceeds 1.5-1.6 km^2 (*Munkácsy*, 2004). The first offshore wind farms in Germany started operation in 2006. On the basis of the plans for wind energy utilization for that region and the characteristics of the North-, and Baltic Sea coasts (water depth, development of the bars and lidos), the aforementioned

hypotheses is not unfounded. It is supported by that most offshore wind farms were established only a few years ago. They are the newest types of practical wind energy utilization. For this reason there are no long time series of monitoring data available on their impacts on the environment. Therefore it would be reasonable to carry out detailed examinations on the questions raised in this paper, since – if there are real problems – extensive research, appropriate planning and realization could prevent anthropogenic landscape evolution processes in those coastal regions.

3. CONCLUSIONS

Wind turbines produce electricity in a clear and environment-friendly way, but in the meantime they can slowly alter their environment.

Onshore wind farms do not create any significant geomorphic forms. Despite their enormous weight, turbines do not cause mass movements, since territories which are hazardous from that aspect are banned. Levelled surfaces and roads created for the construction works are small in area and later they are integrated into the road network as parking places or recreation areas, or they are recultivated.

Offshore wind turbines can alter the mass movement processes of the sea bed significantly, which can affect navigation in those areas.

The degree of the alteration of former natural processes and the extent of new effects should be determined by further detailed studies.

It can be stated that the (anthropo-) geomorphologic effects of instruments of wind energy utilization are insignificant compared to those of fossil fuel exploitation or the utilization of hydropower.

REFERENCES

Borsy, Z., 1992: *Általános természetföldrajz.* [*Physical Geography.* (in Hungarian)] Nemzeti Tankönyvkiadó, Budapest. 429.

Fegyverneky, S., 2004: A szélerőművek telepíthetőségéről. [On the possibilities of the establishment of wind turbines (in Hungarian)] *Mérnökújság 8–9*, 15–16.

Horváth, G., 2005: Szélparkok tervezése környezetvédelmi szempontok alapján. [Planning of Wind Farms on the base of Environmental Considerations (in Hungarian)] *Magyar Tudomány 2005/11*, 1406-1417.

Munkácsy, B., 2004: Tájtervezés Németországban és itthon. [Landscape planning in Germany and Hungary (in Hungarian)] *Épített környezet 1–2*, 34–35.

http://ec.europa.eu/regional_policy/sources/docgener/panorama/pdf/mag20/mag20_hu.pdf

http://www.offshore-wind.de/page/index.php?id=4761

http://www.szelenergia.lap.hu

http://www.windpower.org/de/tour/rd/concrete.htm

http://www.windpower.org/de/tour/rd/gravitat.htm

http://www.windpower.org/de/tour/rd/offintro.htm

http://www.windpowerphotos.com/

http://www.winfo.hu/mediatar.htm

URBAN-RURAL DIFFERENCE IN THE HEATING DEMAND AS A CONSEQUENCE OF THE HEAT ISLAND

J. UNGER and L. MAKRA

Department of Climatology and Landscape Ecology, University of Szeged, P.O.Box 653, 6701 Szeged, Hungary
E-mail: unger@geo.u-szeged.hu

Összefoglalás – A tanulmány alapjául szolgáló adatbázist egy szegedi városi-külterületi állomáspár 1978-1980 közötti mérésadatai szolgáltatták. Az első rész szerint a város klímamódosító hatásával kapcsolatos eredmények nem csak a szigorúan vett 3 éves vizsgálati periódusra, hanem hosszabb időszakra is érvényesek. A Student t-próba egy speciális esetének alkalmazása alapján a területnek az említett 3 évre és az 1961-1990-es periódusra vonatkozó klímajellemzői között nincs jelentős különbség. A második rész a városi hősziget néhány következményével foglalkozik. Az eredmények szerint a hősziget kifejlődése csökkenti a fütési napok (*HD*) számát és a fütési fokszámot (*HDD*), így csökkenti a fütési idény hosszát és a felhasznált energia mennyiségét is. A városi és külterületi *HD*-k és *HDD*-k havi átlagai szerint Szegeden 3 héttel megrövidül a fütési szezon és a fő fütési időszakban az energia igény 10%-kal alacsonyabb, mint a külterületen.

Summary – The database of this study was provided by an urban-rural meteorological station-pair in the period of 1978-1980 in Szeged, Hungary. The first part shows that the results, related to the climate-modifying effect of the city, aren't strictly related to these three years, but they can be extended to a longer period as well. The climatic characteristics of the region in the mentioned three years and the period of 1961-1990 do not show significant differences, which is certified by the application of a special case of the Student t-test. The second part deals with some consequences of the urban heat island. According to the results, the development of the heat island reduces the number of heating days (*HD*) and heating degree-days (*HDD*) thus it reduces the duration of the heating season and the quantity of energy consumption in the city. Monthly means of the urban and rural *HD*s and *HDD*s show that in Szeged the heating season is shorter by more than 3 weeks and the energy demand is about 10% lower than in the rural areas in the main heating season.

Key words: urban climate, time extension of results, heating days, heating degree-days.

1. INTRODUCTION

The modification of the natural surface, the release of artificial energy and polluting materials into of the atmosphere over the cities alter the radiation and energy balance in the urban environments. As a result, a peculiar local climate, the so-called urban climate, develops. Its most obvious manifestation is the urban heat island, which means that, compared to the surroundings, warmer areas appear within the settlements (e.g. *Kuttler*, 2005). This heat excess has lots of practical consequences, which may influence our everyday life.

Szeged is a medium-sized city which had a population of 178,000 in a built-up area of approximately 46 km^2 in the investigated years (*Péter*, 1981). It is situated in Southeastern Hungary (46°N, 20°E) at 79 m above sea level on a flat plain (*Fig. 1*), so

orographical effects do not modify the local climate of the city. The climate of the region is temperate with a continental character (*Cf* type by Köppen's classification).

In the late 1970s, an urban station network was established in Szeged for three years between 1978 and 1980; temperature and humidity observations were carried out 3 or 4 times a day. The continuous urban climatological observations of 10 stations in the city provided the possibility to examine the urban climate of Szeged. While some earlier investigations related to this urban station network dealt with the characteristics of the urban heat island, air humidity and alterations of human comfort sensation in the city (e.g. *Unger*, 1992, 1996, 1999), the second part of this paper discusses some further features and consequences of the urban heat island in Szeged.
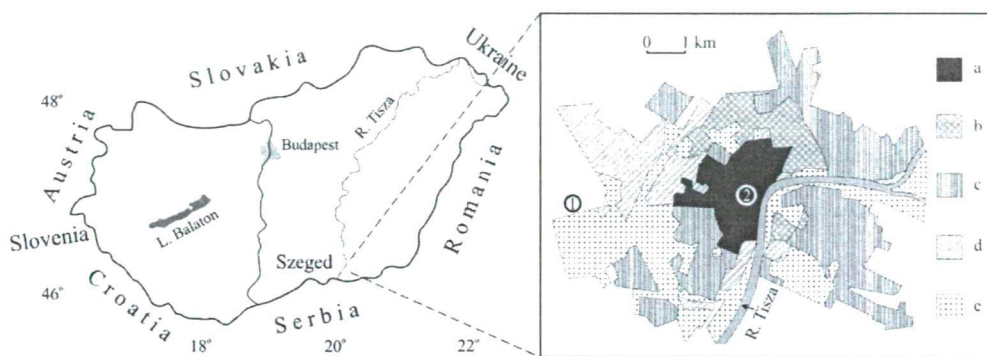

Fig. 1 Location of Szeged in Hungary, sites of rural (1) and urban (2) stations as well as built-up types of the city: a - centre (2-4-storey buildings), b - housing estates with prefabricated concrete slabs (5-10-storey buildings), c - detached houses (1-2-storey buildings), d - industrial areas, e - green areas

Moreover, it is also important to know whether the most significant climatic elements of these 3 years were characteristic for the climate conditions of the Szeged region. The aim of the first part of this study is to compare the climatic conditions (using the parameters such as temperature, vapour pressure, precipitation and wind speed) of these 3 years to a 30-year average (1961-1990) in order to demonstrate the possible deviations of the above-mentioned four climatic elements.

2. CLIMATOLOGY OF SZEGED AREA AND STATISTICAL COMPARISON

Tables 1, 2, 3 and *4* show the monthly and annual averages of temperature, vapour pressure, precipitation and wind speed in the Szeged region in the 3 years (1978-1980) of urban climate investigation and in the 30 years (1961-1990) which are relevant for the climate characterisation of the area using climatological normals.

Table 1 Monthly and annual averages of air temperature of Szeged (°C)
(*CLINO*, 1996; *YHMS*, 1978-1980)

months	J	F	M	A	M	J	J	A	S	O	N	D	year
1961-90	-1.8	0.9	5.6	11.1	16.2	19.2	20.8	20.2	16.5	11.0	5.1	0.6	10.5
1978-80	-2.2	1.2	6.7	9.2	14.8	19.5	19.2	19.3	15.6	10.4	3.8	1.8	10.0

Table 2 Monthly and annual averages of vapour pressure of Szeged (hPa)
(*CLINO*, 1996; *YHMS*, 1978-1980)

months	J	F	M	A	M	J	J	A	S	O	N	D	year
1961-90	5.0	5.6	6.9	8.9	12.3	15.1	16.0	15.8	13.2	9.8	7.6	5.8	10.1
1978-80	4.7	5.9	7.4	8.3	11.5	15.3	15.1	15	12.7	9.6	7.3	6.3	9.9

Table 3 Monthly and annual averages of precipitation of Szeged (mm)
(*CLINO*, 1996; *YHMS*, 1978-1980)

months	J	F	M	A	M	J	J	A	S	O	N	D	year
1961-90	29	25	29	41	51	72	50	57	34	26	41	40	495
1978-80	20	21	31	43	57	91	37	85	26	28	49	45	534

Table 4 Annual wind speed averages separated by directions in Szeged (ms^{-1})
(*CLINO*, 1996; *YHMS*, 1978-80)

directions	NNE	NE	ENE	E	ESE	SE	SSE	S	SSW	SW	WS	W	WNW	NW	NNW	N
1961-90	3.6	3.0	3.3	2.4	2.6	3.3	3.9	3.1	3.0	2.9	3.2	3.2	3.8	4.1	3.8	3.4
1978-80	3.4	3.0	2.6	2.5	2.8	3.2	3.8	3.2	2.8	2.7	2.7	3.1	3.6	4.0	3.6	3.2

In the comparison of the two (3 and 30-year long) databases, the traditional statistical methods could not be applied, because the first database is part of the second one.

In order to establish whether there is any significant change within a given time series of an optional climatic parameter, the Makra-test can be applied (*Tar et al.*, 2001; *Makra et al.*, 2002, 2004a, 2004b). The basic question of this test is whether significant difference can be revealed between the mean of an optional subsample of a given time series and the mean of the whole sample itself, namely that of the given time series. If the answer is yes (that is to say if there is significant difference between the two means), then it can be stated that significant change occurred in the climatic characteristics during the period given by the examined subsample of the whole time series.

The method itself is a special case of the Student t-test. Namely, it makes possible to determine if there is statistically significant difference between the expected values of not independent time series. The following probability variable was produced with $N(0;1)$ distribution:

$$\frac{\overline{M} - \overline{m}}{\sqrt{\frac{N - n}{N \cdot n}} \cdot \sigma}$$

for which $\overline{M}$ is the mean of the whole sample, $\overline{m}$ is the mean of the subsample, N is the number of the elements of the whole time series, n is the number of the elements in the subsample and σ is the standard deviation of the whole time series (it is supposed that the standard deviations of the subsample and the whole time series are equal). Now, from the table of the distribution function of the standard normal distribution an x_p value can be determined for a given $0 < p < 1$ number for which the following equation is true:

$$P\left(\left|\frac{\overline{M} - \overline{m}}{\sqrt{\frac{N-n}{N \cdot n}} \cdot \sigma}\right| > x_p\right) = p$$

If the absolute value of the above-mentioned probability variable with $N(0;1)$ distribution is higher than x_p then it is said that $\overline{M}$ and $\overline{m}$ differ significantly. The 0-hypothesis, according to which there is no difference between these two means, is fulfilled with a probability that is lower or equal to the critical p value. Being supported by this theoretical basis, significant difference can be revealed between the mean of an optional subsample of a given time series and the mean of the whole sample. This means that the period, that is to say the start and end, of the significant change of the examined climatic characteristics can be determined.

The above-mentioned statistical procedure was applied in this study, in order to detect if there was significant difference between the monthly and yearly mean temperatures of the period 1978-1980 and that of 1961-1990 (*Table 5*).

Table 5 Probability variables for determining the significance of differences between the mean temperatures of the whole samples (1961-1990) and the subsamples (1978-1980)

months	J	F	M	A	M	J	J	A	S	O	N	D	year
pr.var.	0.22[1]	0.13[1]	0.84[1]	2.20[2]	1.79[1]	0.40[1]	2.45[2]	1.49[1]	0.94[1]	0.74[1]	1.07[1]	1.14[1]	1.39[1]

[1] not significant
[2] significant at 5% significance level.

According to *Table 5*, it can be stated that the monthly average temperatures of April and July in the period of 1978-1980 differ significantly from those of the whole period (1961-1990). For the whole year and the rest of the months there are no significant differences. According to these results, the above-mentioned short period (1978-1980) can be considered as a representative for characterizing the whole time series (1961-1990). Namely, statistical characteristics coming from the whole time series can be applied for the subsample as well.

3. DATA AND METHODS FOR THE APPLICATION

The location of Station 1 was nearly free from urban modifying effects (Aerological Observatory of the Hungarian Meteorological Service) and it was situated at a distance of 4.4 km west to the city centre. The urban stations represented, more or less, the different types of built-up areas. Among them Station 2 was considered to represent the central urban area (*Fig. 1*).

In this part of the study in order to compare the urban (Station 2) and rural (Station 1) thermal conditions between 1978 and 1980, daily mean temperatures have been used.

The development of the urban heat island has certain influence on the duration of the heating period and the quantity of heating energy consumption. For human comfort there is a need of space heating below a critical temperature level. The more extreme the conditions, the more energy is consumed. Winter conditions can be illustrated through the

examination of the number of heating days and the heating degree-days. They are only functions of air temperature and a given critical threshold. The number of heating days (*HD*) is defined as the number of days, on which, according to Hungarian standards, the daily mean temperature (t_i) is below 12°C. The heating degree-days (*HDD*) are calculated by the following formula:

$$HDD = \Sigma \, (T - t_i)$$

where T is the required room air temperature (20°C) and the summing up refers to the heating days in a heating season. This method assumes that average space heating losses of buildings are proportional to average degree-days and it is used for estimating the energy demand of space heating in buildings (*Harrison et al.*, 1984; *Sailor*, 1998; *Livada et al.*, 2002). Cumulative degree-days are, thus, a direct indicator of the overall thermal climate for a heating season. The ratio of the energy consumption at two sites can be considered equal to the ratio of *HDD*s (*Probáld*, 1974; *Bründl and Höppe*, 1984; *Soule and Suckling*, 1995). It has also to be noted that the number of the heating days is a simpler approach to the climate differences instead of taking the heating degree-days into account, which reflect the amount of heating energy demand as a function of the mean daily temperature.

4. RESULTS AND DISCUSSION

The comparison of the monthly means of urban and rural *HD*s show that the heating season begins in October and lasts until May (*Fig. 2*). Except for the two coldest months (December and January), the monthly means of *HD* in the rural areas exceed those in urban areas and the differences are between 0.7 and 8.7 days in February and October, respectively. As a result, the heating season in the city is more than 3 weeks shorter than in rural areas.
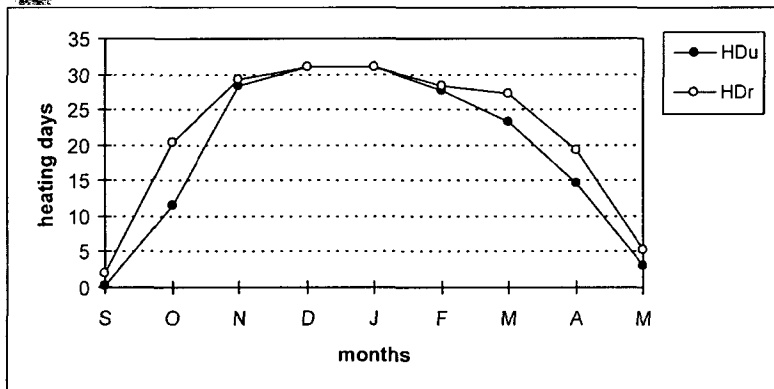
Fig. 2 Monthly mean numbers of urban (*HDu*) and rural (*HDr*) heating days in Szeged (1978-1980)

The heating degree-day is a more exact measure for the comparison of the heating energy consumption. According to *Fig. 3* the heating season characterized by significant heating demand begins in October and lasts until April with the highest values in January at both sites. The most significant difference appears in October (more than 100°C less in

urban than in rural!). While in the coldest winter months the differences are only about 50°C, great differences occur in March and April (65°C and 80°C, respectively). Consequently, the decreasing effect of the city on the heating energy demand is stronger in the transitional months than in other periods of the heating season.
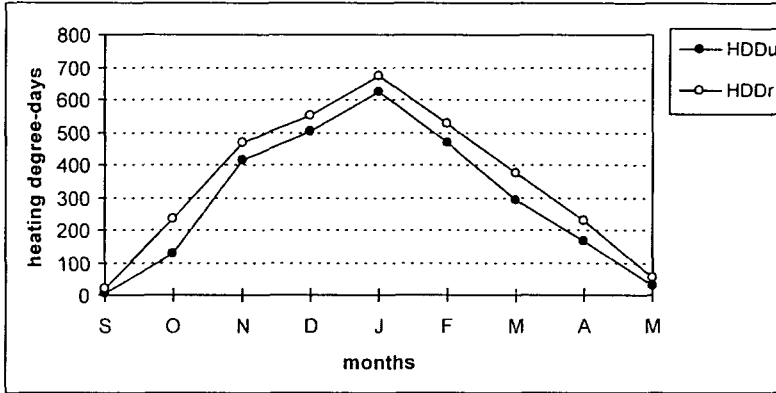

Fig. 3 Monthly means of the urban (*HDDu*) and rural (*HDDr*) heating degree-days (°C) in Szeged (1978-1980)
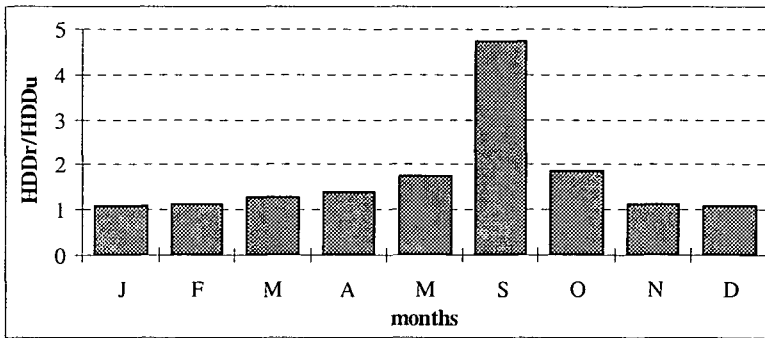

Fig. 4 Ratios of the monthly means of rural and urban heating degree-days (*HDDr/HDDu*) in the heating season in Szeged (1978-1980)

This establisment is supported by the ratios of the monthly means of rural and urban heating degree-days (*Fig. 4*). Except for the value of September (in this month the heating demand is insignificant at both sites, so the ratio is not important), the ratios fluctuate between 1.08 and 1.85 with a minimum in January and a maximum in October, respectively. Thus, in October, the heating energy demand is almost twice as much in rural areas as in the centre. In the winter months the ratios are about 1.1 which means that the energy demand in case of similar buildings is about 10% lower in the city centre than in rural areas in the main heating season. Considering the whole heating season, the difference is already 19%. This result is in good accordance with the values of similar investigations using the heating degree day method for estimation of urban-rural difference in heating demand: 12% in Budapest (*Probáld*, 1974), 20% in Tokyo (*Kawamura*, 1985), 30% in Athens (*Santamouris et al.*, 2001). This fact shows that the urban heating effect results very significant energy and cost savings even in the case of a medium-sized city like Szeged.

5. CONCLUSIONS

The climate modifying effect of the urban heat island in a medium-sized city located in the temperate climate region causes significant thermal alterations which are revealed by our simple measures. These alterations are mostly advantageous for the inhabitants because of the remarkable reduction of the heating season in the winter half year and the reduction of the quantity of heating energy demand in the city centre compared to the rural areas. Therefore, we may conclude that our results can provide useful information for the decision-makers of the local authorities and companies to handle the green areas and to plan the yearly heating energy supply in the urban area of Szeged.

Furthermore, our results about the urban modification effects are valid not only for the 3 years used in urban climatological investigation, but for a longer time period as well.

REFERENCES

Bründl, W. and Höppe, P., 1984: Advantages and disadvantages of the urban heat island - an evaluation according to the hygrothermic effects. *Arch. Meteorol. Geophys. Bioclimatol., Ser. B 35,* 55-66.

Climatological normals (CLINO) for the period 1961-1990. WMO/OMM-No. 847, Geneva. 1996.

Harrison, R., McGoldrick B. and Williams, C.G.B. 1984: Artificial heat release from Greater London, 1971-1976. *Atmos. Environ. 18,* 2291-2304.

Kawamura, T., 1985: Urban climate from the viewpoint of atmospheric environment. *Int. J. Biometeorol. 29,* 138-147.

Kuttler, W., 2005: Stadtklima. In *Hupfer, P. und Kuttler, W.* (eds.): *Witterung und Klima.* Teubner, Stuttgart-Leipzig-Wiesbaden. 371-432.

Livada, I., Santamouris, M., Niachou, K., Papanikolaou, N. and Mihalakakou, G., 2002: Determination of places in the great Athens area where the heat island effect is observed. *Theor. Appl. Climatol. 71,* 219-230.

Makra, L., Horváth, Sz., Pongrácz R. and Mika, J., 2002: Long term climate deviations: an alternative approach and application on the Palmer drought severity index in Hungary. *Physics and Chemistry of the Earth, Part B - Hydrology, Oceans and Atmosphere 27,* 1063-1071.

Makra, L., Juhász, M., Borsos, E. and Béczi, R., 2004a: Meteorological variables connected with airborne ragweed pollen in Southern Hungary. *Int. J. Biometeorol. 49,* 37-47.

Makra, L., Juhász, M., Béczi, R. and Borsos, E., 2004b: The history and impacts of airborne Ambrosia (Asteraceae) pollen in Hungary. *Grana 44,* 57-64.

Péter, L., 1981.: *Szeged.* (in Hungarian) Panoráma, Budapest. 216 p.

Probáld, F., 1974.: *Budapest városklímája. [Urban climate of Budapest.* (in Hungarian)] Akadémiai Kiadó, Budapest 73-75.

Sailor, D.J. 1998. Simulations of annual degree day impacts of urban vegetative augmentation. *Atmos. Environ. 32,* 43-52.

Santamouris, M., Papanikolaou, N., Livada, I., Koronakis, I., Georgakis, C., Argiriou, A. and Asimakopoulos, D., 2001: On the impact of urban climate on the energy consumption of buildings. *Solar Energy 70,* 201-216.

Soule, P.T. and Suckling, P.W., 1995: Variations in heating and cooling degree-days in the South-Eastern USA, 1960-1989. *Int. J. Climatol. 15,* 355-367.

Tar, K., Makra, L., Horváth, Sz. and Kircsi, A., 2001: Temporal change of some statistical characteristics of wind speed in the Great Hungarian Plain. *Theor. Appl. Climatol. 69,* 69-76.

Unger, J., 1992: Diurnal and annual variation of the urban temperature surplus in Szeged, Hungary. *Időjárás 96,* 235-244.

Unger, J., 1996: Heat island intensity with different meteorological conditions in a medium-sized town: Szeged, Hungary. *Theor. Appl. Climatol. 54*, 147-151.

Unger, J., 1999: Comparisons of urban and rural bioclimatological conditions in the case of a Central-European city. *Int. J. Biometeorol. 43*, 139-144.

YHMS (Yearbooks of the Hungarian Meteorological Service). 1978-1980. Budapest

LAND USE CHANGES IN ÓPUSZTASZER

T. VÁMOS and I. BÁRÁNY-KEVEI

Department of Climatology and Landscape Ecology, University of Szeged, P.O.Box 653, 6701 Szeged, Hungary
E-mail: vamos@gmail.com

Összefoglalás – Az ópusztaszeri mintaterületen az utóbbi kétszáz év térképei alapján meghatároztuk azokat a táj-foltokat, amelyeken a tájhasználat módja nem változott. Az állandó tájhasználatú területek és a domborzat között kapcsolat mutatható ki: a magasabb fekvésű területeken főként szántók, települések és erdők találhatók, míg a gye-pek az alacsonyabban elhelyezkedő területeket foglalják el. A tájhasználat kapcsolatrendszerét kutatva szoros kap-csolat mutatható ki a művelés módja és a vizsgált terület népességszámának változása között.

Summary – Permanent land use patches in the Ópusztaszer study area were determined on the evidence of the last two hundred years' maps. A relationship was found between the relief and the permanent land use patches. The ploughland, forest and the built-up area are concentrated on higher elevation. The grassland is located on the low-lying part of study area. By investigating the relations of land use change significant correlation was found between the increase in the number of inhabitants in the study area and the type of land cultivation.

Key words: land use change, relief, population

1. STUDY AREA AND METHODS

The study area is located in the southern part of Hungary, near the river Tisza (*Fig. 1*). It consists of the territories of Ópusztaszer and Baks villages. These villages have existed since 1947 that's why the earlier data refer to the northern part of the Pallavicini estate (*Inventory of the Pallavicin's demesne*, 1868; *Vályi and Zombori*, 1996). Both villages and their territories are situated at the meeting point of three different landscape types. The north-eastern and eastern parts of the study area are a sandy plain belonging to sandy Kiskunság. The northern part is a loess plain with sodic soils and the southern part is an alluvial plain belonging to the alluvium of the river Tisza. The boundary between the flood plain (the average altitude is 78 m above sea level) and the other two landscapes (the average altitude varies between 79 – 81 m above sea level) is a clearly visible step unlike the boundary between loess and sandy landscapes (*Somogyi and Marosi*, 1990).

The aim of our research is to determine the relationship between land use types and geographical factors. Land use change was studied at first. There is no detailed data about land use before the *First Military Survey* (1783-1784 in the study area) so the basis is this military map. Later maps like *Cadastre Maps* (from 1854, 1878, 1883) and *Military Maps* (from 1950, 1991) were compared to the map of the First Military Survey. The result is some patches where, on the evidence of the maps, land use has not changed for more than 200 years. The permanent land use type patches were compared with the relief. The relief was chosen from a range of different geographical factors because it can be represented easily and detailed in the case of this study area and there are not enough data about the soil

and the groundwater system. The relief map was created from a Military Map from 1991. Two types of area were defined in each landscape, based on altitude. One is the base area and the other is the higher area. The altitude of the base area is below 80 m in the floodplain and below 82.5 m above the sea level in sandy and loess landscapes. The higher areas are above the former values. We used ArcView 9.1 program for the comparison. After that we intended to investigate the causes of land use changes. The changes occurred through time so link was found between the change and some geographical time parameters.
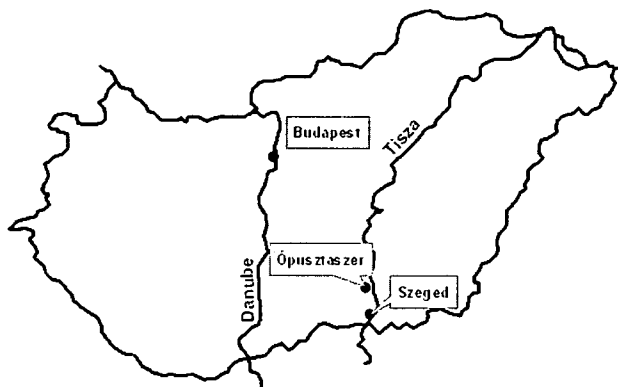

Fig. 1 Situation of the study area in Hungary

2. LAND USE CHANGES IN THE MODEL AREA

The end of the eighteenth century as basis time is advantageous for several reasons. There are enough data and the land use had been similar for centuries. South and Middle Hungary were occupied by the Turkish Empire in the sixteenth and seventeenth century. The population of these areas decreased and extensive animal husbandry predominated because of the prevailing confusion. This farming lasted until the end of the eighteenth century and this situation is described by the First Military Survey. The extension of ploughland increased from the early nineteenth century. It reached its maximum extension in the middle twentieth century. There is a change parallel with the ploughland area increasing; reforestation (*Fig. 2*). The results of the map comparison are the permanent land use patches. There are nine permanent ploughlands, which have been subjected to arable farming for at least 220 years. There are more patches which have been ploughed for 150 years. These patches were compared to the relief of the study area.

2.1. Land use types of the loess plain

There are three permanent cultivated ploughland patches and most of the present ploughland has been under cultivation for at least 150 years. The relationship between the relief and the ploughland is visible (*Table 1*). 51.9% of the permanent cultivated ploughland and 40.71% of the present ploughland are situated on higher elevation. There is little grass land on it, only 4.86% of the total grassland. The rest of the higher areas are forest and built-up areas (*Fig. 3*).

Table 1 The distribution of land use types on loess plain

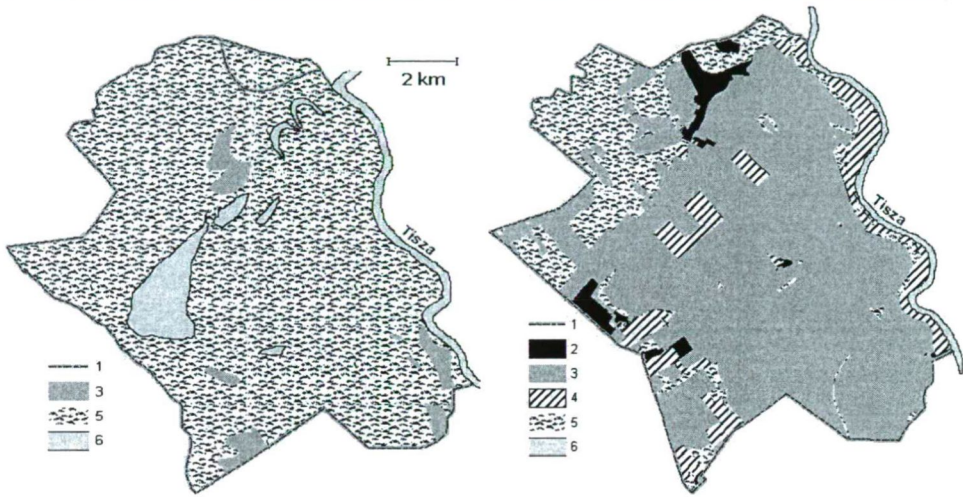|	Loess plain		Higher part of loess plain	
	hectares	%	hectares	%
Ploughland	668	32.21	272	52.20
Grassland	10988	53.01	53	10.26
Forest	106	5.10	54	10.34
Built-up area	201	9.68	141	27.17

Fig. 2 Land use types of the study area in 1784 (above) and in 1990 (below).
Legend 1- boundary of study area; 2- built-up area; 3- ploughland; 4- forest; 5- grassland;
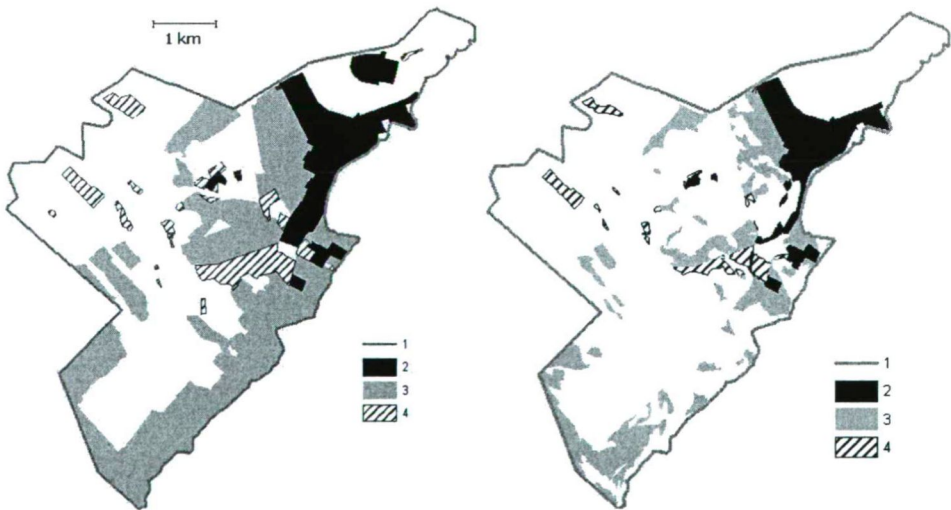6- river, lakes.

Fig. 3 Land use on the loess plain (above) and on the higher part of loess plain (below).
Legend 1- boundary; 2- built-up area; 3- ploughland; 4- forest.

2.2. Land use types of the sandy plain

There are two permanent ploughlands and the present ploughland area has been cultivated for 150 years. The relationship between the land use and the relief is similar as well. 87.58% of the permanent ploughland and 98.13% of the presently cultivated ploughland is on the higher area, but only 50.37% of the higher land is ploughed. The rest of it is either forest or built-up area. However the grassland is situated in both types of altitude areas.

2.3. Land use types of the alluvial plain

The permanent ploughland patches are only situated on the higher area. But there is no relationship between the present cultivated ploughland and the relief. Most parallel of the alluvial plains are protected by dams against the river Tisza. The dams were built from the 1850's and resulted in ploughland spreading on the former flood area. The ploughland extends 85% of the surface today. The exceptions are some former river beds and the present flood area.

The relationship between the type of the land use and the relief is evident. The ploughland, the built-up area and the forest have been concentrated on the higher area. The correlation in case of the ploughland is smaller and decreases the parallel with the ploughland extension. The relationship is not significant particularly in the alluvial plain. The former flood plain is protected by dams and canals against the water. Thus the water system of the alluvial plain is the most transformed from the three land types of the study area. The effect of elevation is negligible on the land use.

3. INTERPRETATION OF THE LAND USE CHANGE

Two geographical time parameters were chosen to investigate the relations of land use. One is rainfall, which represents the water regime. The relationship between relief and land use draws attention to the role of water. Changes in the available amount of water or the water moving transforms land use, like it happened in the alluvial plain. The nearest settlement which has long-term climatologic observations is Szeged where the regular measurements began in 1864 (*Hajósy*, 1975). Budapest has longer term time series than Szeged but Budapest is 150 km from Ópusztaszer. Relationship between the data of the two observatories is strong (correlation coefficient of the annual rainfall 0.767 with 133 data pairs). Thus Buda's data were used completing the data of Szeged in the early term.

The other parameter is the number of inhabitants (*Census of Hungary*, 2001). These data include the population of Ópusztaszer, Baks and Dóc. It was necessary to add inhabitants of Dóc to the population of study area because the data of eighteenth century contain the population of Dóc as well (*Barta*, 1981).

The two parameters mentioned above were compared to the parameters that represent the land use changes. These are the extension of ploughland, forest or grassland at several dates. There is no relationship between the parameters of the land use changes and the ten-year average precipitation. The correlation coefficients are between -0.237 and 0.341 with 7-10 data pairs. If the ten-year average precipitation of each month is compared to the land use change parameters the largest correlation coefficient is -0.689 between the

August average rainfall and the ploughland extension. But this value is too near the value of 5% significance level as well.

The relationship between parameters of land use change and the population is significant. The values of correlation coefficients are 0.961 between the population change and the ploughland extension, 0.791 between the population change and the forest extension and -0.935 between the population change and the grassland extension. All values are above the 1% significance level. Thus there is a clearly visible relationship between the population changes and land use changes. Similar results were published in connection with a Transdanubian study area (*Szilassi*, 2003.).

4. CONCLUSION

Land use is a result of the inhabitants' decisions. The question was what factors influenced the decision. The choice of cultivation type depends on the relief. The relief presumably refers to the role of the groundwater; observations of the groundwater level prove this. The physical landscape factors, like the relief mean only potentialities. The real land use depends on social and economic pressure like the number of inhabitants or increase of population.

This result is acceptable easily in connection with an autarchic community, but this study area was a capitalist estate until 1945. Thus there is the question of whether the change in the number of inhabitants is a cause or a consequence of ploughland increase. This question is difficult to answer because population is considered manpower and consumer at the same time and these are not separated.

REFERENCES

Barta, L., 1981: Az 1828. évi országos összeírás Csongrád megyében. [Country Survey of 1828 in Csongrád county. (in Hungarian)] *Tanulmányok Csongrád megye történetéből 5*, 5-45.
Cadastre map of Pusztaszer 1854. OSZK-TK (National Széchenyi Library, Map Collection)
Cadastre map of Pusztaszer 1877. OSZK-TK (National Széchenyi Library, Map Collection)
Cadastre map of Pusztaszer 1883. OSZK-TK (National Széchenyi Library, Map Collection)
Census of Hungary, 2001: Területi adatok 6.6. Csongrád megye II.kötet. [*Local data 6.6. County of Csongrád volume 2.* (in Hungarian)]
First Military Survey, 1784, HMT (Map Collection of Museum of Hungarian Military History), 1:28800
Hajósy, F., 1975. A csapadékok havi és évi összegei Magyarországon a mérések kezdetétől 1970-ig. [The monthly and annual amount of the rainfall in Hungary from the beginning of the measure till 1970. (in Hungarian)] 355.
Inventory of the Pallavicin's demesne, 1868.
Military map, 1950, HMT (Map Collection of Museum of Hungarian Military History), 1:25000.
Military map, 1991, 1:25000
Somogyi, S. and Marosi, S., 1990: Magyarország kistájainak katasztere. [Cadastre of microregions of Hungary. (in Hungarian)] 87-91.
Szilassi, P., 2003: A területhasználat változásának okai és következményei a Káli-medence példáján. [Causes and consequences of land use change on the example of the Káli Basin (in Hungarian)] *Földrajzi Értesítő 52/3-4*, 189-214.
Vályi, K. and Zombori, I., 1996: Ópusztaszer. Száz magyar falu könyvesháza. [*Ópusztaszer. Book collection of hundred Hungarian willages.* (in Hungarian)] 190.

RISK ANALYSIS OF THE ARIDIFICATION-ENDANGERED SAND-RIDGE AREA IN THE DANUBE-TISZA INTERFLUVE

G. ZSÁKOVICS, F. KOVÁCS, A. KISS and E. PÓCSIK

*Department of Physical Geography and Geoinformatics, University of Szeged, P.O.Box 653, 6701 Szeged,
Hungary, E-mail: zsakovics.gergely@gmail.com*

Összefoglalás – Jelen tanulmányunkban több szempont figyelembe vételével elemeztünk egy, a Duna-Tisza közi Homokhátságon elterülő mintaterületen feltételezhető vízhiányos állapotokat. Ennek feltárásához vizsgálatainkban az 1970 és 2000 közötti havi csapadékadatok alapján készült SPI aszályindex térképeket, az 1971–2000 közötti talajvízszint-változások eredményeit és a terület talajainak vízgazdálkodási tulajdonságait vetettük össze. A mintaterületén ezek alapján létrehoztuk a vízgazdálkodási szempontból különböző mértékben veszélyeztetett területek eredménytérképét, amit összehasonlítottunk az 1992–2001 közötti időtartam NDVI elemzésével kapott, a klíma változékonysága, változása szempontjából potenciálisan veszélyben lévő erdők területével. Az eredménytérkép tájtervezésnél, tájoptimalizáció során hasznos támpontokat adhat azokon a területeken, ahol elengedhetetlen a vízgazdálkodási és hidrometeorológiai szempontok fokozottabb figyelembe vétele.

Summary – In this study a complex analysis was carried out of a sandy area endangered by water-shortage, located in the Danube-Tisza Interfluve. In our investigations, SPI drought index maps based on monthly precipitation data in the period between 1970 and 2000, result maps of groundwater-level changes from 1971 to 2000 as well as maps describing soil characteristics of the area were applied. Based on the above-mentioned database, we generated a result map of endangered areas threatened to different extents from the viewpoint of water management. The result map was compared with the areas of potentially endangered woodlands, which were taken into consideration with respect to the variability and change of the climate. These latter areas were revealed by the analysis of the NDVI (Normalized Vegetation Index) of the period between 1992 and 2001. The result map can provide a good background to landscape planning where it is indispensable to take the aspects of water management and hydrometeorology into consideration.

1. INTRODUCTION

In most parts of Hungary, similarly to the conditions of our study area (*Fig. 1*) located in the Danube-Tisza Interfluve, warm arid and warm-temperate arid climatic regions can be found (*Péczely*, 1979), where from the early 1970s on a continuous, rapid decrease of groundwater level could be detected. The considerable precipitation decrease of the last decades, increasing drought and the intensive use of groundwater resources provide a good reason to study the water economy of the otherwise badly water-balanced area (sandy soils). Additionally, a survey was carried out concerning the distribution of precipitation in the period between 1970 and 2000 applying the evaluation method of the Standardized Precipitation Index (SPI) as well as the average change of groundwater level until 2000 compared to the average of the five years in 1971–1975.
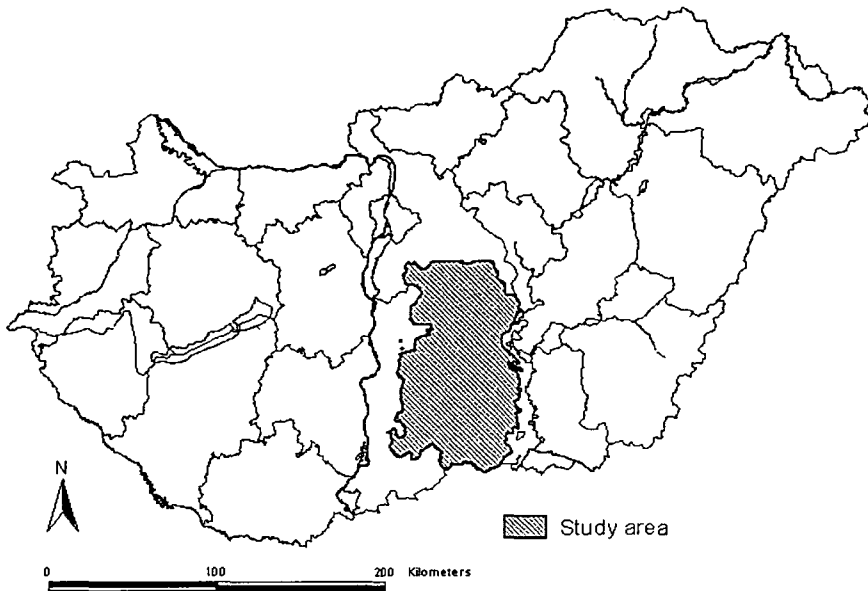
Fig. 1 Location of the study area in the Danube-Tisza Interfluve

The SPI indices express a lack of precipitation and surplus of precipitation respectively on the basis of the precipitation data input. The drop of groundwater level in the study area in the period under survey can be traced back to the combined effects of several factors. The decrease in precipitation, increase in the proportion of woodlands as well as the significant evaporation caused by the increased number of hot days can contribute to this process. A great amount of wells, serving for satisfying the water demand, and the possible groundwater-level decrease due to water-exploitation for agricultural and other utilization cannot be neglected. Therefore, in our study, maps of SPI indices as well as that of the change of groundwater-level were created. Moreover, by using the (Hungarian) Agrotopography Database (AGROTOPO), it is also important to point out those regions of the study area which are endangered to different extents from the viewpoint of water management. Additionally, in order to test our results and for finding the connections with other indicators we compare the result maps with the area of potentially endangered woodlands based on satellite image analysis.

2. MATERIAL AND METHOD

As a backgroud of our investigations, we created the map of the endangered areas by comparing three layers:

As a first layer, SPI indices have been constructed by statistical operations based on the precipitation data of 22 meteorological stations that were represented in our sample area using the chosen interpolation method. Making use of monthly precipitation data we made SPI drought index maps of the study area. The SPI quantitatively determines the lack of precipitation projected to time series. Time series reflect the effects of droughts on the

precipitation measurement points and on the surface generated from these points by the above-mentioned interpolation (for more information, see websites No. 1-3 in the REFERENCES). In the course of our study we used three months' SPI time series that, for instance, in case of the value of March, is based on the total quantities of precipitation in March, February and January. Although several other types of drought indices could have been used (relative evaporation, Pálfai's aridity-index – PAI, Palmer's drought index – PDSI, etc.), the SPI was chosen due to its widespread application and the fact that it requires only precipitation data series to calculate drought indices. Categorization of the SPI is represented in *Table 1*.

Table 1 Categorization of SPI values

2.0 –	extremely wet
1.5 – 1.99	very wet
1.0 – 1.49	moderately wet
-0.99 – 0.99	Average
-1.0 – -1.49	moderately dry
-1.5 – -1.99	very dry
– -2.0	extremely dry

As a second layer, raw data of groundwater-level were provided by the database of the VITUKI (Water Resources Research Center) Zrt. referring to the period of 1971 to 2000, based on the series of 210 wells. We utilized five-year absolute mean of groundwater level calculated from the data of each month in the period between 1971 and 1975. The data of the other years were compared to this five-year mean. The map of the average change of groundwater level in March of the 1976-2000 period was generated by adding up the relative changes of each year that demonstrates the groundwater level of the end of winter hydrological terms (*Rakonczai*, 2006).

As a third layer, data concerning the soil characteristics of the area from the viewpoint of water management were provided by the AGROTOPO database (for more information, see websites No. 4 and 5 in the REFERENCES).

In order to generate surfaces from the above-mentioned database we applied spline interpolation. This method is suitable for producing such surfaces that have little variation in altitudes. On the other hand, it is not suitable for modelling great alterations in relief that denotes large local differences because it minimizes the differences of altitudes (*Bihari*, 2000; *Németh*, 2004).

3. RESULTS AND DISCUSSION

Comparing the drought index maps of the winter and summer hydrological terms (*Fig. 2*) it becomes obvious that the lack of precipitation mainly occurred in the winter terms. In our reference period, this occured mostly in the SPI means of January and February. In the study area, the lowest SPI means could be found in Kecskemét and its surroundings, so this area can be especially sensitive to damages caused by aridity (*Figs. 3-4*).
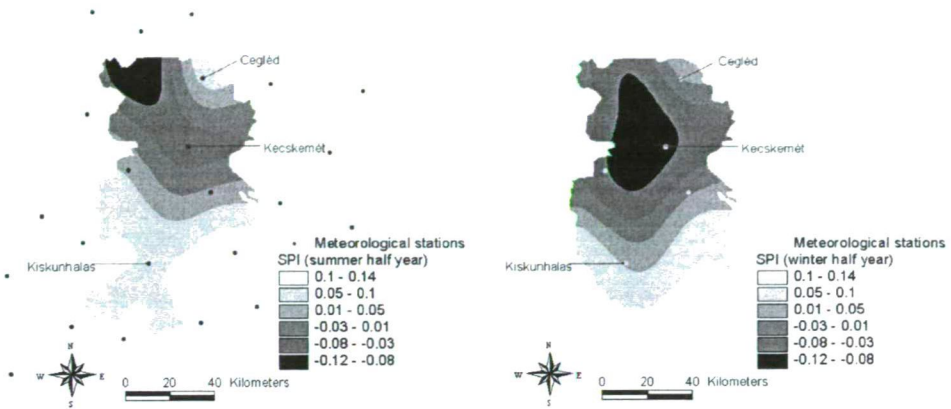
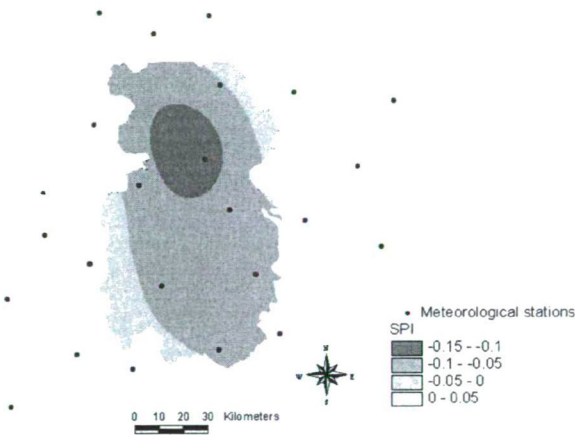*Fig. 2* Means of SPI values in winter and summer terms

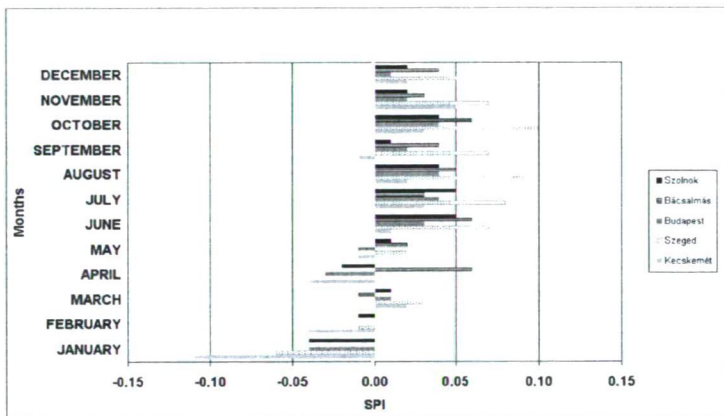*Fig. 3* SPI means of Januaries in the 1970-2000 period

Fig. 4 Monthly mean SPI in some of the measuring stations in the study area

In the 1970s there were four, in the 1980s there were five, while in the 1990s there were already six years that had an average index with negative sign (*Fig. 5*). The latter ones were characterised with lower values, so these years were drier than the earlier period. In this period, in spite of being diversified by wetter years, more and more dry years occurred as time was passing. Among other reasons, this played an important role in the process resulting in the serious drop of groundwater-level, due to the fact that the water consumed in the vegetation season was not retrieved at all in 15 of the 30 years. What is more, on the basis of the drought index maps, between 1970-2000 the most humid year turned out to be 1999, while the driest year occurred in 2000 (*Fig. 6*).
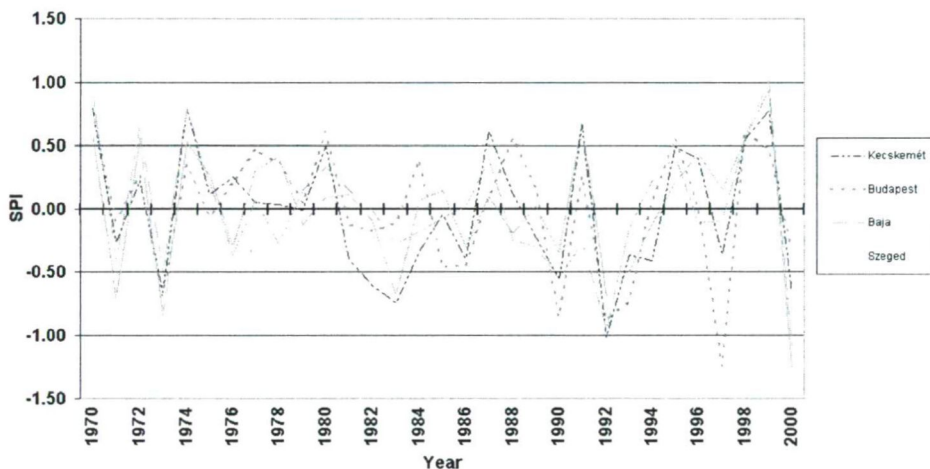
Fig. 5 Annual mean SPI values of the 1970-2000 period

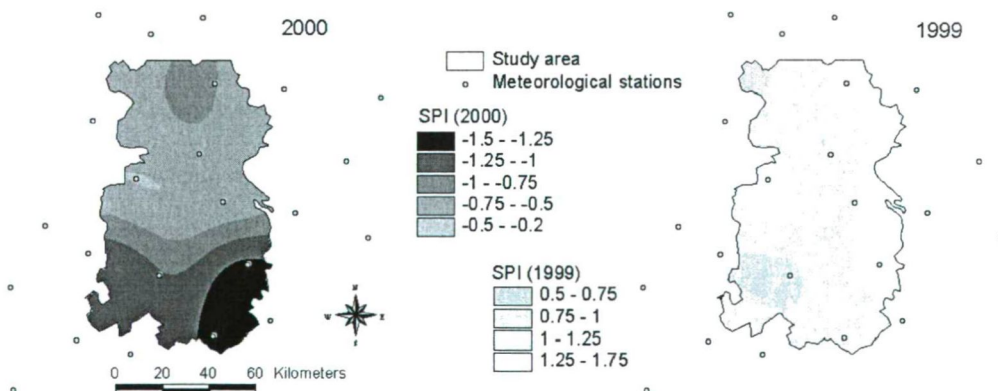*Fig. 6* Annual resolution SPI maps of 1999 and 2000

The winter precipitation – the great lack of which has been previously pointed out – has the role of supplementing the summer loss of groundwater level, so we cross-checked the map of groundwater-level change referring to March with the SPI results of the winter term. Areas of the ridge characterized by great decline were visibly outlined on the

173

groundwater-level change map. Especially the northern and southern parts of the sand ridge had groundwater-levels steadily below the average (*Fig.* 7).
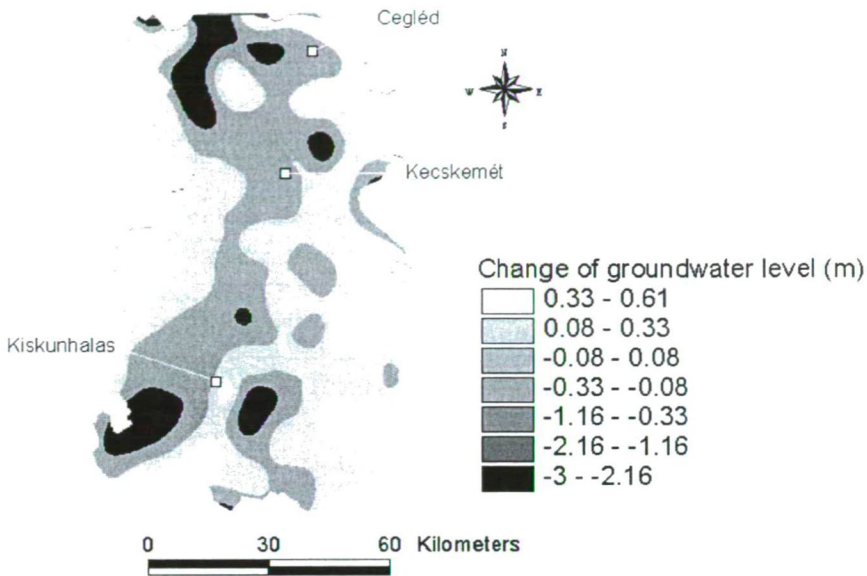

Fig. 7 Map of the mean March groundwater level in the study period

The third layer taken into consideration while marking the endangered areas was constructed on the basis of the data derived from the water economy classification of the AGROTOPO database. Accurate determination of specific aspects was required before starting the selection itself. We reclassified all the three layers in such way that in case of the first and second layers 4-4 categories, while in the case of AGROTOPO database 2 categories were established. The later, different categorisation had to be established due to the disadvantageous (from the viewpoint of water economy) character of the soils in most parts of the study area.

On the basis of this categorization the different soil-types were classified into the following groups. Soils characterized by inadequate water-holding capacity, weak water-storage capacity and very good permeability (sandy soils); soils with strong water-holding capacity and weak water-absorbing capacity (clay) and soils with an extreme water regime are classified into class No. 1. In class No. 2, which is the class of soils with favourable water economy, soils with adequate water-holding and water-absorbing capacity as well as great water-storage capacity (chernozem) can be found (*Fig. 8*).

Four-four restructured classes of the winter-term SPI layer and the surface of the mean groundwater-level change of March were marked with numbers 1, 2, 3 and 4, where class No. 1 was given the interval with the lowest values. New classes accurately demonstrate the spatial distribution of the value domains before classification. In the SPI classification a considerable proportion of the northern part in the study area fell into the first category while in the classification of groundwater level more extended spots showing deep decrease could be found in the southern, southwestern and northwestern parts of the study area (*Fig. 9*).
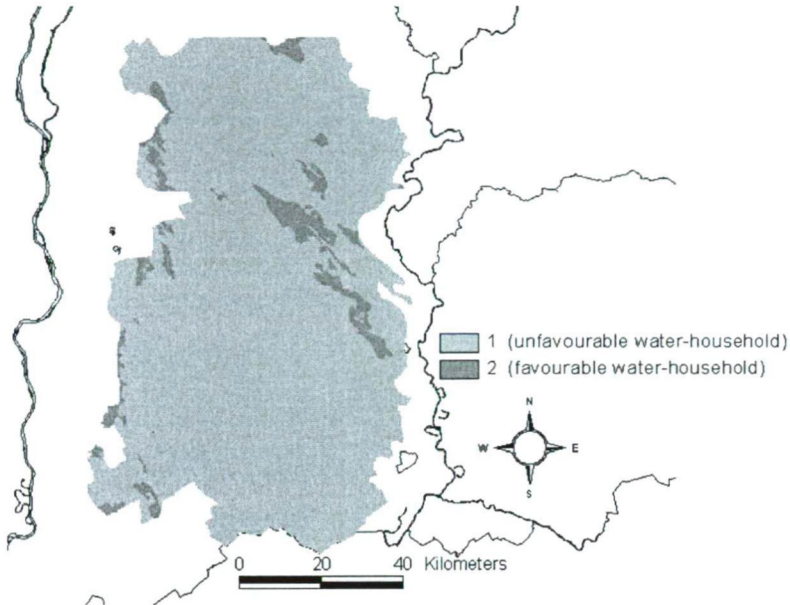
Fig. 8 AGROTOPO layer reclassified from the viewpoint of water economy
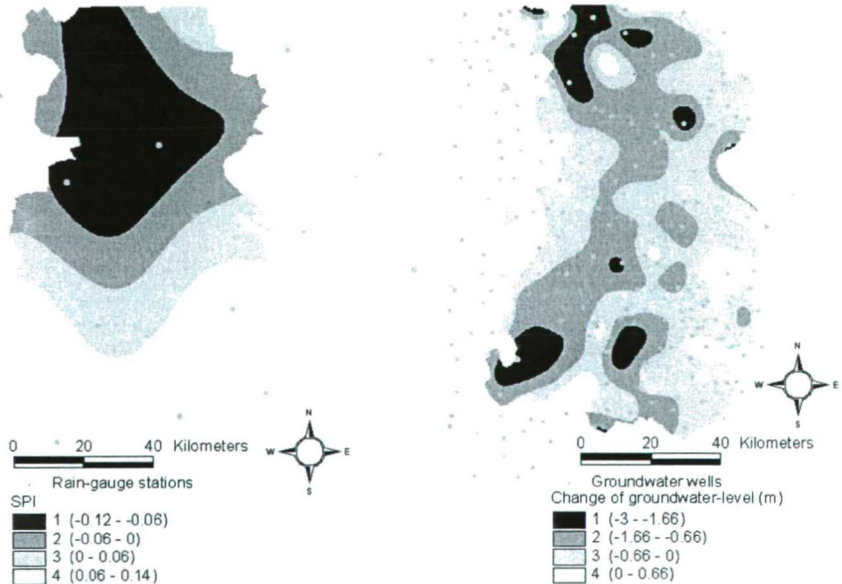

Fig. 9 Reclassified SPI (winter term) and classes of groundwater-level change
with measurement points (wells)

As to mark off the endangered areas, we combined the newly determined classes of the three data-layers. Categories of endangeredness were established as the cross-sections of different combinations. The category of „Increasingly Endangered" means cross sections

of classes of endangeredness marked by 1; here soil conditions are neglected. The cross section of those areas fell into the „Endangered" category that had soils characterized by inadequate water economy and where one of the classes of the SPI or drop of groundwater level (TVSZ-CS) fell into the first category. The cross-section of the first category of the SPI classes and the drop of groundwater level (TVSZ-CS) made up the area of „Moderately Endangered"; in this case the favourable soil conditions were taken into consideration. We included the combination of the second and third and the second and fourth SPI/TVSZ-CS category-classes in the same type taken as a function of unfavourable soil conditions. All the remaining areas came under the „Less Endangered" category (*Table 2*).

Table 2 Categories of endangeredness

Categories	SPI (1-4)	TVSZ-CS (1-4)	T-VIZGAZD (1-2)
Increasingly endangered	1	1	1.2
Endangered	1	2	1
	2	1	1
	2	2	1
	1	3	1
	3	1	1
	1	4	1
	4	1	1
Moderately endangered	2	3	1
	3	2	1
	2	4	1
	4	2	1
	3	3	1
	1	2	2
	2	1	2
	2	2	2
	1	3	2
	3	1	2
	1	4	2
	4	1	2
Less endangered	2	3	2
	3	2	2
	3	3	2
	2	4	2
	4	2	2
	3	4	1.2
	4	3	1.2
	4	4	1.2

Afterwards, we generated the map of endangered areas by combining the above-mentioned categories. As a result, mainly the northern, central and southwestern parts of the study area turned out to be endangered, whereas less endangered areas could be found in the southeastern sections (*Fig. 10*).

For comparison, the area of potentially endangered woodlands, revealed by the analysis of the AVHRR (Advanced Very High Resolution Radiometer) and the NDVI (Normalized Vegetation Index) of the period between 1992 and 2001, were also included in our investigations (*Kovács*, 2006). We examined the extent of the potentially endangered woodlands (using NDVI indices) compared to the location and extent of the areas marked by the categories of „Increasingly Endangered" and „Endangered" in our result map. Areas

characterised in our result maps by these two categories covered 36.89% of the study area, while 56.34% of the endangered woodlands could be found here. We also calculated that only 9.86% of the endangered woodlands are situated in less endangered areas – that cover 23.44% of the study area (*Fig. 11*).
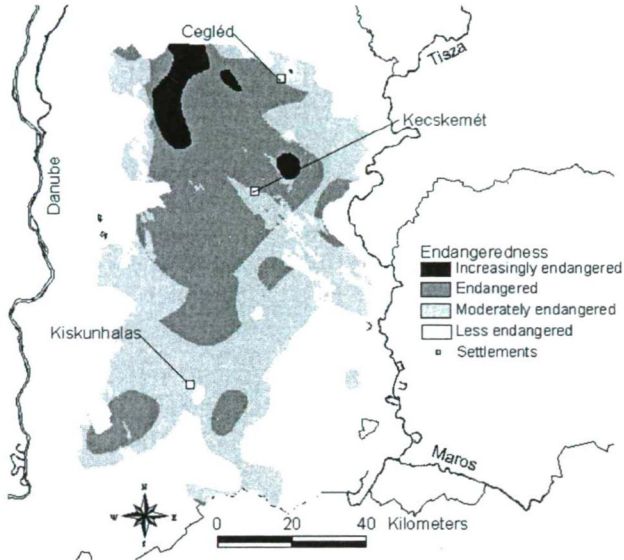
Fig. 10 Categories of endangeredness in the study area
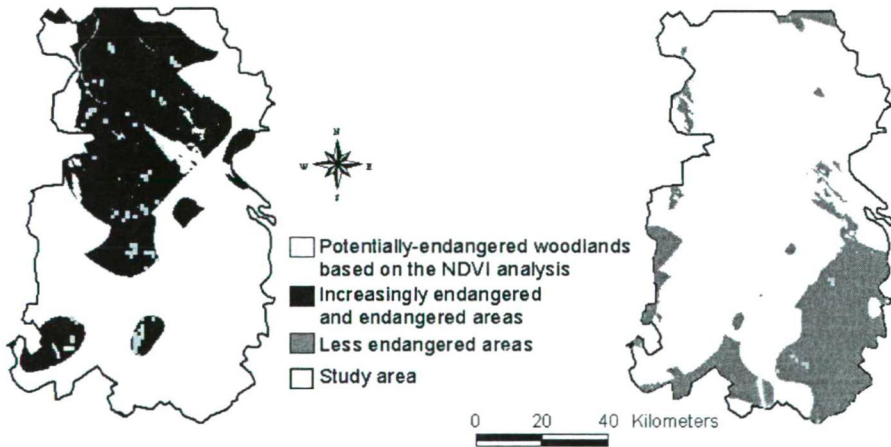
Fig. 11 Area of potentially endangered woodlands (according to the NDVI analysis) located in increasingly endangered, endangered and less endangered areas

Since spatial results concluded are very similar to each other, clear parallels can be detected between our result maps and that of the NDVI analysis. Although the reasons and level of connections should be the topic of further investigations, the map of

endangeredness demonstrates well the differences in the degree of endangeredness of the vegetation in the area which has a given sensitivity from the viewpoint water economy.

4. CONCLUSIONS

Using SPI values we pointed out that the winter term in the reference area is much more arid than the summer term. Moreover, it appeared that Kecskemét and its close surroundings are the areas most exposed to aridification processes. The decrease of groundwater level in the greatest extent could be observed in the northern and southern parts of the study area. As a third layer soil classification, based on water storage capacity and permeability was also carried out in our survey. Using the results of three data layers, a map of endangered areas was generated. It can be stated that the northern, central and southeastern parts of the study area are the most endangered, while in the southeastern parts less endangered areas can be found.

The result map was compared with the area of potentially endangered woodlands. These areas were indicated by the analysis of the NDVI (Normalized Vegetation Index) referring to the period of 1992–2001. In our case, 56.34% of the woodlands fell into the „Increasingly Endangered" or „Endangered" categories which is a considerable proportion compared to the whole size of the study area (3.89%). On the other hand, only 9.86% of the endangered woodlands are situated in the less endangered areas (23.44% of the sample area). Thus, although the detection of possible reasons is a subject of further research, strong parallels could be detected between the condition of the vegetation and our categorization of endangeredness.

REFERENCES

Bihari, Z. 2000: Magyarország új éghajlati térképei. [Recent climatic maps of Hungary. (in Hungarian)] *Élet és Tudomány 55/6,* 175-178.
Kovács, F. 2006: A biomassza-mennyiség regionális változásainak vizsgálata a Duna-Tisza közén műholdfelvételek alapján. (Regional differences of biomass production in the Danube-Tisza Interfluve using satelite image analysis). In *Kiss, A., Mezősi, G.* and *Sümeghy, Z.* (eds.): *Táj, környezet és társadalom. (Landscape, environment and society).* SZTE, Szeged. 413-425.
Németh, Á. 2004: Az aszályérzékenység meghatározása térinformatika alkalmazásával. [Defining drought sensitivity using GIS. (in Hungarian)] *Acta Agraria Kaposváriensis 8/3,* 25-34.
Péczely, Gy. 1979: *Éghajlattan. [Climatology.* (in Hungarian]) Tankönyvkiadó, Budapest. 282-283.
Rakonczai, J. 2006: Klímaváltozás-aridifikáció-változó tájak. (Climate change-aridification-changing landscapes). In *Kiss, A., Mezősi, G.* and *Sümeghy, Z.* (eds.): *Táj, környezet és társadalom. (Landscape, environment and society).* SZTE, Szeged. 593-601.
(1) *http://www.drought.unl.edu/monitor/spi/program/spi_program.htm.*
(2) *http://www.drought.unl.edu/whatis/indices.html.*
(3) *http://www.wrcc.dri.edu/spi/explanation.html.*
(4) *http://gisserver1.date.hu/Uniphorm/workshop/talajadatb.htm.*
(5) *http://www.otk.hu/cd00/3szek/bakacsizsofia.htm* - Agrotopográfiai database (AGROTOPO database).

DESCRIPTION OF THE EFFECTS OF CHEMICAL AND BIOLOGICAL AIR POLLUTANTS BY MEANS OF AIR QUALITY INDICES

T. EÖTVÖS

Department of Climatology and Landscape Ecology, University of Szeged, H-6701 Szeged, P.O.B. 653; Hungary
E-mail: eotvostekla@gmail.com

Összefoglalás – A környezeti levegő minősége alapvetően befolyásolja egészségünket és közérzetünket. A települési környezetek levegője ugyanakkor számos szennyező anyaggal terhelt. Ezek mérése és a mérési eredmények közérthető megjelenítése fontos mind a környezet közigazgatás, mind a civil oldal számára. A levegőminőség jellemzésére és közérthető közzétételére leggyakrabban levegőminőségi indexeket képeznek a mért szennyező anyag koncentrációkból. Az ilyen indexek megalkotása során a mért adatokat általában időben és terület szerint átlagolják, ezáltal az adatok fontos aspektusai veszhetnek el. Az eddig ismert valamennyi levegőminőségi indexre ugyanakkor egyöntetűen jellemző, hogy csak kémiai szennyező anyagok alapján készülnek, miközben egyes biológiai szennyező anyagok a kémiai szennyezők hatásait felerősíthetik és fordítva. A cikk tárgyalja a kémiai és biológiai szennyezők hatásait egyidejűleg figyelembe vevő index megalkotásának indokoltságát. A közérthetőség érdekében megvizsgáljuk az eddigi indexálási gyakorlatok térinformatikai elemekkel történő kiegészítését is.

Summary – Human health is essentially influenced by air quality. Atmospheric air in residential areas contains many pollutants. The monitoring and the plain publishing of the measured values are important both for the authorities and the public. Air quality is often characterised by constructing air quality indices, and these indices are used to inform the public. The construction of an advanced air quality index is usually done by averaging the measured data usually in time and space; hereby important aspects of the data can be lost. All known indices contain only chemical pollutants, while certain biological pollutants can enhance the effects of the chemical pollutants and vice versa. In this paper we discuss the importance of integrating biological pollutants into air quality indices. In order to increase the efficacy of these indices to the civil society we aim to introduce geographic information system (GIS) methods into publishing air quality information.

Key words: air pollutants, air quality index, GIS, chemical air pollutants, biological air pollutants, pollen

1. INTRODUCTION

Atmospheric air is an aero-disperse system: in this gas-mixture solid and liquid particulates are present. Pure air contains nitrogen, oxygen, noble gases (such as Ar, Ne, He,), and carbon-dioxide, but this ideal composition does not exist in nature because it is always polluted by various components.

The pollutants can be classified in several ways according to their origin (natural or anthropogenic, chemical or biological), residence time (persistent, changing or considerably changing), formation mechanism (primary and secondary pollutants), phase (solid, liquid, gaseous), and their effect on human health (toxic, carcinogenic, allergic). The concentration of these pollutants has increased in the atmosphere with the development of technology, industry, transportation and the large-scale spread of the cultivation of industrial crops.

Therefore monitoring air quality has become very important due to the harmful effects on the biosphere and thus on human health. Measurements are being performed at monitoring stations placed in cities, run by environmental or public health authorities. Concentration of sulphur-dioxide, nitrogen-oxides, PM10, ozone and carbon-monoxide are the most often measured components. In addition – owing to the increasing frequency of allergic illnesses – the monitoring of pollen and measurement of its concentration has become increasingly important. The level of air pollution was attempted to be described in different ways to the civil society to make it understandable.

The aim of the study is twofold: firstly, to overview the current air quality indices, and to indicate the need to introduce a new type of air quality index to include the simultaneous effects of chemical and biological pollutants and, secondly, to use GIS methods in order to increase the efficacy of the air quality analysis.

2. CHEMICAL AND BIOLOGICAL POLLUTANTS AND THEIR EFFECT ON HUMAN HEALTH

People, animals and plants need clean air for the appropriate standard of living. In this case clean air means that the concentrations of air pollutants do not exceed certain threshold limits, which were established by empirical and/or experimental means.

The air quality requirements are put forth by legislation, while technical specifications contain the technological compliance in detail. In Hungary, the legislation is based on Act LIII 1995 on the General Convention of the Protection of the Environment. The Act, regarding the air quality protection, specifies the following:

- The protection of the air quality includes the atmosphere as a whole, its composition, the processes within, and the climate.
- The air is to be protected from all artificial impacts imposed by radiating, liquid, gaseous or solid substances affecting the quality of the air or imposing health damage or threatening the state of other elements of the environment via the air.
- At designing, implementing and operating activities or facilities and at processing and using products it is mandatory that the emission of air pollutants is minimal.

Related regulations (no. 21/2001 Government Regulation; no. 17/2001 Regulation, Ministry of Environment; no. 14/2001 Joint Regulation: Ministry of Environment, Ministry of Health, Ministry of Agriculture. and Rural Development; no. 7/2003, Joint Regulation: Ministry of Environment, Ministry of Economy) are in compliance with the Regulations and Directives of the European Union concerning Clean Air Protection.

We can define air pollution as follows: gases, solid particles and aerosols that change the natural composition of the atmosphere. They can be harmful to human health, living organisms, soil, water and other elements of the environment. Of the classification possibilities listed in the introduction, we discuss air pollutants according to their origin.

According to their origin, they can come from natural and anthropogenic sources. The natural sources are forest fires, prairie fires, volcanic activity, flora and fauna. Hence H_2S, SO_2, HCl, NO_x, CO, CO_2, CH_4, NH_3, dust, pollen, fungus spore, bacteria are natural pollutants. All human activities are anthropogenic sources of pollutants. These pollutants are basically the same as the natural ones except maybe the biological pollutants; besides, some specific organic compounds (CFC's, dioxin, benzene, etc.) and soot and ash.

Though all the here-mentioned components are well-known pollutants, regular daily monitoring is limited to only some of them. Furthermore, some of them are typically not

influencing the air quality of residential areas on a daily basis, due to their impact mechanism. Considering these, the paper deals with the following compounds: CO, SO_2, NO_x, O_3, dust (PM10, soot, ash), and of the biological pollutants the pollen of ragweed (Ambrosia).

3. CHEMICAL POLLUTANTS: CO, O_3, SO_2, NO_X, DUST (PM10, SOOT, ASH)

Most of the indices consider these five pollutants, which are also the most frequently measured ones.

Carbon-monoxide is extremely poisonous for people and animals. Breathing it in, it attaches to haemoglobin and squeezes out oxygen. Haemoglobin becomes carbon-monoxide haemoglobin, which causes lack of oxygen in the nervous system and heart muscle. Acute poisoning brings on headache, heavy breathing, heart problems, in serious case unconsciousness and even breath paralysis. Survivors usually suffer from slowly healing nerve injuries. In fresh air acute poisoning never happens. Chronic symptoms are headache, dizziness, insomnia, heart ache, nervous system symptoms and increase of heart attack frequency. In fresh air carbon-monoxide leaves the organism. Elderly people, pregnant women, people who work in polluted air are most exposed.

Sulphur-dioxide is harmful to people and animals if they inhale it. SO_2 is adsorbed to the mucous membrane, of which the acidic reaction has irritant effect. If it enters the bloodstream, haemoglobin becomes sulfo-haemoglobin; hereby it hinders taking oxygen. Clean air restores health. Acute effects are lung, nose and throat mucous membrane irritation, and asthmatic spasm. In fresh air it does not occur. In chronic case respiratory illnesses (bronchitis) occur. Children, elderly people as well as children and adults suffering from asthma are the most endangered.

Nitrogen-oxides irritate the mucous membrane, cause coughing, nausea, headache, dizziness and acute poisoning. These symptoms disappear in a few hours then some hours later pneumonia, pneumonoedema may develop. In fresh air acute poisoning does not occur. Nitrogen-dioxide has twofold impact mechanism. Attached to the mucous membrane, it forms nitrous or nitric acid, which damages the tissues locally. If it enters the bloodstream, haemoglobin is oxidized to methehemoglobin, thus it becomes unable to carry oxygen to the organs. Therefore, longer exposure reduces resistance ability against infections, aggravates asthmatic diseases, causes frequent respiratory illnesses, and, later on, decreased lung-functions occur. Children and people who suffer from asthmatic illnesses, cardio-vascular diseases and respiratory diseases are the most endangered.

Ozone is strongly poisonous to human health. Eyes, nose and throat mucous membrane are irritated. It causes coughing and headache if the time of exposition is short. In chronic cases it contributes to asthma and reduces lung capacity. People suffering from asthma, other respiratory diseases, furthermore those with heart problems, elderly people and manual workers are the most endangered.

Dust particles can irritate and hurt eye and upper respiratory tracts. Dust particles bigger than 10 μm are purified by the ephitelium of the respiratory tracts; while dust particles smaller than 10 μm (PM10) can enter the lungs. The chemical composition, physical properties and concentration of the dust determine the effect on the respiratory system. Breathing in dusty air aggravates the state of people with asthma; reduces the ability of resistance against infections and toxic materials. Dust particles can adsorb viruses, bacteria, fungus, toxic materials and so help them to enter the organs. Those

suffering from respiratory or cardio-vascular diseases as well as elderly people are the most endangered.

4. BIOLOGICAL POLLUTANTS: RAGWEED POLLEN

Ambrosia is one of the most common and most thoroughly studied weed in Hungary. It is supposed to have come from the south part of North-America and by the second half of the 19th century four American species have already become acclimatized in Europe. These are the short (or common) ragweed (Ambrosia artemisiifolia = Ambrosia elatior), the giant ragweed (Ambrosia trifida), the perennial ragweed (Ambrosia psilostachya) and the silver ragweed (Ambrosia tenuifolia). Ambrosia elatior is the most widespread species of these. In Europe, the ragweed pollen pollution is the highest in the Carpathian Basin, sometimes with two orders of magnitude higher than the second Northern Italy and the third Rhone valley.

In Hungary, only Ambrosia elatior can be found of the four species of ragweed mentioned above. During the 1920s, it only existed in Southern Transdanubia, since then it has spread in the whole country. Local climate promotes its quick expansion. Thus blooming and pollen emission is significant. Pollen can survive in the soil for a long time – even decades. The main blooming period is between July and October, but it is most intensive in August.

Ambrosia is dangerous not only for people sensitive to allergy but it can cause severe damage in agriculture as well. It occurs in large quantities along roads, railway embankments, uncultivated fields; it displaces other plants (field crops, for example lucerne). It is hard to eradicate because it does not have natural competitors, since it is a new species in the country.

Allergy is an abnormal reaction against materials, which can be found in the environment and are normally harmless to human health. The immune system of a patient sensitive to allergy exaggerates the reaction against certain materials and perceives them harmful. These materials are the allergens. About 30% of the Hungarian population has some type of allergy, two-third of them has pollen-sensitivity, and at least 60% of this is caused by ragweed (*Járai-Komlódi*, 1998; *Makra et al.*, 2004, 2005, 2006, 2007). About 50-70% of the allergic patients have ragweed-sensitivity (*Mezei et al.*, 1992). The number of patients registered with allergic illnesses doubled and the number of cases of allergic asthma became four times higher by the late 1990s compared to the situation 40 years ago.

When a patient with allergic illness is in touch with the allergen, the following process occurs:

1. The human body, reacting against the allergen, produces specific antibodies; namely, protein molecules. These are IgE (immunglobulin E) molecules.
2. These antibodies attach to special cells. These can be found in the respiratory organs and intestines, where allergens can enter easily.
3. Many chemical compounds are forming; one of them is histamine, which is important in the developing of an allergic reaction.
4. Breathing in chemical compounds can cause nose and eye itching, in more serious cases asthmatic asphyxia, or utricaria, furthermore, mouth and stomach symptoms, diarrhoea can develop.

Extreme concentrations of chemical compounds can cause severe symptoms all over the body: nettle-rash, low blood pressure or even unconsciousness. This group of symptoms is called anaphylaxis.

5. INTRODUCTION TO AIR QUALITY INDICES

The first attempts to formulate air quality state in relation to pollutant levels appeared in the 1960s.

It usually meant that concentration intervals were defined for some pollutants, and these intervals had a detailed description. In this paper the categories of two air pollution indices are shown. Pollutant Standard Index (PSI) seems more complex in a sense that a numerical scale is defined for the concentration intervals, and these numbers indicate, which category the actual air quality falls in (*Table 1*).

Table 1 Pollutant Standard Index (PSI)

PSI value	O_3		PM		CO	SO_2
	8 hours	1 hour	PM2.5, 24 hours, (ppm)	PM10, 24 hours, (ppm)	8 hours, (ppm)	24 hours, (ppm)
50	0.07	–	15	50	4	0.03
100	0.08	0.12	65	150	9	0.12
150	0.10	0.16	100*	250	12	0.25
200	0.12	0.20	150*	350	15	0.30
300	0.40 (1 hr)	0.40	250*	420	30	0.60
400	0.50 (1 hr)	0.50	350	500	40	0.80
500	0.60 (1 hr)	0.60	500	600	50	1.00

Proposed PSI values (*EPA*)

Mayer et al. (2004) developed statistical air stress indices and an impact-related air quality index (DAQx). Their sensitivity depending on emissions and air mass exchange conditions was investigated by test calculations based on air pollution data

The Air Quality Index (AQI) is introduced by the *EPA* (USA). This is a system of quantifying the quality of the ambient air we breathe. The AQI reading for a given day is based on the critical pollutants and upon pollutants with high readings. The major air pollutants used to determine the AQI are ground-level ozone, particulate matter, carbon monoxide, sulphur dioxide and nitrogen dioxide. The Air Quality Index is divided into six categories ranging from good to hazardous. Good is green, and ranges from 0-50. The next level is moderate, which is yellow and ranges from 51-100. The third level is unhealthy for sensitive groups, and is orange. It ranges from 101-150. The fourth level is unhealthy, which is red and ranges from 151-200. Very unhealthy is purple, and ranges from 201 to 300. The hazardous level, rarely seen in the United States, is black and has an AQI of 301+ (*Table 2*).

The components considered, the thresholds and the descriptions are different in most countries. The paper of *Shooter and Brimblecombe* (2007) is a good summary of air quality indices.

In the more complex indices there are previously defined parameters (or only one parameter), which are weighted on the basis of the strength of their effects on human

health. They are averaged in time, the place of the monitoring station is considered and by means of mathematical methods a single value is constructed of the data.

Table 2 Air Quality Index (AQI) (*EPA*)

AIR QUALITY GUIDE			
Air quality	**AQI**	**Caution – Ozone**	**Caution– very small particles (PM2.5)**
Good	0 – 50	No health impacts are expected when air quality is in this range.	No health impacts are expected when air quality is in this range.
Moderate	51 – 100	Unusually sensitive people should consider limiting prolonged outdoor exertion.	No health impacts are expected when air quality is in this range.
Unhealthy for sensitive groups	101 – 150	Active children and adults, and people with respiratory disease, such as asthma, should limit prolonged outdoor exertion.	People with respiratory disease or heart disease, the elderly, and children should limit prolonged exertion.
Unhealthy	151 – 200	Active children and adults, and people with respiratory disease, such as asthma, should avoid prolonged outdoor exertion; everyone else, especially children, should limit prolonged outdoor exertion.	People with respiratory disease or heart disease, the elderly, and children should avoid prolonged exertion; everyone else should limit prolonged exertion.
Very unhealthy	201 – 300	Active children and adults, and people with respiratory disease, such as asthma, should avoid all outdoor exertion; everyone else, especially children, should limit outdoor exertion.	People with respiratory disease or heart disease, the elderly, and children should avoid any outdoor activity; everyone else should avoid prolonged exertion
Hazardous	> 300	Everyone should avoid all outdoor exertion.	

Current *EPA* Air Quality Index and Clean Air Campaign Health Advisory

There is no unified strategy for constructing an air quality index. In every country or even within a country in different cities the value of the air quality index is acquired by different methods. There are suggestions for making simple air quality indices but in practice they are not characteristic. Even simple air quality indices need skills in mathematical statistics (*Bruno and Cocchi*, 2002).

6. DRAWBACKS OF CURRENT AIR QUALITY INDICES

Some objections can be raised against current air quality indices. They are not unified so it is hard to compare them. Though the descriptions are easy to understand for everyone and more or less compatible but the content behind the descriptions may be different due especially to the components considered.

Each of the complex indices considers different components but none of them include biological pollutants (for example ragweed pollen). However, their consideration could be very important because e.g. pollen, especially that of ragweed, through its irritant effect on the mucous membrane may intensify the effects of chemical pollutants.

When creating complex indices, at least temporal and spatial averaging needs to be performed, respectively. Objection can be raised against the temporal averaging of compounds that have no long term effects (for instance CO), since the modified data may not indicate severe short term exposures.

SUGGESTIONS TO SOLVE THE PROBLEMS

There are two suggestions to solve these problems. One of them is to supplement the current and studied air quality parameters with pollen. Pollen levels would be considered as a multiplicator function according to the actual concentration, thus the cumulative effects would appear in air quality indices.

In order to eliminate the lost data caused by averaging in time and space, we suggest using GIS methods. The indices used in this way should consider only the cumulative effects of the actually measured pollutant concentrations at a single location, and the GIS would display these indices at a certain time. In this way human health effects of all the pollutants show up in a way understandable for the public and the concerns can be spatially located. (A good analogy is the publishing of meteorological data with a state-of-the-art method).

REFERENCES

Bruno, F. and Cocchi, D.A., 2002: A unified strategy for building simple air quality indices. *Environmetrics 13(3)*, 243-261.

EPA – Enviromental Protection Agency, 40 CFR Part 58 [FRL- 6198-6] RIN 2060-AH92

Járai-Komlódi, M., 1998: Ragweed in Hungary. In *Spieksma, F.Th.M.* (ed.) 1998: *Ragweed in Europe. Satellite Symp. Proc. 6th Int. Congr. Aerobiol.* Perugia, Italy. Alk – Abello A/S, Horsholm DK. 33-38.

Makra, L., Juhász, M., Borsos, E. and Béczi, R., 2004: Meteorological variables connected with airborne ragweed pollen in Southern Hungary. *Int. J. Biometeorol. 49/1*, 37-47.

Makra, L., Juhász, M., Béczi, R. and Borsos, E., 2005: The history and impacts of airborne Ambrosia (Asteraceae) pollen in Hungary. *Grana 44/1*, 57-64.

Makra, L., Juhász, M., Mika, J., Bartzokas, A., Béczi, R. and Sümeghy, Z., 2006: An objective classification system of air mass types for Szeged, Hungary with special attention to plant pollen levels. *Int. J. Biometeorol. 50/6*, 403-421.

Makra, L., Juhász, M., Mika, J., Bartzokas, A., Béczi, R. and Sümeghy, Z., 2007: Relationship between the Péczely's large-scale weather types and airborne pollen grain concentrations for Szeged, Hungary. *Grana 46/1*, 43-56.

Mayer, H., Makra, L., Kalberlah, F., Ahrens, D. and Reuter, U., 2004: Air stress and air quality indices. *Meteorol. Z. 13*, 395-403.

Mezei, G., Járai-Komlódi, M., Papp, E. and Cserháti, E., 1992: Late summer pollen and allergen spectrum in children with allergic rhinitis and asthma in Budapest. *Pädiatrie & Pädologie 27/3*, 75.

Shooter, D. and Brimblecombe, P., 2007: Air quality indexing. *Int. J. Environ. Pollut.* (in press)

NOTES TO CONTRIBUTORS OF ACTA CLIMATOLOGICA ET CHOROLOGICA

Authors may be of any nationality, but the official language of the journal is English. Papers will be reviewed by unidentified referees.

Manuscripts should be sent to
Editor-in-chief of ACTA CLIMATOLOGICA ET CHOROLOGICA
Department of Climatology and Landscape Ecology
University of Szeged
P.O.Box 653, 6701 Szeged, Hungary

in two copies including all illustrations.

Title part of the paper should contain the concise title, the name(s) of the author(s), the affiliation(s) including postal and E-mail address(es). In case of multiple authors, the cover letter should indicate the corresponding author.

Summary should follow the title. Summary has to contain the purpose, data and methods as well as the basic conclusion. A summary in Hungarian as *Összefoglalás* is expected from Hungarian author(s).

Key words are necessary to help to classify the topic.

The text has to be typed in 1.5 spacing with wide (2.5 cm) margins. Word-processor printing is preferred. The use of SI units is expected. The negative exponent is preferred to solidus. Figures and tables should be consecutively numbered and referred in the text. The text should be no longer than 20,000 characters including notes and references.

Mathematical formulae are expected to be as simple as possible and numbered in parentheses at the right margin.

Tables and figures should be marked by Arabic numbers (*Table 1, Fig. 1*) and set in the text together with their captions. Avoid too lengthy or complicated tables.

References: The text citation should contain the name(s) of the author(s) in *Italics* and the year of publication. In case of one author the form of citation should be as follows: *Johnson* (1989), or if the name of the author cannot be fitted into the text: (*Johnson*, 1989); in the case of two authors: *Oke and Maxwell* (1975); if there are more than two authors: *Smith et al.* (1990). When referring to several papers published in the same year by the same author, the year of publication should be followed by letters a, b etc. At the end of the paper the list of references should be arranged alphabetically. For an article: the name(s) of author(s) in Italics, year, title of article, name of journal, volume number (the latter two in Italics) and pages. E.g. *Jauregui, E.,* 1989: The dust storms of Mexico City. *Int. J. Climatol. 9,* 169-180. For a book: the name(s) of author(s), year, title of the book (all in Italics except the year), publisher and place of publication. E.g. *Junge, C.E.,* 1963: *Air Chemistry and Radioactivity.* Academic Press, New York and London.

The final version should be submitted by e-mail as an attachment. The preferred medium for the text is MS Word 2002 (or Office XP) and for the figures the CorelDraw 9-13 or Excel 2002 (or Office XP) (or in 300 dpi resolution, high quality JPG or TIF formats).

Reprints: authors receive one copy of the relevant issue and 20 reprints free of charge.

More information: unger@geo.u-szeged.hu
keveibar@earth.geo.u-szeged.hu
makra@geo.u-szeged.hu
sumeghy@geo.u-szeged.hu